PhD PROGRAM IN CLINICAL MEDICINE AND PUBLIC HEALTH
Department of Pharmacology

THERAPEUTIC POTENTIAL OF INTESTINAL MESENCHYMAL STROMAL CELLS IN INFLAMMATORY BOWEL DISEASE AND COLORECTAL CANCER

DOCTORAL THESIS

Laura Hidalgo García

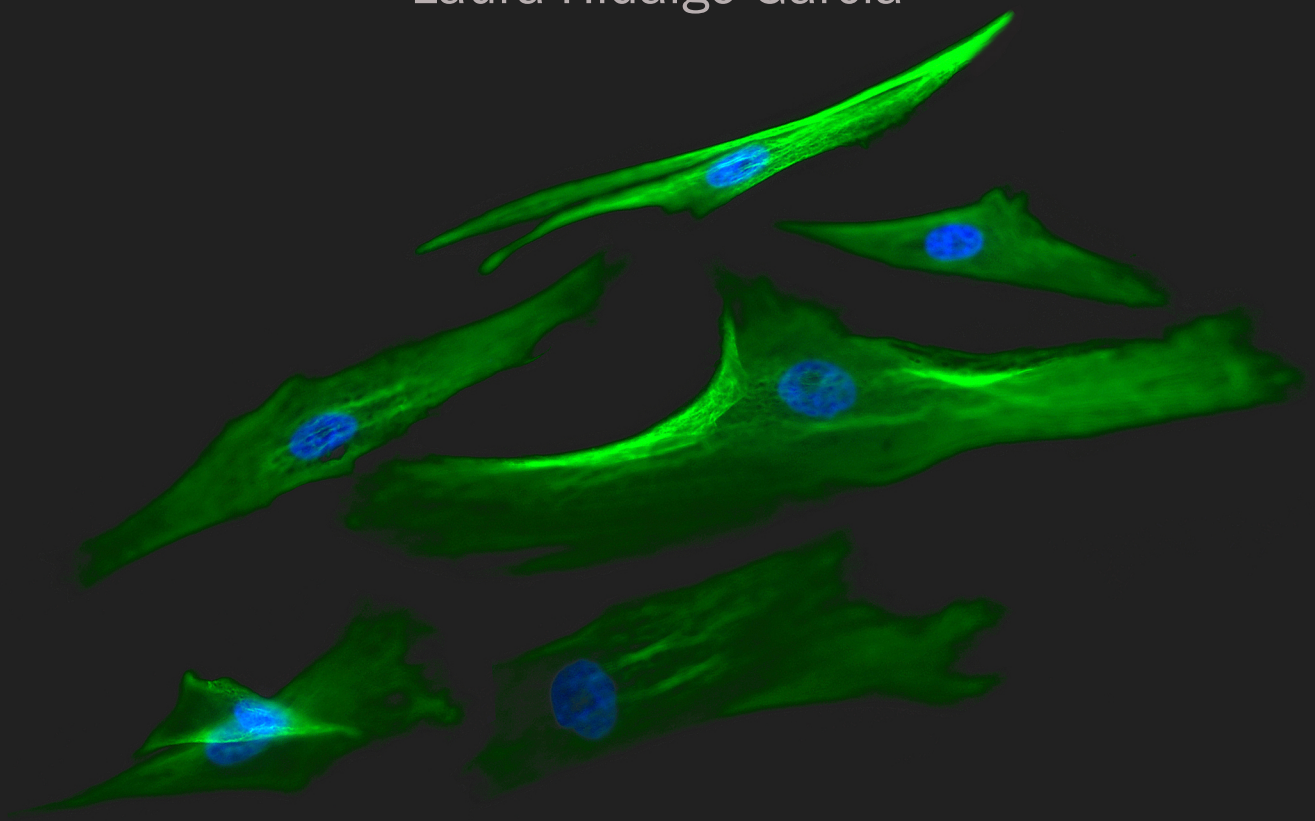

UNIVERSIDAD DE GRANADA

UNIVERSIDAD DE GRANADA

FACULTAD DE FARMACIA

Departamento de Farmacología

Programa de Doctorado en Medicina Clínica y Salud Pública

Therapeutic potential of intestinal mesenchymal stromal cells in inflammatory bowel disease and colorectal cancer

Tesis doctoral para aspirar al Grado de Doctor presentada por

Laura Hidalgo García

Bajo la dirección de los Doctores:

Julio Juan Gálvez Peralta

Per Olof Anderson

Granada, 2022

Editor: Universidad de Granada. Tesis Doctorales
Autor: Laura Hidalgo García
ISBN: 978-84-1117-639-2
URI: https://hdl.handle.net/10481/79476

“I have not failed. I’ve successfully discovered 10,000 things that won’t work”

Thomas Edison

“I am among those who think that science has great beauty”

Marie Curie

El doctorando / The *doctoral candidate* **Laura Hidalgo García** y los directores de la tesis / and the thesis supervisor/s: **Julio Juan Gálvez Peralta y Per Olof Anderson**

Garantizamos, al firmar esta tesis doctoral, que el trabajo ha sido realizado por el doctorando bajo la dirección de los directores de la tesis y hasta donde nuestro conocimiento alcanza, en la realización del trabajo, se han respetado los derechos de otros autores a ser citados, cuando se han utilizado sus resultados o publicaciones.

/

Guarantee, by signing this doctoral thesis, that the work has been done by the doctoral candidate under the direction of the thesis supervisor/s and, as far as our knowledge reaches, in the performance of the work, the rights of other authors to be cited (when their results or publications have been used) have been respected.

Lugar y fecha / Place and date:

Granada, 02 de febrero de 2022

Director/es de la Tesis / *Thesis supervisor/s;* Doctorando / *Doctoral candidate*:

Julio Juan Gálvez Peralta Per Olof Anderson Laura Hidalgo García

Firma / Signed Firma / Signed

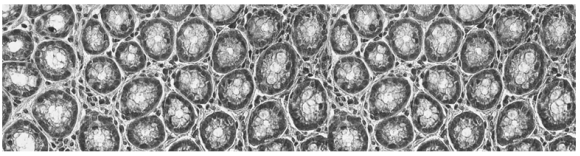

Index

INDEX

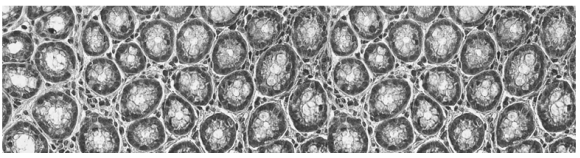

Summary

SUMMARY

Inflammatory bowel disease (IBD) is a chronic disease with increasing incidence and prevalence, currently affecting millions of people worldwide, which can lead to an aggressive colitis-associated cancer (CAC) with a poor prognosis. Its etiology seems to rely on the complex combination of different factors, including environmental determinants, genetic predisposition, microbiota imbalance, and mucosa immune defects. This compromises the intestinal epithelial barrier, leading to an altered immune response characterized by excessive and sustained cytokine production and immune cell recruitment and activation. Thus, the state of intestinal mucosal tolerance, i.e. immunological unresponsiveness to innocuous food antigens and the commensal microbiota, becomes disrupted. Understanding these mechanisms has potential translational value for IBD therapy and management, as well as for preventing the development of CAC.

Human intestinal mesenchymal cells (iMCs) represent a heterogeneous population of various cell types, such as fibroblasts, myofibroblasts, pericytes, smooth muscle cells and resident mesenchymal stromal cells (MSCs), which reside in the subepithelial compartment where they provide much of the structural framework of the intestine. However, iMCs also play important roles regulating the homeostasis/maintenance of the epithelial barrier and promoting immunological tolerance against commensal bacteria and food antigens. Moreover, recent investigations have proposed that iMCs may play dual roles both inhibiting or supporting gut inflammation and injury in IBD, as well as reducing or promoting tumor growth and metastasis, depending on their response to inflammatory mediators and/or TLR agonists.

The study of the stromal compartment of tissues was pioneered by Owen and Friendenstein, who discovered fibroblastic cells in the bone marrow with the capacity to give rise to bone, adipocytes and hematopoiesis-supporting stroma. Such MSCs are defined by a set of criteria postulated by the International Society for Cell Therapy (ISCT), and can be isolated from a variety of adult and neonatal tissues. Importantly, cultured MSCs retain part of their in vivo characteristics and provide a suitable model to analyze various aspects of stromal cells in health and disease. The design of new therapies against IBD and CAC should contemplate the importance of iMCs both in the homeostasis of the healthy intestine and the chronic inflammation even though further studies are needed to fully understand their properties on tissue regeneration and immunomodulation.

In order to address this, we set the following objectives:

1. Isolation and characterization of the immunomodulatory and tissue regenerative properties of intestinal MSCs (iMSCs) in vitro.
2. Analysis of the effect of iMSCs administration in dextran sulfate sodium (DSS)-induced acute colitis in mice: evaluation of disease severity, immune responses, tissue regeneration and microbiota composition.

3. Analysis of the effect of iMSCs administration on cancer progression in a model of colitis-associated cancer: evaluation of tumor growth, immune responses, and microbiota composition.

First, plastic-adherent iMCs were isolated from human intestinal resections and expanded in vitro. We then confirmed their identity as iMSCs according to the definition by ISCT, i.e: (i) expression of CD73, CD90, CD105, while lacking CD31, CD34 and CD45, and (ii) possessing the ability to differentiate into adipocytes, chondroblasts and osteoblasts in vitro.

Then, we explored the immunomodulatory properties of iMSCs in vitro. Our data show that iMSCs significantly repressed $CD4^+$ and $CD8^+$ T cell proliferation, partly through a indoleamine-2,3-dioxygenase (IDO)-dependent mechanism. Furthermore, iMSCs reduced the LPS-mediated induction of TNF-α in THP-1 macrophages, suggesting a polarization into anti-inflammatory M2 macrophages. In addition, isolated iMSCs enhanced wound closure in a scratch wound healing assay, using human normal colon epithelial cells.

Second, we analyzed their properties in vivo in an experimental model of acute intestinal inflammation induced by DSS in C57/bl6 mice, which displays human IBD-like features. One single intraperitoneal injection of iMSCs significantly reduced the disease activity index (DAI), ameliorated the histological damage of the colon and improved the integrity of the intestinal epithelium. The anti-inflammatory effect exerted by iMSCs was associated with a reduced expression of pro-inflammatory cytokines including TNF-α, IL-6 and IL-12, as well as of the adhesion molecule ICAM-1 and iNOS, thus suggesting a M2-polarization of macrophages. Interestingly, when the microbiota was analysed, the treated mice presented a higher species richness (Chao1 index) and diversity (Shannon index), than the untreated colitic mice. Besides, iMSCs modified the abundance of key phyla affected by the DSS, such as *Proteobacteria* and *Actinobacteria*.

Finally, the iMSCs were evaluated in a murine model of CAC consisting of the injection of azoxymethane (AOM) followed by three cycles of DSS to C57/bl6 mice. Two intraperitoneal injections of iMSCs at the peaks of the two last DSS cycles significantly reduced colitis and the associated intestinal tumor development. The iMSCs reduced the colonic expression of several inflammatory mediators that drive CAC, including IL-6, TNF-α, IL-17/IL-23 and COX-2; the activation of the signaling pathways of PI3K/AKT and IL-6/STAT3 as well as the levels of tumor-promoting β-catenin). The iMSCs treatment also lowered the number of intestinal neutrophils and eosinophils in comparison to CAC mice. As shown in the DSS model, iMSCs also decreased the proportion of M1 macrophages, and partly restored the normal intestinal macrophage differentiation. Regarding their effect on microbiota composition, iMSCs ameliorated the CAC-induced dysbiosis, restoring the OTUs and Shannon parameters and diminishing the alterations in the relative abundance of *Bacteroidetes* and *Verrucomicrobia*.

In summary, our data show that human iMSCs isolated from the noninflamed intestine possess potent tissue-regenerative and immunomodulatory capacities in vitro and in vivo, that could be considered as key elements to ameliorate IBD severity and protect against CAC development.

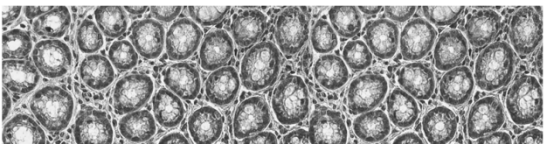

Introduction

INTRODUCTION

1. MESENCHYMAL STROMAL CELLS: DISCOVERY AND DEFINITIONS

The term “stroma” comes from the late latin word *strōma*, which means “bed" or “bed covering” and refers to those parts in the organ or tissue that have a connective or structural role, compassing stromal cells and a complex extracellular matrix. Historically the term “stromal cells” (SCs) have made reference to “non-immune” cells – in a tissue or organ – that provide structural support to the parenchyma, i.e., the parts of the organ that perform a specific function (1). The stroma consists of, heterogeneous cell populations, including mesenchymal stem cells, pericytes and fibroblasts with different phenotypes (2).

Mesenchymal stromal cells (MSCs) were originally identified in the bone marrow by Friedenstein, Owen and colleagues in the 1960s as fibroblastic cells with self-renewal capacity, able to form colony-forming units fibroblast (CFU-F), bone, adipocytes and hematopoiesis-supporting stroma (3-5). These cells were labelled “bone marrow osteogenic stem cells” and represented, at the time, the second example (after hematopoietic stem cells) of an adult tissue-specific stem cell. Subsequently, perivascular cells with self-renewal capacity which could differentiate into adipocytes, osteoblasts and chondroblasts in vitro were found in virtually all adult organs and tissues, including adipose tissue, and Wharton’s jelly of the umbilical cord (6, 7). These apparently common progenitors of mesodermal tissues were named “mesenchymal stem cells” and were proposed to represent a new therapeutic technology for regenerative medicine (8, 9). However, convincing data to support the stemness, as defined by Friedenstein and colleagues, of these cells were lacking, prompting the International Society for Cellular Therapy (ISCT) to propose the term “multipotent mesenchymal stromal cell” when referring to these cells (10) (Figure 1).

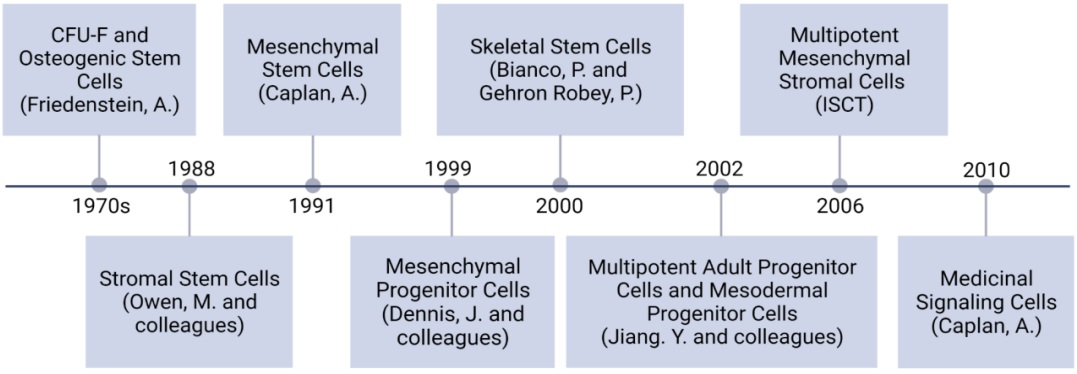

***Figure 1. The history and timeline of Mesenchymal Stromal Cells nomenclature**. MSCs were first described by A. Friedenstein as Colony-Forming Unit fibroblasts (CFU-F) and Osteogenic Stem Cells (3, 11) in the late 60s. Nevertheless, since then, a number of terms have been used when referring to Mesenchymal Stromal Cells (MSCs) found throughout the body including*

"mesenchymal stem cells" (8), "mesenchymal progenitor cells" (12), "skeletal stem cell" (13) or "multipotent adult progenitor cells" (14). Due to the lack of evidence showing their differentiation and self-renew abilities in vivo, the ISCT proposed the term "multipotent mesenchymal stromal cells" in 2006 (15) and proposed three minimum criteria to define them. Four years later, A. Caplan suggested that the acronym MSC could stand for "Medicinal Signaling Cells" which reflects that the beneficial therapeutic effects of MSCs can be attributed to their capacity to secrete bioactive molecules. Figure adapted from R&D systems and created with BioRender.com.

2. MSCs IN VIVO

MSCs isolated from distinct tissues are phenotypically similar based on the definition of MSC described by Dominici in 2006 (16, 17). Crisan et al., found that $CD146^+$ $CD45^-$ $CD34^-$ pericytes isolated from various were indistinguishable from MSCs in terms of adherence, morphology, phenotype and in vitro differentiation capacities (6), suggesting a common pericyte origin for MSCs. However, later studies have shown that MSCs from different tissues exhibit distinct transcriptomic profiles, differentiation and immunomodulatory capacities (17-21).Thus it is now believed that MSCs have a unique identity depending on which tissue they reside in (18, 19). Thus, the tissue-specific role of bone marrow-derived MSCs is to participate in bone remodelling and support hematopoiesis (22, 23).

However, some studies suggest that endogenous MSCs (including BM-MSC) can home, via the bloodstream, to sites of injury, including inflammatory cardiomyopathy (24) ((25)). Furthermore, endogenous MSCs have also been implicated in tumor progression. MSCs from bone marrow and adipose tissue can migrate to the tumor (26), enter the tumor microenvironment, and promote tumor growth and metastasis (27). These processes are carried out through their differentiation into cancer-associated fibroblasts (CAFs) (28) and the expression of growth factors and/or immunomodulatory cytokines that can promote angiogenesis and tumor growth, inhibit anti-cancer immune responses and induce epithelial-mesenchymal transition (EMT) in tumor cells (29).

3. MSC IN VITRO

Ever since Arnold Caplan coined the term "mesenchymal stem cells" and Mark F. Pittenger showed that multipotent MSCs could easily by isolated from adult bone marrow, much attention has been directed at harnessing the possible therapeutic properties of in vitro expanded MSCs (8, 9). However, due to the different approaches in characterizing the cells, comparison between studies became increasingly difficult.

To accurately define human MSCs with the aim of facilitating the exchange/comparison of data between researchers, the Mesenchymal and Tissue Stem Cell Committee of the ISCT proposed a minimum set of criteria that MSCs have to meet (15) (Figure 2).

- First, MSCs must be able to adhere to plastic under culture conditions and present a fibroblast-like shape. In fact, they proliferate to form a heterogeneous population of fibroblast-like cells (colony-forming-unit fibroblasts) that are at varying stages of commitment to differentiation.
- Second, MSCs must present a specific immunophenotype. They have to express CD105 (also known as endoglin), CD73 (ecto-5′-nucleotidase), and CD90 (THY1) on their surface, and be negative for the haematopoietic marker CD45, monocyte or macrophage markers CD14 or CD11b, haematopoietic progenitor and endothelial cell marker CD34, B cell markers CD79α or CD19 or human leukocyte antigen (HLA)-DR.
- Third, to demonstrate their multipotency, MSCs must differentiate in vitro into osteoblasts, adipocytes and chondroblasts.

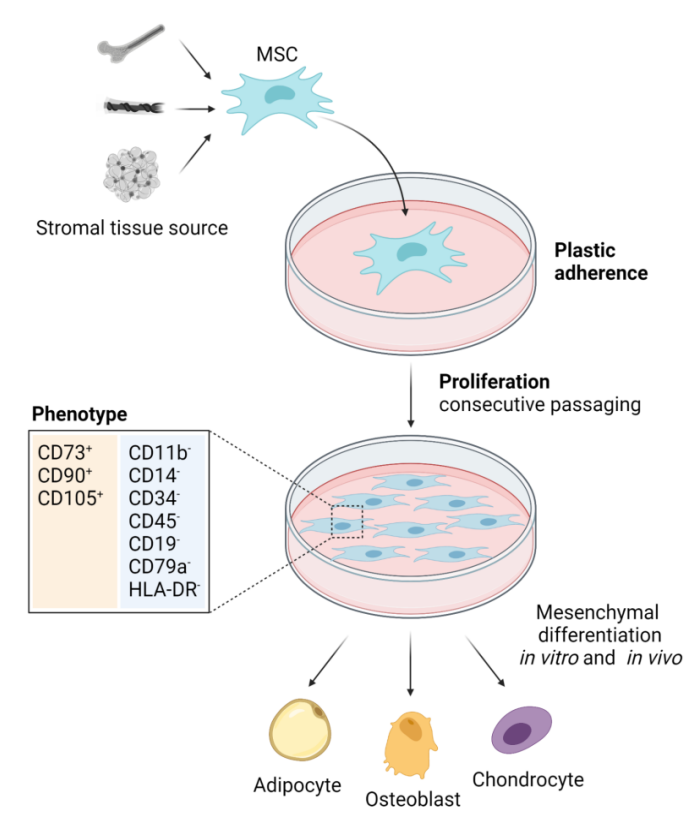

***Figure 2. Minimal criteria for defining human multipotent MSCs according to the ISCT**. After isolation, MSCs can be distinguished from other cell types by their capacity to adhere to plastic. After that, they can proliferate for several consecutive passages to form a heterogeneous population of fibroblast-like cells. Although MSCs do not express a unique cell marker, ISCT proposed a phenotype criteria. Concretely, they established that MSCs must be positive for CD73, CD90 and CD105 and show a lack of expression of other markers typical from other cell types such as CD11b, CD14, CD34, CD45, CD19, CD79a or HLA-DR. Additionally, MSCs have to possess the ability to differentiate in vitro or in vivo into other mesenchymal tissue cells such as*

osteoblast, chondroblasts and adipocytes. Image created with BioRender.com and adapted from (30).

4. IMMUNODULATORY FUNCTION OF IN VITRO EXPANDED MSCS

Importantly, in addition to their high self-renewal capacity and multilineage potential, it has been shown that in vitro expanded MSCs possess broad anti-inflammatory and immunomodulatory capacities *in vitro* and *in vivo*, both in preclinical models (31, 32) and in clinical trials (33-35). MSCs can modulate both innate (macrophages, dendritic cells and NK cells) and adaptive immune (T- cells, B-cells) responses through the production of a variety of mediators, including (i) soluble factors (e.g. cytokines, growth factors, including IL-10, IL-6, tumor necrosis factor α-stimulated gene 6 (TSG-6), hepatocyte growth factor (HGF), and prostaglandin E_2 (PGE_2)), (ii) intracellular enzymes (nitric oxide, indoleamine 2,3-dioxygenase (IDO), and hemeoxhygenase-1 (HO-1)) (iii) membrane bound molecules (e.g. PD-L1, HLA-G) (36). Furthermore, MSCs have been shown to home to sites of inflammation, making them a promising cell therapy for the treatment of inflammatory/immune-mediated diseases (37), including graft-versus host disease, sepsis, inflammatory bowel disease (IBD), and multiple sclerosis.

Interestingly, the capacity of MSCs to suppress or promote inflammation depends on the inflammatory milieu they are subjected to since they are not constitutively immunosuppressive. During the onset of inflammation, low levels of inflammatory mediators such IFN-γ, TNF-α and IL-1β drive MSCs to acquire a proinflammatory state (known as MSC1). During this phase, MSCs generate great amounts of proinflammatory soluble mediators that stimulate activation and migration of neutrophils, and enhance their ability to phagocytize bacteria and promote bacterial clearance (38). On the other hand, during the late phase of inflammation, high levels of proinflammatory cytokines are released, and engrafted MSCs tend to show an anti-inflammatory phenotype (or MSC2). In this context, they suppress activation and effector functions of inflammatory dendritic cells (DCs), macrophages and T, NK and NKT cells, promoting tissue repair and homeostasis (38). The switch towards a proinflammatory or anti-inflammatory phenotype mainly relies on differential activation of toll-like receptors (TLRs) that are expressed on their surface (39). TLR-4 mediated activation influences in the polarization of MSCs towards a MSC1 phenotype, while activation of TLR-3 may lead MSCs to a MSC2 immune-suppressive phenotype. The balance between these pathways probably serves to prevent excessive tissue damage during inflammation and promote host defense (38).

5. INTESTINAL STROMAL CELLS - FROM STRUCTURAL COMPONENTS TO KEY PLAYERS IN EPITHELIAL HOMEOSTASIS AND IMMUNE RESPONSES.

Epithelial and stromal cells are present at the surfaces of most organs, creating a physical barrier, separating the microbiome from the underlying tissues and immune system (40). Numerous

studies have investigated the interactions between the microbiome and the immune system in the healthy and diseased gut, but little attention has been directed at the intestinal stroma. Recently, studies have started to understand their involvement in regulating the homeostasis/maintenance of the epithelial barrier, modulating immune/tissue responses. Importantly intestinal stromal cells exhibit both beneficial and detrimental effects in intestinal pathologies and cancer, as will be discussed below.

A major drawback in the field of intestinal stromal compartment in that, in the literature, the term intestinal SCs (iSCs) has been confusingly used to make reference to cells with mesenchymal origin such as fibroblasts (FBs), smooth muscle cells (SMCs) and pericytes (1, 41, 42) but has also even included lymphatic endothelial cells, blood vessels, neurons and glia (40, 43). Similarly, the term "intestinal mesenchymal cells" (iMCs) encompasses different kinds of cells and is generally used to refer to $CD45^{-}EpCAM^{-}$ non-endothelial ($CD31^{-}$), non-glial and non-neuronal cells, including myofibroblasts (MFBs), FBs, SMCs, pericytes, and mesenchymal stromal/stem cells. But mostly, these two terms - iSCs and iMCs - have been used indistinctly to refer to the same type of cells i.e. cells that share similar origin, marker molecules and integrated biological functions. This, together with the fact that there is no unique specific marker to concretely define these different subsets and allocating functions, has given rise to multiple scientific works referring to the same cells into distinct manners. For these reasons and unless otherwise stated, here we will refer to iMCs as all $CD45^{-}$ (non-hematopoietic) $CD31^{-}$ (non-endothelial) and $EpCam^{-}$ (non-epithelial) cells of unknown or mixed origin in the intestine and, if possible, their specific name will be mentioned.

In general, iMCs are negative for hematopoietic ($CD45^{-}$), epithelial ($EpCAM^{-}$), and endothelial ($CD31^{-}$) markers and positive for combinations of CD90, α–smooth muscle actin (α-SMA, also known as ACTA2), desmin and vimentin. Other proposed markers include platelet-derived growth factor receptor (PDGFR)-α, chondroitin sulfate proteoglycan 4, also known as melanoma-associated chondroitin sulfate proteoglycan or neuron-glial antigen 2 (NG2) and S100 calcium binding protein A4 (S100A4, also known as FSP1). However, the lack of specific markers to distinguish and locate different subsets until recently have made it difficult to assign specific functions to a particular iMC subset, limiting the understanding of the immunobiology of these cells (41, 44). In 2016, NK2 homeobox 3 (NKX2-3) and amine oxidase copper containing 3 (AOC3), a cell surface molecule, were identified as SMC and myofibroblast markers, respectively; short stature homeobox 2 (SHOX2) was found to be a marker for fibroblasts and so, should be used for characterization of this subset (45) (Table 1).

► **KEY CONCEPT | intestinal mesenchymal cells lack specific cells surface markers.** The lack of iMCs specific markers makes it difficult to identify iMCs in tissue and the development of strategies that could modulate their behaviour *in vivo*. Because of that, current research is focused on searching for specific markers for these cells.

Subsets	Markers	Functions
Fibroblasts	α-SMA-, Vimentin+, CD90+, Desmin-, FSP1+, PDGFRα+,PDGFRβ-, VCAM1-, AOC3-, NKX2-3-, SHOX2+, SMM-	Mechanical support, epithelial homeostasis, stem cell niche maintenance, immune regulation
Myofibroblasts	αSMA+, Vimentin+, CD90+, Desmin-, ER-TR7+, PDGFRβ+,VCAM1-, MHC class I,II+, CD80/86+, Collagen I+, NG2+, AOC3+, NKX2-3-, SHOX2-, SMM-, FAP+	ECM maintenance, regulation of angiogenesis and vascular function
Pericytes	αSMA+, Vimentin+, Desmin+, PDGFRα+, PDGFRβ+, VCAM1+,MHC class I,II+, CD80/86+, NG2+, SMM-	Regulation of angiogenesis, cell trafficking, vascular function, stem cell properties
MSCs	Vimentin+, CD90+, PDGFRα+, PDGFRβ+, ICAM1+, VCAM1+,CD73+, CD105+, CD29+, CD44+, SMM-	Stem cell properties
SMCs	αSMA+, Vimentin-, CD90-, Desmin+, FSP1-, PDGFRα+,VCAM1-, NG2+, AOC3+, NKX2-3+, SHOX2-, SMM+	Mechanical support, smooth muscle contraction

***Table 1**. **Subsets of iMCs that are present in the intestine.** AOC3, amine oxidase copper containing 3; CD, cluster of differentiation; FAP, fibroblast activating protein; FSP1, fibroblast-specific protein 1; ICAM1, intercellular adhesion molecule 1; NKX2-3, NK2 Homeobox 3; SHOX2, short stature homeobox 2; SMM, smooth muscle myosin; VCAM1, vascular cell adhesion protein 1. Table adapted from (46).*

In the healthy colon, fibroblasts are usually inactive, with low transcriptomic and metabolic activity. They are found in the lamina propria, which is the connective tissue adjacent to the gut epithelium, and their main functions include the secretion of extracellular matrix (ECM) proteins for the maintenance of the ECM, the secretion of ECM modifying enzymes, and the secretion of mediators that control epithelial differentiation and proliferation (41, 47, 48). However, upon tissue damage and/or inflammation, fibroblasts are activated by multiple factors (including TGF-β, reactive oxygen species (ROS), inflammatory cytokines, chemokines and mechanical stress), and differentiate into myofibroblasts (49, 50). In contrast to fibroblasts, myofibroblasts proliferate, acquire a stellate morphology and are metabolically more active. The principal role of myofibroblasts is to promote tissue repair and wound healing, along with modulation of inflammation (48, 49, 51, 52). After the resolution of the insult, the quantity of myofibroblasts diminishes, partly through a reversion to the quiescent state and apoptosis. As stated before, resident MSCs can be isolated from a myriad of adult tissues and are multipotent progenitor cells that are distinct from completely differentiated, non-hematopoietic intestinal-resident cells. They have the ability to regulate immune responses and to differentiate to different cell types. However,

their precise homeostatic functions and origin are not clearly defined (53-55). Curiously, studies of other tissues have found pericytes as a possible predecessor of MSCs (56).

In line with the use of the cellular markers explained before, the following figure depicts the anatomical structure of the small intestine and colonic lamina propria in order to clarify the organization and relationships of the different intestinal mesenchymal cells (the anatomy of the large intestine is quite similar to the crypts of the small intestine).

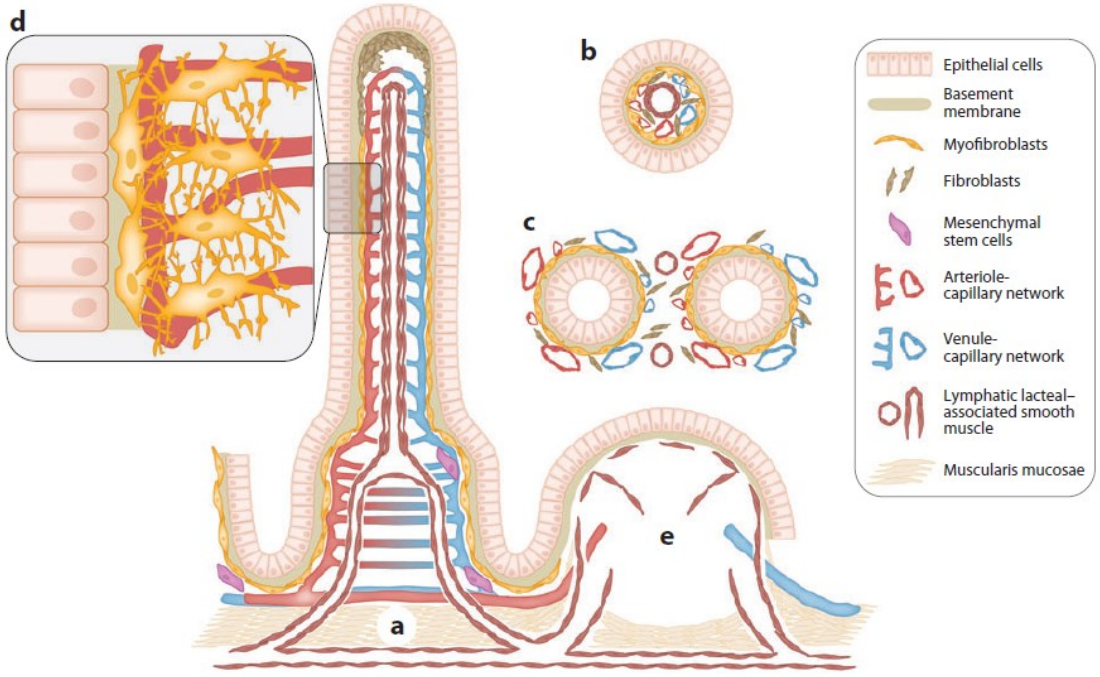

***Figure 3**. **The spatial distribution of the intestinal mesenchymal niche and the epithelial compartment alongside the small intestine.** (a) Longitudinal view of the villus-crypt axis showing the epithelium, lamina propria myofibroblasts, pericytes, resident mesenchymal stem/stromal cells (previously defined as MSCs), and smooth muscle cells in the muscularis mucosa. Fibroblasts are mostly located in the upper part of the villi. (b) Transverse sections through a villus show the lymphatic capillaries associated with smooth muscle cells. (c) Cryptal cross section demonstrating the lymphatic pericytes. As well, images b and c show that subepithelial myofibroblasts are mainly pericytes (d) Illustration of the myofibroblasts and pericytes that support and wrap around the capillaries. (e) A Peyer's patch with its different cellular components. Image taken from (41).*

6. DEVELOPMENTAL ORIGIN OF INTESTINAL MESENCHYMAL CELLS

Understanding the lineage tree of intestinal mesenchymal cells and their developmental origin is fundamental for their study, classification and further characterization. The intestinal mesenchyme evolves at the same time with the epithelium during the development of the embryo

and their cross-talk is crucial during the organogenesis of the intestine (57). Precursor cells are observed at 7-weeks of the developing process, when the intestinal lumen is not still assembled. 2 weeks after, the lumen along with primitive crypt invaginations is organized. At this time, there are also observed vascular structures with pericytes and endothelial cells, collagen fibers, a basement membrane and epithelial cells surrounded by myofibroblast-like and fibroblast-like cells. At the 11th week the intestines possess well-differentiated villi and crypts, composed of secretory and epithelial cells. At the base of the crypts and in the lamina propria myofibroblast-like cells and fibrous extensions (called fibronexi) are present (58). Cells of the intestinal mesenchyme, including the lamina propria, its blood and lymphatic vessels and the muscularis propria are thought to originate mainly from the visceral mesoderm. Other origins proposed are the mesothelium and the neural crest (57). The mesothelium is a monolayer of squamous-like epithelial cells that lines serosal cavities and internal organs. Is believed to generate iMCs via epithelial-mesenchymal transition (EMT) and is derived from the mesoderm (44, 57). In 2012, Rinkevich et al. proved the mesothermal origin of intestinal mesenchymal cell populations. For that purpose, they created a mesothelin (a marker of mesothelial cells) knock-in mouse model to perform lineage tracing experiments between days 10.5-17.5 of the embryo development and showed that mesothelin+ cells are precursors of myofibroblasts of the intestinal mucosa and of SMCs in the gut. By contrast, lineage tracking of cells from the neural crest or circulating cells showed no contribution of the neural crest to the intestinal smooth muscle and the lamina propria mesenchyme (59). In spite of this, the lineage relationships between progenitor cells in the adult gut have not still been clarified. In addition to the complexity over intestinal mesenchymal cell origin, in the last decade there is an increasing interest in the immunomodulatory capacity and therapeutic potential of mesenchymal stromal cells cells (60). In 2004, Brittan & Wright demonstrated that lamina propria pericytes and subepithelial myofibroblasts are repopulated by bone marrow stromal cells, being neoplasia and intestinal injury amplifiers of this process (61). This mechanism also takes place in lungs (62) and liver (63). What specific chemotactic signals and which bone marrow stem cells are the promoters of this mesenchymal replenishment still remains unclear (64). Both MSCs and fibrocytes are candidate cells of bone marrow origin to be the stromal stem cells of the intestine (65, 66). As stated before, MSCs are $CD45^-$, $CD34^-$,α-SMA^+ cells that express variable levels of CD105, CD73, CD44, CD90 and CD71 (transferrin receptor) and do not express antigen-presenting costimulatory markers like CD40, CD80 and CD86 (66). Fibrocytes derive from a small subpopulation of CD14+ PBMCs expressing IgG receptors. They are α-SMA+, $CD45^+$, $CD34^+$ cells that also express CD80, CD86 and MHC-II (65, 67). As well as MSCs, fibrocytes are located in cancers and in inflamed tissues (65). Nevertheless, a better understanding of these two bone marrow-derived cells function would be useful in the area of iMC biology, especially with regards to the modulation of resident mesenchymal cell function/ abundance in the context of stromal cell transplantation for intestinal and liver diseases (64, 68).

7. ROLE OF iMCs: INTESTINAL HOMEOSTASIS

As we have seen, iMCs form a complex system underneath the gut epithelium (41, 69). Due to their localization, they provide structural framework but also take part in a variety of processes in the gut to maintain intestinal homeostasis – they play crucial roles in intestinal repair and wound healing and release mediators for epithelial differentiation and proliferation (70). Hereafter, we are going to see how the bidirectional communication between the epithelium and the mesenchyme compartments fundamentally relies on the release of different soluble mediators that impact in the intestinal epithelium fate and homeostasis (71).

7.1. Wnt signalling

Wnt pathway is the principal pathway that drives epithelial proliferation. The fundamental signalling mediators of this pathway are Wnt proteins, that are classified into canonical (Wnts 3, 6 and 9b) and non-canonical (Wnts 2b, 4, 5a and 5b). Historically, when the Wnt canonical pathway is activated, cytoplasmic β-catenin translocates to the nucleus and promotes the expression of related genes. On the other hand, the term non-canonical pathway refers to Wnts signalling that does not lead to nuclear β-catenin translocation (72). An in deepth analysis of intestinal Wnts reported that canonical Wnts are mainly produced by epithelial cells, while non-canonical Wnts come from the mesenchymal compartment (73). In 2007, Van der Flier et al. (74) found that a series of genes were preferentially expressed within the crypt stem cell niche after Wnt signalling activation, arriving to the conclusion that Wnt signalling is enhanced at that location. Concretely, olfactomedin 4 (Olfm4) and leucine-rich repeat–containing G protein–coupled receptor 5 (Lgr5), were expressed in epithelial stem cells or their predecessors. (74-76). On the other hand, it has been reported that some Wnt antagonists have a mesenchymal origin (77). Then, mesenchymal cells participate in the modulation of the Wnt/β-catenin signalling pathway, preventing an exacerbate activation in the intestinal epithelium.

7.2. BMP signalling

One major pathway that antagonizes Wnt signalling across the epithelium comprises the mesenchymal-derived bone morphogenetic proteins (BMPs) (78, 79). The BMP pathway suppresses Wnt/β-catenin signalling in epithelial stem cells, limiting their self-renewal and expansion and promoting their differentiation (80, 81). BMPs antagonize Wnt signalling by stabilizing Phosphatase and Tensin homolog (PTEN), which in turn, diminishes Akt activity, and therefore inactivates β-catenin translocation (78). BMPs are growth and differentiation factors that belong to the TGF-β superfamily. Their binding promotes the activation of the receptor they have been coupled with, which phosphorylates a SMAD protein (SMAD1, -5, or -8) that then forms a complex with a co-SMAD – SMAD4 in mammals. Right after, the SMAD1/5/8-SMAD4 complex translocates to the nucleus, and activates the transcription of a set of genes (82). BMP signalling takes place also in a SMAD-independent manner. In this case, after BMP binding, a MAPK-dependent signalling cascade is triggered (82). Active Bmp signaling, is detected within

differentiated epithelial cells and throughout the mesenchymal compartment of the lamina propria (81, 83) and as one proceeds in direction to the lumen, the quantity of BMPs increases, creating an environment that supports epithelial differentiation (84) (Figure 4).

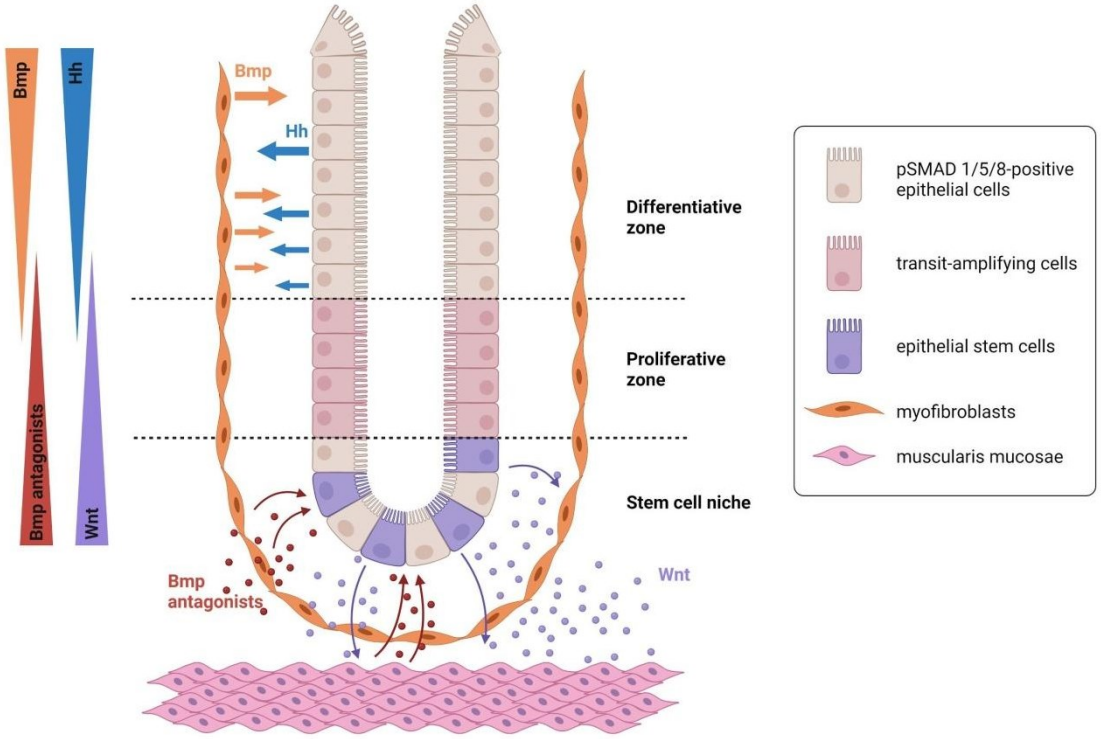

Figure 4. Interactions between the epithelial and mesenchymal compartments in the intestinal crypt. *Hh proteins released by epithelial cells of the differentiative zone promote the synthesis of Bmps by mesenchymal cells. While their lack in the stem cell niche compartment leads to a decreased synthesis. On the other hand, Bmps produced by differentiated epithelial cells support the maintenance of the quiescent and differentiated state. The secretion of canonical Wnts by Paneth and epithelial stem cells supports self-renovation of the stem cell compartment and also triggers the secretion of Bmp antagonists by myofibroblasts and cells from the muscularis mucosae (which further augments Wnt signaling). Image created with BioRender.com adapted from (41).*

7.3. Hedgehog signalling

Epithelial cells can also regulate the mesenchymal cell compartment. One way of regulating it is through the hedgehog pathway. Differentiated epithelial cells express and release Hedgehog proteins (Hh): Indian Hedgehog (IHH), Sonic Hegdehog (SHH) and Desert Hegdehog (DHH), which ensures a lower level of BMPs in the proliferative zone (Figure 4). The first studies came a decade ago, when Kosinski et al reported that IHH is crucial to coordinate intestinal mesenchymal cell formation and proliferation. In turn, iMCs regulate the accurate differentiation and regeneration of the intestinal epithelium (85). This process has to be thoroughly regulated, as a continued activation of the hedgehog pathway results in to crypt abnormalities, elimination of

epithelial cells precursors, and myofibroblasts overgrowth in mice (86, 87). Hh signaling is triggered when a Hh protein binds to its receptor, initiating a signaling cascade that leads to the translocation of the transcription factors Gli1, Gli2, and Gli3 into the nucleus, activating the expression of some related genes like *Gli1 and Ptch1.* Both IIHH and SHH are expressed by intestinal epithelial cells during day 18.5 of embryonic development and it has been shown that *IHH* knockout mice die at birth (41). On the other side, minor mutations in SHH, IHH, or their downstream pathways result in serious malformations on several organs in humans. Within the adult intestine, hedgehog pathway is usually given in an epithelial to mesenchymal direction and is fundamental for the proper development of the intestinal mesenchymal cell compartment (87, 88), bringing to light the key importance of bidirectional epithelial-mesenchymal interactions for intestinal barrier maintenance and homeostasis.

8. ROLE OF IMCS: REGULATORS OF IMMUNE TOLERANCE AND THE MUCOSAL IMMUNE SYSTEM

Historically, iMCs have been thought as mere observers of immune responses, providing only structural support to professional immune cells. However, this concept has changed and iMCs have emerged as direct players of tissue homeostasis and inflammation, in fact they were denominated as “non-professional innate immune cells” (1). Although the cells from the epithelial barrier sense and interact with food antigens, intestinal microbiota and pathogens, we know that sometimes its physical and biochemical action does not prevent these antigens from entering the lamina propria. Therefore, the professional and non-professional immune cells that lie below the epithelial cells represent the second line of defence to antigens that have passed the gut lumen (69). Summarized data below provides convincing evidence that gut mesenchymal cells act as non-professional immune cells that regulate innate and adaptive immunity.

8.1. iMCs and innate response interactions

During the last decade, it has been acknowledged that iMCs have the ability to interact with immune cells of the intestinal lamina propria and are able to sense inflammatory, damage-associated and bacterial signals in their surrounding environment. Early studies were performed in vitro with cultured intestinal mesenchymal cells from mice and humans. They established that iMCs express a wide panel of innate recognition and cytokine receptors and respond to the relevant stimuli by secreting chemokines, cytokines, ECM components and matrix metalloproteinases (MMPs) (89).

Although evidence of the mesenchymal contribution to microbial sensing in vivo is scarce, there is increasing evidence suggesting that iMCs are able to respond promptly to pathogenic agents. As we are going to see, different studies have described that cultured murine and human myofibroblasts express NLRs (NOD-like receptors) and TLRs. That gives evidence of their potential to recognize and respond to immune signals in the gut such as bacteria and their

components (90). In this regard, BMJ Owens et al. showed that CD90⁺ iMCs are able to respond to a *Salmonella typhimurium* infection in vitro, although to a lesser extent than professional APCs such as dendritic cells (90). Nevertheless, evidence showing their mechanism of action in vivo is still lacking.

Additionally, in 2011, Kim el al. reported that NOD2 (*nucleotide-binding oligomerization domain-containing protein 2*) signalling in iMCs was fundamental for handling the recruitment of inflammatory monocytes and, therefore, for promoting bacterial eradication in a mouse model of human pathogenic infection (91). Studies describing the expression of other NLRs in murine iMCs are limited. However, it has been reported that mouse myofibroblasts constitute the principal source of intestinal cells that express NLRP6, a member of the NLR family that regulates epithelial barrier restructure after bacterial infection in vivo (92).

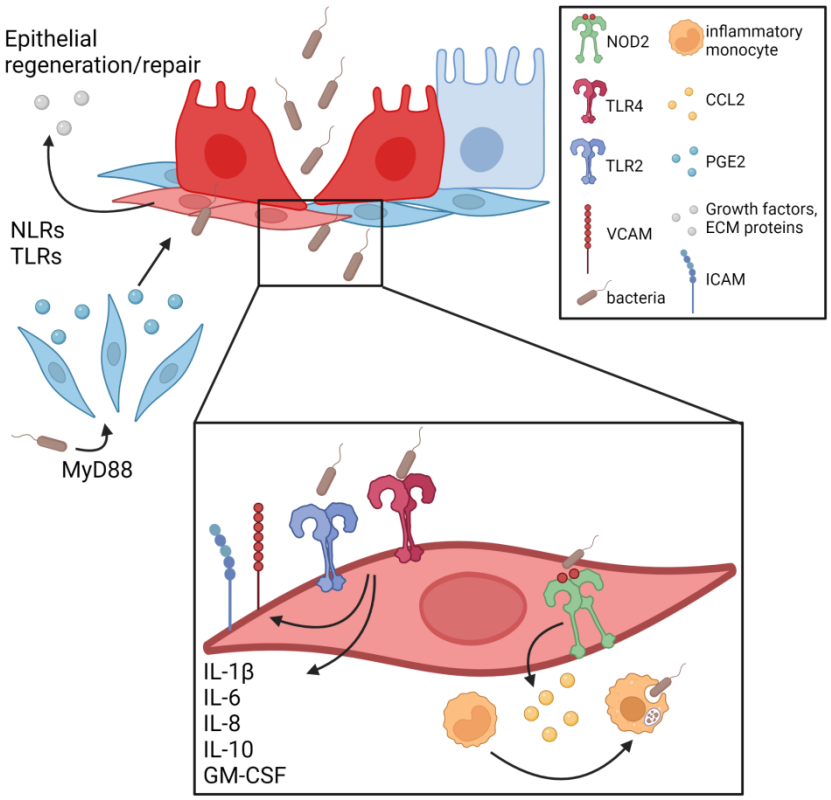

***Figure 5. Intestinal mesenchymal cells possess an important role in bacterial recognition**. Intestinal mesenchymal cells are strategically located to give a response to the intrusive pathogens through NOD2 sensing NOD2, can be triggered which triggers the release of CCL2 and facilitates the recruitment of inflammatory monocytes that take part in the eradication of the pathogenic microorganism. Additionally, it is known that human colonic mesenchymal cells express TLR receptors. For that reason, it would be feasible that upon microbial invasion, iMCs-mediated immune signalling could act in two ways (i) promoting leukocytes recruitment and (ii) generating growths factors and extracellular matrix proteins. MyD88 - myeloid differentiation primary response gene (88), GM-CSF - granulocyte-macrophage colony-stimulating factor, NLR*

- NOD-like receptor, PGE_2 - prostaglandin-E_2, VCAM-1 - vascular cell adhesion molecule-1 and ICAM-1 - intercellular adhesion molecule-1 . Figure created with BioRender.com and adapted from (93).

Also, it has been described that primary murine myofibroblasts, isolated from either the colon or the ileum, express TLR4 and so respond to LPS stimulation by activating p38 MAPK, Akt, NFκB, signalling pathways and secreting immune mediators including CXCL1, IL-6 and PGE_2 (94). Additionally, human colonic myofibroblasts are known to express TLRs, NOD1 and NOD2 receptors (89), and have detectable protein levels of TLR2, TLR4 and TLR5 allowing them to reply to bacterial infections (90). In fact, as in mice, LPS stimulation of human iMCs triggers a variety of reactions (95-97) including the production of IL-10, IL-6, IL-1β and GM-CSF, and the upregulation of the adhesion molecules VCAM-1 (or CD106) and ICAM-1 (or CD54) (98). Also, human iMCs produce functional NOD2 receptors, that act synergically with TLR2 to enhance the expression of different IL-1 family members, regulating mucosal homeostasis (90). They also possess the ability to respond to stimulation with IL-1β, IL-1α, TNF-α and IL-17 which in turn leads to the activation of different mediators (like NF-kB, MAPKs and COX-2) and the secretion of proinflammatory signals (such as IL-6, IL-8 and MCP-1), MMPs and distinct types of collagens (44, 99-102). On the other hand, butyrate and propionate – very well known short-chain fatty acids (SCFA) – attenuate the secretion of matrix metalloproteinases 1 and 3 induced by TNF-α and IL-1β in these cells (103). Therefore, the aforementioned studies established that cytokine detection and antigen recognition along with the signaling pathways they trigger are viable mechanisms in intestinal fibroblasts/myofibroblasts.

In addition to bacterial responses, iMCs subsets are involved in the immune response to parasites. Concretely, SMCs express IL-4Rα, which is fundamental to fight helminth infection in mice, and its related signalling has been related to a Th2 coordinate response and increased intestinal contractility (104, 105).

8.2. iMCs and adaptive immune response

To date, interactions between iMCs and adaptive immune response have been little studied. The main findings are summarized below.

iMCs can influence immune cells via the production of soluble mediators or through direct cell to cell contact. It has been suggested that iMCs can interfere in T cell activity through different mechanisms. Concretely, non-diseased human iMCs can interfere in $CD4^+$ T cell activity via programmed death-ligand 1 (PD-L1) and PD-L2 expression, immune checkpoints that act binding to PD1 in T lymphocyte surface and inhibiting T cell activation (106). Also, it has been shown that after IL-2 priming they can support $CD25^+$ $FoxP3^+$ Treg expansion in a MHCII and PGE_2 dependent process (107). Additionally, it has been reported that human mesenchymal cells can have an impact in lamina propria lymphocyte's survival and proliferation in a process mediated by the α4β1 integrin (108).Some other studies have reported the ability of iMCs to present

antigens and trigger T-cell cloning in vitro. This is due to human iMCs appearing to express HLA-DR in steady state (109). On the other hand, it is still not clear whether mesenchymal cells from the intestine can induce proliferation of a concrete effector T cell population. Nevertheless, it has been described that after a proinflammatory challenge, iMCs can express IL-23p19 (110) and therefore, they could theoretically promote Th17 differentiation.

As mentioned above, iMCs can influence immune cells not only by direct contact but also via the production of soluble molecules. Mediators such as PGE_2, IL-10 and TGFβ1–3 are released after activation of some iMCs such as fibroblast, myofibroblasts and other peripheral stromal cells (111-114). Although there is still lacking evidence of their immunosuppressive activity in the intestinal stroma, we already know that these factors are implicated in the inhibitory activity that MSCs and other stroma cells exert over B and NK cells, macrophages, dendritic cells and $CD4^+$ and $CD8^+$ T lymphocytes (113-116).

Studies covering interactions between iMCs and other cells of the trained immunity such as B cells are limited. In 2011, Fritz J et al. reported that factors secreted by iMCs, together with microbial mediators, participate in the production of a multifunctional IgA-secreting plasma cell population, capable of inducing the production of iNOS and TNF-α (117). Also, it has been found that LTβR signaling into iMCs is fundamental for the production of mucosal IgA (that plays a key role in viral and microbial invasion) (118). Moreover, iMCs are able to induce IgM to IgA class switching in vitro (119), which evidences the role of stromal cells in supporting IgA production. However, further research should be performed to clarify the contribution of these interactions in intestinal immunobiology.

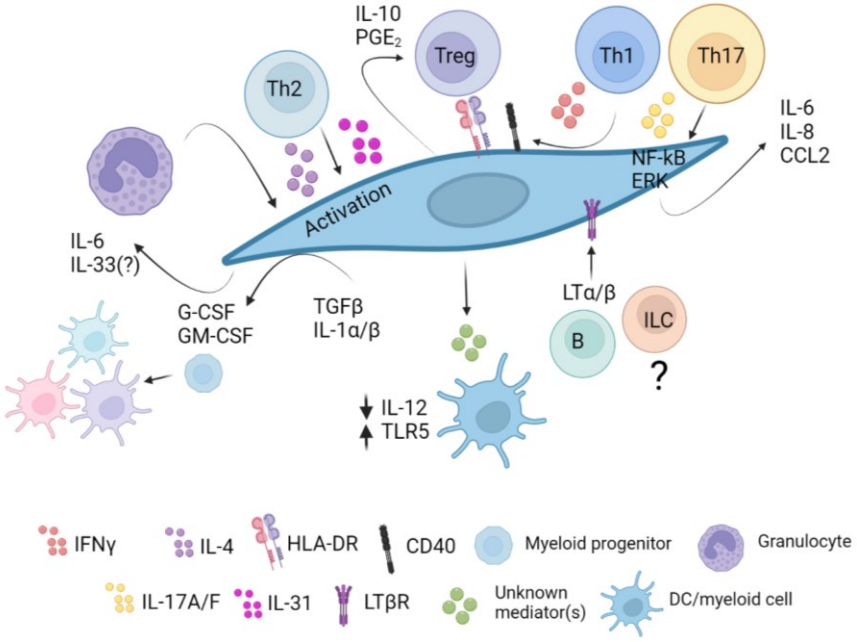

Figure 6. Intestinal mesenchymal cells communicate with multiple immune cell types. *Intestinal mesenchymal cells interact through various means with immune cell populations such*

as Th lymphocytes, Tregs, B cells and granulocytes. Intestinal mesenchymal cells communicate with numerous cells mainly through the release of cell-derived cytokines in the two directions. TGF - transforming growth factor, PGE_2 - prostaglandin E_2, LT – lymphotoxin, gp38 – podoplanin, GM-CSF - granulocyte macrophages colony-stimulating factor, G-CSF - granulocyte colony-stimulating factor, DC - dendritic cell, CCL - C-C motif chemokine ligand . Figure created with BioRender.com adapted from (93).

9. INFLAMMATORY BOWEL DISEASE

Inflammatory bowel disease (IBD) is a chronic idiopathic disease mainly represented by two major forms, ulcerative colitis (UC) and Crohn's disease (CD). Although its etiology still remains undefined, IBD is a multifactorial disease and is thought to stem from a combination of environmental factors, genetic predisposition, microbiota imbalance and mucosa immune defects (120). Patients suffering from these conditions present overlapping signs and symptoms like diarrhoea, rectal bleeding and/or mucus in the stools, fatigue, fever, weight loss, abdominal pain or fatigue, and so their quality of life is tragically impaired (121). Despite the latter, there are some important differences between these two conditions that help in the clinical diagnosis. In CD, any part of the gastrointestinal tract (GIT) can be affected and the intestinal inflammation is transmural (any layer of the intestinal tissue can be compromised), segmental and, very frequently, granulomatous. Also, unlike UC, CD is very frequently associated with fistulas, abscesses and strictures. In UC, however, inflammation is limited to the colon and superficial - only mucosa and submucosa can be affected (is non-transmural), where crypt abscesses and cryptitis are very common (122). The main differences among UC and CD are collected in Table 2.

	Crohn's disease	**Ulcerative colitis**
Affected area	Can appear in any part alongside the GIT, from mouth to anus	Restricted to the colon
Type of inflammation	Discontinuous patchy inflammation	Continuous inflammation
Extent of inflammation	Can affect any layer of the gut wall	Only mucosa and submucosa can be affected
Physiological appearance	Thickened colonic wall and luminal surface can exhibit a cobblestone appearance	Thinned colon wall and ulcerative luminal surface
Rectal bleeding	Hardly ever observed	Very common

***Table 2**. Summary of the main differences between crohn's disease and ulcerative colitis*

9.1. Etiology

As said before, although a big effort has been carried out by the scientific community to elucidate IBD etiology, it remains unclear. Currently, it is widely assumed that the disease appears in genetically predisposed patients as the result of complex interplay between environmental, microbial and immunological factors (123). In fact, it is generally assumed that any individual factor does not have the ability to induce and maintain inflammation *per se*, leading to the idea that the interaction between these distinct components is responsible for the disease clinical onset (124).

9.2. Environmental risk factors

Multiple environmental factors have been associated with IBD, such as westernized diet, geographical location, cigarette smoking, drugs (like antibiotics or oral contraceptives) and social circumstances. These factors might either protect against the development of IBD or contribute to its onset. Also, they can have an impact in the course of the disease and, since there are some differences in the pathogenesis of UC and CD, the same factor can influence in a different manner. Although some factors – like smoking - have been found to be highly correlated, there is still conflicting evidence when it comes to others (125). Another important aspect is hygiene. In this regard, the “hygiene theory” hypothesizes that a low bacterial exposure during childhood can contribute to a less competent immune system, increasing the risk of developing IBD (126).

9.3. Genetic predisposition

Genome-wide association studies (GWAS) have identified 99 non-overlapping genetic susceptibility loci, among them, 28 are shared between CD and UC, which indicates common altered pathways (127, 128). A deep analysis of the results showed that these genes are involved in a myriad of pathways that are fundamental for intestinal equilibrium like gut barrier function (*HNF4A, CDH1, MUC19*), epithelial restitution (*REL, PTGER4, NKX2-3*), microbial defence (*NOD2, CARD9, REL*), innate immune regulation, immune tolerance (*IL10*, *CREM*) production of ROS (*CARD9, UTS2, PEX13*), autophagy (*CUL2*), regulation of adaptive immunity (*IL23R, JAK2, TYK2, TNFSF15*), endoplasmic reticulum stress (*ORMDL3*) and metabolic pathways associated with cellular homeostasis (122).

Multidisease comparative analysis can bring to light shared disease-causing genetic factors and pathways. Concretely, it has been reported that more than half of the loci correlated with an increased IBD susceptibility have also been linked with other autoimmune and inflammatory diseases. Nevertheless, they can have different roles. These overlapping genes can have dissimilar effects depending on the condition, so it is vital to understand their function. For instance, the R620W polymorphism of the *PTPN22* gene is associated with an increased risk for rheumatoid arthritis and type 1 diabetes, however, it diminishes the possibility of suffering from CD(129). On the other hand, shared risk genes between conditions can give a clue on a disease's evolution. For example, genes such as *REL*, *CARD9*, *IL2* and *MST1*, are common in UC and

primary sclerosing cholangitis (PSC), a well-known associated complication (130). Then, this could help us to classify UC patients who are at PSC risk. Moreover, loci that predispose to CD - like *LRRK2 C13orf31* and *NOD2* - unexpectedly overlap with susceptibility regions for *Mycobacterium leprae* infection (131). Additionally, other CD-associated genes are involved in the reaction against mycobacteria - such as *IRGM, ITLN1*, *LTA* and C*ARD9* (127). Therefore, studies covering host responses against mycobacteria or related antigens may be helpful in Crohn's disease as well.

GWAS analysis explain approximately the 20% of the heritability in IBD (127, 128), the rest, might be explained by non-genetic, epigenetic (and environmental) and other genetic factors such as structural and rare variants, and interactions between genes and individual mutations, that are not covered by GWAS. Nevertheless, the success of GWAS resides in their capacity to point out fundamental pathways that have brought light into the IBD pathobiology.

9.4. Microbiota

The gut microbiota constitutes the largest source of bacteria of our body, consisting of approximately 10^{12} cells that belong to more than 1000 species of bacteria and other microorganisms, including archaea, viruses, phages, yeast, fungi and protozoa (132). It is an important modulator of human health and homeostasis through its role in food digestion, energy harvest, immune development, and epithelial homeostasis. The microbiota is shaped early after birth, in part through intricate interactions with the host immune system and colonocyte metabolism (133). During the very first stage of life, microbiota is characterized by the presence of facultative anaerobes, such as *Enterobacteriaceae* and *Staphylococcus.* Right before and after the weaning period, the infant's microbiota is dominated by *Bifidobacterium* and some lactic acid bacteria. With the consumption of solid food, microbiota is colonized with new microorganisms and changes to a more adult-like profile, mainly represented by bacteria from the genera *Clostridium*, *Veillonella*, *Prevotella*, *Ruminococcus*, and *Bacteroides*. During the first 3-5 years of age, the microbiota keeps developing and becomes more and more diversified until it is finally shaped into its adult profile – mainly composed of *Firmicutes* and *Bacteroidetes phyla* (134). Thereafter, its composition remains almost invariable (135). However, life-style-related diseases such as diabetes and obesity, the use of antibiotics, food additives and certain infections, can result in intestinal dysbiosis (136). Dysbiosis causes disease by promoting inflammation, modulating cellular signaling, changing the immune responses, increasing the production of exotoxins that interact with the mucosa, and promoting the formation of carcinogens from dietary elements and xenobiotics. An altered interaction between the gut microbiota and mucosal immune system has been linked to different inflammatory and malignant gastrointestinal diseases, including IBD, irritable bowel syndrome (IBS) and colorectal cancer (CRC) (137-140). Due to its importance in the maintenance of intestinal homeostasis and the involvement of dysbiosis in IBD disease, the intestinal microbiota has lately become a therapeutic target.

The implication of commensal bacteria on IBD is also reflected in *in vivo* models of spontaneous colitis, in which the absence of microbiota (germ free mice) impairs the development of the disease (141, 142). In turn, when bacteria or their purified parts are reintroduced in the gut, spontaneous colitis occurs and the disease persists (143, 144). Additionally, the use of broad-spectrum antibiotics in patients with active UC, promptly reduces intestinal inflammation, indicating how luminal bacteria signaling can drive to mucosal injury (145). Moreover, mechanisms of commensal tolerance in IBD patients are highly dysregulated. This is reflected mainly by two facts. First, T lymphocytes from the mucosa display hyperreactivity against common antigens in the intestinal bacterial milieu (146) and second, they show a dramatic increase in mucosal IgG antibodies against commensal bacteria (under physiological conditions, IgA is the main immunoglobulin in the intestine) (147).

Gut dysbiosis in IBD is characterized by a marked reduction in diversity of bacteria species in comparison with healthy individuals. This alteration is mainly associated with a decrease of bacterial diversity within *Bacteroidetes* and *Firmicutes* phyla - and therefore, *Firmicutes/Bacteroidetes* ratio - as well as in bacteria that potentially protect the intestinal function belonging to the genus *Bacteroides, Eubacterium*, *Bifidobacterium* and *Lactobacillus*, together with the overgrowth of *Escherichia coli* or *Streptococcus faecalis* (148-152). Nevertheless, not all bacteria play the same role since it has been proven that specific microbial species belonging to the genera like *Lactobacillus, Bifidobacterium* and *Faecalibacterium* could actually protect the mucosa through the induction of immune pathways that avoid inflammatory responses (153). In fact, several pre- and clinical studies have shown the beneficial effect of probiotics in IBD and CRC (154-157). However, a deeper understanding of their mechanisms of action is necessary to implement their broad use in the clinic.

9.5. Epithelial barrier, the physical line of defence: mucus, antimicrobial peptides and cell monolayer

The first physical barrier found by food allergens and bacteria is the mucus layer, composed of different gel-forming mucins (being MUC2 the most important one) secreted by goblet cells. These mucins form a dense and firm layer that usually is more porous in its outer part. Mucins are fundamental in bacterial defence. This was highlighted in two different studies in which transgenic *MUC2*-/- mice developed colitis as a consequence of direct contact between bacteria and epithelial cells (158, 159). Besides, within the mucin- matrix we can find peptides with antimicrobial activity (AMPs) – the α- and β-defensins. The first are secreted by Paneth cells while the others are produced via epithelial cells and they act by controlling the composition of the intestinal microbiota. Although some of them are produced constitutively, others are released after bacterial sensing by pattern recognition receptors (PRRs) (160). In fact, defects in Paneth cell function and in the secretion of defensins are observed in CD patients. Concretely, they present a defective expression of HBD2, HBD3 and HBD4 β-defensins when compared to UC patients (161). Right under this intricate matrix, we encounter a monolayer of intestinal epithelial barrier,

that constitutes the second physical layer of defence. This barrier is mainly composed of enterocytes and to a lesser extent, goblet and Paneth cells (the latter ones are only present in the small intestine). Enterocytes are implicated in microbial sensing, and control of immune cell activation through the release of soluble factors. The barrier integrity is sustained by adherens and tight junctions and desmosomes that form the intercellular apical junction complex. Patients with both CD and UC suffer from increased intestinal permeability due to a defective epithelial barrier. Nevertheless, whether this is the cause or consequence of continuous inflammation is still uncertain. Other defects associated with the development of IBD are related with microbial sensing through PRRs. As described before, mutations in the NRL family member NOD2 have been correlated with ileal CD and, until today, is the gene with the strongest association to IBD (162-164).

10. IBD IMMUNE RESPONSES

10.1 Innate immunity

Innate immunity represents our first line of defence against pathogens and is characterized to be fast and non-specific. In addition to epithelial and stromal cells, innate immune cells sense gut microbiota and pathogens, initiating the inflammatory response.

Intestinal $m\varphi_s$ - together with dendritic cells - act as effector cells of the innate response, playing an important role in discerning between potential pathogens from innocuous antigens. Thus, they are able either to initiate a response towards pathogens or ensure local tolerance, being fundamental gatekeepers of gut homeostasis (165).

Their privileged position close to the epithelial barrier in conjunction with their phagocytic activity makes them the perfect cell type to capture and remove any material that has surpassed the epithelial monolayer. They also promote the maintenance of the epithelial barrier integrity, promoting survival and proliferation of epithelial cell precursors via the release of PGE_2, BMP2 and Wnt ligands (165, 166). They are also implicated in tissue remodeling (167) and exhausted epithelial cells engulfment (168). Interestingly, intestinal resident macrophages have the ability to remain unstimulated after TLR signalling or bacterial ingestion (169, 170), preventing an inflammatory response to commensal bacteria (165). They also promote oral tolerance mainly via the secretion of IL-10, which induces the proliferation of Tregs (171).

On the basis of the Ly6C surface marker expression there exists two distinct monocytic subpopulations (172). The $Ly6C^{hi}$ is the largest subset and has been typically designated “classical” monocytes. They are characterized by the expression of high levels of CD62L and CCR2, but low levels of the CX3C chemokine receptor 1 (CX3CR1). They are recruited in a CCR2 dependent manner - CCR2 or CCL2 deficient mice have no circulating monocytes. The $Ly6C^{lo}$ subset is known as the “non-classical” monocytes and they are $CX3CR1^{+}$ and express lower

levels of CD62L and CCR2 (165). They are involved in vasculature maintenance as well as neutrophil recruitment and endothelial cell efferocytosis (173, 174).

Unlike other tissues, the intestinal macrophages pool needs regular replenishment from blood Ly6C^{hi} monocytes (169). After entering the mucosa, circulating monocytes suffer a transformation process to become functional mature macrophages. This takes place through a series of transient CX3CR1^{int} intermediaries that start to express MHCII before losing Ly6C expression. This is followed by upregulation of CD64, F4/80 and CX3CR1 expression, finally acquiring a typical CD11c^{+}, MHCII^{+}, F4/80^{hi}, CD64^{+}, CX3CR1^{hi} phenotype. At the same time this monocyte-macrophage differentiation waterfall takes place, macrophages acquire their typical functions - increased phagocytic activity, unresponsiveness to TLR ligation and IL10 increased production (168, 169, 175).

During intestinal inflammation, there is a drastic shift in macrophage tissue composition that results in the arrest of the monocyte-macrophage differentiation continuum and leads to an accumulation of CX3CR1^{int} MHCII^{-} macrophages. This has been described in different models of colitis, including the DSS-induced and adoptive transfer colitis. These macrophages, unlike tissue resident ones, can respond to TLR stimulation and produce high amounts of proinflammatory cytokines such as TNF-α, IL-6, IL-12, IL-23 and iNOS. Conversely, the quantity of CX3CR1^{hi} resident macrophages changes very little, and in spite of the inflammatory environment, they remain anti-inflammatory (168, 169, 175, 176).

10.2. Adaptive immunity

In contrast to the innate immune system, adaptive immunity is highly specific and it provides long lasting immunity to the host. Usually, distinct components of the adaptive immune response collaborate with the cells of the innate response, resulting in a highly effective pathogen removal. The principal players of this specialized response are T cells, that after activation can differentiate into the different subtypes of T helper cells (Th1, Th2, or Th17). While Th1 cells are necessary for combating intracellular pathogen, Th2 cells mediate allergic and anti-parasite response, while Th17 cells mediate responses against extracellular bacteria and fungi invasion (177, 178). A dysregulation of the T cell response leads to an excessive release of cytokines and chemokines that have multiple pathogenic effects, contributing to the onset of inflammation. In fact, multiple studies have established an association between CD and UC and different levels of T lymphocyte-derived cytokines (179).

10.2.1. Th1, Th2 and Th17 cells in IBD

Th1 cells, traditionally induced by IL-12, are characterized by the production of great amounts of INF-γ, while Th2 typical cytokines are IL-4, IL-5 and IL-13 (177). In CD, the typical T cell cytokine profile in the mucosa is defined by elevated levels of IFN-γ and IL-2. This together with the fact that CD is characterized by higher levels of macrophage-derived IL-12 (when compared to UC), suggest that CD is caused by an aberrant Th1 response, (180, 181). Th1-derived IFN-γ favours

enterocytes apoptosis and the production of TNF-α by intestinal macrophages. This promotes the transition of fibroblasts to myofibroblast that start to secrete MMPs capable of digesting the basal membrane of the enterocytes (182). Then, TNF-α connects innate and adaptive immune responses, playing a crucial role in IBD pathogenesis, as evidenced by the important results obtained with anti-TNF-α therapy (183).

In the case of UC, we find high amounts of the Th2 cytokines IL-5 and IL-13, this last one released by atypical NK T cells (184-186). Some studies have reported an anti-inflammatory effect of IL-13 in the intestine (187, 188), while others have described that IL-13 can increase intestinal permeability and induce enterocyte differentiation and apoptosis (189, 190). A study carried out by Bernardo *et. al* showed the absence of this cytokine in supernatants from UC biopsies cultured *ex vivo* - that were enriched in IL-6 though (191). Therefore, the importance of the Th2 response in IBD onset is still unclear.

Th17 differentiation is induced by a combination of TGF-β and IL-6, and their expansion is promoted by IL-23, a cytokine that has an essential role in initiating an early response against bacteria and mediates the crosstalk between innate and adaptive immunity. They are characterized by the production of large amounts of IL-17A, IL-17F, IL-21 and IL-22 (192). IL-17A has been found to be overexpressed in the lamina propria of IBD patients, as well as in the supernatants of ex vivo cultured mucosa (193). Moreover, IL-21 secreted by Th17 cells is an IL-2 related cytokine highly expressed in the mucosa of IBD patients (194, 195), and it acts inducing Th1/Th17 responses.

10.2.2. Regulatory T cells (Tregs)

T regs are capable of suppressing T_H0 proliferation in vitro and in vivo and they typically express the transcription factor Foxp3 (196). They are highly involved in gut homeostasis, since they prevent the development of an altered immune response against food antigens and commensal microbiota. Concretely, they are in charge of avoiding the activation and action of T effector cells via the secretion of anti-inflammatory cytokines such as TGF-β and IL-10 (197). Tregs are increased in the mucosa of IBD patients and their functions are not impaired (as described in *in vitro* experiments). Nevertheless, it has been reported that effector T cells in the mucosa of IBD patients do not respond to the action of Tregs (198). Thus, a diminished anti-inflammatory Treg activity could contribute, as much as an enhanced T cell effector function, to IBD pathogenesis.

11. iMCs IN INTESTINAL INFLAMMATION

The advantageous contributions of iMCs to the epithelial barrier formation and homeostasis maintenance are clear. Nevertheless, when improperly activated or regulated, iMCs can contribute to pathological mechanisms, which usually occurs during inflammatory immune diseases, such as IBD. Recently, studies using high throughput technologies such as single cell RNAseq or mass cytometry time of flight (CyTOF) have described the different stromal cell

subsets in the colon of healthy and IBD patients (199-201). Kinchen et al. reported the presence of 12 different cell clusters of non-immune, non-epithelial origin in the colon of colitic patients (199). Of these 12 clusters, five were identified as distinct mesenchymal cell types. Among these, four of them were defined as fibroblast-like cells (stromal 1-4 subsets, hereafter S1-4) and the fifth one as myofibroblast (based on the expression of genes with contractile function). S1 was distinguished by the production of elastic fibers and non-fibrillar collagens, while S2 showed marked expression of sheet collagens (like *COL4A5, COL4A6*, which are fundamental for the epithelial base membrane) and S3 was enriched in extracellular and supramolecular fiber organization. With regards to the cells in the S4 cluster, while they were rare in the intestines of healthy participants, this population was highly expanded in patients with UC, constituting the main stromal population in the inflamed intestine. This subset presented a upregulation of podoplanin (PDPN, also known as gp38), IL-33, CCL19, *CXCL5*, *MMP3*, *IL1B* and *IL6* as well as molecules associated with the development, organization and function of tertiary lymphoid structures. It has been proposed that this pro-inflammatory cluster could be, in part, responsible for the epithelial barrier damage by inhibiting the proliferation of the epithelial stem cell niche (199, 202). It is worth noting that the chemokine profile exhibited by iMCs mainly recruits cells from the myeloid lineage, which highlights the possibility that, after an inflammatory insult, stromal cells could be pre-primed to speed up the action of myeloid cells.

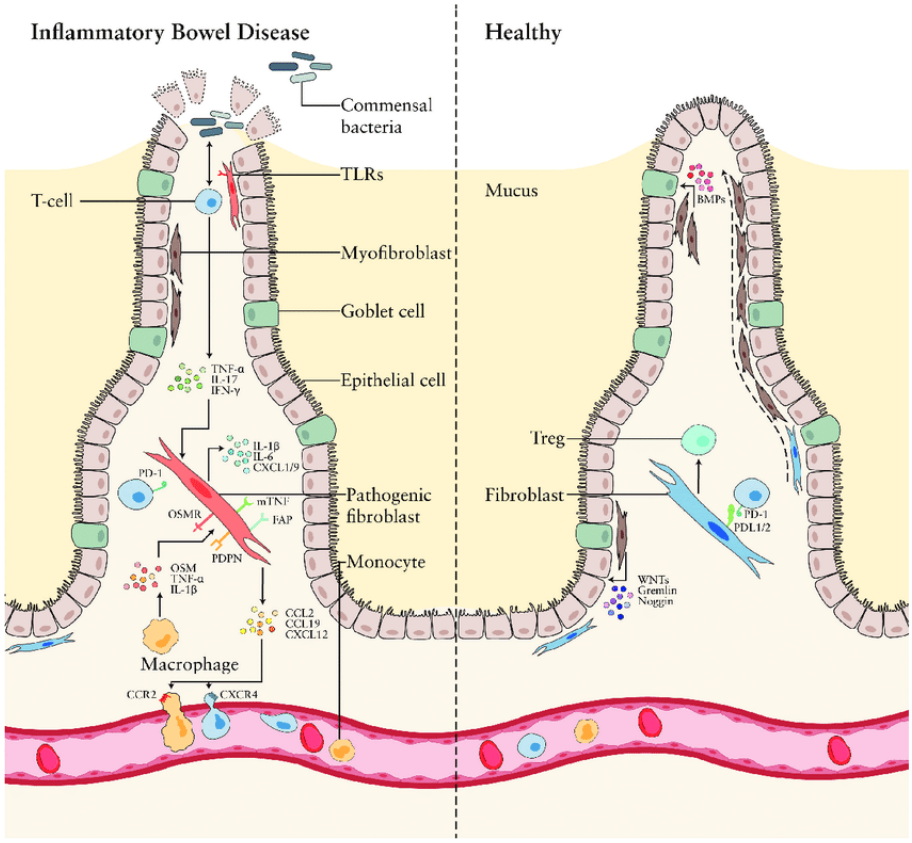

Figure 7. Mesenchymal cells in the intestine of IBD patients versus healthy people. In *IBD a decreased migratory capacity of fibroblasts and fewer mesenchymal cells are found (shown in*

green). Mesenchymal cells possess the ability to respond to the invading microbiota either in a direct or indirect way. Pathogenic iMCs (shown in light red) secrete a myriad of mediators and participate in the recruitment of leukocytes to the site of inflammation. PDPN - podoplanin, OSMR - oncostatin M receptor, FAP- fibroblast activation protein, IFN-γ - interferon gamma, CXCL - CXC motif chemokine, TNFSF-14 - tumor necrosis factor superfamily 14, mTNF - membrane-bound tumor necrosis factor, CCL - chemokine ligand, BMP - bone morphogenetic protein. Figure extracted from (203).

Additionally, Smillie et al. found eight fibroblast-like clusters in healthy and UC colonic samples, one of them highly expanded during disease (200). This last one was designated as IAF (inflammation-associated fibroblasts) and was characterized by expression of *IL-13RA2, FAP*, and *IL-11*. The other cluster mainly differed in the expression of Wnt and BMP genes, which suggest their variable position alongside the crypt-villus axis. On the other hand, Martin et al. focused on the study of paired healthy and compromised resections from the ileum of CD patients (201). They identified different stromal clusters composed of fibroblasts, SMCs, pericytes and endothelial cells. The two fibroblast subsets differed in their expression of platelet-derived growth factor receptors (*PDGFRA* and *PDGFRB*) and prostaglandin. Interestingly, activated fibroblasts strongly expressed CD90, PDPN and some other mediators such as *IL-6, IL-11, CXCL1, CXCL2, CXCL5* and *CXCL8* (201).

iMCs are important not only in the pathology of inflammation but also in colorectal cancer, where they can both support and suppress tumor-growth, promote angiogenesis and might even regulate metastasis ((46, 204, 205) which will be discussed more in detail below.

12. INFLAMMATION-ASSOCIATED COLORECTAL CANCER

Colorectal cancer (CRC) is currently the third most common malignant neoplasm worldwide and the second leading cause of cancer-related deaths, causing approximately 900,000 deaths/year (https://tinyurl.com/rt8jefhc accessed 02/10/2021). Although CRC-related mortality is declining due to the improvement of surgical techniques, patient care and more effective therapies, the global burden of CRC is predicted to rise to 2.2 million new cases and 1.1 million deaths/year by 2030 (206, 207). Colitis-associated cancer (CAC) is the CRC subtype linked to IBD and it represents around 2% of all diagnosed CRC cases. It usually has poor prognosis since is difficult to treat and presents high mortality rates (208).

The concept of inflammation driven cancer goes back to 1863, when Rudolph Virchow observed the presence of a considerable number of immune cells in the tumor microenvironment (209). The first evidence of colorectal cancer in IBD patients occurred in the mid-1920s, when Crohn and Rosenberg described the case of a patient with long-term UC that suffered from colonic adenocarcinoma. Epidemiologic studies in the 60s initially ascribed the higher risk to develop CRC mostly to UC and not to CD in IBD patients. In fact, it was proposed that UC patients had

up to a 10 times greater CRC risk when compared to the general population (210). In contrast, studies could not encounter higher incidence rates in the case of CD (211). Nevertheless, later studies have claimed that the risk for CRC in CD depends on how compromised the large intestine is. Different meta-analysis studies have shown that CRC risk increases with disease severity, extent and duration, reaching up to an 8.3% in CD and 18% in UC, 30 years after the onset of the disease (212, 213). However, real incidence rates could be lower since the last studies were carried out at academic centers, which usually treat more severe stages of the disease (214).

12.1. Genetic mutations lead the initiation of CAC

Nowadays it is well known that chronic inflammation can promote carcinogenesis, exemplified by the connection between bronchitis and IBD with lung cancer and CRC, respectively (215, 216). In CAC, the inflammatory state that drives the disease development is a result of two main processes: (i) the persistent release of inflammatory cytokines in the intestinal tissue, which results in a continuous activation of the NFkB pathway, and (ii) bacterial translocation from the gut lumen. The inflammatory milieu along with the presence of proinflammatory cytokines, promote the generation of reactive nitrogen intermediates (RNI) and ROS, leading to epigenetic changes that result in cumulative mutations in tumor suppressor genes and oncogenes - such as *p53.* Indeed, alterations in p53 are considered to be a key early event during the onset of colitis-associated tumorigenesis. It has been described that p53 mutations take place in approximately 47-85% of colitis-associated cancers (217). Additionally, it has been reported that intestinal genomic alterations can be driven due to inactivation of mismatch repair enzymes or genomic instability. All this together, results in the activation of proliferative and pro-survival pathways - such as NFkB, Wnt/β-catenin, Akt and STAT3 - and the malignant transformation of cancer stem cells (218, 219).

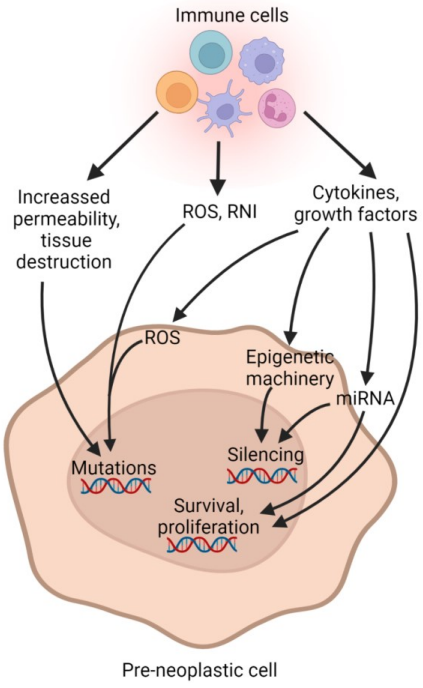

***Figure 8**. **Tumor initiation in colitis-associated cancer.** ROS and RNI released by the inflammatory IBD milieu can alter DNA structure and promote the initiation of the CAC. The production of ROS and RNI can be further increased by cytokines and growth factors released by premalignant cells, resulting in epigenetic modifications and DNA mutations that lead to cell proliferation and survival and thus, the promotion of tumor initiation. Figure created with BioRender.com adapted from (208).*

12.2. Mechanisms of immune signaling that lead to tumor promotion and progression

Once the tumor has been initiated, cell signaling from cancer cells, tissue injury and necrosis results in the release of inflammatory cytokines that play an important role in cancer promotion to a higher grade of dysplasia, as they drive the activation of protumorigenic signaling pathways in cancer cells - such as NF-κB or IL6/STAT3 - that control proliferation, apoptosis, invasiveness or angiogenesis (220-222). Hereafter, we are going to address some of the more important tumor-promoting mechanisms.

12.2.1. The NF-kB pathway and its role in tumor initiation and promotion

Nuclear factor-κB (NF-κB) is a pleiotropic transcription factor that possesses an essential function in coordinating the inflammatory response and it has been proposed to be an important connection between inflammation and tumor formation. The activation of NF-κB signaling is usually due to the presence of microbial antigens and proinflammatory cytokines. Once activated, NFkB promotes the release of so many other proinflammatory molecules - e.g. IL-6 and TNF-a - that have been linked to IBD and CAC development and promotion. At the same time, activation of NFkB can also lead to cell apoptosis inhibition through the release of some protein implicated in cell survival such as Bcl-xL and Bcl-2 (223). NFkB induction can also promote the release of mediators that have a role in tumor invasiveness and metastasis like serine proteases, matrix metalloproteinases and chemokines (224). In colitis-associated cancer, the first hint for the relevant role of the NF-κB pathway was reported by Greten et al. (225). They showed that deletion of the NFkB activator molecule IKK-β in the epithelial compartment results in an impaired Bcl-xL signaling, increased apoptosis and a lower tumor load. In contrast, deletion of IKK-β in the myeloid compartment resulted in a decreased tumor size together with a diminished expression of cytokines such as IL-6, TNF-α or IL-1β in a preclinical model of AOM-DSS. Thus, these data indicate that the activation of NFkB signaling in different cellular compartments participates in tumor initiation as well as in tumor promotion and progression. Additionally, Shaked et al. (2012) reported that mice with chronic epithelial NF-kB activation and germ-line impairment of the tumor-suppressor gene *APC (Adenomatous polyposis coli)* presented a higher tumor development with important DNA damage (223). Also, they found out that mice with a constitutively active IKK-β developed tumors even in the presence of the APC gene (226). Therefore, this data closely correlates with the previous one and, taken together, point out the central role of NF-κB signaling in tumor development.

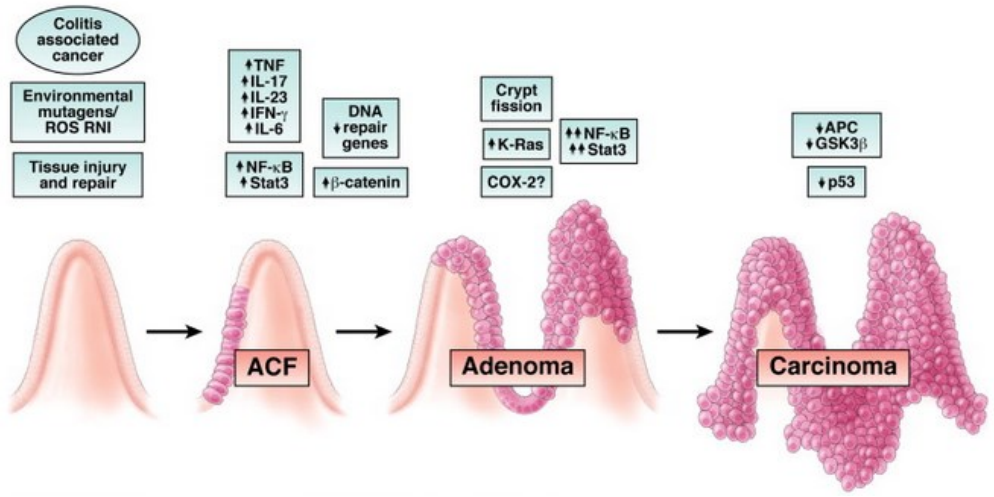

***Figure 9**. **Mechanisms of colitis-associated cancer development.** Chronic inflammation promotes tumor promotion and progression by activating proliferation and inhibiting apoptosis in premalignant cells. Also, the continuous presence of proinflammatory cytokines contribute to genomic instability and mediates the emergence of mutations in important oncogenes and tumor suppressor genes (first in p53, then in K-ras and at late stages in APC). Figure extracted and modified from (208).*

12.2.2. TNF-α signaling

TNF-α has been proposed to be the one of the principal links between IBD and CAC development due to its role in maintaining and supporting chronic inflammation in IBD. Despite its name indicating that it is a mediator involved in tumor necrosis, preclinical research using the AOM/DSS model has shown that TNF-α is actually directly related with the pathogenesis of inflammation-driven cancer. Concretely, it has been reported that the reduction of TNF-α signaling through different strategies - such as administration of anti-TNF-a antibodies or through the impairment/blockade of its receptors - leads to a lower leukocyte infiltration (of neutrophils and macrophages mainly) and ends with a reduced tumor size and number (227). Additionally, some studies have shown that after induction of colitis in mouse models, the expression of TNFR2 (one of the two receptors of TNF-α) is increased (228, 229). This upregulation of TNFR2 in the AOM/DSS model, in turn, leads to the activation of the NF-κB signalling pathway, which promotes tumor initiation and progression (228). To highlight the effects of the other receptor of TNF-α, TNFR1, on tumor development, bone marrow chimera mice were used (227). In this study, Popivanova and colleagues concluded that the effects of TNFR1on tumor growth were mainly due to its expression in hematopoietic cells (227). Therefore, while TNFR2 signaling seems to have an impact in tumor initiation and development through activation of the NF-κB pathway, TNFR1 signalling in immune cells appers to take part in the tumor-promoting role of inflammation (230).

12.2.3. IL-6/STAT3 signaling pathway

Elevated levels of both circulating and mucosal IL-6 are found in IBD patients, and its signalling in mice models of colitis has been attributed to the development of the disease (231). For that reason, together with TNF-α, IL-6 is another of the key cytokines involved in CAC pathogenesis. IL-6 is released by hematopoietic (lymphocytes, monocytes, macrophages), non-hematopoietic (fibroblasts and endothelial cells) and tumorigenic cells (230) upon activation of NFAT or NF-kB. Then, soluble IL-6 can bind to its membrane bound IL-6 receptor (IL-6R) or to its soluble form (sIL-6R), which is released by the TNF-α converting enzyme. Becket and colleagues showed for the first time that epithelial cancer cells present a downregulation of the IL-6R expression and an augmented TNF-α converting enzyme activity, and this is also true for cancer cells from patients with colon cancer (232). For that reason, it was postulated that IL-6 signaling in CAC is mainly mediated through its soluble receptor (233). This process is called "IL-6 trans-signaling" and alows IL-6 to act on cells that do not express the membrane-bound receptor. In the same study, Becker and colleagues specifically blocked this signalling pathway, showing that the tumor-promoting role of IL-6 singaling was mainly attributed to the sIL-6R in an AOM/DSS model (233). Later, other groups found that sIL-6R-mediated activation of STAT3 in tumorigenic cells contributed to their proliferation, suggesting the importance of STAT3 in tumor development (234, 235). Since then, a growing number of studies have highlighted the importance of STAT3 signaling in cancer development and, though individual mechanism that lead to its activation have to be accurately defined, the mounting evidence points out that STAT3 signalling impairment constitutes an interesting therapeutic target in CAC (222, 236, 237).

12.2.4. The Wnt/β-catenin pathway

As we have seen, the canonical Wnt signaling pathway plays a fundamental role in gut homeostasis and intestinal development. In CAC, multiple mutations and alterations in the molecules that are implicated in this signaling pathway are given, driving to a constant activation of the canonical Wnt/β-catenin pathway and favouring uncontrolled stem cell proliferation. In fact, deregulation of the Wnt/β-catenin pathway in IBD and colorectal cancer is well documented (238, 239). In absence of Wnt canonical ligands, cytoplasmic β-catenin remains forming a complex with the proteins Axin, APC, the casein kinase 1 (CK1) and the glycogen synthase kinase 3 (GSK3) and the protein is continuously being ubiquitinated thanks to the phosphorylation of CK1 and GSK3. In the presence of a Wnt ligand, a frizzled receptor is activated upon its binding and the protein complex is disassembled. This allows β-catenin accumulation in the cytoplasm and the translocation to the nucleus, where it forms complexes with TCF/LEF and activates the expression of target genes such as Lgr5, c-myc or cyclin D1 (240). Then, constitutive activation of this pathway leads to excessive stem cell proliferation and fosters cell tumorigenesis. Although the activation of the β-catenin pathway is mainly promoted by APC gene mutations in the early stages of CRC development (241, 242), in CAC, mutations in the APC gene are rarely given at that time (they are more likely to happen in later phases of tumor development). However, nuclear Wnt/β-catenin accumulation is found at early phases of CAC development due to mutations in other

components of the pathway (243) and through the signaling of NFkB and STAT3 (among others) (217).

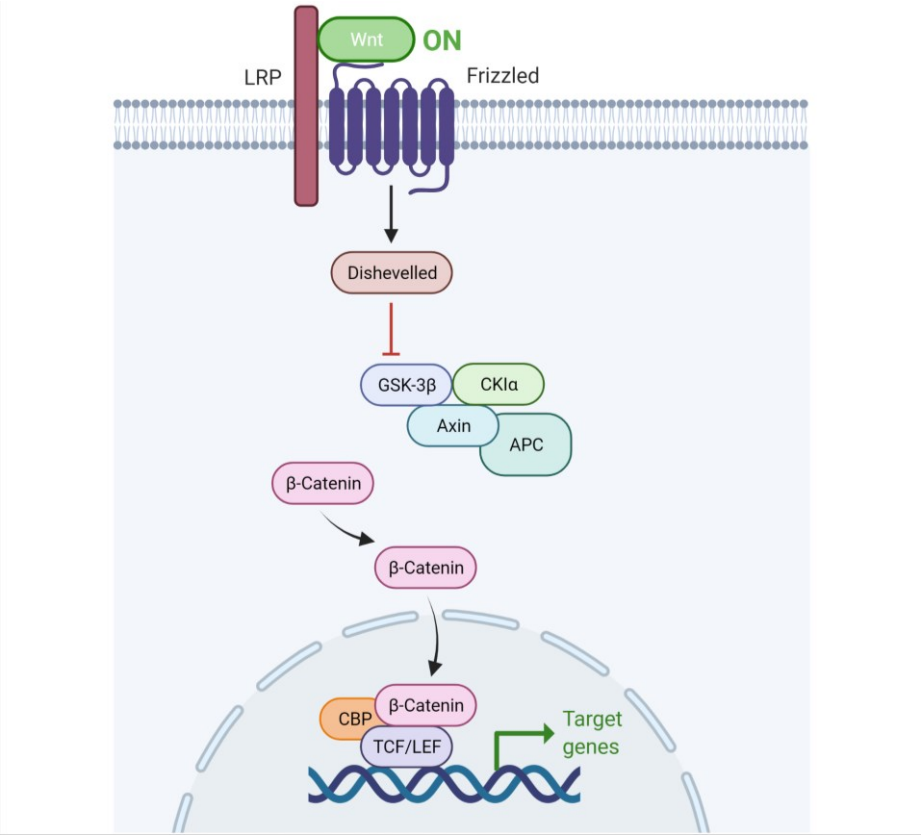

Figure 10. The β-catenin signaling pathway. *Right after wnt binding to a frizzled receptor, the protein complex that β-catenin forms in the cytoplasm with Axin,CK1a, APC and GSK-3 β is dissociated and β-catenin is now able to migrate to the nucleus, where it accumulates and promotes the transcriptions of target genes. Figure adapted from "Wnt Beta-Catenin Signaling Pathway", by BioRender.com (2022). Retrieved from https://app.biorender.com/biorender-templates*

12.2.5. COX-2/PGE_2 pathway

Cytokines such as TNF-α can upregulate COX-2 expression in an NF-κB-dependent way ((244)). The first evidence linking COX-2 to carcinogenesis came from CRC studies in patients (245) and subsequently confirmed in mouse models. Deletion of the COX-2 gene in Apc mutant rodent models resulted in an important decrease in tumor formation (246, 247). Additionally, mice overexpressing COX-2 did not develop colorectal cancer spontaneously but after AOM administration presented a superior tumor load in comparison with the control group (248). The importance of COX-2 signaling in CRC development has been confirmed by population-based studies that show a lower risk of CRC in patients that daily consume non-steroidal anti-inflammatory drugs (NSAIDs) (249). Actually, the beneficial use of NSAIDs has been attributed, in part, through inhibition of PGE_2 release, the production of PGE_2 by COX-2 enhances β-catenin

activity (250, 251). Other COX-2 mechanisms that promote tumor progression are(i) the inhibition of apoptosis via the PI3K-AKT signaling pathway (250) and (ii) the promotion of angiogenesis by the induction of bFGF (basic fibroblast growth factor) and VEGF (vascular endothelial growth factor) release (252) and (iii) by increasing the expression of IL-23 in myeloid cells (253).

12.2.6. Th17 signaling

Other important mediators related to CAC pathogenesis are the cytokines released by Th17 lymphocytes, an important arm of the adaptive immune system during IBD. Although Th17 cells are implicated in the antibacterial response, the release of their associated proinflammatory cytokines such as IL17A, IL17F, IL21 and IL22 has been linked to tumor development (254). Langowski et al provided the first evident that Th17 cells have a role in tumor progression. In a mouse model of cutaneous tumor, they showed that mice lacking IL-23p19 expression - a cytokine that is involved in the differentiation process of Th17 lymphocytes - presented increased resintance to tumor development (255). That study manifests the importance of IL-23 and IL-23 signaling in tumor development and the possible link with Th17 cell signaling. Importantly, Grivennikov et al. reported that IL-23 signaling is principally found in tumoral myeloid cells likely to be activated by commensal bacteria (256) and its expression has been found to be increased in human colorectal tumors, increasing neutrophil and macrophage infiltration (257). In accordance with the later, the treatment with anti-IL17A antibodies or disruption of the *il-17a* gene in mice models of chemically induced/DSS colorectal cancer resulted in a reduced tumor development (258, 259). Equivalent results have been obtained targeting the other members of the Th17 family (65, 66). Because the tumor reduction was associated with a decrease in the levels of proinflammatory cytokines, it was hypothesised that Th17 cells contribute to tumor formation through providing a proinflammatory microenvironment that activates tumor promoting pathways. In fact, IL-22 signaling has been linked with the activation of STAT3 signaling in intestinal epithelial cells in mice and humans (260, 261).

13. ENDOGENOUS IMCS AND COLORECTAL CANCER

Tumours are regarded as chronic injuries which, apart from cancer cells (the parenchyma), contain vascular endothelial cells, cancer-associated fibroblasts (CAFs), immune cells and a complex extracellular matrix (the stroma) (262). The stroma supports and promotes tumor development/metastases, and a high stroma/parenchyma ratio is associated with a poor prognosis in sporadic CRC (263). In CRC, several iMCs subpopulations, including myofibroblasts, fibroblasts, local and bone marrow (BM)-derived MSCs and smooth muscle cells differentiate into CAFs and participate in tumor development (46).

Several animal models have been developed that recapitulate the etiology and pathobiology of human CRC, including the initiation, promotion and progression of the tumors. As has been shown above, the AOM/DSS-model is ideal to analyze the mechanisms/genetics behind the initiation,

promotion, and progression of inflammation-induced CRC, and for the evaluation of genoprotective, and anti-inflammatory treatments (264). The administration of the genotoxic AOM is followed by one or more DSS cycles is a relatively rapid and robust rodent CAC model that mimics several aspects of inflammation-induced CRC tumors in humans, including location, polypoid-like growth, and dysregulation of the Kras and β-catenin/c-Myc pathways, elevated levels of the enzymes COX-2 and iNOS, and dense immune cell infiltration (264-267). In contrast, when tumors are induced by AOM, metastasis is hardly ever seen in wild-type animals (264).

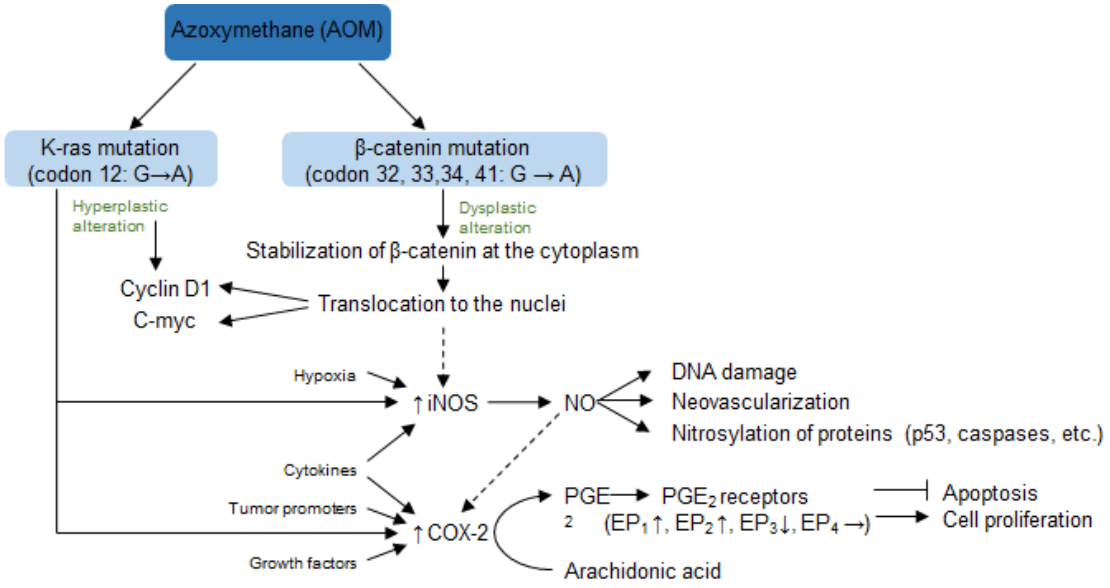

Figure 11. Gene mutations and altered expression of proteins in colon carcinogenesis induced by AOM/DSS*. Figure adapted from (266)*

Several molecules and pathways in iMCs have been implicated in susceptibility to AOM/DSS-induced CAC, including IKKβ which promotes the protumorigenic IL-6/STAT3 axis (268), MAPKAPK2/HSP27 which promotes epithelial proliferation and angiogenesis (269), and MyD88 which enhances CAC by promoting an M2 macrophage polarization (270). In contrast, Hamilton et al., showed that loss of Igf2 mRNA binding protein 1 (IMP1) in iMCs increased tumor numbers and size in the AOM/DSS model (271). However, this was due to the importance of IMP1 in the production of tumor promoting factors, including hepatocyte growth factor. These data suggest that targeting protumorigenic pathways in iMCs could emerge as an effective cancer treatment. Importantly, unlike tumor cells, iMCs within the TME are genetically stable, and thus represent an attractive therapeutic target with reduced risk of resistance and tumor recurrence.

14. Injection of in vitro expanded MSC and Colorectal Cancer

As previously mentioned, both endogenous and in vitro expanded MSCs can migrate to tumors and promote angiogenesis (272), tumor growth (273), and metastases (274, 275). However, MSCs have also been demonstrated to exert antitumorigenic effects in vivo, inducing tumor cell

death (276, 277). At the same time, MSCs have successfully ameliorated IBD severity in clinical trials (278);(33, 279), and have been approved by the FDA, the European Medicines Agency, and recently the Japan Ministry of Health, Labour and Welfare for the local treatment of complex perianal anal fistulas in Crohn´s disease patients. Since IBD patients do have a higher risk of suffering from CAC, it is important to understand the protumorigenic effects of MSCs before administering them to patients. Yet, few studies have analyzed the effects of MSCs on inflammation-induced tumorigenesis.

Using the AOM/DSS model CAC, Nasuno et al., showed that intravenous administration of syngeneic bone marrow (BM)-derived MSCs simultaneously with the AOM injection (before DSS-treatment) significantly reduced the average tumor number in Lewis rats (280). MSC-treated rats showed lower levels of O6-MeG DNA adducts and prevented the dysregulation of the WNT pathway, suggesting an inhibition of tumor initiation. However, delaying the BM-MSCs administration until the first round of DSS colitis did not significantly reduce tumor burden. In contrast, Chen et al., (281) and Tang (282) showed that systemic administration of allogeneic BM-MSCs and human umbilical cord-derived MSCs during the first and second DSS-treatments significantly reduced CAC in C57BL/6 mice, decreasing the levels of proinflammatory cytokines (TNF-α, IL-6 and IL-1β) and inducing Foxp3$^+$ Tregs in the colon, respectively. It is well known that IFN-γ and TNF-α increase the immunomodulatory capacity of MSCs, and their ameliorating effect on colitis (283). Surprisingly, Hu and colleagues recently showed that TNF-α/IFN-γ-prestimulated iMSCs, injected during the DSS-phase, promoted tumor number/size in the AOM/DSS model (284). The low number of studies and contrasting data warrants further studies on the effect of MSCs, from different tissues, on CAC.

15. iMCs AND MICROBIOTA IN IBD AND CAC

Hitherto, numerous studies have investigated the interactions between the microbiome and the immune system. However, little attention has been directed at the intestinal stroma, especially on the interplay between the normal or unbalanced microbiota and iMC subpopulations in health and disease and several interesting areas remain to be explored. Also, whether there is a correlation between the dysbiosis (phyla, genus, species of bacteria) found in IBD and CRC and iMCs function (proinflammatory vs. homeostatic) is not known.

As discussed in section above, iMCs express TLRs and NLRs and respond to bacteria, potentially acting as “non-professional innate immune cells”. However, the majority of studies have analyzed iMC-microbiota interactions in vitro and the effects of normal or dysbiotic microbiota on iMC phenotype and function in vivo has hardly been addressed. In 2014, Beswick et al. found that CD90$^+$ iMCs, via TLR4-induced PD-L1 expression, could promote mucosal immune tolerance (285). In addition, Ciorba et al. found that the probiotic *Lactobacillus rhamnosus* GG (LGG), via TLR2-induced COX-2/PGE2 expression by iMSCs, could protect against radiation-induced intestinal epithelial damage. Later on, in 2018, they discovered the mechanism of action behind

(10.1136/gutjnl-2011-300367). LGG promotes lipoteichoic acid production and binding to TLR2 on pericryptal macrophages, inducing the release of CXCL12 chemokine which in turn binds to CXCR4 receptor on COX-2 expressing iMSCs. This promotes their migration next to the epithelial stem cell niche (286). Considering the ability of the microbiota to reprogram the function of intestinal epithelial cells, it is of particular interest to analyze if the microbiota or their metabolites can “educate” or change the iMC composition in the gut. However, most studies of microbiota imprinting of the immune system have driven their attention on haematopoietic cells. Interestingly Zawair et al., reported that human fetal myofibroblasts possess a more inflammatory phenotype than those isolated from infants, perhaps indicating that acquisition of the microbiota at birth may dampen iMC activity (287). The mechanisms and pathways underlying these effects are largely unknown. However, microbial signals are required for RALDH activity and retinoic acid production in iMCs so this pathway might make a contribution (288). Furthermore, SCFA produced by microbiota diminish MMPs and chemokine production by cytokine stimulated myofibroblast in vitro (103, 289). This suggests that regulation of iMCs by microbial mediators may contribute to preserving a tolerogenic atmosphere in the healthy intestine. Additionally, microbial SCFA together with urolithins have been found to modulate human myofibroblasts prostaglandin synthesis in vitro. Therefore, microbiota could contribute to how iMCs modulate mucus production epithelial function and in vivo (290, 291). Also, there is emerging evidence suggesting that microbiota could influence iMC-mediated pathologies. For example, it is known that overexpression of tumor necrosis factor-like cytokine 1A (TL1A) leads to the induction of intestinal fibrosis. In the absence of resident microbiota, fibroblasts from germ-free mice exhibit impaired collagen production and migration in response to TL1A or bacterial products (292). Thus, microbial priming of iMC may condition their response to concrete stimuli, promoting their switch from a pro-inflammatory state to a more tolerogenic one.

Another area of interest is the understanding how the composition of the microbiota in the gut is shaped by the host at different anatomical locations. Curiously, recent data suggest that certain iMCs in the gut-associated lymphoid tissues regulate bacteria-specific IgA production and the diversity of the gut microbiota (293). In fact, in vitro cultures of BM-MSCs exhibit anti-fungal and bactericidal properties through secretion of antimicrobial peptides like LL-37(294), depletion of extracellular tryptophan (295) and IL-17 production (296). However, whether iMCs, in general or specific subpopulations, play a direct role in shaping the gut microbiota is currently unknown.

In CRC, both in humans and in experimental models, some bacteria are consistently increased (including *Fusobacteria*, *Alistipes*, Porphyromonadaceae, Coriobacteridae, Staphylococcaceae, *Akkermansia* spp. and Methanobacteriales), whereas others are reduced (*Bifidobacterium, Lactobacillus, Ruminococcus, Faecalibacterium* spp., *Roseburia* and *Treponema*) (297). The bacteria most positively associated with tumor presence are Gram-negative, such as *Bacteroides*, *Parabacteroides*, *Alistipes* and *Akkermansia*, whereas Gram-positive *Clostridiales*, including multiple members of *Clostridium* group XIVa, are negatively correlated with tumor development

(298). Dysbiosis may cause disease by promoting inflammation, modulating cellular signaling, changing the immune responses, increasing the production of exotoxins that interact with the mucosa, and promoting the formation of carcinogens from dietary elements and xenobiotics.

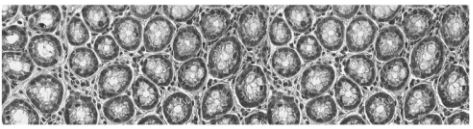

Hypothesis and Aims

HYPOTHESIS

Intestinal mesenchymal cells play important roles in intestinal homeostasis through their interactions with the epithelium, immune system and intestinal microbiota. Due to their ambiguous role in intestinal inflammation during IBD and in the initiation, promotion, and progression of colitis-induced cancer, a further analysis of their capacity to promote epithelial repair and regulate immune/inflammatory responses is of great importance when designing new therapies for intestinal inflammatory diseases and cancer.

AIMS

1. Isolation and characterization of the immunomodulatory, and tissue regenerative properties of iMSCs in vitro.
2. Analysis of the effect of iMSC administration on DSS-induced acute colitis in mice: evaluation of disease severity, immune responses, tissue regeneration and dysbiosis
3. Analysis of the effect of iMSC administration on cancer progression in a model of colitis-associated cancer: evaluation of tumor growth, immune responses, and CAC-induced dysbiosis.

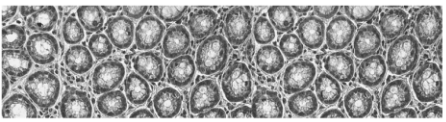

Materials & methods

MATERIALS AND METHODS

1. ISOLATION, CULTURE AND CHARACTERIZATION OF MSCS FROM HUMAN INTESTINAL TISSUE

1.1. Handling and processing of intestinal resections

Intestinal resections were obtained from patients who signed the corresponding informed written consent before undergoing surgery in Hospital Virgen de las Nieves (Granada, Spain). These patients had been previously admitted for bowel resection because of malignant conditions, including colon cancer, benign polyps and diverticulitis. iMSCs were isolated from non-comprised tissue (i.e. tissue that distances a minimum of 5 cm from the affected area).

Freshly isolated intestinal resections were washed thrice with sterile PBS supplemented with 2% penicillin/streptomycin to remove debris, stools, and erythrocytes. The tissue was weighed, cut into 0.5 cm pieces and resuspended in 15 mL of HBSS (4-5 mg tissue/mL) without calcium and magnesium (Lonza, Basel, Switzerland, Cat.#BE10-543F) supplemented with 1mM dithiothreitol (DTT), 5 mM EDTA, 2% penicillin/streptomycin, 2% amphotericin B, 25 µg/mL of gentamycin and 10 mM HEPES. The tissue was incubated for 30 min at 37ºC in a shaking water-bath (~150 rpm) to remove intestinal epithelial cells. Next, the supernatant was discarded and the tissue was washed vigorously 3-4 times in sterile PBS to remove as much EDTA as possible, due to its inhibitory effect on collagenase activity. Tissue pieces were then collected and minced into 2-3 mm fragments, facilitating the following tissue-dissociation step. After that, tissue pieces were resuspended in 15 mL of DMEM Advanced (Gibco, ThermoFisher Scientific, Waltham, MA, USA, Cat.# 12491-023) containing 400 U/mL DNase (Sigma-Aldrich, Spain, Cat.#DN25), 500 U/mL collagenase type IV (Sigma-Aldrich, Spain, Cat.#C5138), 0.09 U/mL dispase II (Roche Applied System, Germany, Cat.#04942078001), 2% penicillin/streptomycin (Lonza, Basel, Switzerland Cat.#DE17-602E), 2% amphotericin B (Sigma-Aldrich, Cat.#A2942), 25 µg/mL of gentamycin, 10 mM HEPES and 0.36 mM $CaCl_2$, and incubated for 60-90 minutes at 37ºC in a shaking water-bath (~150 rpm). The digest was washed thrice with cold PBS containing 2 mM EDTA and filtered through a 70 µm and a 100 µm nylon mesh. Finally, cells were resuspended in complete DMEM Advanced containing 10% fetal bovine serum, 2 mM Ultraglutamine (Lonza, Basel, Switzerland), 2% penicillin/streptomycin, 2% amphotericin B and 25 µg/mL of gentamycin, and cultured at 37ºC and 5% CO_2 (this media was used until passage 1).

After 24 hours, three 1x sterile PBS washes were carried out to remove non-adherent cells and debris. This step was repeated every 2-3 days until obtaining a pure MSC culture with a fibroblast-like morphology. Usually, isolated cells covered 90% of the culture surface after 10 days post isolation.

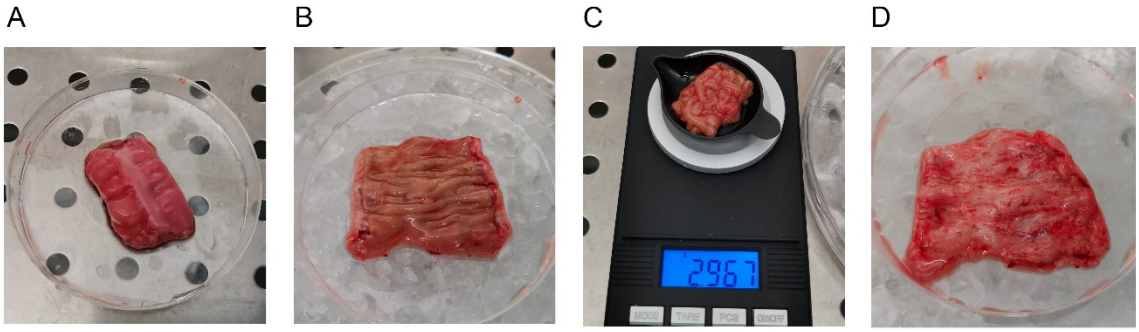

Figure 12.. Mechanical isolation of mucosa from intestinal human resections*. A) Intestinal colonic resection without mesenteric fat. B) Longitudinally opened tissue section with mucosa facing upwards C) Weighed mucosal sections obtained from the later sample and D) intestinal resection after mucosa excision.*

1.2. iMSCs maintenance and culture

Cells were maintained at 37ºC and 5% of CO_2 in a Galaxy R+ incubator (RSBiotech). Cell handling was carried out in a sterile laminar flow cabinet and media exchange was performed every 3-4 days. The media used was complete DMEM Advanced (Gibco, ThermoFisher Scientific, Waltham, MA, USA) supplemented with 10% fetal bovine serum (FBS) previously heated up to 56ºC for 30 minutes and filtered (Gibco, ThermoFisher Scientific, Waltham, MA, USA, Cat.# 10270-106), 2 mM Ultraglutamine (Lonza, Basel, Switzerland), 1% penicillin/streptomycin (Lonza, Basel, Switzerland) and 1% amphotericin B (Sigma).

When cultured cells reached 90% confluence, they were divided (usually in a 1:2-1:3 dilution) or stored in liquid nitrogen in freezing media (95%FBS, 5% DMSO). First, cells were washed with 1x PBS and then detached from the flask surface with TrypLE (ThermoFisher Scientific, Waltham, MA, USA). After 5 min at 37ºC, cells in suspension were neutralized with FBS containing media and pelleted at 300 x g for 5 minutes at room temperature. Then, supernatant was discarded, cell quantification performed and iMSCs resuspended in an appropriate volume. All iMSCs were used at passages 1 to 8.

1.3. Colony forming units-fibroblast (CFU-F) assay

CFU-F assay was carried out as previously described by Pochampally (299). Briefly, cells were detached and filtered through a 70 µm nylon mesh to avoid cell aggregates. Then, cells were pelleted and counted and 1000 iMSCs were plated in 6-well plates in complete DMEM Advanced. Culture medium was replaced every 3-4 days. After 12 days, cells were washed with PBS, fixed at room temperature in pure ethanol (20 minutes) and stained with 1% crystal violet (1 minute). After that, crystal violet was removed and running tap water was used to eliminate remaining crystal violet. Resulting colonies were stained in purple and observed under a stereomicroscope.

1.4. iMSCs differentiation capacity

1.4.1. Adipogenic differentiation and Oil Red O staining

For adipogenic differentiation 4000 cells/cm^2 were seeded into 6-well plates. Cellular differentiation was induced using a specific medium (Table 3). In parallel, cells maintained in complete DMEM Advanced were used as negative differentiation controls. Culture medium was replaced every 3-4 days.

Components	Concentration	Reference	Company
DMEM (1g/L glucose)	-	L0066-500	Biowest
FBS	10% (v/v)	10270-106	Gibco
Penicillin/Streptomycin	1% (v/v)	H3DE17-602E	Lonza
Insulin	1% (v/v)	I0516	Sigma
Indomethacin	0.2 mM	I7378	Sigma
Dexamethasone	0.1 µM	D4902	Sigma
IBMX	0.05 mM	I5879	Sigma

***Table 3**. Culture media composition used in adipogenic differentiation*

After 4 weeks, cellular differentiation was assessed via morphological examination of the cellular accumulation of lipid droplets by Oil red O staining assay. For this purpose, cells were washed with PBS and fixed for 20 minutes with 4% PFA. Subsequently, cells were washed with sterile distilled water and then with 60% isopropanol. Then, cells were incubated with Oil Red O working solution for 5-10 minutes at room temperature. After that, wells were washed with running tap water and imaged using a light microscope.

1.4.2. Osteogenic differentiation and Alizarin Red S staining

For osteogenic differentiation iMSCs at a density of 3.000 cells/cm^2 were plated into 6-well plates. Cellular differentiation was obtained using a specific medium (Table 4). Cells grown in complete DMEM Advanced were used as negative differentiation controls. Culture medium was replaced every 3-4 days.

Components	Concentration	Reference	Company
DMEM (1g/L glucose)	-	L0066-500	Biowest
FBS	10 % (v/v)	10270-106	Gibco
β-glycerophosphate	10 mM	50020	Sigma
Penicillin/Streptomycin	1% (v/v)	H3DE17-602E	Lonza
Dexamethasone	0.1 µM	D4902	Sigma
Ascorbic acid	0.05 mM	49752	Sigma

***Table 4**. Culture media composition used in osteogenic differentiation*

After 4 weeks, the presence of calcific depositions by cells was assessed with Alizarin Red S. For this purpose, cells were washed with PBS, fixed for 20 minutes with 4% PFA and washed again with sterile distilled water. Subsequently, cells were incubated for 20 minutes with 40 mM, Alizarin Red S working solution (pH 4.1-4.3, Cat.# 1.06278, Merck Millipore, Spain), after which they were washed thrice with distilled water and observed under a light microscope.

1.4.3. Chondrogenic differentiation and Alcian blue staining

A celular pellet of $2 \cdot 10^5$ iMSCs was placed in a 15 mL tube with 3 mL of differentiation medium (Table 5). Culture medium was replaced every 3-4 days during 4 weeks.

Components	Concentration	Reference	Company
DMEM (4.5 g/L glucose)	-	BE12-709F	Lonza
Penicillin/Streptomycin	1% (v/v)	H3DE17-602E	Lonza
Dexamethasone	0.1 µM	D4902	Sigma
Ascorbic acid	0.05 mM	49752	Sigma
Insulin-transferrin-selenium	10%	41400-045	Gibco
TGF-β3	10 ng/mL	100-36E	Peprotech

***Table 5**. Culture media composition used in chondrogenic differentiation*

After this period, spheroids were fixed with 4% PFA, dehydrated in serial higher concentrations of ethanol and then, embedded in paraffin. After that, paraffin blocks were stored at 4ºC (to ease sectioning) and then cut into 3 µm sections and placed in microscope slides (Marienfeld superior, Cat.# 810000). Then, sections were deparaffinized, hydrated and stained with alcian blue 8GX (pH 2.5) for 20 minutes, which stains extracellular matrix proteoglycans. Finally, sections were clarified in xylene (Casa Álvarez, Spain) (two incubations of 5 minutes/each) and mounted with DPX mounting media (Casa Álvarez, Spain).

1.5. Immunophenotypic characterization of iMSCs

1.5.1. Flow cytometry

iMSCs at passage number 2-3 and later on at passage number 7-8 were harvested using TrypLE (ThermoFisher Scientific, Waltham, MA, USA), washed with PBS and incubated (20000-30000 cells/staining) with 7-aminoactinomycin D (7-AAD) (Nalgene, Nalgen Nunc International Corporation, Rochester, NY, USA) or fixable live/dead stain Zombie Aqua (Bioegend, San Diego,. CA, USA) on PBS for 15 minutes at 4ºC. Cells were subsequently stained with combinations of the antibodies shown in Table X diluted in FACs buffer (0.1%Bovine Serum Albumin (BSA) and 2mM EDTA.) for 30 minutes at 4ºC. Corresponding isotype antibodies were used to evaluate background staining. Compensation controls were prepared using OneComp eBeads™ (eBioscience, ThermoFisher Scientific, Waltham, MA, USA). Data was acquired using either the BD FACSCanto™ II flow cytometer or BD FACSAria™ IIIu cell sorter (BD Biosciences, San Diego, CA, USA) and analyzed using the Flowjo v10.6.2 software (FlowJo LLC, Ashland, OR, USA).

Marker	Fluorochrome	Reference	Company
CD45	APC	17-9459-42	Invitrogen
CD73	PE	12-0739-42	Invitrogen
CD90	FITC	11-0909-42	Invitrogen
CD105	PE-Cy7	17-1057-42	Invitrogen
CD31	FITC	303103	BD Biosciences
EpCAM	PerCP-Cy5.5	347199	BD Biosciences
CD34	APC	343607	BioLegend
PD-L1(CD274)	PE	557924	BD Biosciences
7-AAD	≈ PerCP-Cy5.5	00-6993-50	Invitrogen
L/D Zombie aqua™	≈ BV510	423101	BioLegend

***Table 6**. Antibody list used for immunophenotypic characterization of iMSCs*

1.5.2. Immunocytochemistry

iMSCs were detached, seeded in a Nunc Lab-Tek Chamber slide™ (Sigma-Aldrich, Cat.#C7182) and maintained at 37ºC, 5% CO_2 until they reached 70-80% of confluence. At this point, they were fixed in 4% paraformaldehyde in PBS (pH 7.4) for 15 minutes at room temperature and washed thrice with 1x PBS. Then, fixed cells were permeabilized and blocked with a 0.1% saponin, 1% BSA solution for 1 hour. Then, vimentin unconjugated primary antibody (Cat.# ab92547 Abcam, Cambridge, UK, dilution 1:200,) was incubated at 4ºC overnight. Excess antibody was eliminated through three gentle washes with 1x PBS. After that, incubation with goat anti-rabbit IgG H&L (Alexa Fluor 488 Cat.# ab150077, dilution 1:1000) secondary antibody was performed for 2 hours. Anti-rabbit IgG isotype control (catalog# 02-6102, Invitrogen, ThermoFisher Scientific, Waltham, MA, USA) was used as negative control. Excess secondary antibody was washed away and nuclei stained with Hoechst 33342 (Invitrogen, ThermoFisher Scientific, Waltham, MA, USA). Finally, the chamber gasket was removed and the resulting slide mounted with ProLong™ glass antifade mountant (Invitrogen, ThermoFisher Scientific, USA) and a 1.5 mm coverslip. Samples were visualized in a Nikon eclipse Ni-U epifluorescence microscope.

2. IN VITRO EXPERIMENTS

2.1. Effect of iMSCs on T cell proliferation

2.1.1. iMSCs cycle arrest with mitomycin C

iMSCs were harvested and viable cells counted with a hemocytometer and 0.5% alcian blue. After that, cells were resuspended (10^5 to 10^6 cells) in 500 µL of sterile PBS containing 50 µg/mL of mitomycin C (Sigma-Aldrich, Spain, Cat.#M4287) in a 15 mL tube. Then, cells were incubated at 37ºC for 20 minutes out of light. By this stage, cells were washed twice with tempered complete DMEM Advanced and supernatant discarded. Cells were counted again and plated at 5,000, 10,000 and 20,000 cells/well in triplicate in flat bottomed 96-well plates. The day after, cells were used to evaluate their effect in T cell proliferation.

In the case of prestimulated iMSCs, after seeding cells were subsequently cultured with 3 ng/mL TNF-α (Peprotech EC Ltd, London, UK) and 10 ng/mL IFN-γ (Peprotech EC Ltd, London, UK) for 24 hours. Unstimulated cells were used as negative control.

2.1.2. PBMCs isolation from peripheral blood and T cell suppression assay

Peripheral blood mononuclear cells (PBMCs) from healthy donors were isolated from 25-30 mL of blood. Blood was diluted 1:4 with PBS and carefully layered above half volume of room temperature Lymphoprep™ (StemCell Technologies, Vancouver, Canada). Then, tubes were centrifuged at 400 x g for 40 minutes at room temperature in a program set up with no acceleration or deceleration. Buffy coats were then collected with a sterile pasteur pipette and washed three times with PBS (300 x g for 15 min).

The resultant cellular pellet was then quickly labelled with 1 µM carboxyfluorescein succinimidyl ester (CFSE) (Sigma-Aldrich, Madrid, Spain) and then incubated at 37ºC for 12 minutes out of light. At this point, the CFSE signal was quenched with 14 mL of prewarmed PBS containing 5% FBS for 20 minutes at 37ºC. After that, cells were counted and 200,000 PBMCs seeded on top of the different concentrations of iMSCs (any in the case of controls). Then, 2.5 µg/mL of the T cell mitogen phytohemagglutinin-L (PHA-L) (eBioscience, ThermoFisher Scientific, Waltham, MA, USA) were added to the iMSC-PBMC cocultures. CFSE labelled PBMCs in the presence or not of PHA-L were used as positive and negative controls, respectively. In some experiments, 1-methyl tryptophan ((1-MT); 1 mM, Sigma-Aldrich, Madrid, Spain) or indomethacin (20 µM, Sigma-Aldrich, Madrid, Spain) were added to the cocultures. In all cases, the final well volume was adjusted to be the same in every different condition.

On day 6, supernatants were collected and PBMCs carefully harvested and stained with anti-CD4-PE (BD Biosciences, Madrid, Spain), anti-CD3-APC (BioLegend, San Diego, CA, USA) and Zombie Aqua™ (BioLegend, San Diego, CA, USA) as viability dye. Labelled cells were acquired on a BD FACSAria™ IIIu cell sorter (BD Biosciences, Madrid, Spain) and the cell division (proliferation index based on CFSE signal intensity) of $CD4^+$ and $CD8^+$ ($CD3^+CD4^-$) T cells was analyzed using the FlowJo v10.6.2 software (FlowJo LLC; Becton, Dickinson and Company, Franklin Lakes, NJ, USA).

2.1.3. Detection of indoleamine 2,3-dioxygenase activity by UHPLC–MS/MS in conditioned PBMC:iMSC supernants

IDO activity was evaluated by quantifying tryptophan and L-kynurenine concentrations in supernatants from the PBMC:iMSC-cultures on day 6 by UHPLC-MS/MS. All chemicals used for quantification were of analytical HPLC-MS grade. Water was obtained by purification with a Milli-Q system from Millipore (Bedford, MA, USA). Formic acid and acetonitrile for mobile phases were purchased from Scharlab (Barcelona, Spain).

UHPLC-MS/MS analysis was performed on a Waters Acquity UPLC™ H-Class from Waters (Manchester, UK). A Xevo TQS tandem quadrupole mass spectrometer (Waters) equipped with an orthogonal Z-spray™ electrospray ionization (ESI) source was used for tryptophan and L-kynurenine detection. Separation of compounds was obtained with a BEH (Ethylene Bridged Hybrid) column C18 50*2.7 mm 1.7 µm particle size (Waters, UK). The compounds were separated using a gradient mobile phase consisting of solvent A (LC–MS grade water plus 0.1% of formic acid) and solvent B (LC–MS grade acetonitrile plus 0.1% formic acid). Thus, the elution program was a multi-step linear gradient at a flow rate of 0.55 mL/minute. Gradient conditions were: 0.0-3.0 minutes 1% phase B; 3.0-5.0 minutes, 10-25% phase B; 5.0-7.0 minutes, 25-90% phase B and back to 1% in 0.1 minutes. Total run time was 11.0 minutes. The injection volume was 10 µL and the column temperature was maintained at 45ºC.

For mass spectrometric analysis, ESI was performed in positive ion mode. The tandem mass spectrometer was operated in the multiple reactions monitoring (MRM) mode. Instrument parameters were as follows: capillary voltage, 2.00 kV; source temperature, 150ºC; desolvation temperature, 600ºC; cone gas flow, 150 L/h; desolvation gas flow, 1000 L/h; collision gas flow, 0.15 mL/minute, and nebulizer gas flow, 7.0 bar. Dwell time was set at 25 ms. Collision energies and cone voltages were optimized for both analytes.

In order to quantify the individual content of the analytes, two calibration curves were prepared using tryptophan and L-kynurenine commercial standards (Sigma-Aldrich, Madrid, Spain). Concentrations were determined by interpolation in the corresponding calibration curve using the peak area. MassLynx 4.1 software was used for instrument control, peak detection and integration.

2.2. Effect of iMSCs and their conditioned media in THP-1 cells

In order to prepare conditioned media for this experiment and the following ones, iMSCs from four unrelated donors were seeded in 24-well plates at a density of 50,000 cells/mL. Once they reached confluence, the medium was replaced with fresh basal medium and incubated for 48 hours at 37ºC and 5% CO_2. The conditioned media (iMSC-CM) were harvested, centrifuged at 500 x g and stored at -20ºC in aliquots until use.

The human monocytic cell line THP-1 was obtained from Centre for Scientific Instrumentation (University of Granada, Granada, Spain), maintained in complete RPMI 1640 (Gibco; Thermofisher Scientific, Waltham, MA, USA) supplemented with 0.05 mM β-mercaptoethanol (Sigma-Aldrich, Madrid, Spain) and incubated at 37ºC in a humidified atmosphere containing 5% CO_2. Cell cultures were maintained at a density ranging from 200000 to 900000 cells/mL. For co-culture experiments, THP-1 cells were first differentiated into adherent macrophages with 50 ng/mL of PMA (Sigma-Aldrich, Madrid, Spain) in 24-well plates (250000 cells/mL). After 48 hours, iMSCs (10,0000 cells) or iMSC-CM were added to the adherent THP-1 macrophages. 48 hours later, cells were stimulated with 1 µg/mL LPS (Sigma-Aldrich, Madrid, Spain) for 24 hours. Then, supernatants were collected for cytokine determination by ELISA.

2.3. Scratch wound healing assay

Normal Colonic Mucosa (NCM)-356 human epithelial cells were kindly provided by Laura Medrano González and Ezra Aksoy (William Harvey Research Institute, Queen Mary University of London, London, UK). Cells were cultured in DMEM Advanced supplemented with 10% heat inactivated FBS, 1% pen/strep 1% amphotericin B (Sigma-Aldrich, Madrid, Spain) and 2mM ultraglutamine (Lonza, Basel, Switzerland). Cells were seeded onto 6-well plates at a density of 150000 cells/mL and grown until confluence. When cultures reached confluence, monolayers were scraped in straight lines. For this purpose, 200 µL pipette tips coupled to a vacuum system were used in order to create scratch wounds of homogenous width. After a wash with prewarmed PBS, cells were cultured in control or conditioned media, both diluted 1:1 with fresh basal medium.

To track the scratch-wound closure, the scratches were observed by an Olympus-CKX41 inverted microscope (Olympus Europa SE & Co. KG, Germany) and equivalent photos were taken at 0, 24 and 48 hours. Finally, the scratched area was measured using the ImageJ software (Free Software Foundation Inc., Boston, MA, USA). These experiments were performed with iMSC-CM from iMSCs of 4 different donors.

2.4. iMSCs stimulation with TNF-α and IFN-γ – time course

To analyze the effect of proinflammatory cytokines on the expression of immunomodulatory mediators by iMSCs, cells isolated from three different donors were cultured with TNF-α (3 ng/ml, Peprotech EC Ltd, London, UK) and IFN-γ (10 ng/mL, Peprotech EC Ltd, UK) for 1, 2, 6 and 24 hours. For negative controls, basal media without any stimuli was used. At the indicated time points, supernatant was aspirated, cells washed with 1x sterile PBS and RNA isolated as indicated in section 3.7.1.

2.5. Preparation of iMSCs for in vivo administration

iMSCs were grown in complete DMEM Advanced in T-75 flasks until 90-100% confluence. At this point, cells were detached with TrypLE (Gibco, invitrogen) for 5 minutes at 37ºC, followed by neutralization using media containing 10% FBS. Cells were quantified using a hemocytometer, centrifuged at 300 xg for 5 minutes at room temperature and resuspended in sterile PBS at a concentration of $2.5x10^5$ or $5x10^5$ cells per 100 µL (depending on the experiment). This preparation was maintained at 4ºC until immediately IP injection with 1 mL insulin syringes and 23G needles.

3. ASSESSMENT OF THE INTESTINAL INFLAMMATORY PROCESS AND TUMOR DEVELOPMENT

All animal studies were carried out in accordance with the “Guide for the Care and Use of Laboratory Animals” as promulgated by the National Institute of Health and the protocols approved by the Ethic Committee of Laboratory Animals of the University of Granada (Spain) (CEEA 17/09/2019/156). All the animals were housed in makrolon cages, maintained in an air-conditioned atmosphere with a 12 hour light-dark cycle and provided with free access to tap water and food.

3.1. Induction of colitis with dextran sulfate sodium (DSS)

Acute colitis was induced in male C57BL/6J mice (7-9 weeks old) (Charles River, Barcelona, Spain) by adding 3% DSS (36-50 KDa, MP Biomedicals, Santa Ana, CA, USA) from day 0 to day 4 in the drinking water. On day 1, mice were injected intraperitoneally (i.p) with 1×10^6 human iMSCs in 200 µL of sterile PBS. The control and DSS groups received i.p. injections of 200 µL sterile 1 x PBS. Mice were euthanized on day 6. Disease activity index (DAI) was assessed daily as described in section 3.2. Once the animals were euthanized on day 6, the colons were

aseptically removed, rinsed with PBS, weighed, and its length was measured under a constant load (2 g). The colonic tissue was then sectioned in different fragments for subsequent histological and immunological evaluation. Spleens were weighted and blood drained to evaluate intestinal permeability (see section 3.3.).

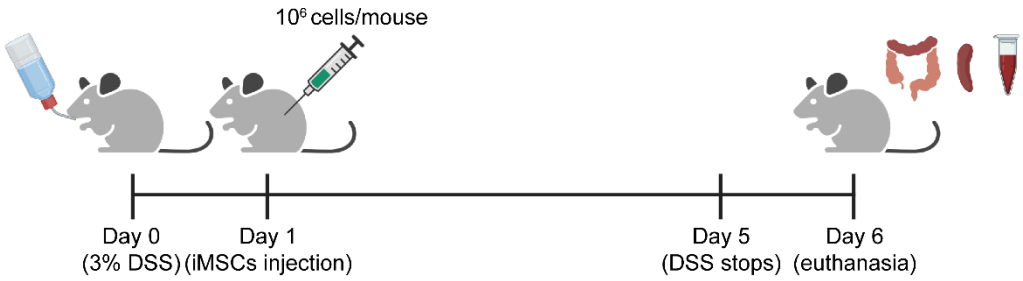

Figure 13. *Experimental design of DSS acute colitis induction. Image created with BioRender.com*

3.2. Determination of DAI in DSS induced colitis

The disease activity index (scale 0-4) was determined by evaluating weight loss, stool consistency, and presence of fecal blood in each mouse. A score was assigned to each one of these parameters according to the criteria previously proposed (300).

Score	Weight loss	Stool consistency	Rectal bleeding
0	None	normal	None
1	1-5%	Mucous traces	Perianal blood traces
2	5-10%	Loose stools	Blood traces on stools
3	10-20%	Diarrhoea	Bleeding
4	>20%	Gross diarrhoea	Gross bleeding

Table 7. *DAI value is the media of weight loss, stool consistency and bleeding scores*

3.3. Evaluation of intestinal permeability in colitic mice

The day before sacrifice, mice from the different experimental groups (n=8/group) were fasted for 12 hours and administered DX-4000-FITC (Sigma-Aldrich, Madrid, Spain) by oral gavage (350 mg/kg body weight). Four hours after administration, just before mice sacrifice, blood was drawn via intracardiac puncture and centrifuged at 4000 x g for 10 minutes at 4ºC. Plasma was diluted (1:10) in PBS and analyzed for DX-4000-FITC concentration with a fluorescence spectrophotometer (Fluorostart, BMG Lab Technologies, Offenburg, Germany) at an excitation

wavelength of 485 nm and emission wavelength of 535 nm. A standard curve was obtained by serial dilutions of FITC-dextran (Sigma-Aldrich, Madrid, Spain) in PBS (301).

3.4. Colonic explant culture

Three whole thick colonic punch biopsies (Miltex, York, PA, USA) were obtained from distal, medial and proximal regions and incubated in 0.5 mL of complete DMEM for 24 hours. After that, supernatants were collected and IL-1β concentration (pg/mL) was measured by ELISA as described in section 3.8.3.

3.5. Induction of colitis associated cancer – the azoxymethane (AOM)/DSS model

Colitis associated cancer (CAC) was induced in 8-9 weeks old C57BL/6J female mice provided by the Centre for Scientific Instrumentation (University of Granada, Granada, Spain) as previously described (302, 303). Briefly, mice were injected i.p. with 10 mg/kg AOM (Sigma-Aldrich, Spain Cat.# A5486-25MG). One week later, 2% (v/v) DSS was added in the drinking water for 5-7 days and this was repeated for a total of three DSS cycles with an interval of two weeks between each cycle. At the disease peak of the second and third DSS cycles, 0.5 x 10^6 human iMSCs were i.p. injected in 200 µLof sterile PBS. DAI was evaluated daily as described in section 3.2.

Once the animals were euthanized on week 15, colons were removed and macroscopically visible tumors were counted and measured. The distal colonic tissue was then sectioned in different fragments for subsequent evaluation. Also, mesenteric lymph nodes (MLNs) and spleens were removed and blood drained to accomplish different evaluations.

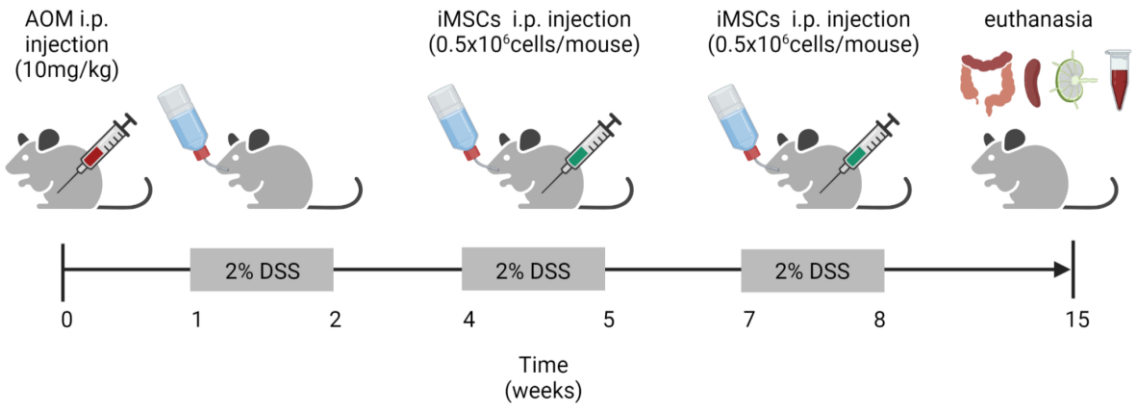

Figure 14. *Experimental design of AOM/DSS cancer associated colitis. Image created with BioRender.com*

Later, tumor volumes were estimated following the formula $V= (D x d^2 x \pi)/6$ that calculates the volume of an ellipsoid, where V= volume, D=larger diameter and d=smaller diameter.

3.6. Colitis and tumor scoring by colonoscopy

By the end of the AOM/DSS study, colon state was screened by means of a Coloview miniendoscopic system (Karl Storz, Madrid, Spain). Mice were anesthetized with isoflurane and tumor size was evaluated as described by Becker et al. (2007) (304). This resulted in the tumor size grade score. Tumour sizes were graded as follows:

Tumor size	Score
very small, just detectable	1
covers up to one eighth of the colonic circumference	2
covers up to a quarter of the colonic circumference	3
covers up to half of the colonic circumference	4
covers more than half of the colonic circumference	5

***Table 8**. Grading of tumor relative to the circumference of colon*

Colitis was also assessed by a scoring system developed by Becker et al. (2007) as well (304), shown in the following table:

	Endoscopic index of colitis severity				
	0	1	2	3	Total
Thickening of the colon	Transparent	Moderate	Marked	Non-transparent	0-3
Changes on the vascular pattern	Normal	Moderate	Marked	Bleeding	0-3
Fibrin visible	None	Little	Marked	Extreme	0-3
Granularity of the mucosal surface	None	Moderate	Marked	Extreme	0-3
Stool consistency	Normal+solid	Still shaped	Unshaped	Spread	0-3

***Table 9**. Endoscopic colitis score based on the observed sign of inflammation. Overall score: 0-15*

3.7. Analysis of gene expression by RT-qPCR

3.7.1. RNA extraction

Total RNA from iMSCs was extracted using cold NucleoZOL (Macherey-Nagel, Düren, Germany) following manufacturer's instructions and then standard phenol/chloroform isolation was performed. In the case of colonic samples, they were first homogenized using a Precellys 24 tissue homogenizer (Bertin Technologies, Montigny-Le bretonneux, France) and then RNA was isolated with the RNeasy® Mini Kit (Qiagen, Hilden, Germany) following manufacturer's indications. The resulting RNA was then quantified in a NanoDrop™2000 (ThermoFisher Scientific, Waltham, MA, USA) and sample purity was considered by the 260/230 and 260/280 ratios.

3.7.2. RNA retrotranscription

1-2 µg of total RNA per sample were reverse transcribed into cDNA using the M-MLV reverse transcriptase (Cat.# M1705), oligo (dT) primers (Cat.# C110A), RNasin® ribonuclease inhibitor (Cat.# N2511) and a 10mM dNTP mix (all from Promega, Madison, WI, USA) following manufacturer's indications. Resulting cDNA was then stored at -20ºC until its further use.

3.7.3. Gene expression analysis by quantitative PCR (qPCR)

Amplified cDNA was thawed and qPCRs for different genes were performed using the MasterMix qPCR SyGreen kit (PCR Biosystems Ltd, London, UK) that employs SYBR green as reporter.

Reactions were carried out in optical-grade 48-well plates, employing an Eco™ Real-Time PCR thermocycler (Illumina, San Diego, CA, USA). Ct values of the housekeeping gene glyceraldehyde-3-phosphate dehydrogenase (*Gapdh*) were used to normalize the values obtained for each of the evaluated genes. Relative gene expression was calculated by means of ΔΔCt formula and expressed as fold-change (compared to the corresponding control). Specific primer sequences (Sigma-Aldrich, Madrid, Spain) are presented in the following table.

Gene	Primer sequence 5'→3'	Species	Annealing T (ºC)	RefSeq accession number
Gapdh	FW 5'-CCATCACCATCTTCCAGGAG RV 5'-CCTGCTTCACCACCTTCTTG	mouse/ human	60	NM_001289726.1
Zo-1	FW 5'-GGGGCCTACACTGATCAAGA RV 5'- TGGAGATGAGGCTTCTGCTT	mouse	56	NM_009386.2
Villin	FW 5'-CTCCGAGCAGATTGAGAAGG RV 5'-GGTGCTGCCACTCTTCTACC	mouse	60	NM_009510.2
Inos	FW 5'-GTTGAAGACTGAGACTCTGG RV 5'-GACTAGGCTACTCCGTGGA	mouse	56	NM_010927.4
Tnf-α	FW 5'-AACTAGTGGTGCCAGCCGAT RV 5'-CTTCACAGAGCAATGACTCC	mouse	56	NM_001278601.1
Il-6	FW 5'-TAGTCCTTCCTACCCCAATTTCC RV 5'-TTGGTCCTTAGCCACTCCTTC	mouse	60	NM_031168.2
Icam-1	FW 5'-GAGGAGGTGAATGTATAAGTTATG RV 5'-GGATGTGGAGGAGCAGAG	mouse	60	NM_010493.3
Il-12	FW 5'-CATCGATGAGCTGATGCAGT RV 5'-CAGATAGCCCATCACCCTGT	mouse	59	NM_008351.3
Arg1	FW 5'-TTGCGAGACGTAGACCCTGG RV 5'- CAAAGCTCAGGTGAATCGGC	mouse	63	NM_007482.3
Cox-2	FW 5'-AAGCAGGCTAATACTGATAGG RV 5'-TGTTGAAAAGTAGTTCTGGG	mouse	56	NM_000963.4
Il-17a	FW 5'-TCCAGAAGGCCCTCAGACTA RV 5'-AGCATCTTCTCGACCCTGAA	mouse	60	NM_010552.3
Il-23-p19	FW 5'-AATCTCTGCATGCTAGCCTG RV 5'-AGTTGGCTGAGTCCTAGTAG	mouse	60	NM_031252.2
Mmp9	FW 5'-TGGGGGGCAACTCGGC RV 5'-GGAATGATCTAAGCCCAG	mouse	60	NM_013599.5
Angpt2	FW 5'- CAACTACAGGATTCACCTTAC RV 5'- GTACTGTGCATTCAAGTTGG	mouse	55	NM_007426.4
IDO1	FW 5'-TTGTTCTCATTTCGTGATGG RV 5'-TACTTTGATTGCAGAAGCAG	human	56	NM_002164.6
Il-10	FW 5'-TGGTGAAACCCCGTCTCTAC RV 5'-CTGGAGTACAGGGGCATGAT	human	60	NM_001382624.1
Tsg-6	FW 5'-CCAAATGAGTACGAAGATAACC	human	55	NM_007115.4

	RV 5'- CACAGTATCTTCCCACAAAG			
Hgf	FW 5'-GCAATTTTTGGTTTGGCTGT RV 5'-CCTGCCCACAGCATATAGGT	human	60	NM_001010932.3
Il-6	FW 5'-GCAGAAAAAGGCAAAGAATC RV 5'-CTACATTTGCCGAAGAGC	human	55	NM_001371096.1
Tpl-2	FW 5'-AACATTGCTGATTCTTCGTG RV 5'-CCCGAACAAGATTGAAGTAG	human	55	NM_001320961.2

Table 10. *RT-qPCR primer sequences and associated RefSeq accession numbers*

3.8. Analysis of protein expression

3.8.1. Protein extraction and quantification

Colonic samples were weighed, minced on an ice-cold plate and suspended (1:5 w/v) in a lysis buffer containing 20 mM HEPES (pH 7.5), 10 mM EGTA, 40 mM β-glycerophosphate, 2.5 mM $MgCl_2$, 1% Igepal®, protease inhibitors – 1mM DTT, 2 µg/mL aprotinin (Cat.# A1153), 5 µg/mL leupeptin (Cat.#L9783), 1 mM PMSF (Cat.#P7626), 1 µg/mL iodoacetamide (Cat.#I6125) – and phosphatase inhibitors – 2 mM sodium orthovanadate (Cat.#S6508), 5 mM sodium fluoride (Cat.#S1504) and 1 mM sodium molybdate (Cat.# 331058) (all of them from Sigma-Aldrich, Madrid, Spain). Then, tissue homogenates were left for 2 hours in a tube rotator at 4ºC. Thereafter, homogenates were frozen and stored until its further use. Samples were then defrosted and centrifuged at 10,000 x g for 15 minutes at 4ºC. Then, supernatant was transferred to new tubes and protein concentration determined by the bicinchoninic (Cat.# D8284) acid method described by Smith et al. (1985) using BSA (Cat.# A4503) as standard (both from Sigma-Aldrich, Spain).

3.8.2. Western blot

40-60 µg of total protein were mixed with 4x Laemmli sample buffer (Bio-Rad, Hercules, CA, USA) and boiled at 95ºC for 5 minutes. Then, samples were quickly placed on ice and proteins were resolved by sodium dodecyl sulphate-polyacrylamide gel electrophoresis (SDS-PAGE) under reducing conditions. After gel electrophoresis, proteins were subsequently electrotransferred to a immobilon-P PVDF membrane (Sigma, Spain, Cat.# IPVH00010). After blocking for 1 hour with 5% non-fat dry milk or 3% BSA (Sigma-Aldrich) diluted in PBS-T, membranes were probed overnight with primary antibodies against: iNOS (1:500, BD biosciences, Cat.# 610333), β-catenin (1:1000, Santa Cruz Biotechnology, Cat.# SC-7963), IL-6 (1:500, Cell signaling, Cat.# 12912), Akt (1:1000, Cell signaling, Cat.# 9272), p-Akt(Ser473) (1:1000, Cell signaling, Cat.# 9271), Bax (1:200, Santa Cruz Biotechnology, Cat.# SC-7480), Bcl-2 (1:500, Santa Cruz Biotechnology, SC-7382), Cox-2 (1:1000, Cell signaling, Cat.# 12282), STAT-3 (1:1000, Cell signaling, Cat.#4904) and pSTAT3(Tyr705)(1:1000, Cell signaling, Cat.#9145). Secondary HRP conjugated antibodies were purchased either by Sigma-Aldrich (1:5000 anti-rabbit IgG, Cat.#A9169) or Cell signaling (1:3000 anti-mouse IgG, Cat.#7076S) and incubated for 1 hour. Control of protein loading and transfer was conducted by detection of β-actin levels with a directly conjugated HRP antibody

(1:1000, Santa Cruz Biotechnology, Cat.#SC-47778). Signal development was performed with the Clarity western ECL substrate (Bio-Rad, Hercules, CA, USA) and signal acquisition using a LAS-4000 image system (Fujifilm, Life Science, USA) or a ChemiDoc image system ((Bio-Rad, Hercules, CA, USA). The quantification of bands was performed by densitometry analysis using either ImageJ (Free Software Foundation Inc) or Image Lab software (Bio-Rad, Hercules, CA, USA).

3.8.3. Cytokine determination by ELISA

For cytokine determination, supernatants from cell cultures or tissue explants were thawed and analyzed using mouse IL-1β (Peprotech, Cat.# 900-K47), human IL-10 (Peprotech, Cat.# 900-K21), human IL-12 (Peprotech, Cat.# 900-K96) or human TNF-α (Peprotech, Cat.# 900-T25) ELISA development kits. Briefly, capture antibody was diluted to its working concentration in PBS and 100 µL added per well in a 96-well high binding ELISA microplate (Corning Costar, Glendale, AR, USA, Cat.#3590). Capture antibody was incubated at room temperature overnight. The following day, wells were washed three times with wash buffer (0.05% Tween 20 in PBS) and wells blocked for 1 hour with 1% BSA in PBS. After washing the blocking buffer, 100 µL of test samples and standards were incubated for 2 hours at room temperature. After gentle washing, 100 µL of detection antibody were added to each well. 2 hours later, the detection antibody was removed and the plate incubated with 100 µL of streptavidin/avidin-HRP conjugate for 20 minutes out of light. Thereafter, the ELISA plate was washed again three times and 100 µL of substrate solution (either with TMB or ABTS, depending on the kit) added to each well. After a 20-minute incubation period, stop solution (2N H_2SO_4) was administered and optical density measured in an infinite F50 ELISA plate reader (Tecan Life Sciences, Switzerland).

3.9. Histological studies

At the day of sacrifice, representative colonic specimens were taken 1 cm from the rectum and fixed for 24 hours in 4% paraformaldehyde. Depending on the further application, tissues were then dehydrated in distinct solutions:

1) Increasing concentrations of ethanol (70%, 85%, 95% and 100%), then embedded in paraffin and trimmed in 5 µm sections – for haematoxylin and eosin staining.
2) A sucrose gradient (first at 15% and then at 30%), then embedded in OCT and trimmed in a cryostat in 8 µm sections – for immunofluorescence experiments.

3.9.1. Haematoxylin and eosin staining

To perform haematoxylin and eosin (H&E) staining, first, sectioned paraffin samples were deparaffinized and rehydrated. For that purpose, they were immersed two times in xylene (20 minutes/each) and then, in decreasing concentrations of ethanol (100%, 96%, 80%, 70% 50%, dH_2O and tap water) for 10 minutes/each. Once the samples were rehydrated, they were prepared for the staining procedure. When histochemical staining of mucins was carried out, sections were

first incubated in 1% alcian blue 3% in acetic acid (in 70% ethanol) for 30 minutes. Then, excess staining was removed in running tap water and conventional haematoxylin and eosin staining was accomplished. Briefly, slides were soaked for 1 minute in undiluted Harris Haematoxylin (Cat.# 10-2332, Casa Álvarez, Spain). Then differentiation and bluing were achieved by immersion in 3% acetic acid and tap water, respectively. After that, samples were dipped in 0.5% eosin (Cat.#10-3002, Casa Álvarez, Spain) for 30 seconds and then, tissue sections were dehydrated in increasing concentrations of ethanol and clarified in xylene before being mounted with DPX media (Casa Álvarez, Spain, Cat.# 10-3500).

3.9.2. Histological damage evaluation

In the DSS colitis model, after H&E staining, samples were submitted to histological tissue damage evaluation by a blind observer – according to a previously established scoring system. This system takes into account the presence of ulceration, immune cell infiltration, edema and the condition of the crypts (305). The scoring criteria is shown in the following table:

Mucosal epithelium and lamina propria
Ulceration: none (0); mild surface (0–25%) (1); moderate (25–50%) (2); severe (50–75%) (3); extensive-full thickness (more 75%) (4).
Polymorphonuclear cell infiltrate
Mononuclear cell infiltrate and fibrosis
Oedema and dilation of lacteals
Crypts
Mitotic activity: lower third (0); mild mid third (1); moderate mid third (2); upper third (3)
Dilations
Goblet cell depletion
Submucosa
Polymorphonuclear cell infiltrate
Mononuclear cell infiltrate
Oedema
Vascularity
Muscular layer
Polymorphonuclear cell infiltrate
Mononuclear cell infiltrate
Oedema
Infiltration in the serosa

Scoring scale: 0 none; 1 slight; 2 mild; 3 moderate; 4 severe. Maximum score:59

***Table 11**. Scoring criteria of full-thickness distal colon sections adapted from (300).*

3.9.3. Immunofluororescence

First, cryosections were brought to room temperature for 10 minutes. After this time, OCT was carefully peeled off from the tissue surroundings and the staining area was delimited with a hydrophobic pen (Cat.# Z377821, Sigma-Aldrich, Spain). Then, depending on the specific application, different steps were followed:

3.9.3.1. Assessment of cell proliferation by Ki67 expression

To determine tissue cell proliferation samples were then hydrated for 10 minutes in 1x PBS before being permeabilized and blocked for 1 hour with a 0.1% saponin, 1% BSA and 0.05% sodium azide PBS solution at room temperature (all from Sigma-Aldrich, Madrid, Spain). Then, slides were probed with primary polyclonal rabbit anti-Ki67 antibody (1:500 dilution) in blocking buffer (Cat.# ab64693 Abcam, Cambridge, UK) at 4ºC overnight, followed by three PBS washes. Then, to amplify the resulting signal, a goat anti-rabbit IgG AF488 secondary antibody (1:1000 dilution Cat.# ab150077, Abcam, Cambridge, UK) was incubated for 2 hours. Hoechst 33342 (Invitrogen, ThermoFisher Scientific, Waltham, MA, USA) was used to stain the nuclei. Anti-rabbit IgG isotype control (Cat.# 02-6102, Invitrogen, ThermoFisher Scientific, Waltham, MA, USA) was used as negative control. Images were acquired with a Nikon Eclipse Ti-E A1 confocal microscope (Centre for Scientific Instrumentation, University of Granada, Granada, Spain) equipped with a 20x objective. Acquisition of green channel (positive signals) was performed using the 488 nm laser and 505-550 nm emission filter. Quantification of $Ki67^+$ cells per crypt was done using 15 random crypts per slide. Images were analyzed with ImageJ software (Free Software Foundation Inc., Boston, MA, USA).

3.9.3.2. Assessment of apoptosis by TUNEL assay

To evaluate cell apoptosis the DeadEnd Fluorometric Tunel system (Cat.#3250, Promega, Madison, WI, USA) was used following manufacturer's indications with some modifications. Briefly, after tissue delimitation, samples were hydrated for 10 minutes with 1x PBS. Then, tissue permeabilization was achieved through incubation with proteinase K (20µg/ml) for 10 minutes. Next, samples were washed and incubated with equilibration buffer (200 mM dimethylarsinic acid, 25 mMTris-HCl, 0.2 mM DTT, 0.25 mg/ml BSA and 2.5 mM cobalt chloride) for 10 minutes before being incubated for 1 hour at 37ºC with the rTdT incubation buffer (out of light in a humidified chamber):

Buffer component	Volume per reaction
Equilibration buffer	22.5 µL
Nucleotide mix (fluorescently labeled)	2.5 µL
rTdT enzyme	0.5 µL

Table 12. *Composition of the rTdT incubation buffer.*

For negative controls this buffer was prepared without the rTdT enzyme. After 1 hour, sections were washed with 2x saline sodium citrate (SSC) buffer for 15 minutes and then three times with 1x PBS. Finally, Hoechst 33342 (Invitrogen, ThermoFisher Scientific, Waltham, MA, USA) was used to stain nuclei and samples were mounted with ProLong™ glass antifade mountant

(Invitrogen, ThermoFisher Scientific, USA). Images were acquired with a Leica TCS-SP5 II spectral multiphoton confocal microscope (Centre for Scientific Instrumentation, University of Granada, Granada, Spain) equipped with a 20x objective. Acquisition of green channel (positive signals) was performed using the 488 nm laser and 505-550 nm emission filter. Quantification of $TUNEL^+$ per field was done using 5 random fields per slide. Images were then analyzed with ImageJ software (Free Software Foundation Inc., Boston, MA, USA).

3.9.3.3. Assessment of iMSCs homing to intestine

To assess iMSCs homing in colon samples, sections were then hydrated for 10 min in 1x PBS. Thereafter, sections were then treated with a solution containing 0.1% saponin, 1% BSA and 0.05% sodium azide for 1 hour at room temperature. Then, slides were incubated with the anti-nuclei antibody conjugated with AF488 (1:100 dilution, Sigma-Aldrich, Madrid, Spain, Cat.#MAB1281A4) at 4ºC overnight. This antibody recognises the nuclei of human cells and does not bind to mouse or rat cells, enabling the detection of iMSCs in mouse tissue samples. The following day, sections were washed three times with 1x PBS and all nuclei counterstained with Hoechst 33342 (Invitrogen, ThermoFisher Scientific, Waltham, MA, USA). As a positive control, iMSCs grown in a Nunc Lab-Tek Chamber slide™ were subjected to the same procedure following the immunocytochemistry protocol described in section 1.5.2.

3.10. Flow cytometry

To analyze the expression of some relevant cellular markers and therefore, study the abundance of some immunologic cell subpopulations, FACs analysis was performed in different tissues.

3.10.1. Blood

At the day of euthanasia, AOM/DSS mice were anesthetized with xylazine (10 mg/kg) and ketamine (100 mg/kg) and blood drained with a 25 gauge heparinized needle and quickly transferred to a tube with anticoagulant. Then, 2 cycles of red cells lysis were done and blood cells counted. About $2x10^6$ cells/sample were stained as follows:

1) First, cells were incubated with live/dead Zombie Aqua fixable viability dye (BioLegend, San Diego, CA, USA), anti-CD16/32 (BioLegend, San Diego, CA, USA, Cat.# 101319) and 123 counting eBeads™ (Invitrogen, ThermoFisher Scientific, Waltham, MA, USA, Cat.#01-1234-42) previously diluted in 1x PBS.
2) Next, samples and Fluorescence minus one (FMO) controls were stained for 30 minutes at 4ºC with the next antibody mix diluted in FACs buffer (0.1%BSA and 2 mM EDTA):

Fluorochrome	Antibody target	Reference	Company
VioBlue	MHCII	130-102-145	Miltenyi Biotec
BV785	Ly6C	128041	BioLegend
FITC	CD11c	130-110-700	Miltenyi Biotec
PE	CD64	130-103-808	Miltenyi Biotec
PerCP-Cy5.5	CD11b	550993	BD Biosciences
PE-Vio770	CCR2	130-108-724	Miltenyi Biotec

***Table 13**. Antibody mix used to analyze abundance of blood monocytes populations*

Then samples were washed with PBS 1x to remove excess antibody, fixed with a paraformaldehyde based solution (Invitrogen, ThermoFisher Scientific, Cat.#00-8222) and resuspended in 200 µL of FACs buffer. Data was acquired using a BD FACSymphony™ A5 Cell Analyzer and results were analyzed with the Flowjo v10.6.2 software (FlowJo LLC, Ashland, OR, USA) following the next gating strategy:

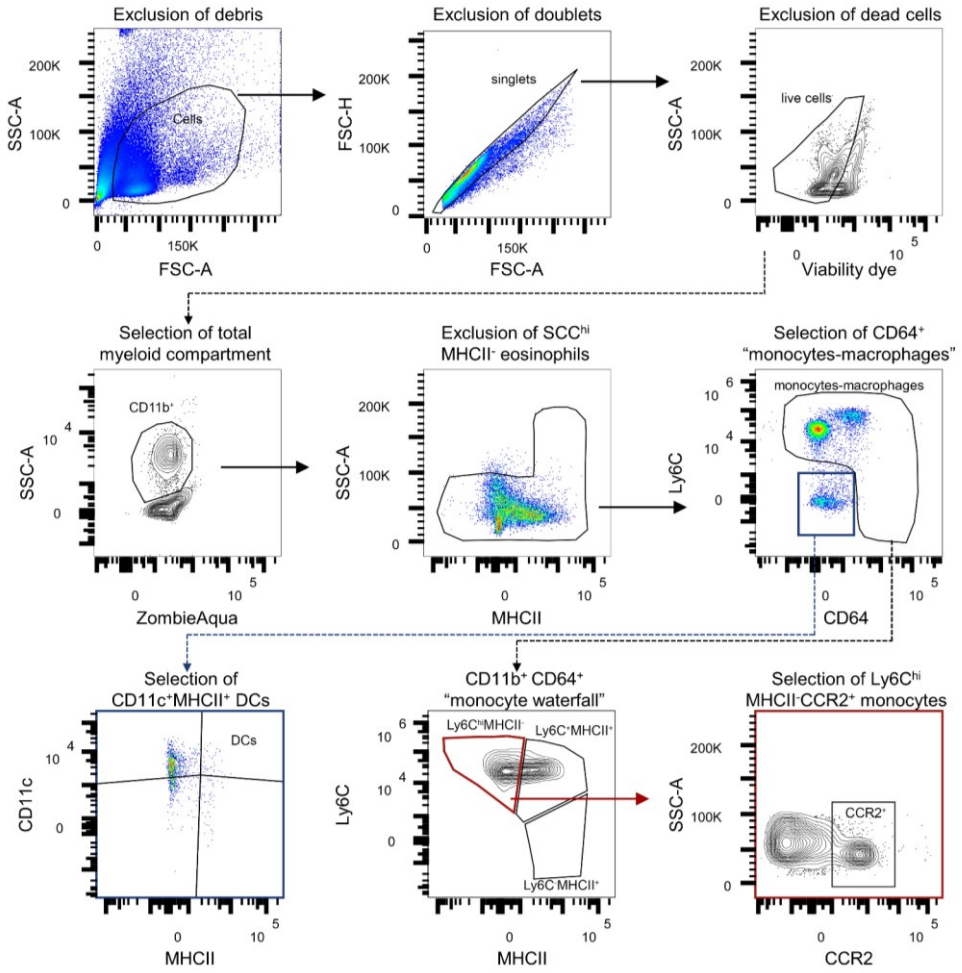

***Figure 15**. Gating strategy employed for the analysis of blood monocytes populations in AOM/DSS mice.*

3.10.2. Intestinal samples

Colonic tissue from AOM/DSS mice was removed and extensively washed with 1x PBS and longitudinally opened and kept on ice. Next, every colon was incubated with 5 mL of a prewarmed solution of HBSS (without Ca^{2+} and Mg^{2+}) supplemented with 1mTT and 5 mM EDTA for 30 min at 37ºC and 150 rpm. After that, supernatant was discarded and tissue washed 3-4 times with 1x sterile PBS to remove remaining EDTA and then, colons were cut into pieces on ice. The tissue was then incubated in DMEM containing 400U/ml collagenase XI (Sigma-Aldrich, Cat.# C7657), 100 U/mL DNase I (Sigma-Aldrich, Spain, Cat.#DN25) and 0.09 U/mL dispase II (Roche Applied System, Germany, Cat.#04942078001) for 40-50 minutes at 37ºC and 150 rpm. After this time, cell suspension was then filled up to 20-30 mL with 2mM EDTA PBS, passed through a 70 µm presoaked nylon mesh and pelleted. Then, cell concentration was assessed and 2-3x10^6 total cells were stained as follows:

1) First, cells were incubated with live/dead Zombie Aqua fixable viability dye (BioLegend, San Diego, CA, USA), FcR blocking (BioLegend, San Diego, CA, USA, Cat.# 101319) and 123 counting eBeads™ (Invitrogen, ThermoFisher Scientific, Waltham, MA, USA, Cat.#01-1234-42) previously diluted in 1x PBS.
2) Then, samples and FMO controls were stained for 30 minutes at 4ºC with the next antibody mix diluted in FACs buffer (0.1%BSA and 2 mM EDTA):

Fluorochrome	Antibody target	Reference	Company
BV421	CD206	141717	BioLegend
BV785	Ly6C	128041	BioLegend
FITC	CD86	553681	BD Biosciences
PE	CD45	130-102-596	Miltenyi Biotec
PerCP-Vio700	F4/80	130-102-161	Miltenyi Biotec
PE-Vio770	Ly6G	130-107-915	Miltenyi Biotec
APC	MHCII	17-5323-82	eBioscience
APC-Cy7	CD11b	101226	BioLegend

***Table 14**. Antibody mix used to analyze abundance of intestinal macrophages populations*

Then samples were washed with PBS 1x to remove excess antibody, fixed with a paraformaldehyde based solution (Invitrogen, ThermoFisher Scientific, Cat.#00-8222) and resuspended in 200 µL of FACs buffer. Data was acquired using a BD FACSymphony™ A5 Cell Analyzer and results were analyzed with the Flowjo v10.6.2 software (FlowJo LLC, Ashland, OR, USA) following the next gating strategy:

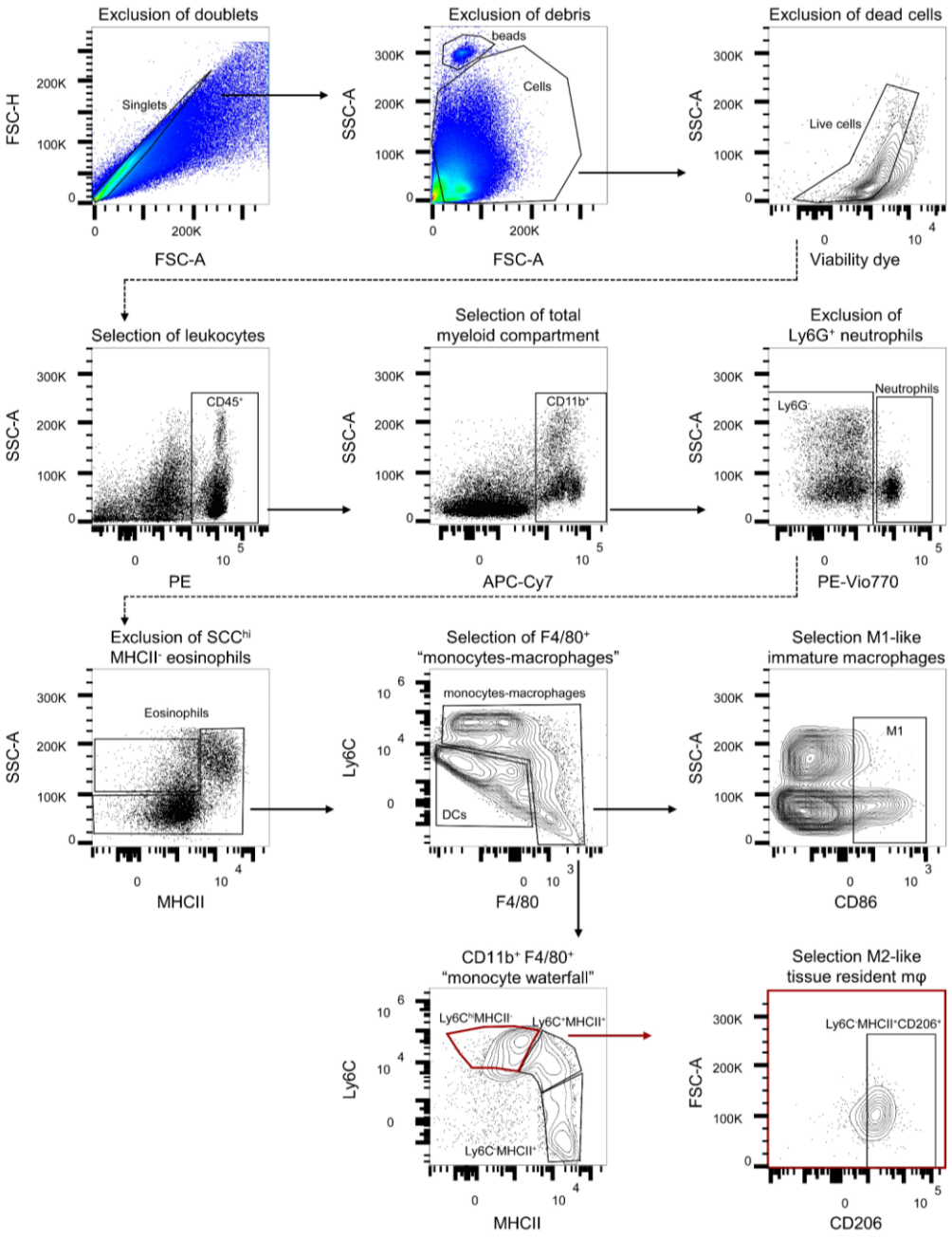

***Figure** 16. Gating strategy employed for the analysis of intestinal immune populations in CAC mice.*

3.10.3. Mesenteric lymph nodes (MLNs)

MLNs from AOM/DSS mice were removed and mashed between nylon filters in a precooled plate. Cells in suspension were then collected and filtered through a 70 µM presoaked nylon mesh. Next, cells were pelleted and counted and 2-3x10^6 cells were processed as it follows:

1) Cells in suspension were incubated for 4.5 hours (37ºC, 5% CO_2) in 1 mL of medium containing 50 ng/mL PMA (Sigma),1 µg/mL ionomycin (Sigma) and a solution containing the Golgi apparatus inhibitor Brefeldin A (1:1000 dilution, BD

Biosciences, Cat.# 555029). After this time, cells were centrifuged at 400 x g for 5 minutes.

2) Then, cells were incubated with live/dead eFluor780 fixable viability dye (Invitrogen, ThermoFisher Scientific, Waltham, MA, USA, Cat.# 65-0865-14), FcR blocking (BioLegend, San Diego, CA, USA, Cat.# 101319) and 123 counting eBeads™ (Invitrogen, ThermoFisher Scientific, Waltham, MA, USA, Cat.#01-1234-42) previously diluted in 1x PBS.
3) Later, samples and FMO controls were stained for 30 minutes at 4ºC with the next antibody cocktail diluted in FACs buffer (0.1%BSA and 2 mM EDTA):

Fluorochrome	Antibody target	Reference	Company
VioBlue	CD4	130-110-310	Miltenyi Biotec
BV510	CD3ε	100353	BioLegend
PE-Vio615	CD8a	130-109-251	Miltenyi Biotec

***Table 15**. Antibody cocktail employed to stain surface markers present in T cells*

4) Subsequently, excess antibody was removed and cells were permeabilized and fixed by means of FoxP3/Transcription factor staining buffer set (Invitrogen, Cat.#00-5523) following manufacturer's instructions. Next, cells and FMO controls were incubated with the intracellular antibody mix shown in the following table:

Fluorochrome	Antibody target	Reference	Company
BV786	IL-4	564006	BD Biosciences
FITC	IFN-γ	130-109-721	Miltenyi Biotec
PE	IL-17A	559502	BD Biosciences
APC	FoxP3	15-5773-80	Invitrogen

***Table 16.** Antibody mix used to stain intracellular markers present in T cell subpopulations*

Finally, cells washed with PBS 1x to remove excess antibody and resuspended in 200 µL of FACs buffer. Data was acquired using a BD FACSymphony™ A5 Cell Analyzer and results were analyzed with the Flowjo v10.6.2 software (FlowJo LLC, Ashland, OR, USA) following this gating strategy:

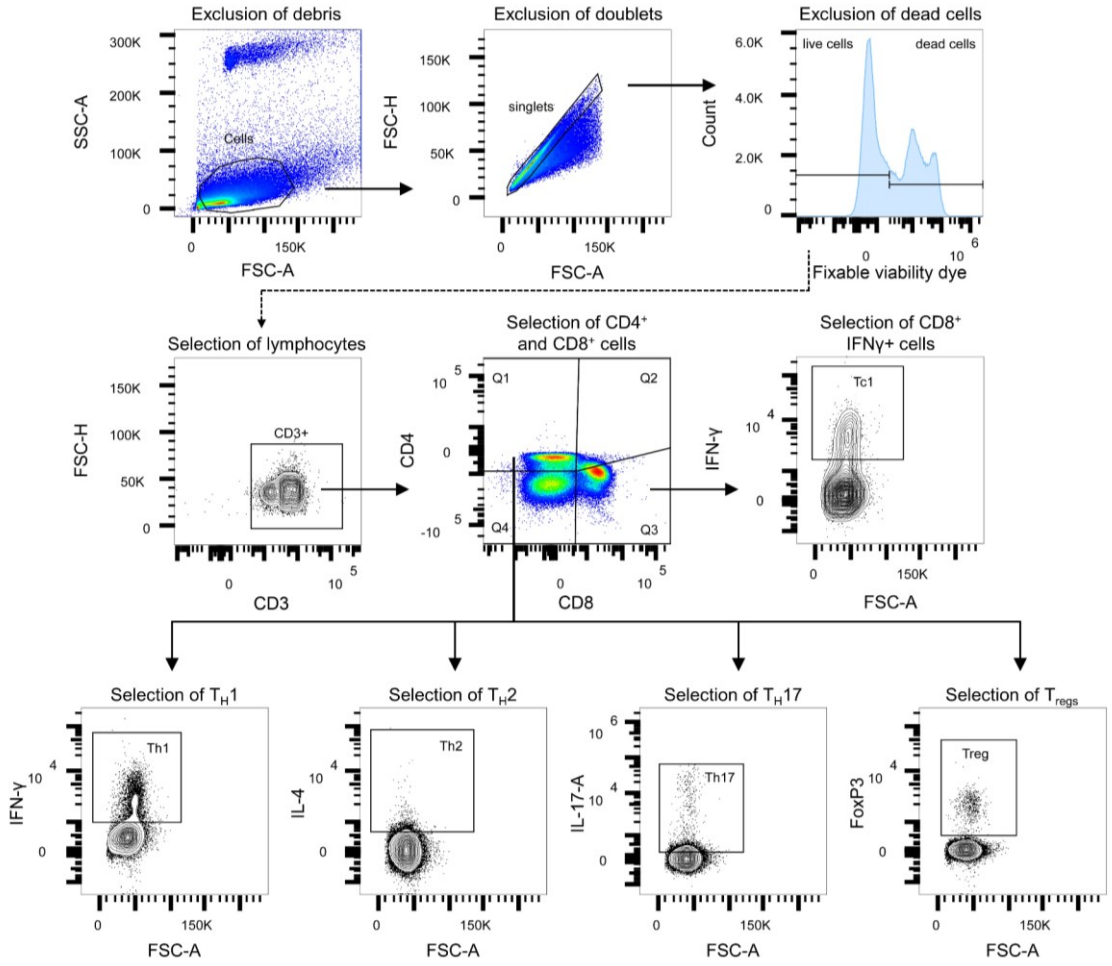

***Figure 17**. Gating strategy employed for T lymphocyte subpopulation analysis in AOM/DSS mice.*

3.11. DNA extraction and sequencing analysis from feces

Colonic luminal contents were collected from all mice at the end of the treatment and kept immediately at −80 °C until DNA extraction. Total DNA was isolated following the procedure described by Rodriguez-Nogales et al. (306). PCR amplification of targeted regions was performed by using “fusion primers”, targeting 16S V4-V5 regions with multiplexing on the Illumina MiSeq machine (Illumina Inc., San Diego, CA, USA). The PCR products with proper size were selected by 2% agarose gel electrophoresis. Same amount of PCR products from each sample were then pooled to make one library to be quantified fluorometrically before sequencing. After the sequencing was completed, all reads were scored for quality, and any poor quality and short reads were removed.

For microbiome analyses, paired-end reads were assigned to samples based on their unique barcodes and truncated by cutting off the barcode and primer sequences. Paired-end reads were merged using FLASH (V1.2.7) (307). Quality filtering on the raw tags were performed to obtain the high-quality clean tags (308) using the Qiime (V1.7.0) quality controlled process (309). The tags were compared with the SILVA reference database using UCHIME algorithm (310) to detect

and remove chimera sequences (311). Lastly, the Effective Tags were obtained. With the effective tag were obtained the OTU cluster and Taxonomic annotation using Uparse software ((312)) Sequences with ≥97% similarity were assigned to the same OTUs. Representative sequence for each OTU was screened for further annotation. For each representative sequence, Qiime in Mothur method was performed against the SSUrRNA database of SILVA Database (313) for species annotation at each taxonomic rank (314). OTUs abundance information were normalized using a standard of sequence number corresponding to the sample with the least sequences. Subsequent analysis of alpha diversity and beta diversity were all performed basing on this output normalized data. Alpha and beta diversity was calculated with QIIME and displayed with R software (Version 2.15.3).

4. STATISTICAL ANALYSIS

Statistical analysis was performed using the GraphPad Prism version 7 software (GraphPad Software, Inc, La Jolla, CA, USA). All data are represented as mean(SEM) of at least 3 independent experiments/biological replicates unless otherwise stated in the figure legends. The Mann–Whitney U-test for non-parametric data was used for the analysis of the DAI and microscopic score. For the PBMCs proliferation experiment analysis a two-way ANOVA followed by the Bonferroni post hoc test. For the rest of the data, multiple comparisons between groups were performed using the one-way ANOVA, followed by the Bonferroni post hoc test. A p-value <0.05 was considered significant.

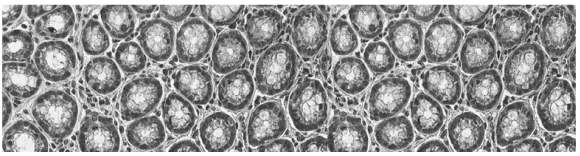

Results

RESULTS

1. CULTURED IMSCS SHOW A MSC-LIKE BEHAVIOUR

iMSCs isolated from intestinal resections presented a fibroblast-like morphology upon *in vitro* culture (Figure 18A) and had the ability to form colony-forming units fibroblasts (CFU-F), which is a measure of proliferation potential and self-renewal capacity associated with MSCs (Figure 18B). iMSCs showed to have trilineage differentiation potential and were able to differentiate into three different cell types *in vitro*: osteoblasts (Figure 18C, left), adipocytes (Figure 18C, middle) and chondroblasts (Figure 18C, right), using standard differentiation assays.

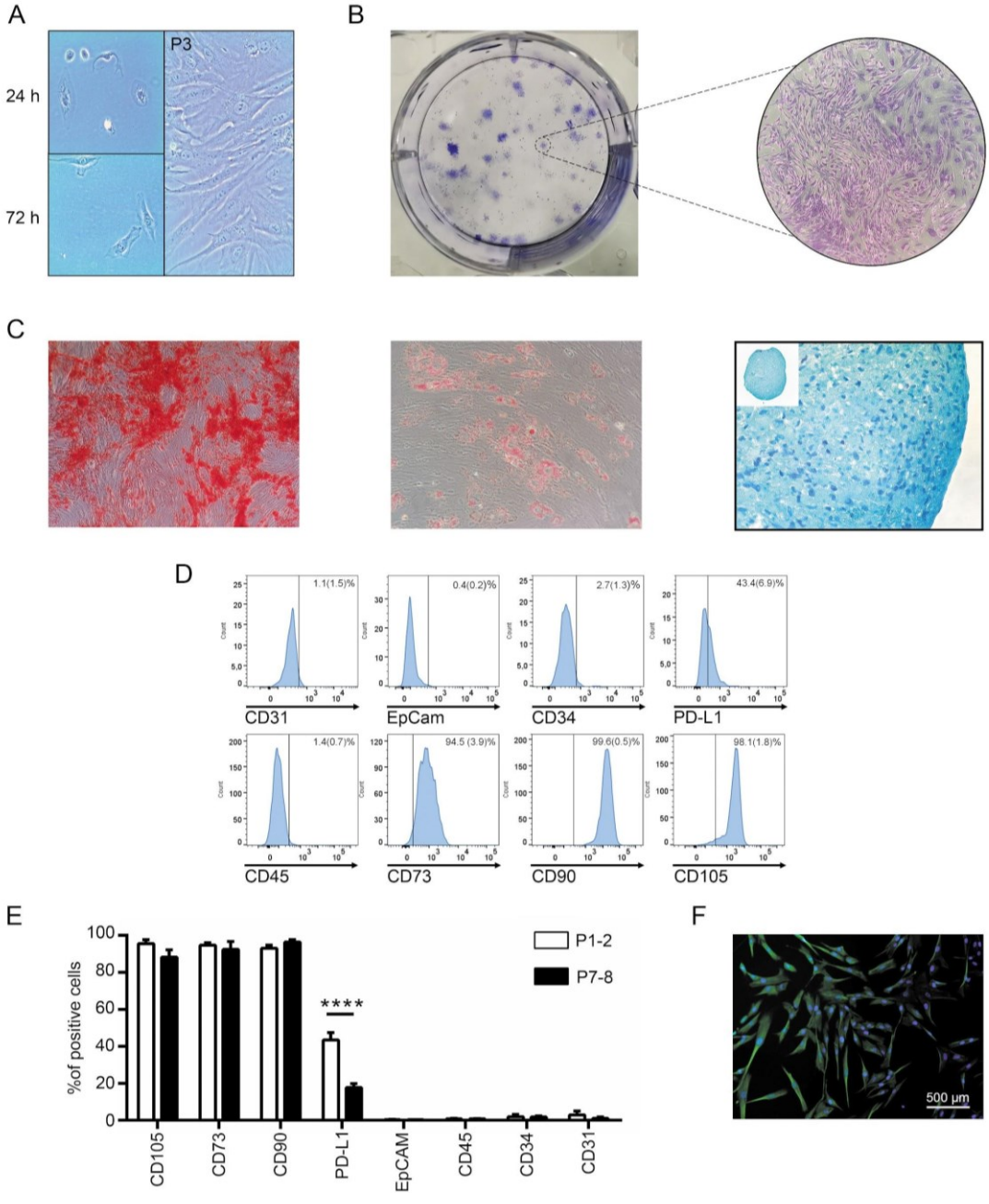

Figure 18. Characterization of human iMSCs. (A) *iMSCs were isolated through plastic adherence for 24 hours as described in materials and methods. After 72 hours, the adherent cells adopted a fibroblastic morphology. At passage 3 (P3), the cultures consisted of homogeneously larger fibroblastic cells.* ***(B)*** *iMSCs were seeded at low density and cultured for 12 days. Colonies (CFU-F) were stained with crystal violet.* ***(C)*** *iMSCs were differentiated for 3-4 weeks into (1) osteoblasts (left) - calcium deposits stained with alizarin red -, (2) adipocytes (middle) - lipid droplets stained with oil red - and (3) chondroblasts - aggrecan stained with alcian blue and nuclei with haematoxylin.* ***(D)*** *P2-3 iMSCs were harvested and stained with a panel of antibodies specific for endothelial (CD34), epithelial (CD31, EpCam), hematopoietic (CD45), mesenchymal (CD73, CD90, CD105) markers, and the immunomodulatory marker PD-L1 (CD274) and analyzed by flow cytometry. Representative histograms demonstrate specific stainings and the vertical lines represent the background staining using the corresponding isotype controls. The FlowJo software was used for FACs data analysis.* ***(E)*** *Average expression levels (% of positive cells in relation to isotype control stainings) of the above mentioned markers in iMSCs at passage 1-2 and 7-8 isolated from 6 donors.* ***(F)*** *P2-3 iMSCs were harvested, seeded and grown in immunofluorescence Nunc Lab-Tek Chamber slides. After that, the presence of vimentin (green) and nuclei (blue) was evaluated with a Nikon eclipse Ni-U epifluorescence microscope. Background staining was established using an isotype control. Data are shown as mean(SEM). ****=P<0.0001.*

Flow cytometry analysis at different passage numbers (P1-2 and P7-8) revealed that iMSCs lacked hematopoietic (CD45), epithelial (CD31, EpCam) and endothelial (CD34) markers, while expressing PD-L1 (programmed death-ligand-1/CD274), CD73 (ecto-5'-nucleotidase), CD90 (thymocyte differentiation antigen 1) and CD105 (endoglin, a surface membrane glycoprotein part of the TGF-β receptor complex) (Figure 18D). These last markers are general MSC-markers and are transmitted to their mesenchymal lineage descendants, such as muscle cells and fibroblast (315). As shown in Figure 18E, this phenotype was stable across serial cell passages (from P1-2 to P7-8), being PD-L1 the only cell marker that was significantly decreased at a later passage. Additionally, an immunocytochemistry analysis of these cells showed that iMSCs expressed vimentin, another typical mesenchymal marker (Figure 18F). In summary, these data suggest that iMSCs meet all the criteria proposed by the ISCT to be defined as mesenchymal stromal cells (15).

2. iMSCs PRODUCE SMALL EXTRACELLULAR VESICLES

Exosomes are small (30-150 nm)extracellular vesicles (EVs) that are released by a myriad of cells and have an important role in intracellular communication. MSCs from different tissues have been shown to produce exosomes, but few studies have confirmed their production by iMSCs (316). Exosomes isolated from iMSCs of different patients were visualized by TEM (Figure 19A, red arrows point out exosomes, recognisable by their lipid bilayer) and nanoparticle tracking

analysis (NTA) (Figure 19B). Exosomes appeared to have a rounded shape and an average size of 93.7 ± 3.4 nm (data from 6 different preparations of conditioned media) and the tracking analysis revealed one (or two in some cases) main population of small vesicles which size ranging from 79.6 to 158 nm. Exosomes are characterized by the expression of tetraspanins (CD9, CD63 and CD81) and some other molecular markers such as Flotillin, Hsp70, Hsp90 and Alix, while they are negative for annexin V (a marker for apoptotic bodies). The presence of some of these markers was evaluated by western blot (Figure 19C) or flow cytometry (Figure 19D) in iMSC-derived exosomes. We found that small extracellular vesicles produced by iMSCs express CD9, flotillin (Figure 19C) and CD63 (Figure 19D, left) in their surface, while they are negative for annexin V (Figure 19D, right). Taken together, these data suggest that the extracellular vesicles isolated from iMSCs were predominantly exosomes and not apoptotic bodies or other larger extracellular vesicles, e.g. microvesicles.

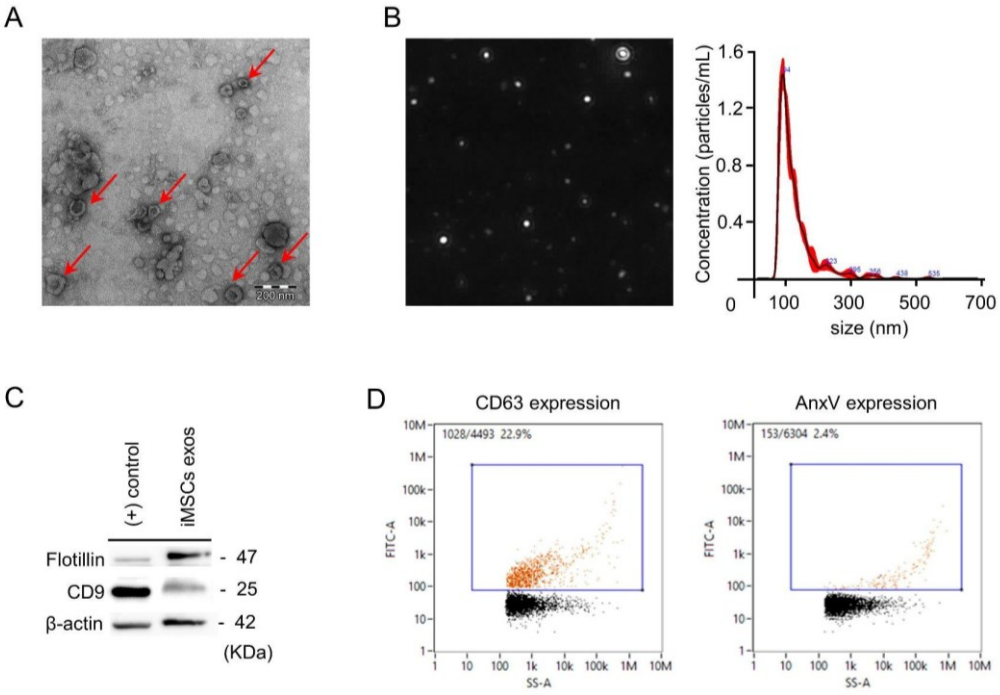

Figure 19. iMSCs are able to produce exosomes. (A) *Red arrows indicate the presence of small EVs visualized by TEM.* ***(B)*** *Diluted small EVs visualized by a nanosight NS300 (left image) and concentration and size analysis performed by NTA. Isolated exosomes were about 93.7 nm in diameter and the generated graphic was mainly characterized by a single peak, which indicates little contamination with microvesicles or proteins (right graph).* ***(C)*** *Western blot analysis of Flotillin, CD9 and β-actin expression in exosomes secreted from iMSCs* ***(D)*** *Flow cytometry analysis that shows 22.9% of the exosomes were positive for CD63 (the expression usually ranges from 10 to 70%) and only 2.4% were positive for the apoptotic body marker annexin V.*

3. iMSCs INHIBIT T CELL PROLIFERATION, PARTLY THROUGH IDO

To study the immunomodulatory characteristics of iMSCs, their effect on T cell proliferation was analysed. It has been previously reported that MSCs need to be "licensed" by IFN-γ and inflammatory cytokines, including TNF-α, to acquire suppressive capacities (317, 318) Thus, we co-cultured different concentrations of non-stimulated and TNF-α/IFN-γ-pre-stimulated iMSCs with CFSE-labeled PBMCs in the presence of the T cell mitogen PHA-L (Figure 20A, peaks indicate the number of cell cycle divisions). In the PHA-L-stimulated cultures, the highest concentration of iMSCs (20000 iMSCs) significantly inhibited the proliferation of $CD4^+$ and $CD8^+$ T cells (Figure 20B and C). Furthermore, cytokine-priming of iMSC significantly increased their capacity to inhibit the proliferation of $CD4^+$ T cells, with a similar trend seen for the suppression of $CD8^+$ T cells (Figure 20B, and C). IDO, PGE_2 and IL-10 have been implicated in the immunomodulatory capacity of MSCs (319). TNF-α/IFN-γ-stimulation of iMSCs resulted in a rapid increase in the mRNA expression of both IDO and COX-2, a key enzyme involved in the production of PGE_2 (Figure 20D).

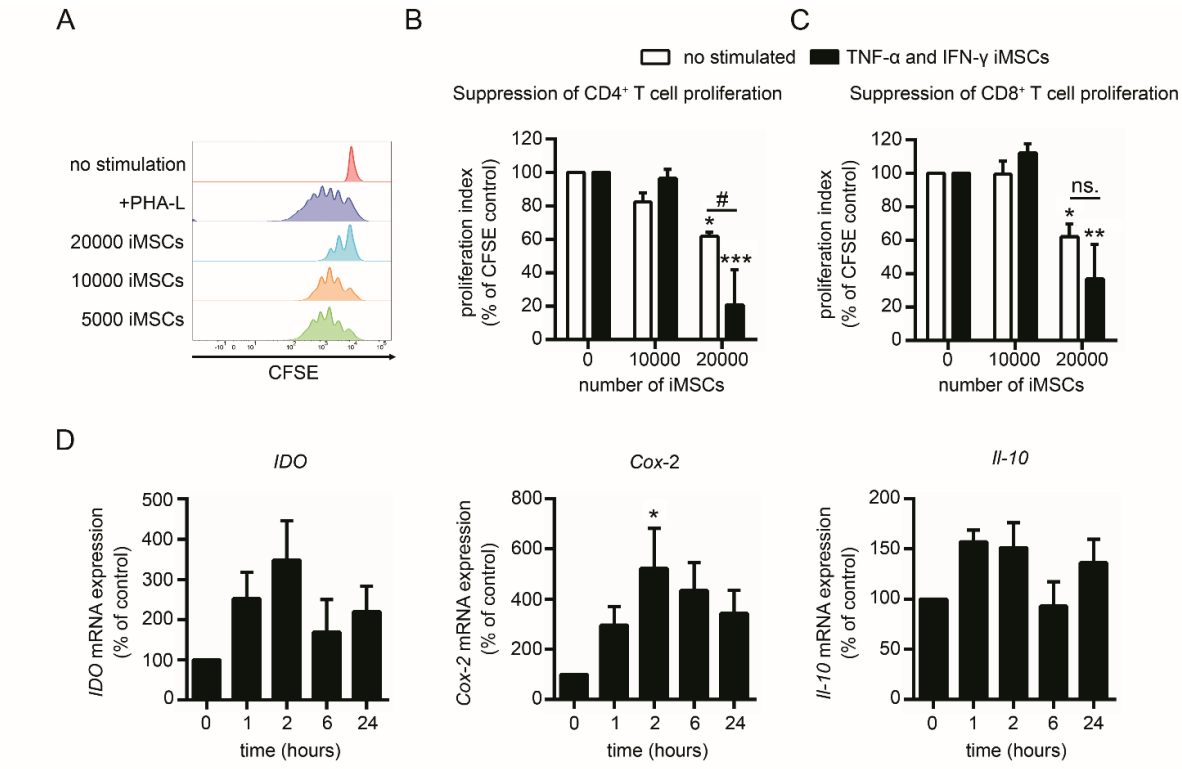

Figure 20. iMSCs inhibit CD4⁺ and CD8⁺ T cell proliferation in vitro. *CFSE-labeled PBMCs were stimulated with PHA-L in the presence or absence of increasing numbers of non-stimulated or TNF-α/IFN-γ prestimulated iMSCs. Six days later, supernatants were collected for the evaluation of IDO activity and cells were acquired on a FACs Aria IIIu cell sorter and the proliferation of $CD4^+$ and $CD8^+$ T cells was quantified using the FlowJo software.* ***(A)*** *Representative histograms showing CFSE-dilution of PHA-L-activated $CD4^+$ T cells cultured with*

or without different numbers of non-stimulated iMSCs. ***(B)*** *Proliferation index of CD4⁺ T cells cultured in the presence of non-stimulated (white bars) and TNF-α/IFN-γ prestimulated (black bars) iMSCs. Percentage of CFSE control refers to CFSE levels in PBMCs alone stimulated with PHA-L at day 6. Data are shown as mean(SEM) of 3 independent experiments. *=P<0.05 and ***=P<0.001 vs. "0 iMSCs", #=P<0.05.* ***(C)*** *Proliferation of CD8⁺ T cells cultured in the presence of non-stimulated (white bars) and TNF-α/IFN-γ prestimulated (black bars) iMSCs. Data are shown as mean(SEM) of 3 independent experiments. *=P<0.05 and **=P<0.01 vs. "0 iMSCs".* ***(D)*** *iMSCs were stimulated with TNF-α/IFN-γ for 1, 2, 6 and 24 hours and mRNA expression of IDO (left graph), Cox-2 (middle graph) and il-10 (right graph) were measured by qPCR. Data are shown as mean(SEM) of three independent experiments. *=P<0.05 vs. "0".*

To analyze the role of IDO and PGE_2 in the iMSCs-mediated inhibition of T cells, we added 1-MT and indomethacin, which are specific inhibitors of IDO and COX-1/2 activity, respectively (Figures 4B and C). We observed a small, but significant, reduction in the suppressive capacity of the iMSCs in the presence of 1-MT (Figure 21B), but not with indomethacin (Figure 21C). Furthermore, the IDO activity was assessed in the cell cultures by determining the concentrations of tryptophan (Figure 21D, left graph) and its metabolite L-kynurenine (Figure 21D, middle graph) in the supernatants by UHPLC-MS/MS. The IDO activity, defined as the L-kynurenine/tryptophan ratio, was significantly increased in the PBMC:iMSC co-cultures in comparison to PBMCs alone (Figure 21D, right graph). As expected, the addition of 1-MT significantly reduced the IDO activity. These data further suggest a role of iMSC-derived IDO in the inhibition of T cell proliferation.

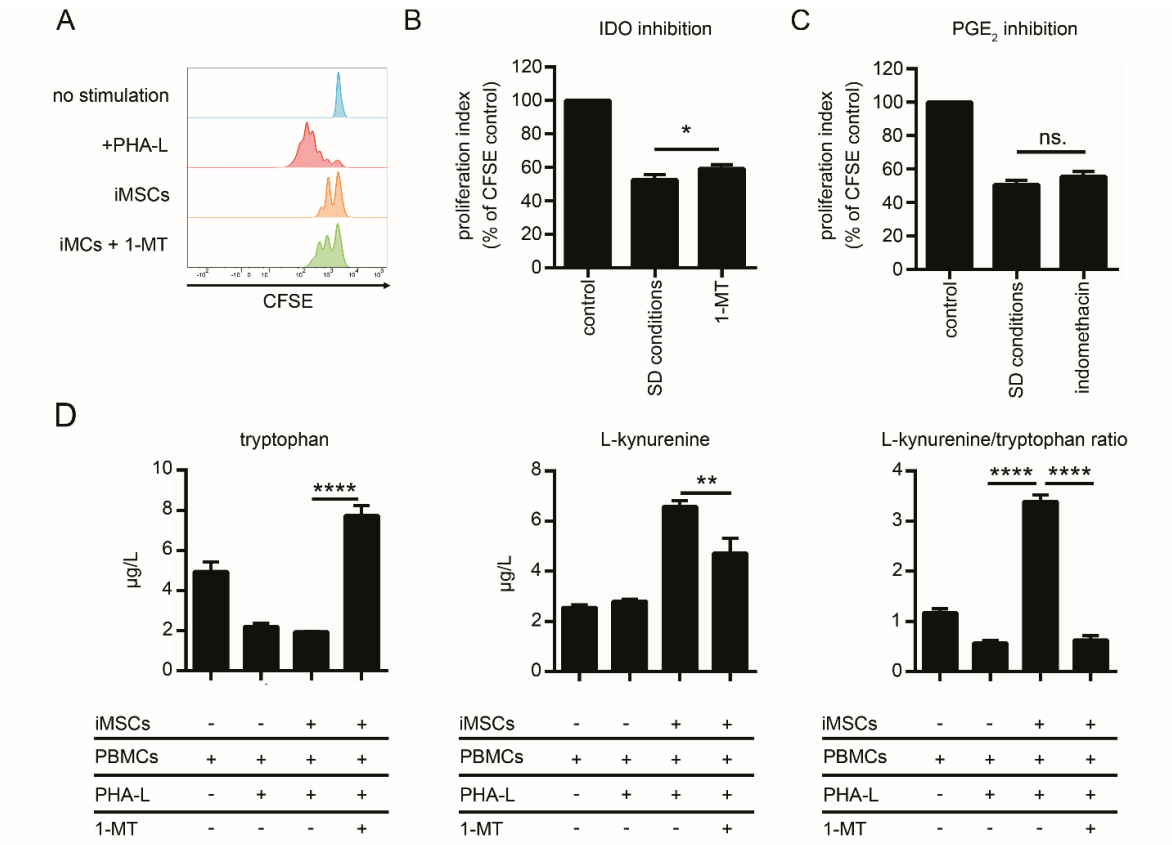

Figure 21. iMSCs inhibit T cell proliferation partly through IDO. (A) *Representative histograms showing CFSE-dilution of CD4⁺ T cells cultured with 20000 iMSCs in the absence or presence of 1-MT.* ***(B)*** *Proliferation index of CD4⁺ T cells co-cultured with 20000 iMSCs with 1-MT or standard media (SD conditions). Data are shown as mean(SEM) from 6 independent experiments. *=P<0.05.* ***(C)*** *Proliferation index of CD4⁺ T cells co-cultured with 20000 iMSCs with indomethacin or standard media. Data are shown as mean(SEM) from 6 independent experiments.* ***(D)*** *Supernatants from PBMC cultures were collected on day 6 and the concentrations of tryptophan (left graph) and L-kynurenine (middle graph) were determined by UHPLC-MS/MS. After that, the L-kynurenine/tryptophan ratio (right graph) was calculated. Data are shown as mean(SEM) from 6 independent experiments.*

4. iMSCs INHIBIT THE LPS-INDUCED EXPRESSION OF TNF-A IN THP-1 MACROPHAGES

To evaluate the effect of iMSCs on macrophage function, THP-1 macrophages were pretreated with iMSCs or iMSC-CM, and the expression of anti-inflammatory and pro-inflammatory cytokines upon LPS stimulation was measured. As shown in Figure 5, iMSCs stimulated with LPS (1 µg/mL) secreted low concentrations of TNF-α, whereas TNF-α secretion from THP-1 cells was highly increased after LPS stimulation. In contrast, THP-1 cells cultured in the presence of iMSCs or iMSC-CM produced significantly less TNF-α upon LPS stimulation (Figure 22A). On the other hand, the expression levels of IL-10 were not found to be significantly different between the groups (Figure 22B).

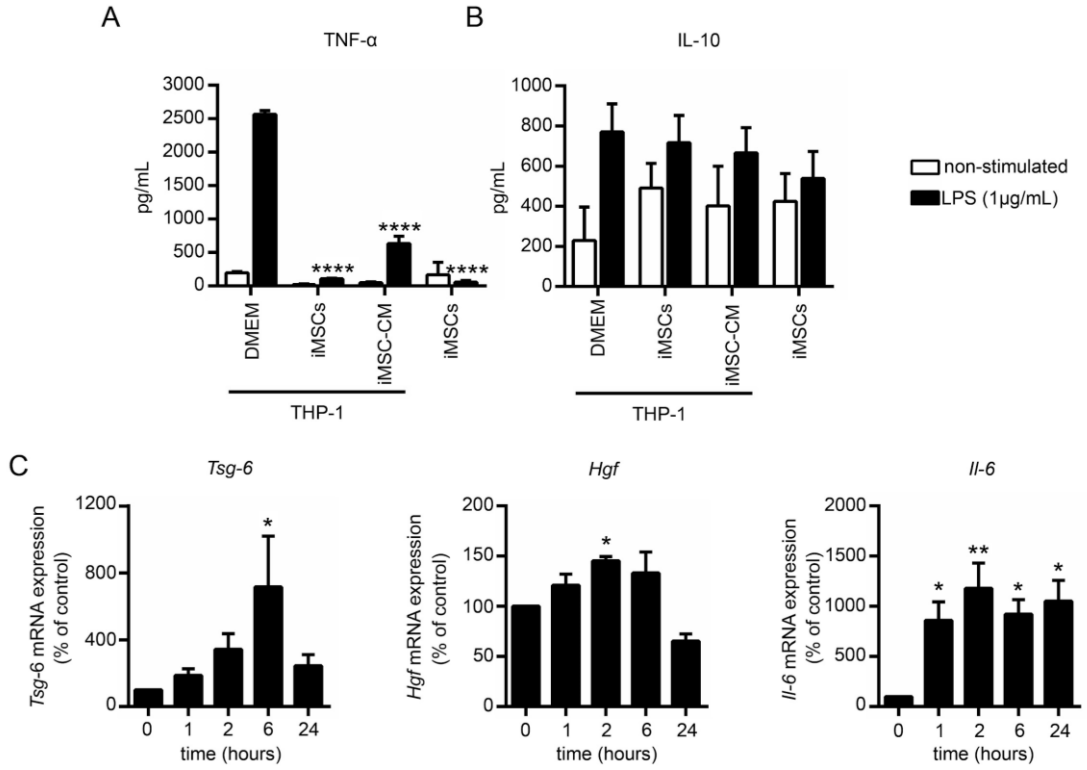

Figure 22. iMSCs inhibit macrophage activation in vitro. *PMA-activated THP-1 cells were cocultured with 100000 iMSCs or treated with iMSC-CM for 48 hours. Cells were subsequently cultured without (white bars) or with LPS for 24 hours (black bars) and the levels of TNF-α* ***(A)*** *and IL-10* ***(B)*** *in the culture supernatants were analyzed by ELISA. ****=P<0.0001 vs. DMEM (+ LPS) group.* ***(C)*** *iMSCs were stimulated with TNF-α/IFN-γ for 1, 2, 6 and 24 hours and mRNA expression of Tsg-6 (left graph), Hgf (middle graph) and Il-6 (right graph) were measured by qPCR. Data are shown as mean(SEM) of 3 independent experiments. *=P<0.05, **=P<0.01 vs. "0".*

Furthermore, IFN-γ/TNF-α stimulation of iMSCs resulted in the induction of several genes involved in the polarization of macrophages into anti-inflammatory M2 macrophages, including TSG-6, hepatocyte growth factor (HGF) and IL-6 (320), suggesting their possible involvement in the observed reduction in TNF-α production by THP-1 cells (Figure 22C).

5. CONDITIONED MEDIA FROM IMSCS PROMOTES *IN VITRO* WOUND HEALING

The impact of iMSC-CM on human NCM356 colonic epithelial cells migration/proliferation was analysed using an *in vitro* scratch wound healing assay. At 24 and 48 hours after wounding, the wound closure was significantly accelerated in iMSC-CM-treated wells when compared with the control (DMEM) (Figure 23A and 6B). In addition, we found that stimulation of iMSCs with TNF-α/IFN-γ rapidly induced the gene expression of tumor progression locus-2 (TPL-2) (Figure 23C). These data are in agreement with the proposed role of TLP-2 in maintaining epithelial cell homeostatic responses by increasing its proliferation (321).

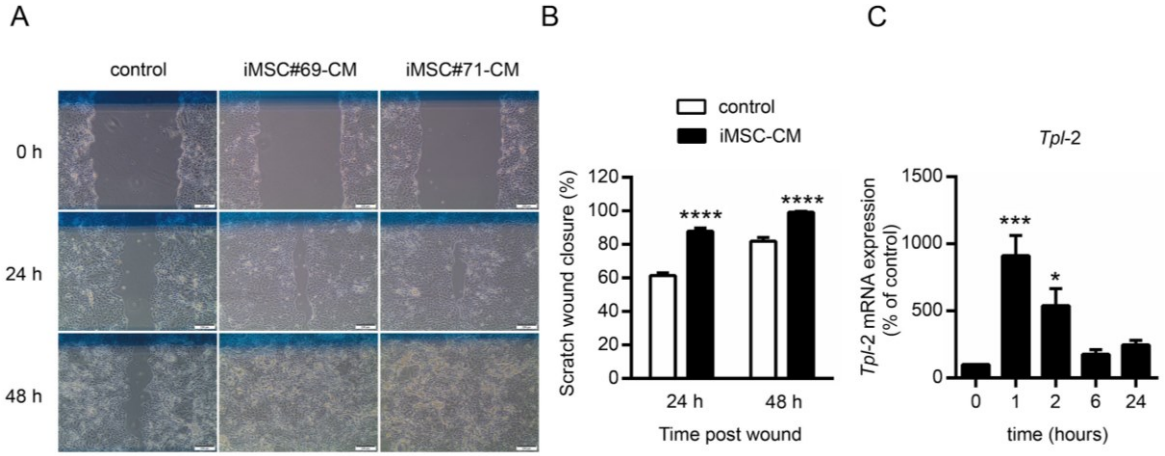

Figure 23. iMSC-CM promotes wound closure using the NCM356 human colonic epithelial cell scratch assay. (A) *Representative phase contrast images of NCM356 epithelial cell layers cultured in DMEM or iMSC-CM from four individual donors (iMSC#69, iMSC#71) were taken at 0, 24 and 48 hours after wounding (white line represents 200 µm. Original magnification 4x)* ***(B)*** *The regeneration of the wound was measured as described in materials and methods. Data are shown as mean(SEM) of 4 independent experiments, ****=P<0.0001 vs. control.* ***(C)*** *iMSCs were*

*stimulated with TNF-α/IFN-γ for 1, 2, 6 and 24 hours and mRNA expression of Tpl-2 was measured by qPCR. Data are shown as mean(SEM) of 3 independent experiments. *=P<0.05, ***=P<0.001 vs. "0".*

6. iMSCs AMELIORATE DSS-INDUCED ACUTE COLITIS

Once the immunosuppressive and wound-healing activities of iMSCs were confirmed *in vitro*, these effects of iMSCs were analysed in an experimental model of acute intestinal inflammation induced by DSS, which displays human IBD-like clinical, histopathological and immunological features. Oral administration of 3% (w/v) of DSS during five consecutive days resulted in a progressive increase in disease activity index (DAI) values, characterized by sustained weight loss and excretion of diarrheic/bleeding faeces. However, mice treated with a systemic administration of iMSCs one day after the initiation of the DSS-treatment showed a reduced DAI (Figure 24A), diminished body weight loss (Figure 24B), a less pronounced increase in spleen weight (Figure 24C) but with no apparent reduction in the colon weight/length ratio (Figure 24D).

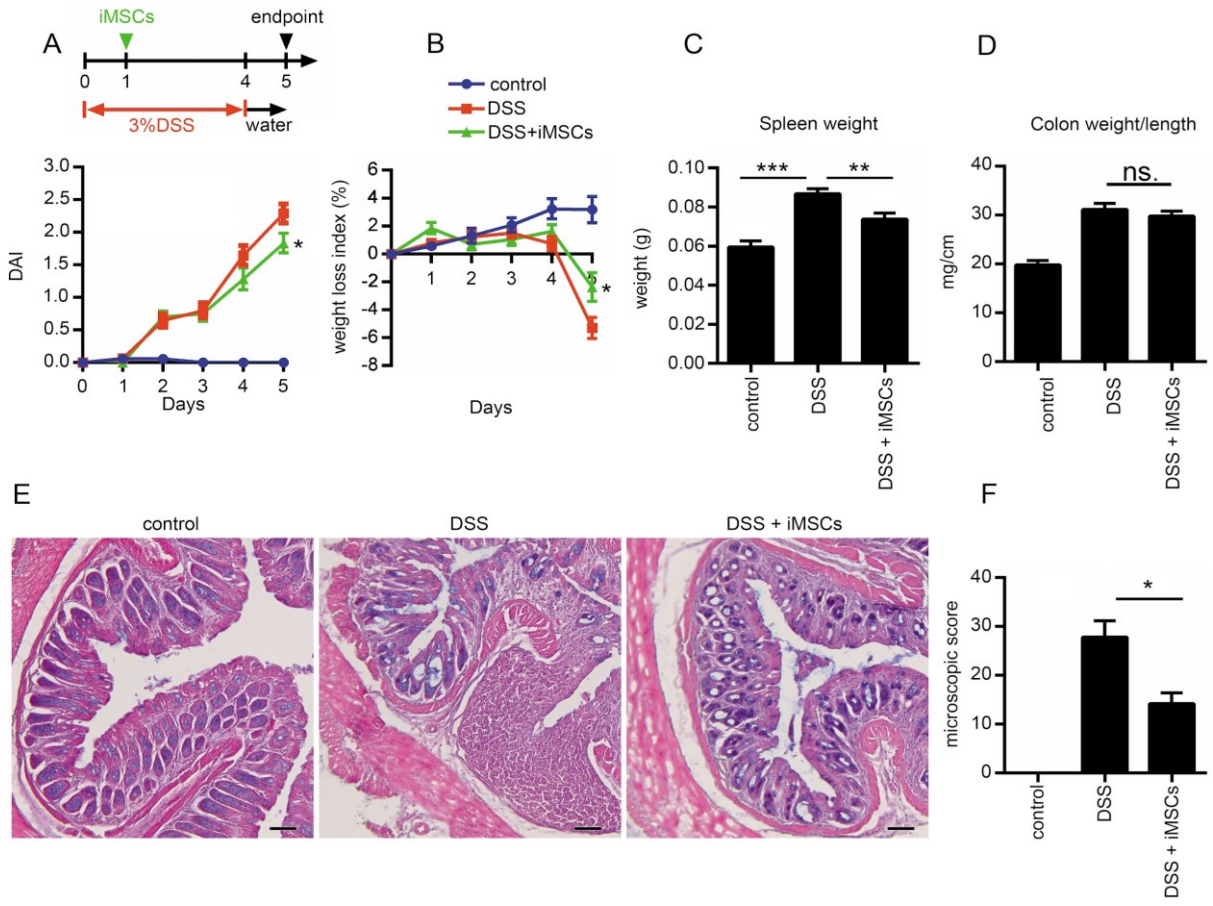

Figure 24. Treatment with iMSCs ameliorates DSS-induced acute colitis. *Mice (n=10) received 3% DSS in the drinking water ad libitum from day 0 to day 4. iMSCs (10^6/mouse) were injected intraperitoneally (n=10) on day 1. Mice receiving tap water instead of DSS were used as control mice (n=10) group.* ***(A)*** *Disease activity index and* ***(B)*** *weight loss index were determined*

daily. ***(C)*** *Spleen weight and* ***(D)*** *colon weight/length were determined on day 5.* ***(E)*** *Representative histological images of colonic tissue stained with alcian blue (mucins), haematoxylin and eosin showing the effect of iMSCs on DSS-induced colitis.* ***(F)*** *Histological evaluation of control, DSS and iMSC-treated mice. Data are shown as mean(SEM) of 5-6 individual mice/group. *P<0.05 vs. DSS mice.*

Images of the histological examination of colonic tissue stained with alcian blue, haematoxylin and eosin showed the effect of iMSCs on DSS-induced colitis (Figure 24E). In the DSS group there were appreciable changes in the mucosa with areas of ulceration on the epithelial layer, in addition to a lower number of goblet cells, decrease in mucins and an intense inflammatory cell infiltrate. In the iMSCs group an improvement of the colonic histology with a reduced area of ulceration was found, more abundance of goblet cells and a diminished infiltration of inflammatory cells (Figure 24F).

7. iMSC ADMINISTRATION PROTECTS THE INTEGRITY OF THE INTESTINAL BARRIER IN DSS-TREATED MICE

To characterize the effects of the iMSCs on the impaired colonic epithelial permeability in colitic mice, intestinal barrier function was determined by oral administration of 4 kDa FITC-dextran. As shown in Figure 25A, colitic mice suffered a significant increase in intestinal permeability in comparison with the control group. However, this epithelial barrier impairment was significantly reduced in the iMSCs-treated group. Additionally, the mRNA expression of proteins involved in the maintenance of epithelial integrity, including *Zonula occludens-1* (*Zo-1*) and *Villin* was significantly reduced in the DSS group in comparison with the control mice, whereas the iMSC-administration significantly increased expression of these markers (Figure 25B and C). To further investigate the mechanisms behind this iMSC-mediated protection of the intestinal barrier, we analyzed the amount of proliferation (Ki67 immunohistochemistry) and apoptosis (TUNEL assay) of cells in intestinal tissue sections from the control, DSS and DSS + iMSC groups. To our surprise, we found an increased number of $Ki67^{+}$ cells in the DSS mice compared to the iMSC-treated group (Figure 25D). In addition, the TUNEL assay showed a significant increase in apoptotic cells in the intestines of iMSC-treated mice in comparison to DSS colitic mice (Figure 25E).

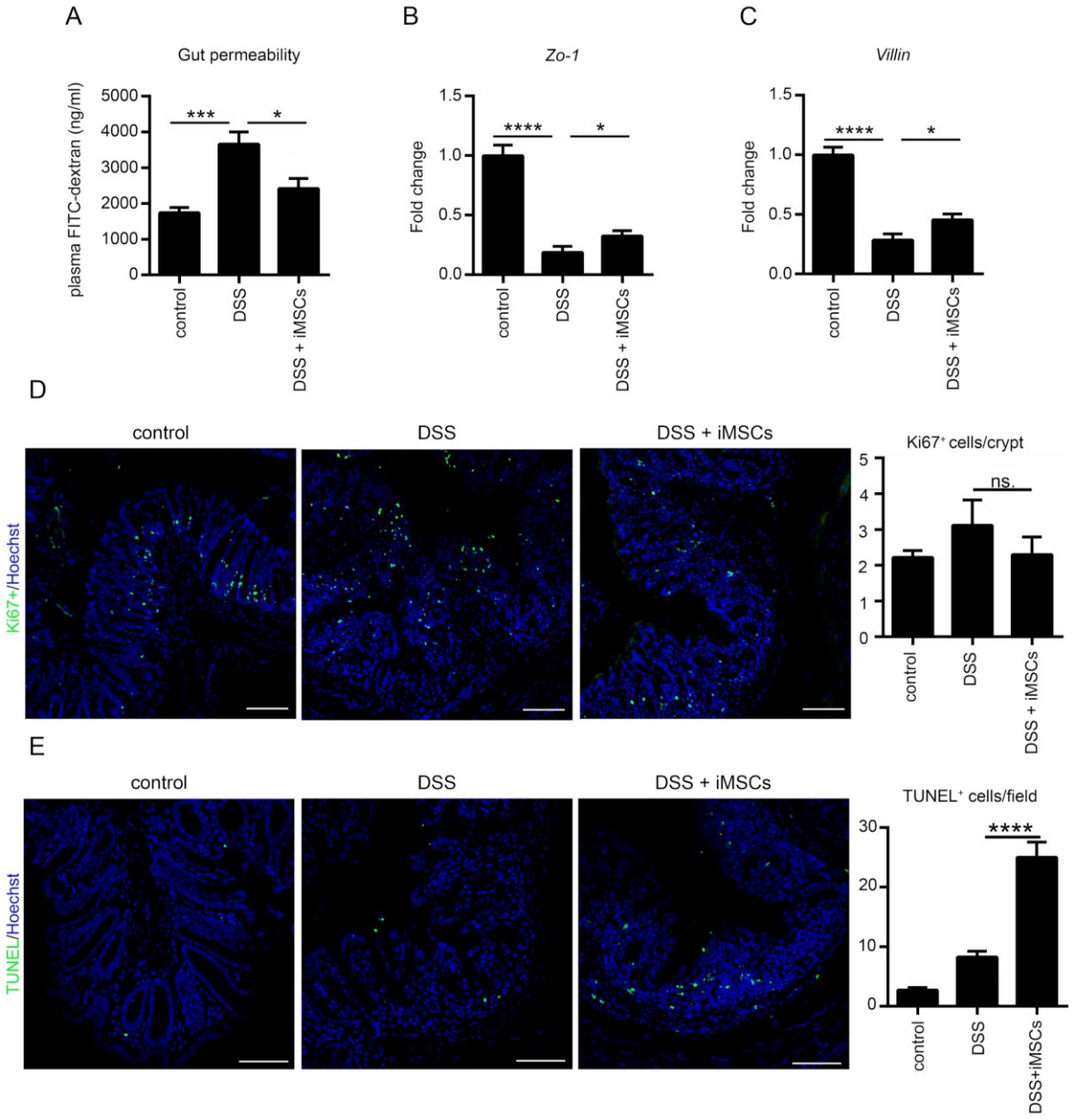

Figure 25. iMSCs promote intestinal epithelial barrier integrity. (A) *Gut permeability was determined on day 5 by plasma concentration of FITC-dextran. mRNA expression of epithelial integrity proteins* ***(B)*** *Zonula occludens-1 (Zo-1) and* ***(C)*** *Villin was quantified by RT-qPCR. Fold-changes are expressed as mean(SEM). *=P<0.05, **=P<0.01, ***=P<0.001, ****=P<0.0001 vs. DSS mice.* ***(D)*** *Representative images showing cell proliferation in colon sections evaluated by immunofluorescence staining of Ki67. Ki67⁺ cells are shown in green and nuclei are shown in blue (Hoechst). White bars represent 100 µm. Data show Ki67⁺ cells/crypt and are represented as mean(SEM) of 5 mice/group. ns. = not significant.* ***(E)*** *Representative images of TUNEL stained colonic tissue sections from control, DSS and DSS + iMSCs experimental groups showing cell apoptosis. Apoptotic cells are stained in green and nuclei in blue (Hoechst). Data show*

*TUNEL⁺ cells/field, and are represented as mean(SEM) of 5 mice/group. ****=P<0.0001 vs. DSS mice.*

8. iMSC ADMINISTRATION REDUCES INFLAMMATORY RESPONSES IN COLITIC MICE

The biochemical analysis of the colonic tissue corroborated the intestinal anti-inflammatory effect of iMSCs, revealing the positive impact on the altered colonic immune response induced by DSS. DSS-induced colitis was characterized by increased expression of the pro-inflammatory cytokines *Tnf-α*, *Il-6* and *Il-12*, as well as the adhesion molecule *Icam-1*, and *Inos* (Figure 26A-E). iMSCs administration significantly reduced the expression of these cytokines, whereas only a trend in reducing *Icam-1* expression was observed (Figure 26D).

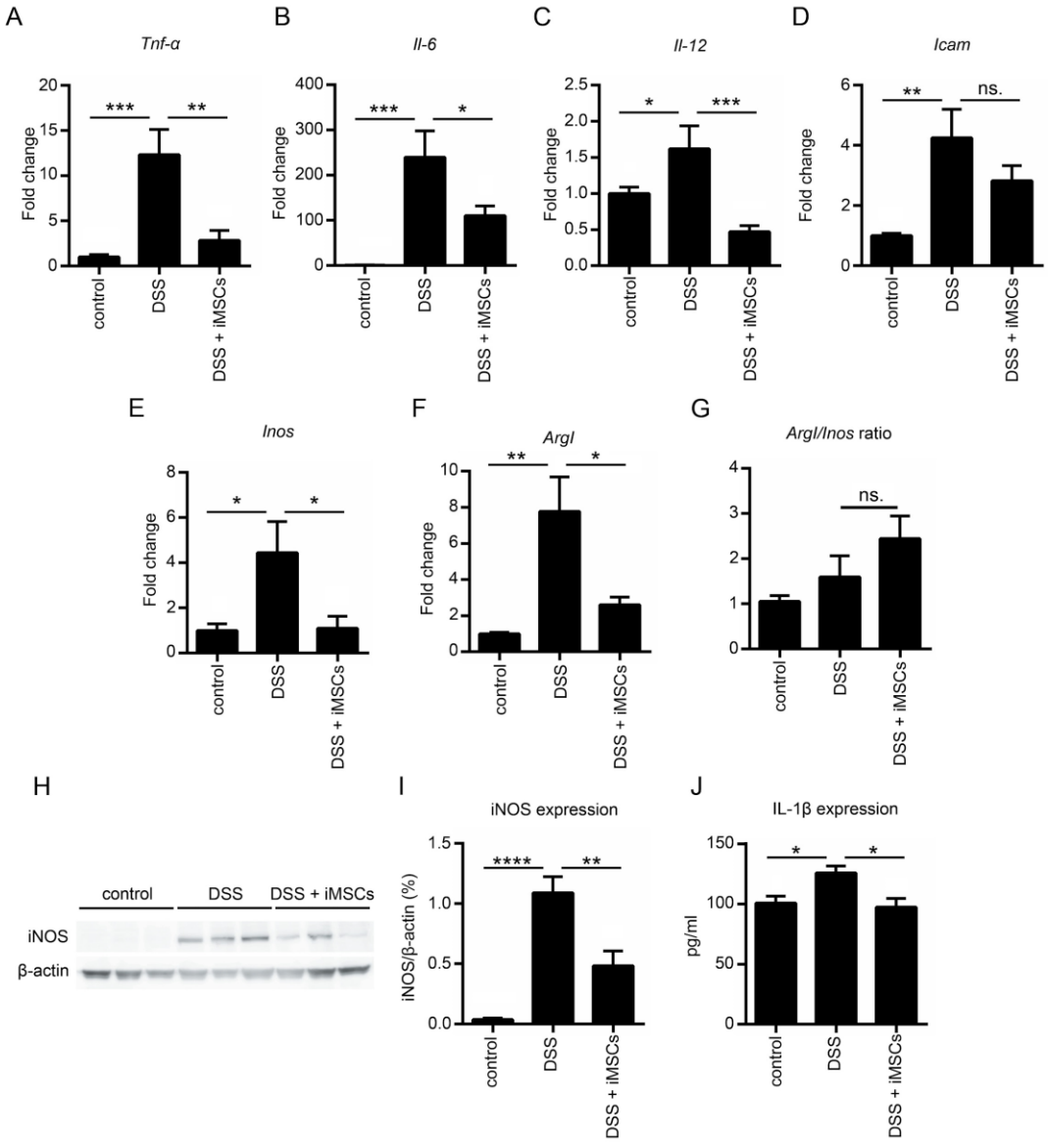

Figure 26. iMSCs inhibit DSS-induced inflammation in colitic mice. *Mice with DSS-induced acute colitis were treated with iMSCs on day 1. Total RNA was extracted from colons collected on day 5 and the gene expression of various inflammatory mediators was determined by RT-qPCR. Colonic gene expression of the cytokines* ***(A)*** *Tnf-α,* ***(B)*** *Il-6,* ***(C)*** *Il-12,* ***(D)*** *the adhesion molecule Icam,* ***(E)*** *the inducible enzyme Inos and* ***(F)*** *ArgI were analyzed by RT-qPCR. *=P<0.05, **=P<0.01, ***=P<0.001, ****=P<0.0001 vs. DSS mice.* ***(G)*** *Based on the RT-qPCR results,the ArgI/Inos ratio was calculated. Data are shown as mean(SEM) of 10 mice/group of two separate experiments.* ***(H)*** *Effect of iMSCs on colonic iNOS expression evaluated by Western blot in DSS colitic mice.* ***(I)*** *Densitometric analysis of the corresponding bands.* ***(J)*** *Effect of iMSCs on colonic IL-1β protein levels measured by ELISA in culture supernatants of colonic fragments from mice of each experimental group incubated for 24 hours in complete DMEM as described in materials and methods. *=P<0.05 vs. DSS group.*

We also analyzed the expression of the M2 macrophage-related gene *ArgI* (Figure 26F). Although *ArgI* expression was highest in DSS-treated mice, the ratio *ArgI/Inos* was increased, albeit not significantly, in iMSC-treated mice suggesting a possible polarization towards an anti-inflammatory M2 macrophage response (Figure 26G) (322). The intestinal anti-inflammatory activity exerted by iMSCs was also corroborated when the pro-inflammatory inducible enzyme iNOS was evaluated by western blot. In contrast to healthy control animals, mice from the DSS group showed an increased expression of this enzyme in the colon. However, the systemic administration of iMSCs significantly down-regulated the colonic expression of iNOS (Figures 9H and I). Additionally, protein levels of the pro-inflammatory cytokine IL-1β were measured in culture supernatants of colonic explants by ELISA. IL-1β levels were significantly lower in the iMSCs-treated colitic group when compared with the DSS control group (Figure 26J).

9. iMSCs TREATMENT AMELIORATES THE GUT DYSBIOSIS IN COLITIC MICE

The effect of iMSCs administration on the gut microbiota was explored since microbial dysbiosis is known to play a fundamental role in ulcerative colitis. Different features of the gut microbial were analysed. Firstly, the analysis of the relative abundance of the main taxonomic phyla was performed (Figure 27A). The results revealed that the most abundant phyla were *Bacteriodetes* (B), *Firmicutes* (F) and *Verrumicrobia* in all experimental groups, although DSS supplementation induced a dramatic shift in these phyla when compared to control mice, significantly increasing *Firmicutes*, reducing *Bacteroidetes* and *Verrucomicrobia* (Figure 27A) . These changes were significantly restored by iMSCs administration, showing similar values to the control group (Figure 27A). To further investigate this remarkable shift in the gut microbial environment after iMSCs treatment, the principal coordinates analysis (PCoA) score plot of gut microbiota at the genus level was determined. The results showed clear differences between control and DSS group (Figure 27B). When iMSCs were administered to colitic mice, marked differences could be appreciated in comparison with the untreated-colitis group (Figure 27B). Finally, several

ecological parameters, including observed OTUs (count of unique OTUs in each sample) (Figure 27C); Chao richness (an estimate of a total community) (Figure 27D) and Shannon diversity (the combined parameter of richness and evenness) (Figure 27E) were evaluated. Observed OTUs, microbial richness and diversity index were significantly decreased in the DSS group compared to the control mice, whereas iMSCs treatment was able to restore all these ecological parameters (Figure 27 C-E).

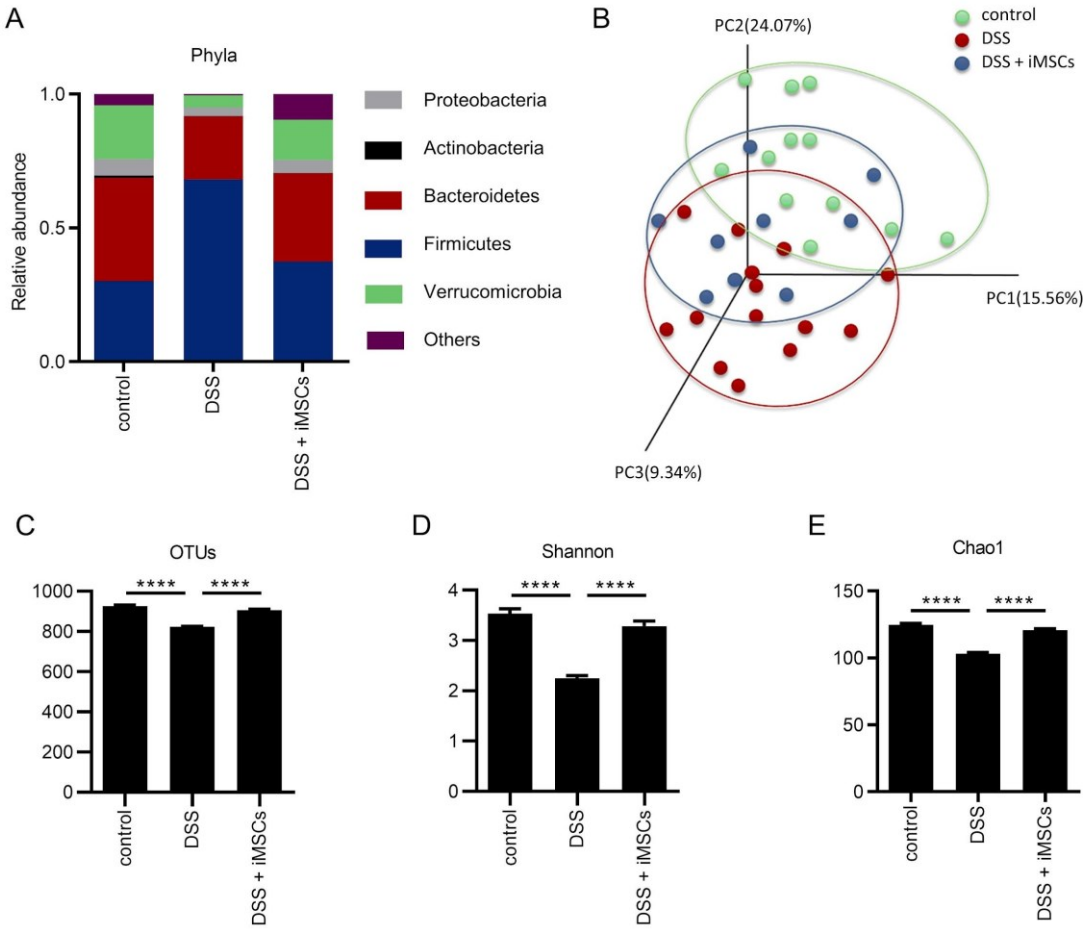

Figure 27. iMSC administration ameliorates the gut dysbiosis in colitic mice. *Concretely, the effect on (**A**) bacterial community at phylum level, (**B**) Beta-diversity by principal coordinate analysis score plot and microbiome diversity by (**C**) Observed OTUs, (**D**) Shannon diversity and (**E**) Chao1 richness were assessed. Data are expressed as mean(SEM). ****=P<0.0001 vs. DSS group.*

10. iMSC ADMINISTRATION AT THE PEAK OF COLITIS REDUCES DISEASE SEVERITY IN CAC MICE

Once the activity of iMSCs was confirmed in colitis, the effect of iMSCs was analysed in an experimental model of colitis associated cancer (CAC) which presents human CAC-like features

and resulted in tumor initiation and development. CAC was induced in C57BL/6J female mice by the injection of AOM followed by three cycles of DSS (2% w/v) DSS. At the peaks of the last two cycles of DSS, iMSCs were injected i.p. with $0.5x10^6$ cells/mice (Figure 28A). During the three DSS cycles weight loss (Figure 28B, left) and disease activity index (Figure 28B, right) were monitored as described in materials and methods. As expected, CAC mice exhibited an important weight loss and a reproducible increase in DAI during each DSS cycle. Interestingly, the first systemic administration of iMSCs during the 2nd DSS cycle did not affect weight loss/DAI score, but showed a protective effect during the third DSS cycle (Figure 28B). The disease ameliorating effects of the iMSC administrations persisted as reflected by a significant reduction in both spleen weight and colon weight/length ratio, seven weeks after the last DSS cycle (Figures 11C, and D).

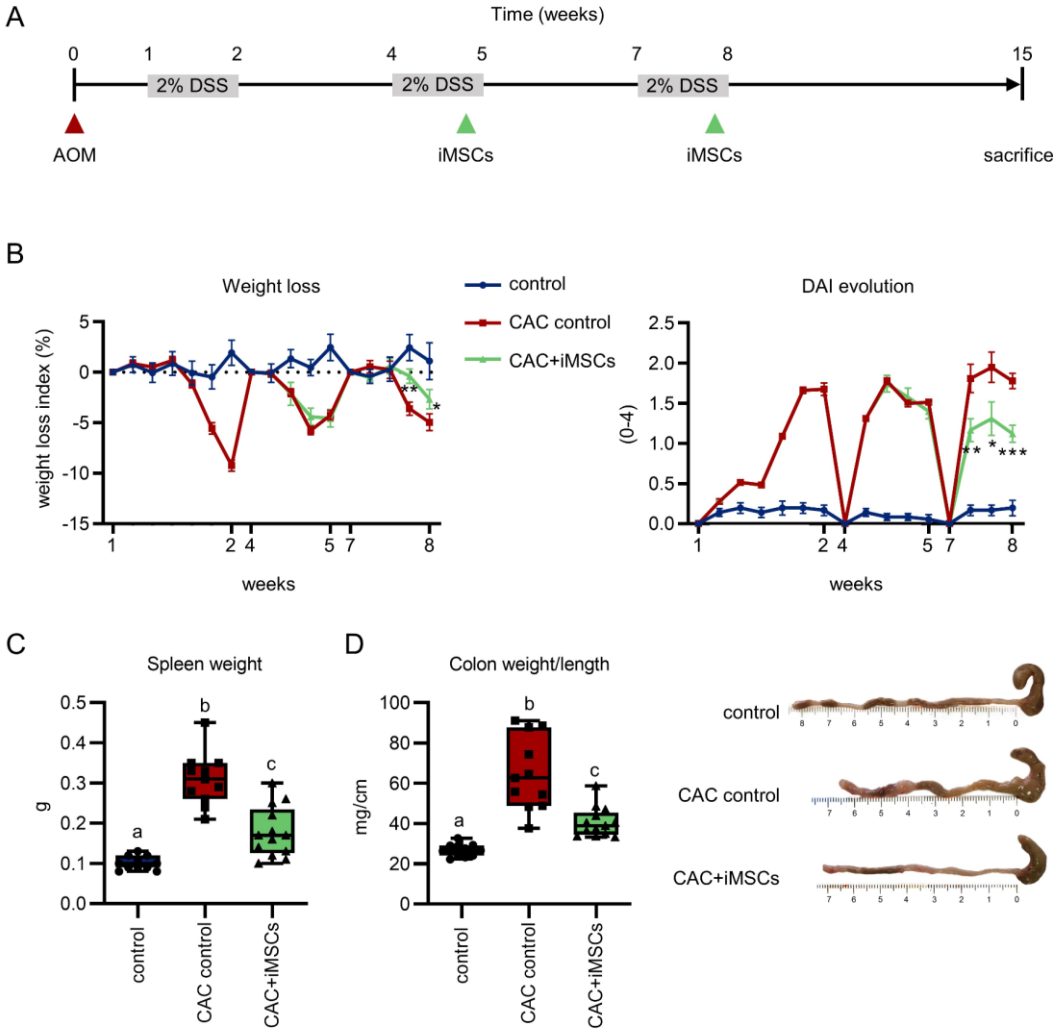

Figure 28. iMSC administration at the peak of colitis reduces disease severity in the AOM/DSS model. (A) *To induce the development of CAC, mice (n=13) were injected intraperitoneally with 10 mg/Kg of AOM. One week after, they received 2.5% DSS in the drinking water ad libitum in three different cycles with two weeks of sterile water between cycles. iMSCs ($0.5x10^6$/mouse) were injected intraperitoneally (n=13) at the peak of the second and third cycles*

of DSS. Mice receiving tap water instead of DSS were used as control mice (n=12)/group. ***(B)*** *Weight loss index (left) and Disease Activity Index (right) were determined daily during the three DSS cycles.* ***(C)*** *Spleen weight and* ***(D)*** *Colon weight/length (left) were determined on week 15, after the euthanasia of mice. Before caecum removal, photos of the colons from the three groups were taken (right). Data are expressed as mean(SEM). CAC+iMSCs group significantly differs from the CAC control group (P < 0.05). * =P < 0.05, **=P <0.01, ***=P<0.001 vs. CAC control mice. Different groups with different letters (a-c) show significant differences (P < 0.05).*

11. iMSC ADMINISTRATION TO AOM/DSS-TREATED MICE REDUCES TUMOR NUMBER/SIZE

In this model, tumor development can normally be detected about 6 to 8 weeks after AOM injection and administration of 2-3 cycles of 3% DSS. The implementation of endoscopic equipment for small animals has enabled the monitoring of tumour development in individual animals without the necessity of their sacrifice. For that purpose, the week before the sacrifice of the mice, we performed a colonic endoscopy (n=4-5) to evaluate the extent of tumor development, using a scoring system of tumor size developed by Becker and colleagues (2006) (304), as described in the materials and methods section. Mice receiving iMSCs exhibited a significantly reduced tumor size grade (Figure 29A). In addition, an endoscopic analysis of colitis severity showed a reduction in intestinal inflammation in iMSC-treated mice (Figure 29B) which is in accordance with the DAI, and colon weight/length ratio previously mentioned.

After sacrifice, colons were opened longitudinally and tumor load and size assessed. Tumor volume was then calculated as detailed in the materials and methods section. In line with the predominant localization of CRC in humans AOM/DSS induced tumors were located in the distal part of the colon and rectum (Figure 29C). Moreover, comparable to their human counterparts, AOM-induced tumors showed a polypoid-like growth. We observed that iMSC-treated mice had significantly fewer tumors, compared to untreated AOM/DSS mice (Figure 29D). In contrast to other studies ((280-282, 323-325), we also found that tumors in iMSC-treated mice were significantly smaller (Figure 29E, and F), compared to those of untreated AOM/DSS mice.

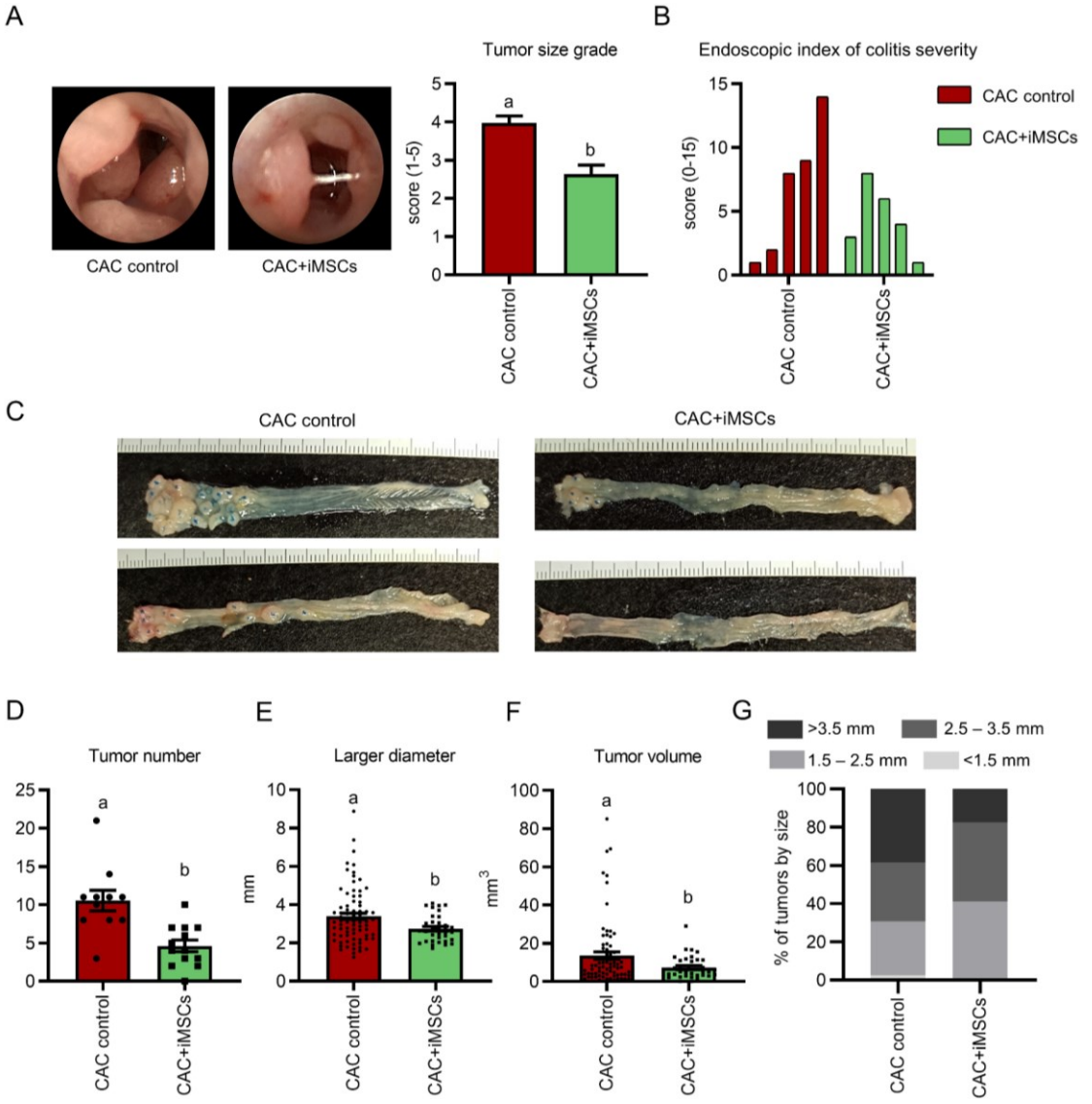

Figure 29. iMSC administration to AOM/DSS-treated mice reduces tumor number and size. ***(A)*** *One week before mice sacrifice colonoscopy was performed in 4-5 mice/group and. Representative images were taken (left) and tumor size grade (right) and* ***(B)*** *colitis severity in colonoscopies were analysed as described by Becker C et al. (2007) (304).* ***(C)*** *Representative images of colons removed from CAC control (left) and CAC+iMSCs (right) mice after their sacrifice. Then,* ***(D)*** *tumor number,* ***(E)*** *tumor larger diameter,* ***(F)*** *tumor volume and,* ***(G)*** *tumor size distribution were assessed. Groups with distinct letters (a-b) show significant differences (P < 0.05). Values are represented as mean (SEM).*

12. EFFECT OF IMSCS ON COLONIC TISSUE INFLAMMATION, TUMOR PROGRESSION AND APOPTOSIS

At the day of sacrifice, representative colonic specimens (n=6) were taken precisely 1 cm from the rectum and transversal colon sections were processed as previously described to perform a

H&E staining. Then, the stage of development of the tumors was assessed by a pathologist. In the case of CAC control samples, 5 out of 6 presented at least one polypoid adenocarcinoma covering almost the whole colonic lumen (data not shown). Nevertheless, the presence of tumors in iMSCs treated mice was less frequent - only 1 sample out of 6 presented a tumoral mass, which correlates with the previous tumor load data. In general, tumors were classified as polypoid adenocarcinomas in situ, since tumor invasion into muscularis mucosae was only evident in two samples (one from each group). The epithelial compartment showed to have lost cellular polarity and a cribriform pattern with intraglandular necrotic debris. When it comes to inflammation, the AOM/DSS control group exhibited a lower number of goblet cells combined with areas of edema and ulceration and bigger areas of lymphoplasmacytic infiltration. These data suggest that late iMSCs administration at the peak of the disease induced a protection against a further DSS cycle and exerted a sustained suppression of the intestinal inflammation.

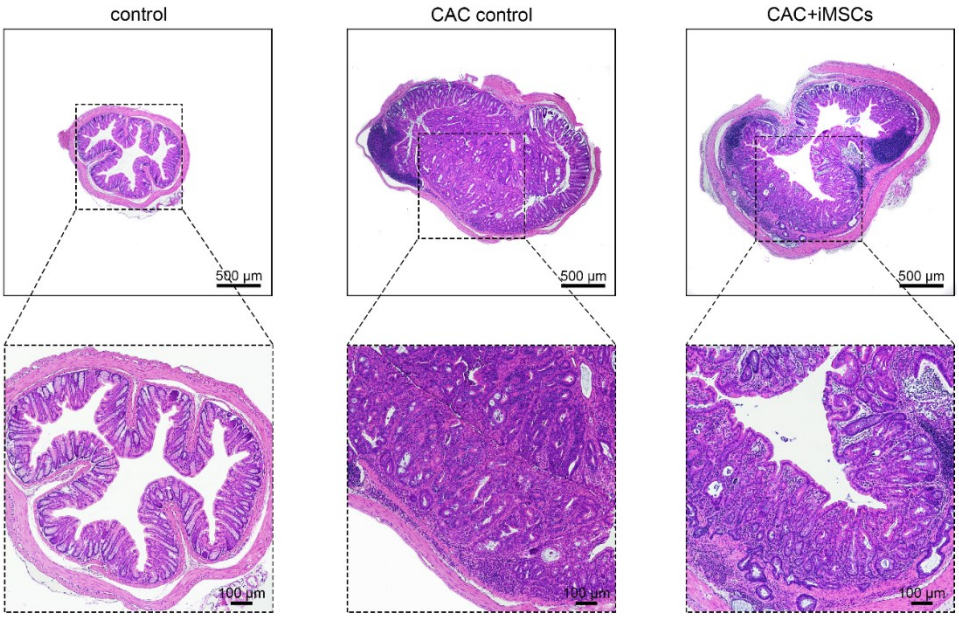

***Figure 30. Histological H&E sections of representative colonic samples**. (**Left**), representative colonic section of a control mouse in which normal tissue architecture is completely conserved, (**middle**), representative colonic section of a CAC control mouse where we can observe a bigger diameter colon size when compared to the healthy control. In the higher magnification image, we can observe the above mentioned cribriform pattern together with intraglandular necrotic debris and a neoplastic stroma, and (**right**), colonic section of a iMSC-treated mouse in which we can observe an atypical glandular disposition in combination with some glandular infiltration to the muscularis mucosae. Also, signs of inflammation are present but tissue architecture is, in general, better preserved.*

Despite the strong anti-inflammatory effects and the reduction of tumor burden in the colon of iMSC-treated mice, we could not detect the iMSCs presence in the distal colons by IHC employing an anti-human nuclei specific antibody. As shown in Figure 31, iMSCs positive control was

properly stained with the AF488 anti-human nuclei antibody. Nevertheless, any positive signal was detected in iMSCs-treated mice colons (bigger images) when compared to CAC control sections (smaller images) (Figure 31A).

Also, to further understand the mechanisms involved in the iMSCs-mediated protection and subsequent reduced carcinogenesis, a basic cellular function, as it is apoptosis, was evaluated by the TUNEL assay (Figure 31B). We found that cell death was significantly higher in CAC control mice when compared to healthy control ones. In turn, iMSCs treated mice presented in-between cell death levels (Figure 31C). These data correlate with the H&E histological findings described above, and as described by Koliaraki et al. (2015), decreased levels of apoptosis indicate a reduction in the tissue damage typically observed after a DSS challenge (268). This leads to a lower urgency of compensatory proliferation and so, could be related with a reduced dysplasia.

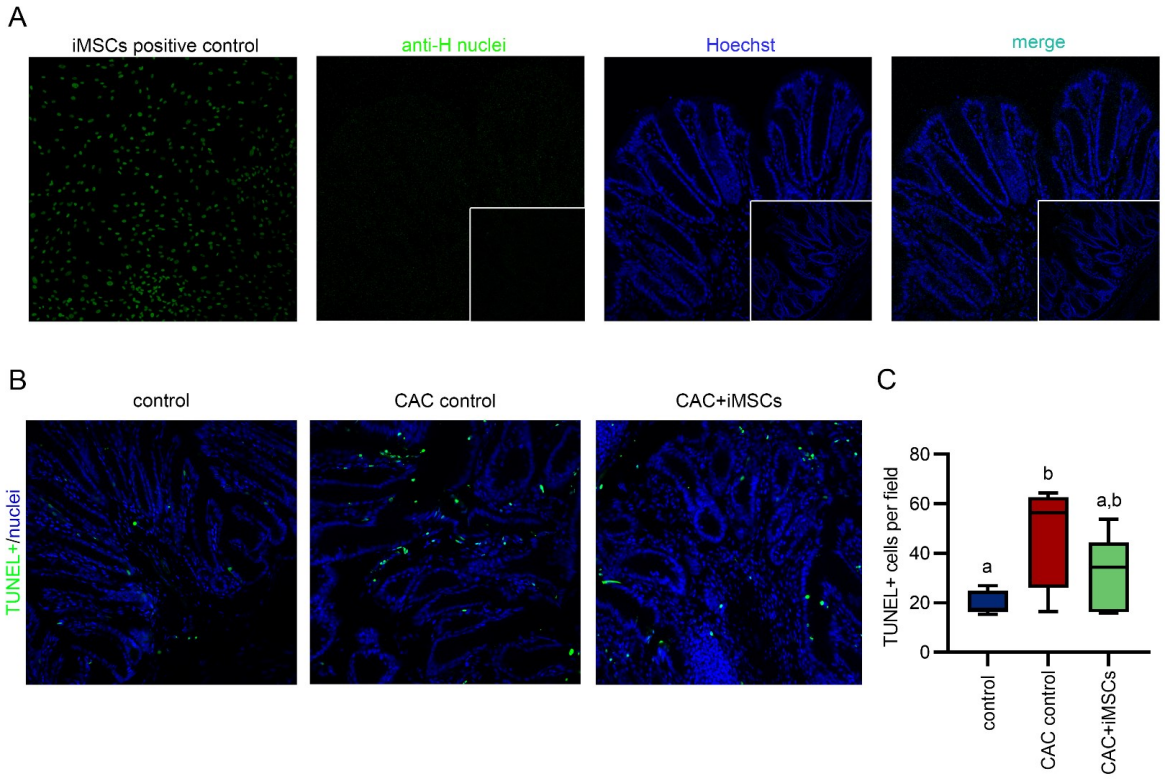

Figure 31. Treated CAC colon sections lack iMSCs homing and present a reduced cell death. *(**A**) Colonic tissue sections from iMSC-treated mice (bigger images) showed no iMSC homing in comparison with the untreated CAC negative controls (smaller images). A iMSCs culture was used as positive control (leftmost image). (**B**) Representative images of TUNEL stained colon sections from control, CAC control and CAC+iMSCs experimental groups showing cell death through apoptosis. Apoptotic cells are stained in green and nuclei in blue (Hoechst 33342). (**C**) The graph shows TUNEL⁺ cells/field, and data are represented as ±SEM range, median (middle line) and extreme values (whiskers) of 4-5 mice/group. Groups with different letters (a-b) show significant differences (P < 0.05).*

13. iMSC ADMINISTRATION DOWNREGULATES INFLAMMATORY MEDIATORS THAT DRIVE TUMORIGENESIS.

We next analyzed the expression of immune/inflammatory mediators that promote CAC in the AOM/DSS model and also, in IBD patients. Gene expression analysis in the colonic tissue showed that the proinflammatory cytokines *il-6* and *tnf-α* were significantly increased in CAC control mice, whereas iMSC-treated mice exhibited reduced levels (Figure 32A). Similarly, both *il-17* and *il-23* (p19 subunit), which are known cytokines that promote CAC development (255, 256), were significantly upregulated in CAC control mice in contrast to healthy controls, and presented a lower expression in iMSC-treated mice (Figure 32A). In addition, the IL-23-inducible gene *mmp-9*, involved in extracellular matrix degradation, and *angiopoietin-2* (*Angpt-2*), that participates in angiogenesis, were reduced in iMSC-treated mice in comparison to CAC untreated ones (Figure 32A). Both are prognostic factors associated with poor survival in CRC (255, 326).

The expression/activation of some relevant mediators of inflammation-induced cancer in mice and humans like IL-6 (Figure15C, left), pSTAT3/STAT3 (Figure 32C, right), COX-2 (Figure 32E, left) pAKT/AKT (Figure 32E, right), β-catenin (Figure 32G, left) or Bax/Bcl-2 (Figure 32G, right) were analyzed by Western blot in colonic protein lysates from control, CAC and iMSC-treated mice (n=4). Overall, we found a significantly higher expression of these proteins in CAC control mice when compared to healthy control mice. Only, in the case of IL-6 differences in expression levels were slight (Figure 32C, left). However, the expression or activation of mediators was significantly reduced in the colon of iMSCs treated mice (Figure 32C, and D). It is well known that DSS acts disrupting the intestinal epithelial barrier, which results in the exposure of the submucosa to various luminal antigens and the induction of high expression levels of inflammatory molecules such as cyclooxygenase-2 (COX-2), inducible nitric oxide synthase (iNOS), or IL-6 (265, 266, 302). In the AOM/DSS mice model, augmented IL-6 levels and COX-2 promote the activation of the JAK1-2/STAT-3 and PI3K/AKT signaling pathways, leading to an increased tumoral epithelial proliferation, resistance to apoptosis and so, tumor multiplicity (217). Administration of iMSCs to AOM/DSS treated mice significantly decreased the expression of all these intermediaries (Figure15 B, C, D and E).

One of the many other molecular features that the AOM/DSS model of CAC recapitulates of human CRC, is the dysregulation of the Wnt/β-catenin axis in part due to mutations in the *Ctnnb1* gene, overexpression of COX-2 and dysregulation of some miRNAs expression (208, 264, 327-329). Despite the described COX-2 upregulation in CAC mice, the CRC-associated low-molecular weight (LMW) β-catenin was not significantly increased when compared to CAC untreated mice (330). However, an increasing tendency could be observed (Figure 32G, right). Interestingly, in the case of Bax/Bcl-2 ratio we found a statistically significant higher ratio in CAC control mice in comparison to the CAC+iMSCs group. These data correlate with the previous TUNEL assay findings (Figure 31D), indicating augmented levels of apoptosis in colonic cells. Taken together,

these data suggest that even late administration of iMSCs can prevent the inflammation-induced dysregulation of tumor promoting pathways.

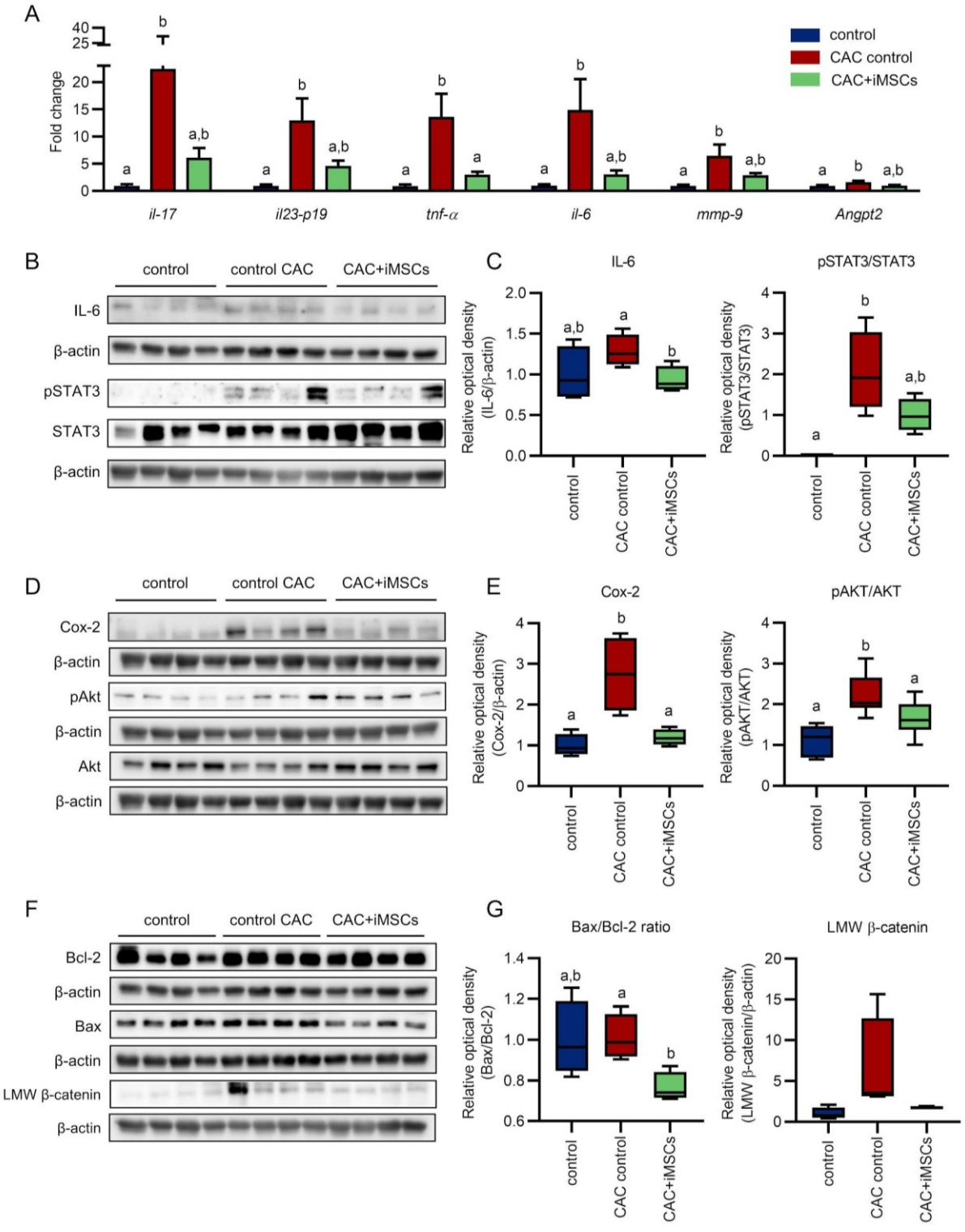

***Figure 32**. iMSCs downregulate the expression of some key molecules that drive CAC development and progression in AOM/DSS mice. (A)Total RNA was extracted from colons collected on the day of sacrifice and the gene expression of various inflammatory mediators was*

determined by RT-qPCR. Concretely, gene expression of the cytokines Il-17, Il-23-p19, Tnf-α, Il-6, mmp-9 and Angpt2 was assessed. Data expressed as mean(SEM) of n=8 mice/group. The effect of iMSC administration on some key proteins was evaluated by western blot in colonic lysates (n=4). Specifically, we performed a (B) IL-6, pSTAT3, STAT3, (D) Cox-2, pAkt, Akt and (F) Bcl-2, Bax and LMW β-catenin western blot analysis and then calculated the corresponding expression of these proteins by (C),(E) and (G) densitometric analysis, respectively. Except for the case of the protein ratios pSTAT3/STAT3 and pAkt/Akt, β-actin was used as loading control. Groups with different letters (a-b) exhibit statistically significant differences (P<0.05). Graphs without letters reflect no significant differences between groups. Box plots represent ±SEM range, median (middle line) and extreme values (whiskers).

14. AOM/DSS CONTROL MICE PRESENT HIGHER AMOUNTS OF INFLAMMATORY Ly6C^{HI} MHCII^{-} CCR2^{+} MONOCYTES

We aimed to characterize the mechanisms by which iMSCs lessen AOM/DSS driven CAC development. With that purpose, at the day of euthanasia, blood was drained from mice (n=5) and the evaluation of monocytic subpopulations was performed through flow cytometry analysis. The gating strategy is described in the materials and methods section. The analysis of blood leukocytes in blood showed clear differences between CAC control and healthy control mice, with the number of circulating CD11b^{+} myeloid cells being significantly raised in the latter (Figure 33A). Importantly, the CD11b^{+} predominant population was the monocytic-macrophagic one, as shown in Figure 33B, and C.

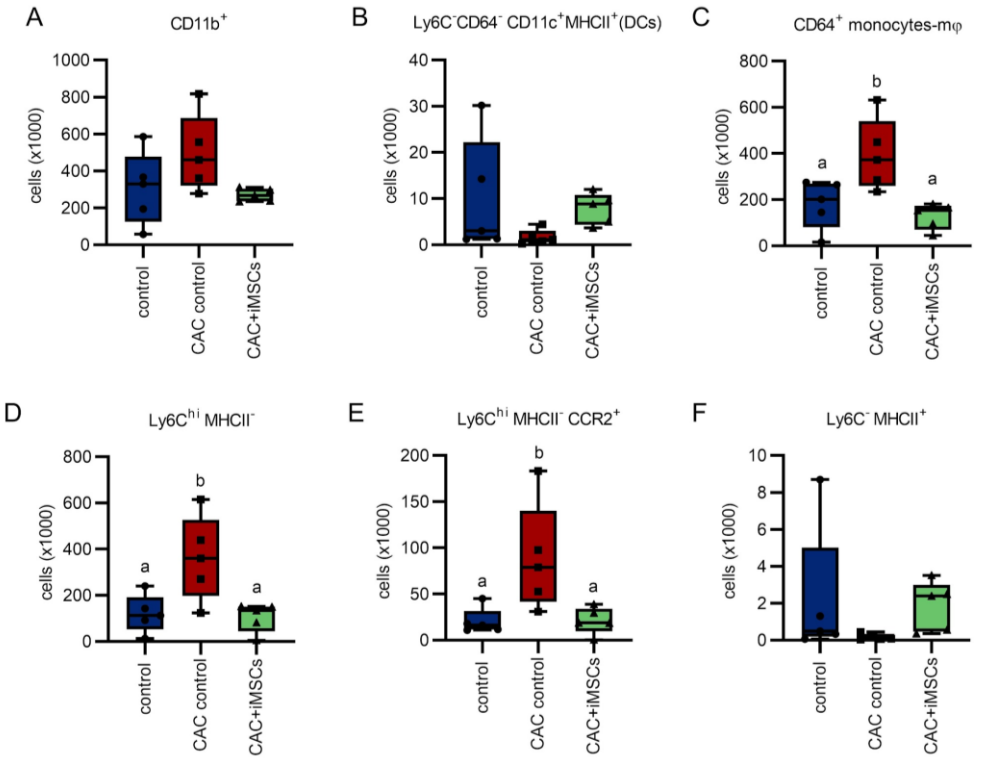

Figure 33. iMSC administration modulates the monocyte subpopulations composition in blood of AOM/DSS mice. *Total number of* ***(A)*** *CD11b$^+$ myeloid cells,* ***(B)*** *Ly6C$^-$ CD64$^-$ CD11c$^+$ MHCII$^+$ dendritic cells, and (**C**) CD64$^+$ monocytes-macrophages in blood of CAC mice. (**D**) Total number of Ly6C^{hi} MHCII$^-$ monocytes in the three different groups. (**E**) From the latter, a high number also expressed the CCR2 chemokine receptor, known to be fundamental in monocyte migration to inflamed tissues. (**F**) Ly6C$^-$MHCII$^+$ non-classical total monocytes present in the three experimental groups. Box plots represent ±SEM range, median (middle line) and extreme values (whiskers). Groups with different letters (a-b) exhibit statistically significant differences (P<0.05). Graphs without letters reflect no significant differences between groups.*

During homeostasis Ly6C^{hi}MHCI$^-$ monocytes are known to travel to the intestine in a CCR2-CCL2 dependent manner. Once in the lamina propria, they maturate and ensure tissue resident macrophages replenishment (165, 175, 331). In figure 33 we show an accumulation of Ly6C^{hi}MHCII$^-$ (classical) inflammatory monocytes (Figure 33E) that also expressed CCR2$^+$ (Figure 33F) in CAC control mice blood in comparison with healthy control and iMSCs treated animals. Thus, the accumulation of this population confirms higher levels of inflammation in CAC control mice and supports iMSCs antiinflammatory activity. Although no significant differences were found, marked tendencies appeared in other relevant immune populations such as dendritic cells (Figure 33B) or non-classical Ly6C$^-$ MHCII$^+$ macrophages (Figure 33G). In both cases, iMSCs treated mice presented a number of cells similar to that found in healthy control mice.

15. iMSC ADMINISTRATION MODULATES THE INNATE IMMUNE CELL COMPOSITION IN THE DISTAL COLON IN AOM/DSS MICE

In view of the described blood findings, we also aimed to analyze the immune cell composition in the colons of healthy, CAC, and iMSC-treated mice. For that, we dissociated colonic tissue from each group (n=3-4) and performed a flow cytometric analysis, assessing several innate immune cell populations. Consistent with the increased colon weight of CAC control animals (Figure 28D), total number of intestinal cells was also increased in CAC control mice (media=16x10^6 cells) in comparison with healthy controls (media = 3.8x10^6 cells) and the iMSC treated group (6.9x10^6 cells). Although we did not observe any statistically significant differences between groups - mainly due to low sample number - some of the analysed populations presented clear tendencies. Among them, CD11b$^+$ myeloid cells (Figure 34B), neutrophils (CD45$^+$/CD11b$^+$/Ly6G$^+$) (Figure 34C), eosinophils (CD45$^+$/CD11b$^+$/Ly6G$^-$/MHCII$^-$/SSC^{hi}) (Figure 34D) and Ly6C^{hi}MHCII$^-$ monocytes (Figure 34F), presented the bigger differences among the CD45$^+$ leukocyte compartment (Figure 34A). Importantly, these populations were also the most abundant in colonic tissue. As previously reported, neutrophils and eosinophils are good estimators of the grade of inflammation, being usually increased in colonic samples of ulcerative colitis (332-334). These correlates with our results, in which neutrophil and eosinophil cell number was increased in the CAC control group in comparison with healthy and iMSC-treated animals (Figures 17C, and D).

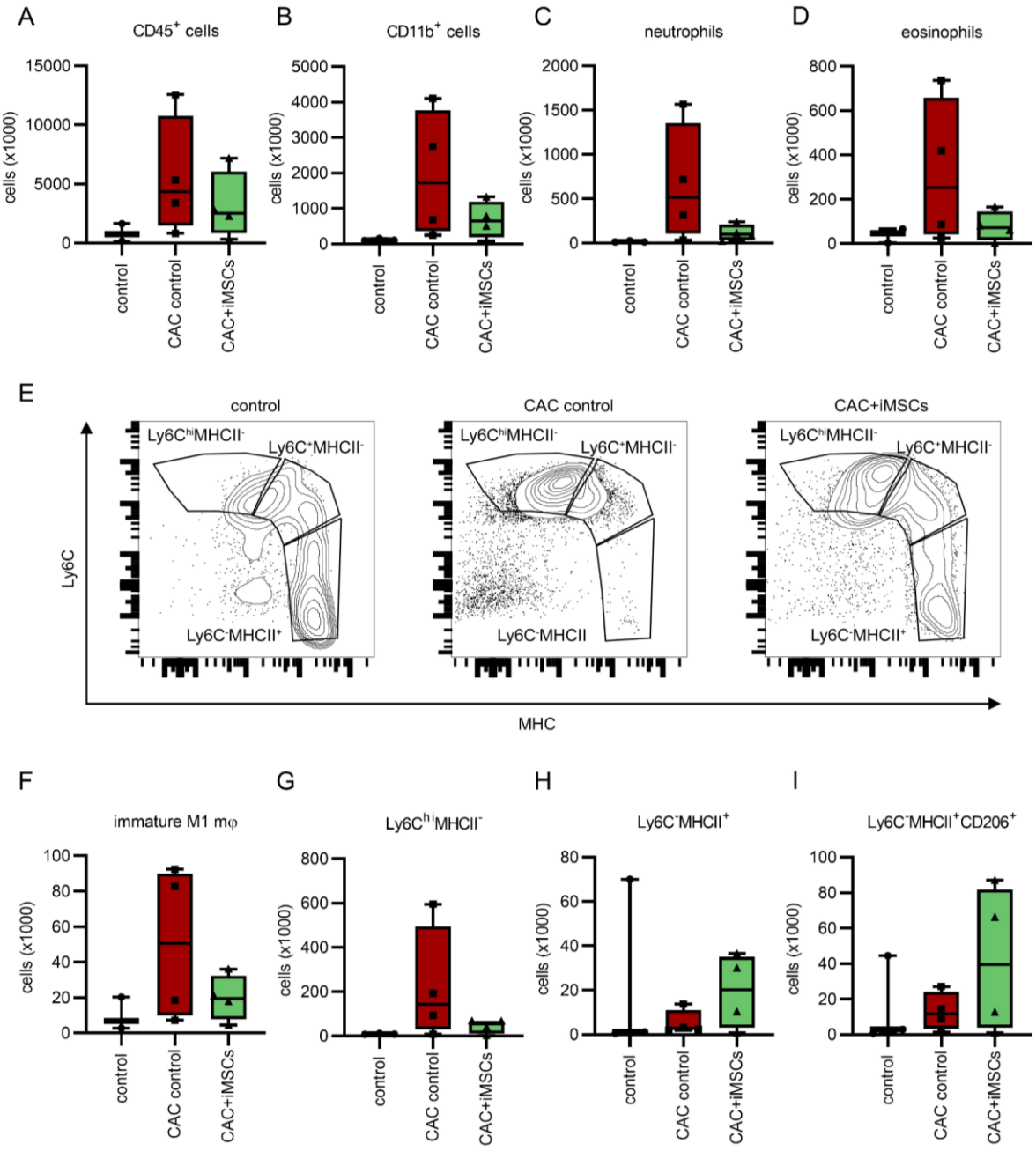

Figure 34. The monocytic-macrophage compartment appears to be altered in colonic tissue of CAC mice. *Total number of* ***(A)*** *CD45⁺ cells,* ***(B)*** *CD11b⁺,* ***(C)*** *neutrophils and,* ***(D)*** *eosinophils in colonic tissue of AOM/DSS treated mice. (****E****) Representative gates from control, CAC control and CAC+iMSCs mice showing the F4/80⁺ monocyte-macrophage differentiation waterfall. Total number of (****F****) immature CD86⁺ macrophages, (****G****) Ly6C^{hi}MHCII⁻ and, (****H****) Ly6C⁻MHCII⁺ monocytes and, (****I****) mature Ly6C⁻MHCII⁺CD206⁺ macrophages in the three experimental groups. Graphs without letters reflect no significant differences between groups.*

Also, as stated above, it has been demonstrated that the CCL2-CCR2 axis mediates the recruitment of Ly6C^{hi} monocytes to the intestine both in steady state and in inflammatory conditions. Once in the lamina propria, Ly6C^{hi} monocytes differentiate into Ly6C⁻MHCII⁺ tissue

resident macrophages through a monocyte-macrophage differentiation waterfall. In an inflammatory context, this maturation waterfall is arrested at the Ly6C^{hi}MHCII^{-} stage and these cells accumulate as inflammatory macrophages with a M1-like inflammatory phenotype that supports the preexistent inflammatory milieu (168). This monocyte-macrophage maturation waterfall is shown in Figure 34E, which illustrates the accumulation of the initial Ly6C^{hi} population in the inflamed colon of CAC animals as well. Again, the administration of iMSCs almost restored the balance of newly recruited/mature macrophages in the colon, similar to that of healthy mice (Figure 34G, and H). In accordance with the previously described, M1 (CD86^{+}) immature macrophages (variable expression of F4/80, MHCII and Ly6C), we did observe an increase of this population in the CAC mice in comparison to tumor free and iMSC-treated mice (Figure 34F). In contrast, the quantity of tissue resident-like Ly6C^{-} MHCII^{+} CD206^{+} macrophages (Figure 34I) was higher in iMSC-treated animals in comparison with both control groups. In summary, our data highlight a substantial modulation of innate immunity in the colons of CAC mice. Furthermore, the therapeutic capacity of iMSCs could correlate with their ability to skew the composition of innate immune cells towards that observed in healthy mice. Nevertheless, no significant differences were obtained.

16. THE T CELL COMPARTMENT COMPOSITION IN MESENTERIC LYMPH NODES (MLNS) FROM AOM/DSS CONTROL MICE DIFFERS FROM THAT IN IMSC-TREATED MICE

We also aimed at characterising the immune cell population at local secondary lymphoid organs (MLNs). With that purpose, cells isolated from MLNs were assessed by FACs (n=5). Interestingly, flow cytometry analysis showed that the CD4^{+} cell number was slightly higher in the CAC control than in the CAC+iMSCs group (Figure 35A). Th1 (CD4^{+}IFN-γ^{+}) and, specially, Th2 (CD4^{+}IL4^{+}) cells were strongly increased when compared to healthy controls (Figure 35B, and C). The last being directly related with the onset of ulcerative colitis (buscar referencia). iMSC treatment partially restored Th2 (Figure 35C) cells levels and, to a lesser extent, Th1 ones (Figure 35B). By contrast, Th17 (Figure 35D) and Tregs (Figure 35F) numbers were mainly increased in the CAC+iMSCs group, and intermediate levels were found in CAC control mice. Both are relevant mediators of tumorigenesis and though Th17 can have a protective role during the onset of inflammation, exacerbated Th17 responses can lead to chronic inflammation and tissue injury, promoting tumor development. On their part, Tregs control exacerbated immune responses, limiting Th17 response among others (335). Additionally, Th17/Treg ratio (Figure 35G) has been described to be altered in IBD patients(336) and, though we did not find significant differences, a marked upward tendency appeared in the CAC control group. In relation with one of the most important compartments in cancer immunosurveillance, an important increase of CD8^{+} and Tc1 (CD8^{+}IFN-γ^{+}) cells (Figure 35H, and I) was observed in CAC+iMSCs mice in comparison to CAC

control mice. In conclusion, our data point out a considerable modulation of the T cell compartment in the MLNs of AOM/DSS mice.

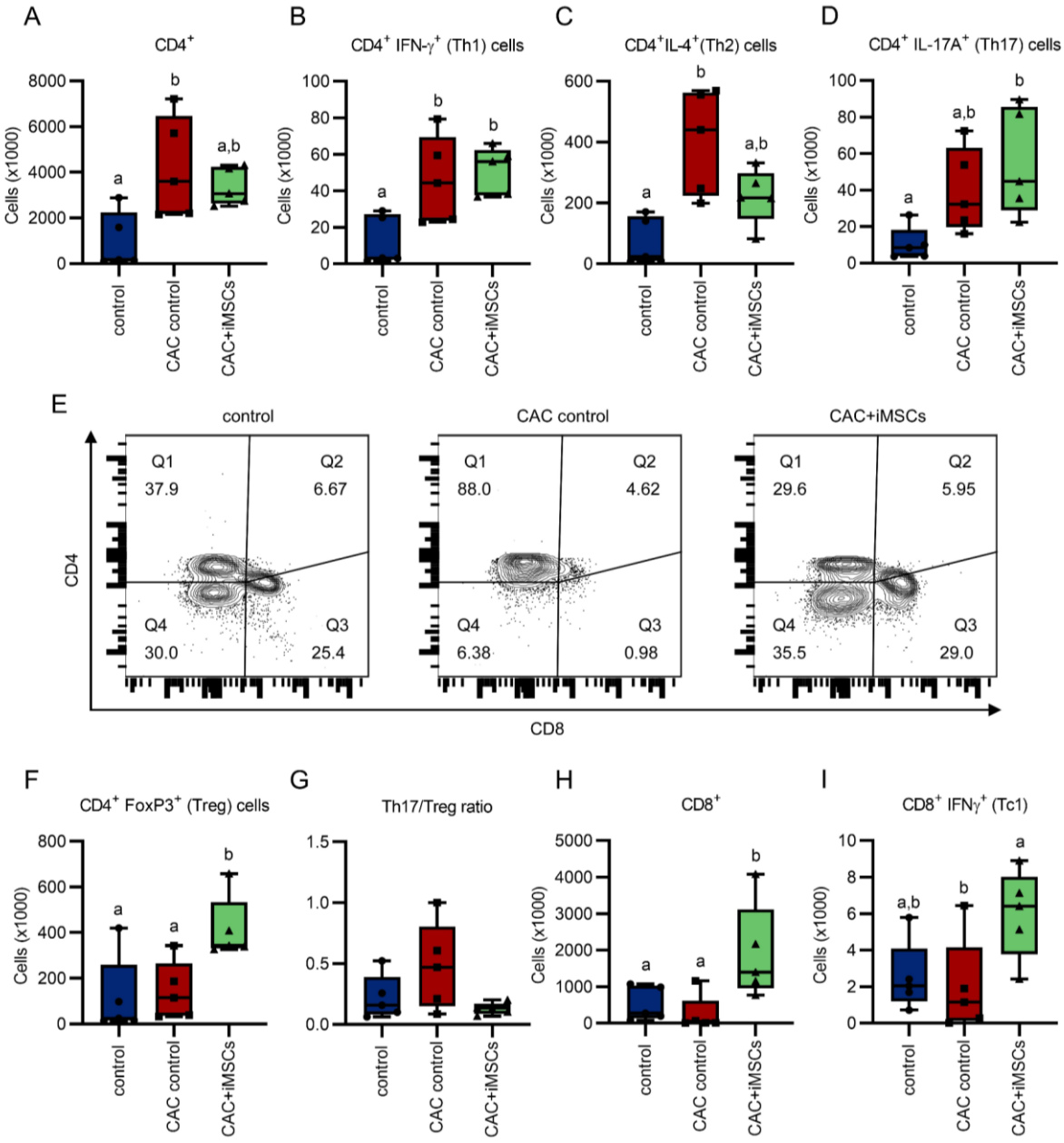

***Figure 35**. **iMSC administration modulates the T lymphocyte response in MLNs of AOM/DSS mice.** (**A**) Total CD3⁺CD4⁺, (**B**)Th1 (CD4⁺ IFN-γ⁺), (**C**) Th2 (CD4⁺ IL-4⁺), (**D**) Th17 (CD4⁺ IL-17A⁺) and (**F**) Tregs cells measured in mesenteric lymph nodes in CAC mice. (**E**) Representative gates from control, CAC control and CAC+iMSCs mice showing the CD4 vs. CD8 T lymphocyte distribution, where we can mainly observe CD4+ cells outnumber the almost missing CD8+ compartment in CAC control mice. (**G**) Resultant Th17/Treg ratio from the previous data. (**H**) Total CD3+CD8+ and (**I**)Tc1 (CD8⁺IFN-γ⁺) cells in MLNs of AOM/DSS mice. Box plots represent ±SEM range, median (middle line) and extreme values (whiskers). Groups with different*

letters (a-b) exhibit statistically significant differences (P<0.05). Graphs without letters reflect no significant differences between groups.

17. iMSCs ADMINISTRATION AMELIORATES THE GUT DYSBIOSIS IN CAC MICE

The effects of iMSCs treatment on the gut microbiota were explored since gut dysbiosis plays a crucial role in many diseases, including colorectal cancer. Thus, when faecal microbiota was evaluated by Illumina sequencing, the distribution histogram of relative abundance of taxa showed that although *Bacteroidetes* and *Firmicutes* were the most abundant phyla found in faecal microbiota other phyla including *Verrucomicrobia* and *Actinobacteria* could be crucial in this study (Figure 36A). In fact, as previously reported, the microbiome composition is altered in the AOM/DSS mice model. Accordingly, our results revealed an increase of *Firmicutes* and *Actinobacteria* abundances in CAC control mice, while the relative abundance of *Bacteroidetes* and *Verrucomicrobia* was reduced in this group (Figure 36A) in comparison to control mice. The administration of iMSCs improved these shifts to values similar to the control group (Figure 36A).

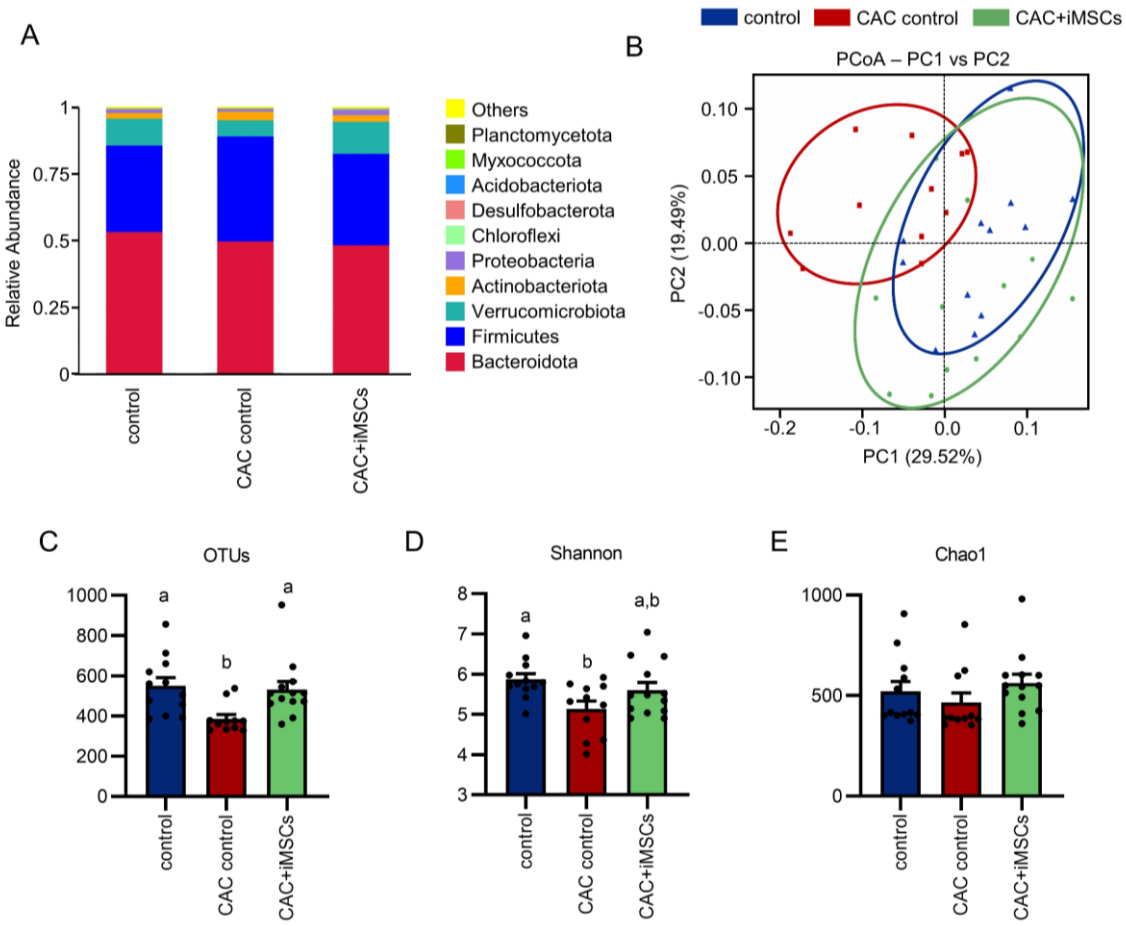

***Figure 36**. **Impact of iMSCs administration on CAC mice microbiota composition**. Concretely, it was evaluated (**A**) the effect on bacterial community at phylum level, (**B**) beta-diversity by principal coordinate analysis score plot and microbiome diversity by (**C**) Observed OTUs, (**D**) Shannon diversity and (**E**) Chao1 richness. Data are expressed as mean(SEM). Groups with different letters (a-b) exhibit statistically significant differences (P<0.05). Graphs without letters reflect no significant differences between groups.*

Additionally, the principal component analysis (PCoA) based on weighted unifrac separation resulted in different separated bacterial communities. The bacterial communities from the CAC+iMSCs mice were closer to the healthy control group than to the CAC control mice (Figure 36B). Several ecological features of the gut bacterial communities were also evaluated in the three experimental groups by different parameters including Observed OTUs (Figure 36C), Shannon diversity (Figure 36D) and Chao1 richness (Figure 36E). While any change was observed in Chao1 richness index (Figure 36E), OTUs and Shannon parameters were significantly reduced in the CAC control group compared to the control mice (Figures 36C, and E). iMSC administration was able to restore both ecological parameters to normal values (Observed OTUs: p= 0.0233; Shannon diversity: p= 0.1730) (Figures 36D, and E).

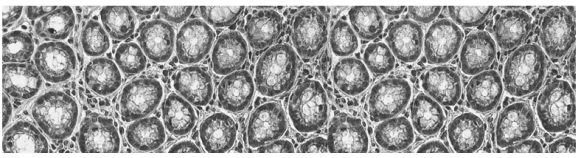

Discussion

DISCUSSION

In the intestine, epithelial cells and iMCs create a physical barrier, effectively separating the microbiome from the underlying tissues and immune system (337). Although it is well documented that iMCs play important roles in intestinal health and disease, the true nature of their immunomodulatory capacity is not clear and warrants further research. The aim of the current thesis has been to characterize the tissue regenerative and immunomodulatory capacities of human iMSCs *in vitro* and *in vivo*, in two experimental mouse models of ulcerative colitis and AOM/DSS derived cancer.

1. ISOLATION AND CHARACTERIZATION OF iMSCs

As mentioned above, MSCs from different tissues exhibit distinct transcriptomic profiles, differentiation and immunomodulatory capacities (17-21). A study by Xu et al. (showed that the BM-MSCs have a stronger osteogenic potential compared to adipose-tissue derived MSCs (ASCs), whereas ASCs are more prone to adipocyte differentiation (338). This contrasting differentiation potential correlated with the methylation status of the main transcription factors controlling MSC fate, demonstrating a tissue-specific epigenetic memory that is maintained upon *in vitro* culture. The same has been demonstrated for MSC in the intestine. Pinchuk and colleagues showed that $CD90^+$ intestinal stromal cells expressed PD-L1 and PD-L2 in situ. Importantly, PD-L1/-L2 expression was maintained on these cells upon in vitro culture and further experiments showed their importance in suppressing the proliferation of CD3/CD28-activated T cells in a cell contact-dependent manner (106). In another study, Saada showed that colon myofibroblasts (CMF) express HLA class II in situ and in vitro. Studies in vitro showed that CMFs had the ability to process and present MHC class II-restricted antigens to $CD4^+$ T cells, suggesting role as nonprofessional APCs capable of modulating mucosal immune responses (109). Taken together, these data show that MSCs retain, at least in part, their tissue specific characteristics through multiple passages in vitro, making it feasible to analyze, at least to some extent, the tissue-specific properties of iMSCs in vitro.

Evidence suggests that iMSCs derive from bone marrow-derived $gremlin^+$ MSCs (339). In this study we have isolated iMSCs based on plastic adherence, resulting in the selection of a heterogeneous collection of fibroblastic cells that probably includes fibroblasts and myofibroblasts. After 2-3 passages *in vitro* these cells adopted a homogenous phenotype ($CD31^-$ $CD34^-$ $EpCam^-$ $CD45^-$ $CD73^+$ $CD90^+$ $CD105^+$ Vim^+), similar to that of MSCs from bone marrow and adipose tissue (340, 341), which was maintained in culture upon serial passaging. They also showed the ability to form discrete colonies (CFU-F) when seeded at low density, and possessed the capacity to differentiate into adipocytes, osteoblasts and chondroblasts, following then the minimal criteria defined by the ISCT to be considered MSCs (15).

2. COCULTURE OF iMSCS WITH PBMCS

Several reports have shown a role of human iMCs in intestinal immune tolerance. Firstly, human colonic myofibroblasts promote intestinal tolerance through the expansion of $CD4^+CD25^{high}Foxp3^+$ regulatory T cells (107). Secondly, human colonic $CD90^+$ stromal cells express programmed death-ligand (PD-L)-1 and PD-L2 which they use to suppress the proliferation of $CD45RA^+CD4^+$ T cells in a cell contact–dependent manner (106). We found that iMSCs could inhibit the proliferation of PBMCs (both $CD4^+$ and $CD8^+$ T cells) induced by PHA-L. Pre-stimulation of iMSCs with TNF-α and IFN-γ increased their immunosuppressive capacity *in vitro*, which correlated with an induction of IDO mRNA expression. IDO is highly up-regulated in the inflamed intestinal mucosa, but its expression has primarily been detected in intestinal dendritic cells and colon epithelial cells in IBD patients. Inhibition of IDO increases disease severity, while TLR9-mediated induction of IDO protects against experimental colitis (341, 342) highlighting the relevance of IDO in regulating intestinal inflammation.

While IDO is a well-known IFN-γ-inducible inhibitor of T cell proliferation used by human BM-MSCs and ASCs (340, 343), to our knowledge, no study has analysed the expression/function of IDO in iMSCs. In addition to the transcriptional induction of IDO in iMSCs, we found a significant increase in IDO enzyme activity in the PBMC:iMSC cocultures. However, inhibition of IDO did not result in a complete reversion of suppression, indicating that iMSCs use additional mechanisms to inhibit T cell responses. Interestingly, we found that some iMSC cell lines depended to a higher degree on IDO, suggesting that their immunomodulatory capacity and its underlying mechanisms vary with donor, and most likely, experimental conditions (344). In summary, our data demonstrate that iMSCs can use IDO to inhibit T cell proliferation.

While IDO activity would be beneficial in suppressing inflammation/immune responses in IBD, it has been shown that IDO is expressed by cancer-associated fibroblasts in human esophageal cancers, likely contributing to an immunosuppressive tumor microenvironment (345). Thus, context is of key importance when modulating IDO activity in human disease. Finally, human BM-MSCs cells have been shown to exhibit broad-spectrum antimicrobial effector function mediated by IDO (295). Whether iMSCs/iMCs, via IDO, can play a role in shaping the gut microbiota is unknown.

3. iMSCS MODULATION OF CULTURED THP-1 CELLS

Although iMCs have been shown to promote mucosal tolerance, several reports have highlighted a pro-inflammatory role of iMCs in IBD. Kinchen and colleagues observed a remodeling of the colonic mesenchyme in IBD patients characterized by the emergence of a pro-inflammatory iMC population which prevented epithelial healing and promoted disease (199). Furthermore, West and colleagues showed that oncostatin M (OCM) is up-regulated in IBD patients compared to

healthy controls which induces a pro-inflammatory response in intestinal mesenchymal cells (346). Importantly, high levels of OCM correlated with a decreased responsiveness to anti-TNF-α therapy. Recently, Martin et al. (201) and Smillie et al. (200) characterized inflammatory cell modules in the affected intestinal mucosa of CD and UC patients which associate with resistance to anti-TNF-α therapy. In addition to epithelial and immune cells, these modules contained inflammatory iMCs with the ability to recruit monocytes to the site of inflammation. Monocytes/macrophages play important roles in the pathogenesis of IBD (347) and recent data suggest that anti-TNF-α monoclonal antibodies exert their beneficial effect on IBD through the induction of immunomodulatory macrophages (348). BM-MSCs and ASCs have previously been shown to induce anti-inflammatory macrophages with which ameliorate experimental sepsis and colitis (349, 350). However, few studies have analyzed the effect of human iMSCs on macrophage polarization (351) and to this end we employed the human leukemia monocytic THP-1 cell line which is an adequate model for analyzing macrophage polarization into the M1 and M2 activation states (352). We show that iMSCs, as well as their conditioned medium, could inhibit the LPS-induced production of TNF-α by THP-1-derived macrophages. This is in agreement with previous studies, where murine and human BM-MSCs and ASCs induce M2 macrophages, mainly via production of PGE_2 (320). How iMSCs reduce the production of TNF-α by THP-1 macrophages is not known. We found that TNF-α/IFN-γ induced the expression of several genes involved in the polarization of M2 macrophages, including TSG-6, HGF and IL-6 (320). However, additional studies are necessary to specifically evaluate the involvement of these factors in the immunomodulatory function of iMSCs. Further insight into how iMSC can induce anti-inflammatory macrophages could help in re-educating the inflammatory iMSC populations that appear in IBD patients.

4. EFFECT OF IMSCS ADMINISTRATION IN A MOUSE MODEL OF ULCERATIVE COLITIS

In order to confirm the immunomodulatory and tissue regenerative properties of iMSC in vitro, we decided to analyze their effects *in vivo*, using the DSS-model of acute intestinal inflammation in C57BL/6J mice. This is a convenient and reproducible experimental model that resembles the main manifestations of IBD, concretely, this model has been used to study the innate immune mechanisms in intestinal inflammation and simulates human IBD by promoting an exaggerated Th2 immune response (). Due to similarities in intestinal development, the diversity of species within the Firmicutes, Bacteroidetes, and Proteobacteria phyla, and the nature of the immune responses between mice and humans, these models have markedly advanced our understanding of human IBD (353). Although only a fraction of all biologics that have been evaluated in experimental colitis has reached the clinic (including monoclonal antibodies targeting TNF-α, IL-12/IL-23, and α4-integrin), a better knowledge of the characteristics of the employed models and an improved targeting specificity will surely increase the future translational success rate (354, 355). The use of the mouse colitis model allows a precise control of the induction and progression

of the disease, something that cannot be replicated easily using human biopsies/resections from IBD patients.

It needs to be pointed out that we have evaluated the human iMSC in a xenogeneic setting. Some reports have highlighted species incompatibilities that prevent the proper evaluation of human MSCs in rodent models (343, 356). A notable difference is that murine MSCs use iNOS to inhibit T cells, whereas human MSCs use IDO (357). Despite this, human MSCs have been shown to inhibit the proliferation of murine T cells, in part via PGE_2 (358, 359). In addition, the immunomodulatory and tissue regenerative capacity of human MSCs has been evaluated in multiple xenogeneic mouse models of disease with successful results, comparable to those of murine MSCs (360). These data suggest that xenogeneic models for the evaluation of human MSCs are valid and robust. Still, care needs to be taken when evaluating data from xenogeneic experimental settings.

We injected the iMSCs intraperitoneally since this route has proven the most adequate based on therapeutic efficacy and migration of MSCs towards the inflamed intestine (361, 362). We show for the first time that injection of iMSC, one day after the start of DSS administration, significantly decreased the colitis severity and weight loss. Injection of iMSCs resulted in a reduction of colonic inflammation, evidenced by a decreased immune infiltration and down-regulation of inflammatory mediators in the colon. In addition, we observed an increment, although not significant, in the *Argl/Inos* ratio, suggesting a polarization of macrophages towards an M2 response, which is in agreement with our in vitro results using THP-1 cells. These data are in accordance with the anti-inflammatory effects seen using MSCs from different tissues in experimental colitis (363) and again shows that iMSCs from the healthy intestine possess immunomodulatory capacity.

We found that administration of iMSCs protected the intestinal epithelial barrier against the DSS-induced damage, which is consistent with our observation that the iMSC-CM can promote wound regeneration *in vitro*. This is also supported by recent studies demonstrating that murine $CD90^+CD34^+gp38^+$ iMCs are important for the maintenance of intestinal epithelial stem cells (364, 365). One possible mediator providing this protection could be PGE_2, which is known to stimulate epithelial growth, inhibit epithelial apoptosis during insults and potentiate WNT-signaling (53, 366). However, we found higher levels of proliferating ($Ki67^+$) cells in the colons of DSS mice compared to iMSC-treated mice which is in contrast to studies showing an increased intestinal epithelial proliferation after MSC administration to colitic mice (367). Nevertheless, several studies have demonstrated that DSS-induced epithelial damage is followed by a compensatory increase in epithelial cell proliferation (368-371). Consequently, our data suggests that, in our experiments, iMSC administration does not promote intestinal barrier integrity by promoting epithelial cell proliferation, but rather by protecting against DSS-induced tissue damage.

We thus proceeded to evaluate the extent of apoptosis in the colonic tissue in our experimental groups. Although there was an increase in TUNEL-positive/apoptotic cells between healthy and

DSS-treated mice, we unexpectedly found a significantly higher number of TUNEL-positive cells in the iMSC-treated group compared to DSS mice. Although surprising, this agrees with several studies demonstrating that MSCs, via IDO (372) or FAS-L (373) can induce apoptosis of T cells, playing a pivotal role in their ability to ameliorate colitis (373, 374). In addition, it has also been reported that MSC-derived membrane particles can induce selective apoptosis of pro-inflammatory monocytes (375). Although our data show that iMSC administration results in a clear improvement of the integrity of the intestinal barrier in colitic mice, further investigations are needed to understand the mechanisms behind this observation.

Interestingly, several recent studies have shown that BM-MSCs can be polarized into pro-inflammatory “MSC1” or anti-inflammatory “MSC2” phenotypes when primed via TLR4 and TLR3, respectively (39, 376). Regarding iMCs, Beswick recently reported that the expression of PD-L1 on iMCs in CD decreases, making them unable to efficiently control the pathogenic Th1 responses. Furthermore, TLR4 signaling increased the PD-L1-dependent inhibition of T cells by iMCs (285). These data suggest that the microbiota can modulate both the tissue regenerative and immunomodulatory capacity of iMSCs. As the dysbiotic microbiome seen in IBD patients has been shown to drive IBD pathogenesis, further studies should investigate its effect on immunomodulatory properties of iMSC.

In summary, we have shown that iMSCs isolated from the healthy human intestine promote epithelial wound closure and possess the capacity to modulate immune/inflammatory responses *in vitro* and *in vivo*. Our data might be relevant for the development of new therapies targeting the dysregulated intestinal stroma in IBD.

5. iMSCs AND AOM/DSS ASSOCIATED CANCER DEVELOPMENT

Colorectal cancer is a serious complication of IBD, induced by chronic inflammation and resulting in tumors with a worse prognosis compared to sporadic CRC (377, 378). Current treatments of IBD, including immunosuppressive thiopurines and anti-TNF-α monoclonal antibodies can reduce the incidence of CAC (379, 380). However, varying response rates and adverse effects, including a possible promotion of new or recurrent cancers due to inhibition of immune responses against tumor cells and oncogenic viruses warrant the search for complementary treatments (381, 382).

As previously stated, MSCs hold great promise as a cell therapy for inflammatory/autoimmune diseases and are currently approved for the treatment of complex perianal fistulas in CD patients (383). However, it has been shown that in vitro-expanded MSCs can adopt protumorigenic properties in vivo as mentioned in the introduction. Since IBD patients have a higher risk of developing intestinal tumors, it is important to evaluate their CRC-promoting properties under such conditions. Furthermore, MSCs have been proposed as a vector when trying to deliver anti-cancer drugs to tumors but such an approach could be potentially dangerous if one ignores the tumor-promoting effects of MSCs.

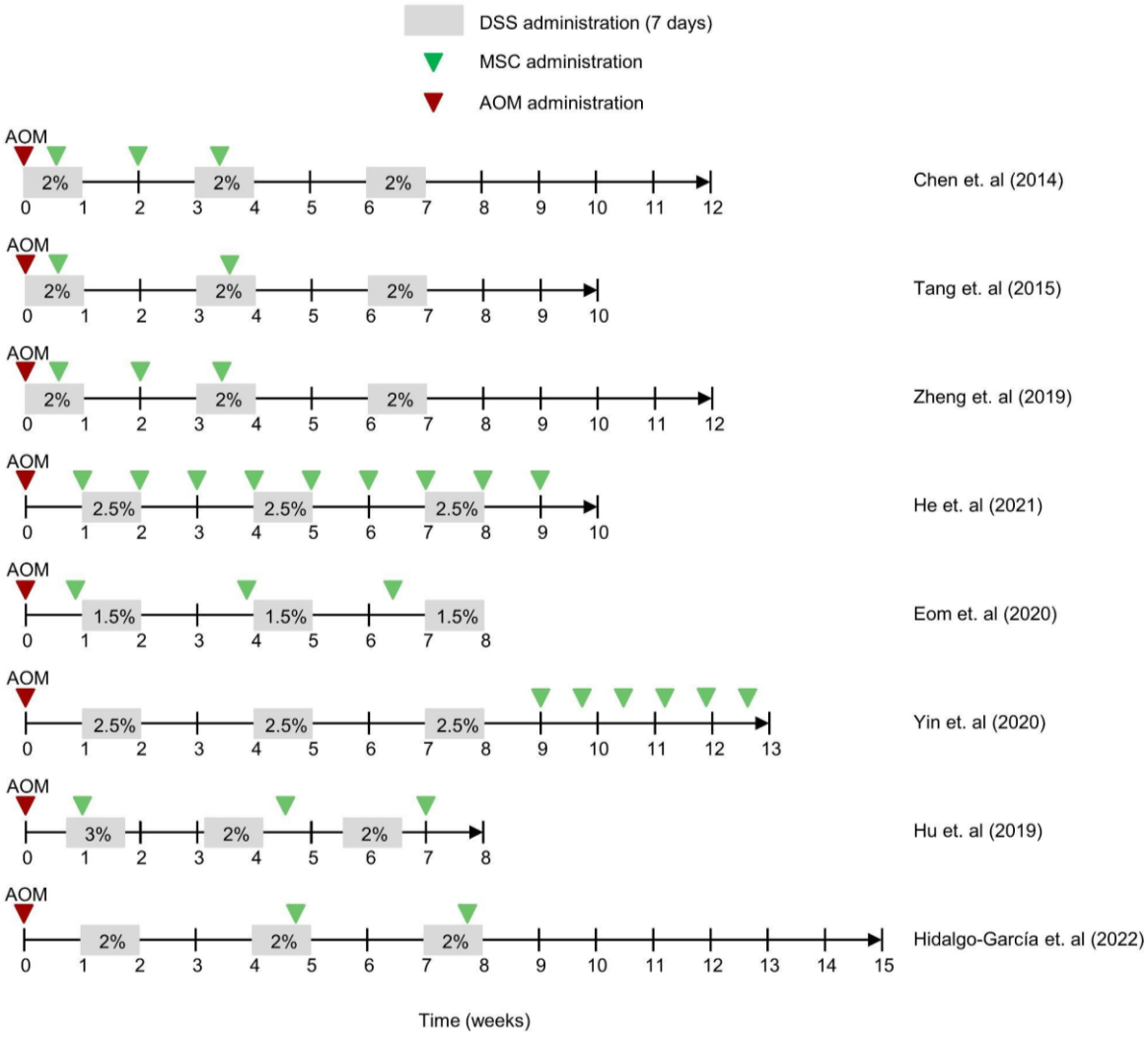

Figure 37. Summary of previous CAC studies administering MSCs. *Different protocols based on administration of AOM in combination with DSS are schematically represented.*

To date only a few studies have analyzed the effects of non-genetically modified syn-, allo- and xenogeneic MSC on tumor induction/growth and immune responses in rodent models of CAC (Figure 37). While MSC administration generally reduced tumor formation/growth to various degrees, TNF-α/IFN-γ-prestimulated iMSC surprisingly promoted tumor development (280-282, 284, 323). The low number of studies and contrasting data warrants further studies on the effect of MSCs, from different tissues, on CAC. Thus, having demonstrated that iMSCs from the healthy human intestine inhibit experimental colitis, we wanted to confirm this immunomodulatory potential, but also evaluate possible protumorigenic properties of iMSCs, in a model of CAC. To this end, we selected a model based on the use of AOM in combination with DSS, due to our interest in the study of tumor progression driven by chronic colitis. Although some other authors have previously reported the development of CAC in a model in which mice develop tumors within a period of 20 weeks after a single cycle of DSS (265, 383), we used the model described by Neufert et. al (2007), based on three cycles of DSS. This protocol reproduces chronic

inflammation - including flares of remission or higher activity - which is thought to be the driving force of tumor progression development in CAC (302). Importantly, this model, as mentioned in the introduction, mimics several aspects of inflammation-induced CRC in humans (264, 265, 267). In the AOM/DSS CAC model, aberrant crypt foci can be seen about two weeks after the initial AOM injection, while macroscopically visible lesions can be observed from week 3-4 (233, 384).

As shown in Figure 37, in contrast to previous studies, we injected iMSCs at the disease peaks of the second (week 4-5) and third DSS administration (week 7-8), i.e. at a time when visible lesions are already present. Despite the increased serum levels of both IFN-γ and TNF-α observed during active colitis (284), our late injections of iMSCs did not adopt the pro-tumorigenic phenotype described by Hu and colleagues (284), but instead significantly and permanently reduced both the intestinal inflammation and tumor numbers. Furthermore, in contrast to published data, we detected a decrease in both tumor number and size (280, 281, 323, 324). This reduction in inflammation was also manifested by a marked reduction in edema, ulceration and leukocyte infiltration together with a lower frequency of tumors in equivalent haematoxylin and eosin colonic tissue sections. These findings, in part, justify the increased colonic apoptosis found in CAC control mice in comparison to iMSC treated ones, since lower levels of apoptosis are indicative of a higher integrity of the epithelial barrier, usually disrupted after a DSS challenge (268). This observation was also confirmed by higher Bax/Bcl-2 ratios in CAC control mice.

We did not detect the injected iMSCs in the intestine at the time of sacrifice (seven weeks after the last injection), which is consistent with their rapid disappearance and limited engraftment in mouse models (325) and in human patients (385). These data suggest that a delayed MSC administration results in a transient modulation, albeit with long lasting effects, of the intestinal immune response which results in an efficient inhibition of CAC severity through a reduction in cancer initiation (linked with a reduced number of tumors) and progression (linked to a reduced tumor size) (302). This immunomodulation exerted by iMSCs resulted also in a lower weight of the spleens extracted from CAC+iMSCs mice (Figure 28C), in comparison with the CAC control group, which is related to the grade of inflammation (386).

As stated before, the development of this subtype of inflammatory CRC is associated with a continuous inflammatory response. For that reason, we can find some upregulated levels of certain proinflammatory cytokines that are also reported to be elevated in IBD. Concretely, we measured the presence of the inflammatory related cytokines IL-23a (subunit p19), IL-17, TNF-α and IL-6 at mRNA level. We found that all these inflammatory mediators were significantly increased in CAC control mice in comparison with healthy controls, while the CAC+iMSCs group presented reduced levels that were statistically significant in the case of *tnf-a*. IL-23 and IL-17, are known protumorigenic drivers that are implicated in colorectal cancer development (256) usually linked to poor prognosis and a more aggressive disease (387). In 2012, Grivennikov and colleagues reported that IL-23 can be released by tumoral myeloid cells - mainly macrophages - activated by microbial products signaling (256). Then, IL-23 can activate the Th17 mediated

immune response, leading to the release of high amounts of IL-17A and the activation of the STAT3 signaling pathway on malignant cells. This can be achieved either by IL-17A direct engagement with its receptors or by IL-17A induction of the IL-6-producing myeloid compartment (387). In fact, AOM/DSS-induced CAC is also characterized by high IL-6 levels and dense immune cell infiltration/stromal increase (265, 266, 302, 388) and activation of the transcription factor STAT3 through IL-6/sIL-6R trans-signaling has been reported to lead to enterocyte survival and proliferation, which enhances tumor multiplication (233, 235, 389). *il-6* mRNA elevated colonic levels were also confirmed at protein level in CAC controls and were accompanied by a significant increase in STAT3 activation. The CAC+iMSCs group presented reduced levels of these two mediators that were statistically significant in the case of IL-6. TNF-α levels are also known to be highly induced in IBD (390) and CAC (227). Importantly, TNF-α can both activate, and be upregulated by, NF-κB signaling, which contributes in perpetuating inflammation and, in consequence, promotes tumorigenesis (217).

Among other similarities between the AOM/DSS-induced CAC model and human CAC, we find frequent mutations in *Kras,* dysregulation of the Apc/β-catenin signalling pathway and increased levels of the enzymes COX-2 and iNOS (265, 266, 302, 388)). In agreement, we found an increased expression of CRC-associated β-catenin and COX-2 - statistically significant in this case - in the intestines of CAC mice that was reduced in iMSC-treated mice, correlating with the tumor burden within the groups (Figures15 E and G). In fact, one of the described procarcinogenic effects of COX-2 is through the modulation of β-catenin, since aberrant COX-2 signalling stimulates the transcription of the *Ctnnb1* gene (217, 251). COX-2 signalling has also been related with Akt phosphorylation and induction of the PI3K/Akt signalling pathway (391, 392), usually found active in human carcinomas and associated with enhanced cell growth, survival and metabolism. At the same time, PI3K/Akt activation leads to the phosphorylation of the β-catenin regulator GS3K-3β, resulting in an enhanced activation of the β-catenin signaling pathway. In accordance, we found a significant elevated ratio of pAkt/Akt expression in the colon of CAC control mice when compared to healthy control and iMSC treated mice.

6. iMSC MODULATION OF THE CAC DEVELOPMENT THROUGH THE INTESTINAL IMMUNE SYSTEM – INNATE AND ADAPTIVE CELLS

As said before, this model is characterized by an elevated presence of cytokines that are involved in the migration of myeloid cells to the inflamed intestine such as CCL2 (393). This correlates with the fact that during intestinal inflammation, neutrophils and Ly6C^{hi}MHCII^{-} inflammatory monocytes are gradually recruited in a CCR2-CCL2 manner to mount an appropriate immune response. In steady state, these newly recruited Ly6C^{hi}MHCII^{-} monocytes promptly differentiate into mature tissue resident Ly6C^{-}MHCII^{+} monocytes through a monocyte-macrophage differentiation waterfall (394). However, during inflammation, the standard differentiation process is disrupted and newly arrived Ly6C^{hi}MHCII^{-} monocytes together with early intermediary macrophages accumulate in the

intestine. These accumulated monocytes and macrophages are responsive to TLR ligands and have been described to be proinflammatory (175). In line with the latter, we found that CAC control mice presented significantly increased numbers of circulating Ly6C^{hi}MHCII^{-}CCR2^{+} monocytes, and at the same time this population also increased in the colon. Moreover, we observe a higher, although not significant, total number of immature CD86^{+} M1-like inflammatory monocytes when compared to the healthy control and the CAC+iMSCs groups. This finding connects with the previously reported elevated *il-23* expression in the intestine, since as we discussed, IL-23 release is directly attributed to TLR activated M1-like macrophages (256). Additionally, these release inflammatory mediators such as NO, ROI, TNF-α, IL-12, IL-23, IL-6 and IL-1β which cause tissue damage, as well as activating other inflammatory cells including Th1 or Th17 effector cells (331). Moreover, previous studies have suggested that monocytic cells recruitment through the CCL2-CCR2 axis increases colon tumor numbers in mice (389);(395)). Then, these CCL2-recruited monocytes could contribute to tumor survival by being polarized to TAMs (tumor associated macrophages) (396).

In CRC, granulocytes and macrophages in the tumor microenvironment (TME) produce ROS and RNS that can cause DNA damage and resulting mutations (397, 398). In addition, Bogdan et al (399) found that neutrophil-derived hypochlorous acid can increase the levels of 5-chlorocytosine in the DNA which results in CpG mutations in the genome. Furthermore, tumor-infiltrating cytotoxic T lymphocytes release IFN-γ which induces copy number alterations in tumor cells due to the modulation of DNA damage response/repair pathways (400). Thus, both chronic inflammation and antitumoral immune responses can promote genomic instability and carcinogenesis.

Neutrophils are not usually found in the healthy intestine (401). However, in recent years it has become clear that neutrophils play an important role in promoting tumorigenesis through several mechanisms (402). Shang et al. showed that progression of CAC in the AOM/DSS model was accompanied by an increased infiltration of neutrophils expressing CXCR2 into the colonic submucosa. Remarkably, injection of neutrophil-neutralizing antibodies after the last DSS cycle reduced the number and size of tumors (403). In addition, it has been well established that IL-17 promotes the activation and accumulation of neutrophils at sites of inflammation (404). In accordance, we observed a marked decrease in the numbers of neutrophils in the colons of iMSC-treated mice in comparison to CAC mice, which correlated with the mRNA levels of IL-17 in each group.

Apart from neutrophils, eosinophils are thought to play a major proinflammatory role in IBD and are increased in the intestinal mucosa in both CD and UC patients (332). In a series of elegant experiments, Polosukhina and colleagues demonstrated that DSS-administration induced a significant increase in colonic eosinophils in colitic mice compared to control mice. Disruption of *Ccl11*, an eosinophil chemoattractant, markedly reduced the numbers of intestinal eosinophils in colitic mice. Furthermore, *Ccl11*$^{-/-}$ mice, when subjected to AOM/DSS, had decreased histologic

injury, fewer tumors, and a reduced colonic eosinophil infiltration in comparison to wild type mice ((405)). In accordance, we detected an increased number in eosinophils in CAC mice that was reduced in iMSC-treated mice.

In summary, we show that iMSCs have the capacity to markedly decrease colonic inflammation, partly restoring the monocyte/macrophage balance, and reducing granulocyte infiltration in the colonic mucosa. It is well known that TNF-α and IFN-γ stimulation of MSCs and iMSC increase their capacity to inhibit T cell responses, partly through the induction of IDO (406-408). Injection of IFN-γ receptor-deficient MSCs cannot reduce GvHD.(406), and IFN-γ/polyI:C pretreatment of MSCs increase their therapeutic effect in DSS-colitis, via the induction of IDO (409). It is therefore surprising that administration of TNF-α/IFN-γ pre-stimulated MSCs to the AOM/DSS model results in an increased tumor promotion and progression as shown by Hu et al. (284). However, TNF-α stimulation of human BM-MSCs induced the secretion of CCL5, which promoted CRC growth in vitro and in vivo, upregulating the β-catenin pathway (410). Summarizing the reports on MSCs in AOM/DSS-induced CAC, non-primed MSCs injected into the AOM/DSS model home to the inflamed intestine only when injected i.v. In addition, there is a possibility that the MSCs that reach the tumor site could, depending on their stimulation in the TME, promote tumor growth via their differentiation into cancer-associated fibroblasts or via their immnosuppressive capacities. In this sense, IFN-γ induces IDO expression in MSCs (411), and high IDO expression in the intestine can promote CRC by promoting a local tryptophan depletion and inactivating T cells (412, 413). However, based on our experiments, we could not detect any protumorigenic properties of iMSCs isolated from healthy tissues. Additionally, we did not find iMSCs homing neither in the CAC model (probably due to the time period after the last injection) and neither in the 7 days-DSS study (data not shown). Therefore, all these data lead us to conclude that injected iMSCs do not reach and/or persist in the inflamed colon and rather induce a systemic immunosuppression by other means, as previously reported by other groups (363).

7. MICROBIOTA IN IBD AND CAC

It is widely known the connection between chronic inflammation and the origin of cancer, although the pathophysiological mechanisms of IBD and CAC is not clear, many studies have highlighted the relationship between the commensal gut microbiota and host immune system as a key factor in the promotion of colitis and then CAC (414, 415). In fact, the activation of immune signaling pathways by bacterial components can break homeostasis and generate a pro-neoplastic inflammatory environment. Many metagenomic analyses have provided strong evidence that not only microbial populations in CRC tissues differ from the microbiota of healthy host tissues, but also that specific members of the microbiota may contribute to the development of a proinflammatory atmosphere that triggers CRC. In this sense, several human and animal studies have shown that both conditions, IBD and CRC (including CAC), present an altered gut microbiota and, more concretely, a reduction in microbial richness and diversity (416-418). Accordingly, we

obtained similar results in the DSS colitis and AOM/DSS -induced CAC models, which showed, in both cases, a modified microbial profile with decreased diversity and richness. As commented before, this is in agreement with previously published data (155, 323, 419). Interestingly, when the control group was compared with DSS mice in both animal models, the relative abundance of *Firmicutes* was increased and the abundance of *Bacteroidetes* and *Verrucomicrobia* was reduced. It has been suggested that bacteria belonging to the *Firmicutes* phyla, such as *Clostridium difficile* and *Ruminococcus gnavus,* are specific to the faecal microbiota of patients with preneoplastic lesions, including adenomas and hyperplastic polyps (420, 421) and colitis (422, 423). Therefore, the overgrowth of this phylum that we have observed both in the DSS mice and CAC group could be explained by the overgrowth of these species. Conversely, the reduced abundance of *Bacteroidetes* and *Verrucomicrobia* observed in DSS and CAC mice versus the control group is in accordance with several studies that have shown the implication of these phyla in the normal development of the gastrointestinal tract. Regarding *Bacteroidetes* phylum, its composition with different butyrate-producing species would explain our results. It is well known that butyrate has an important role in maintaining a healthy gut, restoring the energy metabolism and reducing the inflammatory process in experimental colitis due to its immunomodulatory activity, but also it has demonstrated a potential protective effect against colorectal cancer (424-426). Furthermore, in our results *Verrucomicrobia* was found to be more abundant in control mice in both animal models. Akkermansia is a crucial genus from *Verrucomicrobia phylum.* Many studies have revealed that *Akkermansia* has an important role in regulatory effects on gut homeostasis by producing beneficial metabolites. In fact, the authors have reported that lower colonization and abundance of *Akkermansia* are characteristic of colitis and CRC (including CAC) conditions (427-429). These studies are in agreement with our findings. When the MSCs treatment was evaluated, the results revealed that iMSCs administration managed to restore the microbial profile as well as increase the beta and alpha diversity. Very little has been done regarding the effects of iMSCs treatment on gut microbiota composition, but a recent study explored the preventive effects of bone-marrow derived MSCs on the same CAC model and also found that they could change β-diversity but not abundance of the gut microbiome (323). The interplay between iMCs and microbiota needs to be further explored, but it seems to be a two-way communication. On one hand, iMCs express TLRs and NLR and respond to bacteria, potentially acting as “non-professional innate immune cells” (1). Moreover, Beswick et al. found that $CD90^+$ iMSCs, via TLR4-induced PD-L1 expression, could promote mucosal immune tolerance (285), and certain iMCs in the gut-associated lymphoid tissues could regulate bacteria-specific IgA production and thus the diversity of the gut microbiota (293). On the other hand, Ciorba et al. found that the probiotic *Lactobacillus rhamnosus*, via TLR2-induced COX-2/PGE_2 expression by iMSCs, could protect against radiation-induced intestinal epithelial damage (430). Considering the ability of the microbiota to reprogram the function of intestinal epithelial cells, it would be plausible that the microbiota or their metabolites could “educate” or change the iMCs composition and/or function, thus promoting a healthy or a diseased gut, as occurs in IBD and

CRC. In the same way, an altered stroma could also promote dysbiosis that could play a crucial role in the development of these diseases.

8. SUMMARY

Applicability/scientific importance of our work

We belive that understanding the biology of iMSCs is important for several reasons. First, recent studies have shown that iMSC can adopt a proinflammatory, disease-promoting phenotype in IBD. Beswick recently reported a decrease in the expression of PD-L1 on iMCs in Crohn's disease, making them unable to efficiently control the pathogenic Th1 responses in the colon (285). Thus, a continuous characterization of the tissue regenerative and immunodulatory capacities of iMSCs in vitro can provide novel parameters to study in a disease setting, and if compromised, restore them (therapeutic targets).

Second, our studies of iMSCs can also be important for improving current cell therapies using MSCs from other tissue origins. We do not consider intestinal resections to be a source of MSCs for cell therapy purposes. However, a recent study showed that Serpina3n, expressed by the cells in the intestinal stroma, is important for the resolution of inflammation in colitis (431). This information could help us in designing allogeneic MSC therapies for IBD, selecting MSCs by their capacity to produce serpina3n and/or PD-L1 expression. Thus, our current and future characterization/analysis of iMSCs could aid in designing allogeneic MSC therapies for IBD or CRC, with the aim of replacing/reeducating resident iMCs that are exhausted or have diverted from their physiological functions, as suggested by Signore et al., (432) and Barnhoorn and colleagues (203).

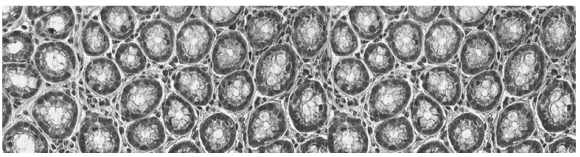

Conclusions

CONCLUSIONS

1. In vitro expanded iMSCs from human intestinal resections are MSC according to the minimal criteria proposed by the ISCT, and can be used for analyzing their properties in vitro and in vivo.
2. iMSCs inhibit T cell proliferation and LPS-induced expression of TNF-α in macrophages, and promote wound healing *in vitro,* behaving as MSCs from other tissues.
3. iMSCs ameliorate DSS-induced acute colitis in mice, reducing the inflammatory responses, protecting the integrity of the intestinal barrier and restoring the altered gut microbiota.
4. iMSCs reduces tumor progression in CAC in mice due to their potent anti-inflammatory/immunomodulatory effects, also reverting the gut dysbiosis induced by the disease.
5. New drugs for the treatment of IBD and CAC could be developed aiming to restore/enhance the properties of iMCs.

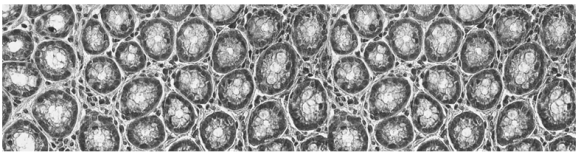

Bibliography

BIBLIOGRAPHY

1. Owens BM. Inflammation, Innate Immunity, and the Intestinal Stromal Cell Niche: Opportunities and Challenges. Front Immunol. 2015;6:319.

2. Hinz B, Lagares D. Evasion of apoptosis by myofibroblasts: a hallmark of fibrotic diseases. Nat Rev Rheumatol. 2020;16(1):11-31.

3. Friedenstein AJ, Chailakhjan RK, Lalykina KS. The development of fibroblast colonies in monolayer cultures of guinea-pig bone marrow and spleen cells. Cell Tissue Kinet. 1970;3(4):393-403.

4. Owen M, Friedenstein AJ. Stromal stem cells: marrow-derived osteogenic precursors. Ciba Found Symp. 1988;136:42-60.

5. Robey PG, Kuznetsov SA, Riminucci M, Bianco P. Bone marrow stromal cell assays: in vitro and in vivo. Methods Mol Biol. 2014;1130:279-93.

6. Crisan M, Yap S, Casteilla L, Chen CW, Corselli M, Park TS, et al. A perivascular origin for mesenchymal stem cells in multiple human organs. Cell Stem Cell. 2008;3(3):301-13.

7. da Silva Meirelles L, Chagastelles PC, Nardi NB. Mesenchymal stem cells reside in virtually all post-natal organs and tissues. J Cell Sci. 2006;119(Pt 11):2204-13.

8. Caplan AI. Mesenchymal stem cells. J Orthop Res. 1991;9(5):641-50.

9. Pittenger MF, Mackay AM, Beck SC, Jaiswal RK, Douglas R, Mosca JD, et al. Multilineage potential of adult human mesenchymal stem cells. Science. 1999;284(5411):143-7.

10. Horwitz EM, Le Blanc K, Dominici M, Mueller I, Slaper-Cortenbach I, Marini FC, et al. Clarification of the nomenclature for MSC: The International Society for Cellular Therapy position statement. Cytotherapy. 2005;7(5):393-5.

11. Friedenstein AJ, Petrakova KV, Kurolesova AI, Frolova GP. Heterotopic of bone marrow. Analysis of precursor cells for osteogenic and hematopoietic tissues. Transplantation. 1968;6(2):230-47.

12. Dennis JE, Merriam A, Awadallah A, Yoo JU, Johnstone B, Caplan AI. A quadripotential mesenchymal progenitor cell isolated from the marrow of an adult mouse. J Bone Miner Res. 1999;14(5):700-9.

13. Bianco P, Gehron Robey P. Marrow stromal stem cells. J Clin Invest. 2000;105(12):1663-8.

14. Jiang Y, Jahagirdar BN, Reinhardt RL, Schwartz RE, Keene CD, Ortiz-Gonzalez XR, et al. Pluripotency of mesenchymal stem cells derived from adult marrow. Nature. 2002;418(6893):41-9.

15. Dominici M, Le Blanc K, Mueller I, Slaper-Cortenbach I, Marini F, Krause D, et al. Minimal criteria for defining multipotent mesenchymal stromal cells. The International Society for Cellular Therapy position statement. Cytotherapy. 2006;8(4):315-7.

16. Kern S, Eichler H, Stoeve J, Kluter H, Bieback K. Comparative analysis of mesenchymal stem cells from bone marrow, umbilical cord blood, or adipose tissue. Stem Cells. 2006;24(5):1294-301.

17. Heo JS, Choi Y, Kim HS, Kim HO. Comparison of molecular profiles of human mesenchymal stem cells derived from bone marrow, umbilical cord blood, placenta and adipose tissue. Int J Mol Med. 2016;37(1):115-25.

18. Sacchetti B, Funari A, Remoli C, Giannicola G, Kogler G, Liedtke S, et al. No Identical "Mesenchymal Stem Cells" at Different Times and Sites: Human Committed Progenitors of Distinct Origin and Differentiation Potential Are Incorporated as Adventitial Cells in Microvessels. Stem Cell Reports. 2016;6(6):897-913.

19. Lemos DR, Duffield JS. Tissue-resident mesenchymal stromal cells: Implications for tissue-specific antifibrotic therapies. Sci Transl Med. 2018;10(426).

20. Al-Nbaheen M, Vishnubalaji R, Ali D, Bouslimi A, Al-Jassir F, Megges M, et al. Human stromal (mesenchymal) stem cells from bone marrow, adipose tissue and skin exhibit differences in molecular phenotype and differentiation potential. Stem Cell Rev Rep. 2013;9(1):32-43.

21. Ziegra CJ, Oswald RE, Bass AH. [3H]kainate localization in goldfish brain: receptor autoradiography and membrane binding. Brain Res. 1990;527(2):308-17.

22. Mendez-Ferrer S, Michurina TV, Ferraro F, Mazloom AR, Macarthur BD, Lira SA, et al. Mesenchymal and haematopoietic stem cells form a unique bone marrow niche. Nature. 2010;466(7308):829-34.

23. Crane JL, Cao X. Bone marrow mesenchymal stem cells and TGF-beta signaling in bone remodeling. J Clin Invest. 2014;124(2):466-72.

24. Schmidt-Lucke C, Escher F, Van Linthout S, Kuhl U, Miteva K, Ringe J, et al. Cardiac migration of endogenous mesenchymal stromal cells in patients with inflammatory cardiomyopathy. Mediators Inflamm. 2015;2015:308185.

25. Ullah M, Liu DD, Thakor AS. Mesenchymal Stromal Cell Homing: Mechanisms and Strategies for Improvement. iScience. 2019;15:421-38.

26. Kidd S, Spaeth E, Watson K, Burks J, Lu H, Klopp A, et al. Origins of the tumor microenvironment: quantitative assessment of adipose-derived and bone marrow-derived stroma. PLoS One. 2012;7(2):e30563.

27. Shinagawa K, Kitadai Y, Tanaka M, Sumida T, Kodama M, Higashi Y, et al. Mesenchymal stem cells enhance growth and metastasis of colon cancer. Int J Cancer. 2010;127(10):2323-33.

28. Mishra PJ, Mishra PJ, Humeniuk R, Medina DJ, Alexe G, Mesirov JP, et al. Carcinoma-associated fibroblast-like differentiation of human mesenchymal stem cells. Cancer Res. 2008;68(11):4331-9.

29. Sun Z, Wang S, Zhao RC. The roles of mesenchymal stem cells in tumor inflammatory microenvironment. J Hematol Oncol. 2014;7:14.

30. Le Blanc K, Mougiakakos D. Multipotent mesenchymal stromal cells and the innate immune system. Nat Rev Immunol. 2012;12(5):383-96.

31. Gonzalez-Rey E, Anderson P, Gonzalez MA, Rico L, Buscher D, Delgado M. Human adult stem cells derived from adipose tissue protect against experimental colitis and sepsis. Gut. 2009;58(7):929-39.

32. Anderson P, Gonzalez-Rey E, O'Valle F, Martin F, Oliver FJ, Delgado M. Allogeneic Adipose-Derived Mesenchymal Stromal Cells Ameliorate Experimental Autoimmune Encephalomyelitis by Regulating Self-Reactive T Cell Responses and Dendritic Cell Function. Stem Cells Int. 2017;2017:2389753.

33. Ciccocioppo R, Bernardo ME, Sgarella A, Maccario R, Avanzini MA, Ubezio C, et al. Autologous bone marrow-derived mesenchymal stromal cells in the treatment of fistulising Crohn's disease. Gut. 2011;60(6):788-98.

34. Kolf CM, Cho E, Tuan RS. Mesenchymal stromal cells. Biology of adult mesenchymal stem cells: regulation of niche, self-renewal and differentiation. Arthritis Res Ther. 2007;9(1):204.

35. Le Blanc K, Rasmusson I, Sundberg B, Gotherstrom C, Hassan M, Uzunel M, et al. Treatment of severe acute graft-versus-host disease with third party haploidentical mesenchymal stem cells. Lancet. 2004;363(9419):1439-41.

36. Volarevic V, Gazdic M, Simovic Markovic B, Jovicic N, Djonov V, Arsenijevic N. Mesenchymal stem cell-derived factors: Immuno-modulatory effects and therapeutic potential. Biofactors. 2017;43(5):633-44.

37. Volarevic V, Nurkovic J, Arsenijevic N, Stojkovic M. Concise review: Therapeutic potential of mesenchymal stem cells for the treatment of acute liver failure and cirrhosis. Stem Cells. 2014;32(11):2818-23.

38. Gazdic M, Volarevic V, Arsenijevic N, Stojkovic M. Mesenchymal stem cells: a friend or foe in immune-mediated diseases. Stem Cell Rev Rep. 2015;11(2):280-7.

39. Waterman RS, Tomchuck SL, Henkle SL, Betancourt AM. A new mesenchymal stem cell (MSC) paradigm: polarization into a pro-inflammatory MSC1 or an Immunosuppressive MSC2 phenotype. PLoS One. 2010;5(4):e10088.

40. Nowarski R, Jackson R, Flavell RA. The Stromal Intervention: Regulation of Immunity and Inflammation at the Epithelial-Mesenchymal Barrier. Cell. 2017;168(3):362-75.

41. Powell DW, Pinchuk IV, Saada JI, Chen X, Mifflin RC. Mesenchymal cells of the intestinal lamina propria. Annu Rev Physiol. 2011;73:213-37.

42. Roulis M, Flavell RA. Fibroblasts and myofibroblasts of the intestinal lamina propria in physiology and disease. Differentiation. 2016;92(3):116-31.

43. Ruhl A. Glial cells in the gut. Neurogastroenterol Motil. 2005;17(6):777-90.

44. Mifflin RC, Pinchuk IV, Saada JI, Powell DW. Intestinal myofibroblasts: targets for stem cell therapy. Am J Physiol Gastrointest Liver Physiol. 2011;300(5):G684-96.

45. Hsia LT, Ashley N, Ouaret D, Wang LM, Wilding J, Bodmer WF. Myofibroblasts are distinguished from activated skin fibroblasts by the expression of AOC3 and other associated markers. Proc Natl Acad Sci U S A. 2016;113(15):E2162-71.

46. Koliaraki V, Pallangyo CK, Greten FR, Kollias G. Mesenchymal Cells in Colon Cancer. Gastroenterology. 2017;152(5):964-79.

47. Kalluri R, Zeisberg M. Fibroblasts in cancer. Nat Rev Cancer. 2006;6(5):392-401.

48. Tommelein J, Verset L, Boterberg T, Demetter P, Bracke M, De Wever O. Cancer-associated fibroblasts connect metastasis-promoting communication in colorectal cancer. Front Oncol. 2015;5:63.

49. Rasanen K, Vaheri A. Activation of fibroblasts in cancer stroma. Exp Cell Res. 2010;316(17):2713-22.

50. D'Urso M, Kurniawan NA. Mechanical and Physical Regulation of Fibroblast-Myofibroblast Transition: From Cellular Mechanoresponse to Tissue Pathology. Front Bioeng Biotechnol. 2020;8:609653.

51. Servais C, Erez N. From sentinel cells to inflammatory culprits: cancer-associated fibroblasts in tumour-related inflammation. J Pathol. 2013;229(2):198-207.

52. De LKT, Whiting CV, Bland PW. Proinflammatory cytokine synthesis by mucosal fibroblasts from mouse colitis is enhanced by interferon-gamma-mediated up-regulation of CD40 signalling. Clin Exp Immunol. 2007;147(2):313-23.

53. Brown SL, Riehl TE, Walker MR, Geske MJ, Doherty JM, Stenson WF, et al. Myd88-dependent positioning of Ptgs2-expressing stromal cells maintains colonic epithelial proliferation during injury. J Clin Invest. 2007;117(1):258-69.

54. Walker MR, Brown SL, Riehl TE, Stenson WF, Stappenbeck TS. Growth factor regulation of prostaglandin-endoperoxide synthase 2 (Ptgs2) expression in colonic mesenchymal stem cells. J Biol Chem. 2010;285(7):5026-39.

55. Manieri NA, Drylewicz MR, Miyoshi H, Stappenbeck TS. Igf2bp1 is required for full induction of Ptgs2 mRNA in colonic mesenchymal stem cells in mice. Gastroenterology. 2012;143(1):110-21 e10.

56. Armulik A, Genove G, Betsholtz C. Pericytes: developmental, physiological, and pathological perspectives, problems, and promises. Dev Cell. 2011;21(2):193-215.

57. McLin VA, Henning SJ, Jamrich M. The role of the visceral mesoderm in the development of the gastrointestinal tract. Gastroenterology. 2009;136(7):2074-91.

58. Artells R, Navarro A, Diaz T, Monzo M. Ultrastructural and immunohistochemical analysis of intestinal myofibroblasts during the early organogenesis of the human small intestine. Anat Rec (Hoboken). 2011;294(3):462-71.

59. Rinkevich Y, Mori T, Sahoo D, Xu PX, Bermingham JR, Jr., Weissman IL. Identification and prospective isolation of a mesothelial precursor lineage giving rise to smooth muscle cells and fibroblasts for mammalian internal organs, and their vasculature. Nat Cell Biol. 2012;14(12):1251-60.

60. Dazzi F, Lopes L, Weng L. Mesenchymal stromal cells: a key player in 'innate tolerance'? Immunology. 2012;137(3):206-13.

61. Brittan M, Wright NA. Stem cell in gastrointestinal structure and neoplastic development. Gut. 2004;53(6):899-910.

62. Murphy J, Summer R, Fine A. Stem cells in airway smooth muscle: state of the art. Proc Am Thorac Soc. 2008;5(1):11-4.

63. Forbes SJ, Russo FP, Rey V, Burra P, Rugge M, Wright NA, et al. A significant proportion of myofibroblasts are of bone marrow origin in human liver fibrosis. Gastroenterology. 2004;126(4):955-63.

64. Stappenbeck TS, Miyoshi H. The role of stromal stem cells in tissue regeneration and wound repair. Science. 2009;324(5935):1666-9.

65. Bellini A, Mattoli S. The role of the fibrocyte, a bone marrow-derived mesenchymal progenitor, in reactive and reparative fibroses. Lab Invest. 2007;87(9):858-70.

66. Uccelli A, Moretta L, Pistoia V. Mesenchymal stem cells in health and disease. Nat Rev Immunol. 2008;8(9):726-36.

67. Abe R, Donnelly SC, Peng T, Bucala R, Metz CN. Peripheral blood fibrocytes: differentiation pathway and migration to wound sites. J Immunol. 2001;166(12):7556-62.

68. Swenson E, Theise N. Stem cell therapeutics: potential in the treatment of inflammatory bowel disease. Clin Exp Gastroenterol. 2010;3:1-10.

69. Pinchuk IV, Mifflin RC, Saada JI, Powell DW. Intestinal mesenchymal cells. Curr Gastroenterol Rep. 2010;12(5):310-8.

70. Lahar N, Lei NY, Wang J, Jabaji Z, Tung SC, Joshi V, et al. Intestinal subepithelial myofibroblasts support in vitro and in vivo growth of human small intestinal epithelium. PLoS One. 2011;6(11):e26898.

71. Samuel S, Walsh R, Webb J, Robins A, Potten C, Mahida YR. Characterization of putative stem cells in isolated human colonic crypt epithelial cells and their interactions with myofibroblasts. Am J Physiol Cell Physiol. 2009;296(2):C296-305.

72. Corda G, Sala A. Non-canonical WNT/PCP signalling in cancer: Fzd6 takes centre stage. Oncogenesis. 2017;6(7):e364.

73. Gregorieff A, Pinto D, Begthel H, Destree O, Kielman M, Clevers H. Expression pattern of Wnt signaling components in the adult intestine. Gastroenterology. 2005;129(2):626-38.

74. Van der Flier LG, Sabates-Bellver J, Oving I, Haegebarth A, De Palo M, Anti M, et al. The Intestinal Wnt/TCF Signature. Gastroenterology. 2007;132(2):628-32.

75. van der Flier LG, Haegebarth A, Stange DE, van de Wetering M, Clevers H. OLFM4 is a robust marker for stem cells in human intestine and marks a subset of colorectal cancer cells. Gastroenterology. 2009;137(1):15-7.

76. Barker N, van Es JH, Kuipers J, Kujala P, van den Born M, Cozijnsen M, et al. Identification of stem cells in small intestine and colon by marker gene Lgr5. Nature. 2007;449(7165):1003-7.

77. Li X, Madison BB, Zacharias W, Kolterud A, States D, Gumucio DL. Deconvoluting the intestine: molecular evidence for a major role of the mesenchyme in the modulation of signaling cross talk. Physiol Genomics. 2007;29(3):290-301.

78. Waite KA, Eng C. From developmental disorder to heritable cancer: it's all in the BMP/TGF-beta family. Nat Rev Genet. 2003;4(10):763-73.

79. Zhang J, Li L. BMP signaling and stem cell regulation. Dev Biol. 2005;284(1):1-11.

80. Sneddon JB, Zhen HH, Montgomery K, van de Rijn M, Tward AD, West R, et al. Bone morphogenetic protein antagonist gremlin 1 is widely expressed by cancer-associated stromal cells and can promote tumor cell proliferation. Proc Natl Acad Sci U S A. 2006;103(40):14842-7.

81. He XC, Zhang J, Tong WG, Tawfik O, Ross J, Scoville DH, et al. BMP signaling inhibits intestinal stem cell self-renewal through suppression of Wnt-beta-catenin signaling. Nat Genet. 2004;36(10):1117-21.

82. Miyazono K, Kamiya Y, Morikawa M. Bone morphogenetic protein receptors and signal transduction. J Biochem. 2010;147(1):35-51.

83. Hardwick JC, Kodach LL, Offerhaus GJ, van den Brink GR. Bone morphogenetic protein signalling in colorectal cancer. Nat Rev Cancer. 2008;8(10):806-12.

84. Kosinski C, Li VS, Chan AS, Zhang J, Ho C, Tsui WY, et al. Gene expression patterns of human colon tops and basal crypts and BMP antagonists as intestinal stem cell niche factors. Proc Natl Acad Sci U S A. 2007;104(39):15418-23.

85. Kosinski C, Stange DE, Xu C, Chan AS, Ho C, Yuen ST, et al. Indian hedgehog regulates intestinal stem cell fate through epithelial-mesenchymal interactions during development. Gastroenterology. 2010;139(3):893-903.

86. Zacharias WJ, Li X, Madison BB, Kretovich K, Kao JY, Merchant JL, et al. Hedgehog is an anti-inflammatory epithelial signal for the intestinal lamina propria. Gastroenterology. 2010;138(7):2368-77, 77 e1-4.

87. van Dop WA, Uhmann A, Wijgerde M, Sleddens-Linkels E, Heijmans J, Offerhaus GJ, et al. Depletion of the colonic epithelial precursor cell compartment upon conditional activation of the hedgehog pathway. Gastroenterology. 2009;136(7):2195-203 e1-7.

88. Madison BB, Braunstein K, Kuizon E, Portman K, Qiao XT, Gumucio DL. Epithelial hedgehog signals pattern the intestinal crypt-villus axis. Development. 2005;132(2):279-89.

89. Otte JM, Rosenberg IM, Podolsky DK. Intestinal myofibroblasts in innate immune responses of the intestine. Gastroenterology. 2003;124(7):1866-78.

90. Owens BM, Steevels TA, Dudek M, Walcott D, Sun MY, Mayer A, et al. CD90(+) Stromal Cells are Non-Professional Innate Immune Effectors of the Human Colonic Mucosa. Front Immunol. 2013;4:307.

91. Kim YG, Kamada N, Shaw MH, Warner N, Chen GY, Franchi L, et al. The Nod2 sensor promotes intestinal pathogen eradication via the chemokine CCL2-dependent recruitment of inflammatory monocytes. Immunity. 2011;34(5):769-80.

92. Normand S, Delanoye-Crespin A, Bressenot A, Huot L, Grandjean T, Peyrin-Biroulet L, et al. Nod-like receptor pyrin domain-containing protein 6 (NLRP6) controls epithelial self-renewal and colorectal carcinogenesis upon injury. Proc Natl Acad Sci U S A. 2011;108(23):9601-6.

93. Owens BM, Simmons A. Intestinal stromal cells in mucosal immunity and homeostasis. Mucosal Immunol. 2013;6(2):224-34.

94. Walton KD, Kolterud A, Czerwinski MJ, Bell MJ, Prakash A, Kushwaha J, et al. Hedgehog-responsive mesenchymal clusters direct patterning and emergence of intestinal villi. Proc Natl Acad Sci U S A. 2012;109(39):15817-22.

95. Zhang Z, Andoh A, Inatomi O, Bamba S, Takayanagi A, Shimizu N, et al. Interleukin-17 and lipopolysaccharides synergistically induce cyclooxygenase-2 expression in human intestinal myofibroblasts. J Gastroenterol Hepatol. 2005;20(4):619-27.

96. Walton KL, Holt L, Sartor RB. Lipopolysaccharide activates innate immune responses in murine intestinal myofibroblasts through multiple signaling pathways. Am J Physiol Gastrointest Liver Physiol. 2009;296(3):G601-11.

97. Burke JP, Cunningham MF, Watson RW, Docherty NG, Coffey JC, O'Connell PR. Bacterial lipopolysaccharide promotes profibrotic activation of intestinal fibroblasts. Br J Surg. 2010;97(7):1126-34.

98. Pang G, Couch L, Batey R, Clancy R, Cripps A. GM-CSF, IL-1 alpha, IL-1 beta, IL-6, IL-8, IL-10, ICAM-1 and VCAM-1 gene expression and cytokine production in human duodenal fibroblasts stimulated with lipopolysaccharide, IL-1 alpha and TNF-alpha. Clin Exp Immunol. 1994;96(3):437-43.

99. Okuno T, Andoh A, Bamba S, Araki Y, Fujiyama Y, Fujiyama M, et al. Interleukin-1beta and tumor necrosis factor-alpha induce chemokine and matrix metalloproteinase gene expression in human colonic subepithelial myofibroblasts. Scand J Gastroenterol. 2002;37(3):317-24.

100. Bamba S, Andoh A, Yasui H, Araki Y, Bamba T, Fujiyama Y. Matrix metalloproteinase-3 secretion from human colonic subepithelial myofibroblasts: role of interleukin-17. J Gastroenterol. 2003;38(6):548-54.

101. Lee YS, Yang H, Yang JY, Kim Y, Lee SH, Kim JH, et al. Interleukin-1 (IL-1) signaling in intestinal stromal cells controls KC/ CXCL1 secretion, which correlates with recruitment of IL-22-secreting neutrophils at early stages of Citrobacter rodentium infection. Infect Immun. 2015;83(8):3257-67.

102. Hata K, Andoh A, Shimada M, Fujino S, Bamba S, Araki Y, et al. IL-17 stimulates inflammatory responses via NF-kappaB and MAP kinase pathways in human colonic myofibroblasts. Am J Physiol Gastrointest Liver Physiol. 2002;282(6):G1035-44.

103. Kawamura T, Andoh A, Nishida A, Shioya M, Yagi Y, Nishimura T, et al. Inhibitory effects of short-chain fatty acids on matrix metalloproteinase secretion from human colonic subepithelial myofibroblasts. Dig Dis Sci. 2009;54(2):238-45.

104. Horsnell WG, Cutler AJ, Hoving JC, Mearns H, Myburgh E, Arendse B, et al. Delayed goblet cell hyperplasia, acetylcholine receptor expression, and worm expulsion in SMC-specific IL-4Ralpha-deficient mice. PLoS Pathog. 2007;3(1):e1.

105. Marillier RG, Brombacher TM, Dewals B, Leeto M, Barkhuizen M, Govender D, et al. IL-4R{alpha}-responsive smooth muscle cells increase intestinal hypercontractility and contribute to resistance during acute Schistosomiasis. Am J Physiol Gastrointest Liver Physiol. 2010;298(6):G943-51.

106. Pinchuk IV, Saada JI, Beswick EJ, Boya G, Qiu SM, Mifflin RC, et al. PD-1 ligand expression by human colonic myofibroblasts/fibroblasts regulates CD4+ T-cell activity. Gastroenterology. 2008;135(4):1228-37, 37 e1-2.

107. Pinchuk IV, Beswick EJ, Saada JI, Boya G, Schmitt D, Raju GS, et al. Human colonic myofibroblasts promote expansion of CD4+ CD25high Foxp3+ regulatory T cells. Gastroenterology. 2011;140(7):2019-30.

108. Roberts AI, Nadler SC, Ebert EC. Mesenchymal cells stimulate human intestinal intraepithelial lymphocytes. Gastroenterology. 1997;113(1):144-50.

109. Saada JI, Pinchuk IV, Barrera CA, Adegboyega PA, Suarez G, Mifflin RC, et al. Subepithelial myofibroblasts are novel nonprofessional APCs in the human colonic mucosa. J Immunol. 2006;177(9):5968-79.

110. Zhang Z, Andoh A, Yasui H, Inatomi O, Hata K, Tsujikawa T, et al. Interleukin-1beta and tumor necrosis factor-alpha upregulate interleukin-23 subunit p19 gene expression in human colonic subepithelial myofibroblasts. Int J Mol Med. 2005;15(1):79-83.

111. Mahida YR, Beltinger J, Makh S, Goke M, Gray T, Podolsky DK, et al. Adult human colonic subepithelial myofibroblasts express extracellular matrix proteins and cyclooxygenase-1 and -2. Am J Physiol. 1997;273(6):G1341-8.

112. McKaig BC, Hughes K, Tighe PJ, Mahida YR. Differential expression of TGF-beta isoforms by normal and inflammatory bowel disease intestinal myofibroblasts. Am J Physiol Cell Physiol. 2002;282(1):C172-82.

113. Maby-El Hajjami H, Ame-Thomas P, Pangault C, Tribut O, DeVos J, Jean R, et al. Functional alteration of the lymphoma stromal cell niche by the cytokine context: role of indoleamine-2,3 dioxygenase. Cancer Res. 2009;69(7):3228-37.

114. Haniffa MA, Wang XN, Holtick U, Rae M, Isaacs JD, Dickinson AM, et al. Adult human fibroblasts are potent immunoregulatory cells and functionally equivalent to mesenchymal stem cells. J Immunol. 2007;179(3):1595-604.

115. Nazareth MR, Broderick L, Simpson-Abelson MR, Kelleher RJ, Jr., Yokota SJ, Bankert RB. Characterization of human lung tumor-associated fibroblasts and their ability to modulate the activation of tumor-associated T cells. J Immunol. 2007;178(9):5552-62.

116. Balsamo M, Scordamaglia F, Pietra G, Manzini C, Cantoni C, Boitano M, et al. Melanoma-associated fibroblasts modulate NK cell phenotype and antitumor cytotoxicity. Proc Natl Acad Sci U S A. 2009;106(49):20847-52.

117. Fritz JH, Rojas OL, Simard N, McCarthy DD, Hapfelmeier S, Rubino S, et al. Acquisition of a multifunctional IgA+ plasma cell phenotype in the gut. Nature. 2011;481(7380):199-203.

118. Kang HS, Chin RK, Wang Y, Yu P, Wang J, Newell KA, et al. Signaling via LTbetaR on the lamina propria stromal cells of the gut is required for IgA production. Nat Immunol. 2002;3(6):576-82.

119. Fagarasan S, Kinoshita K, Muramatsu M, Ikuta K, Honjo T. In situ class switching and differentiation to IgA-producing cells in the gut lamina propria. Nature. 2001;413(6856):639-43.

120. Abdel Salam AG, Ata HM, Salman TM, Rashed LA, Sabry D, Schaalan MF. Potential therapeutic utility of mesenchymal stem cells in inflammatory bowel disease in mice. Int Immunopharmacol. 2014;22(2):515-21.

121. Lopez-Posadas R, Neurath MF, Atreya I. Molecular pathways driving disease-specific alterations of intestinal epithelial cells. Cell Mol Life Sci. 2017;74(5):803-26.

122. Khor B, Gardet A, Xavier RJ. Genetics and pathogenesis of inflammatory bowel disease. Nature. 2011;474(7351):307-17.

123. Maloy KJ, Powrie F. Intestinal homeostasis and its breakdown in inflammatory bowel disease. Nature. 2011;474(7351):298-306.

124. Triantafillidis JK, Merikas E, Georgopoulos F. Current and emerging drugs for the treatment of inflammatory bowel disease. Drug Des Devel Ther. 2011;5:185-210.

125. Dutta AK, Chacko A. Influence of environmental factors on the onset and course of inflammatory bowel disease. World J Gastroenterol. 2016;22(3):1088-100.

126. Koloski NA, Bret L, Radford-Smith G. Hygiene hypothesis in inflammatory bowel disease: a critical review of the literature. World J Gastroenterol. 2008;14(2):165-73.

127. Franke A, McGovern DP, Barrett JC, Wang K, Radford-Smith GL, Ahmad T, et al. Genome-wide meta-analysis increases to 71 the number of confirmed Crohn's disease susceptibility loci. Nat Genet. 2010;42(12):1118-25.

128. Anderson CA, Boucher G, Lees CW, Franke A, D'Amato M, Taylor KD, et al. Meta-analysis identifies 29 additional ulcerative colitis risk loci, increasing the number of confirmed associations to 47. Nat Genet. 2011;43(3):246-52.

129. Sharp RC, Abdulrahim M, Naser ES, Naser SA. Genetic Variations of PTPN2 and PTPN22: Role in the Pathogenesis of Type 1 Diabetes and Crohn's Disease. Front Cell Infect Microbiol. 2015;5:95.

130. Janse M, Lamberts LE, Franke L, Raychaudhuri S, Ellinghaus E, Muri Boberg K, et al. Three ulcerative colitis susceptibility loci are associated with primary sclerosing cholangitis and indicate a role for IL2, REL, and CARD9. Hepatology. 2011;53(6):1977-85.

131. Cardoso CC, Pereira AC, de Sales Marques C, Moraes MO. Leprosy susceptibility: genetic variations regulate innate and adaptive immunity, and disease outcome. Future Microbiol. 2011;6(5):533-49.

132. Cani PD. Human gut microbiome: hopes, threats and promises. Gut. 2018;67(9):1716-25.

133. Litvak Y, Byndloss MX, Baumler AJ. Colonocyte metabolism shapes the gut microbiota. Science. 2018;362(6418).

134. Tanaka M, Nakayama J. Development of the gut microbiota in infancy and its impact on health in later life. Allergol Int. 2017;66(4):515-22.

135. Rodriguez JM, Murphy K, Stanton C, Ross RP, Kober OI, Juge N, et al. The composition of the gut microbiota throughout life, with an emphasis on early life. Microb Ecol Health Dis. 2015;26:26050.

136. Nicholson JK, Holmes E, Kinross J, Burcelin R, Gibson G, Jia W, et al. Host-gut microbiota metabolic interactions. Science. 2012;336(6086):1262-7.

137. Bajaj JS, Barbara G, DuPont HL, Mearin F, Gasbarrini A, Tack J. New concepts on intestinal microbiota and the role of the non-absorbable antibiotics with special reference to rifaximin in digestive diseases. Dig Liver Dis. 2018;50(8):741-9.

138. Tilg H, Adolph TE, Gerner RR, Moschen AR. The Intestinal Microbiota in Colorectal Cancer. Cancer Cell. 2018;33(6):954-64.

139. Sartor RB. Microbial influences in inflammatory bowel diseases. Gastroenterology. 2008;134(2):577-94.

140. Guarner F. What is the role of the enteric commensal flora in IBD? Inflamm Bowel Dis. 2008;14 Suppl 2:S83-4.

141. Resta-Lenert S, Smitham J, Barrett KE. Epithelial dysfunction associated with the development of colitis in conventionally housed mdr1a-/- mice. Am J Physiol Gastrointest Liver Physiol. 2005;289(1):G153-62.

142. Taurog JD, Richardson JA, Croft JT, Simmons WA, Zhou M, Fernandez-Sueiro JL, et al. The germfree state prevents development of gut and joint inflammatory disease in HLA-B27 transgenic rats. J Exp Med. 1994;180(6):2359-64.

143. Rath HC, Herfarth HH, Ikeda JS, Grenther WB, Hamm TE, Jr., Balish E, et al. Normal luminal bacteria, especially Bacteroides species, mediate chronic colitis, gastritis, and arthritis in HLA-B27/human beta2 microglobulin transgenic rats. J Clin Invest. 1996;98(4):945-53.

144. Sartor RB, Cromartie WJ, Powell DW, Schwab JH. Granulomatous enterocolitis induced in rats by purified bacterial cell wall fragments. Gastroenterology. 1985;89(3):587-95.

145. Casellas F, Borruel N, Papo M, Guarner F, Antolin M, Videla S, et al. Antiinflammatory effects of enterically coated amoxicillin-clavulanic acid in active ulcerative colitis. Inflamm Bowel Dis. 1998;4(1):1-5.

146. Pirzer U, Schonhaar A, Fleischer B, Hermann E, Meyer zum Buschenfelde KH. Reactivity of infiltrating T lymphocytes with microbial antigens in Crohn's disease. Lancet. 1991;338(8777):1238-9.

147. Macpherson A, Khoo UY, Forgacs I, Philpott-Howard J, Bjarnason I. Mucosal antibodies in inflammatory bowel disease are directed against intestinal bacteria. Gut. 1996;38(3):365-75.

148. Macfarlane S, Furrie E, Cummings JH, Macfarlane GT. Chemotaxonomic analysis of bacterial populations colonizing the rectal mucosa in patients with ulcerative colitis. Clin Infect Dis. 2004;38(12):1690-9.

149. Marteau P. Bacterial flora in inflammatory bowel disease. Dig Dis. 2009;27 Suppl 1:99-103.

150. Lupp C, Robertson ML, Wickham ME, Sekirov I, Champion OL, Gaynor EC, et al. Host-mediated inflammation disrupts the intestinal microbiota and promotes the overgrowth of Enterobacteriaceae. Cell Host Microbe. 2007;2(2):119-29.

151. Frank DN, St Amand AL, Feldman RA, Boedeker EC, Harpaz N, Pace NR. Molecular-phylogenetic characterization of microbial community imbalances in human inflammatory bowel diseases. Proc Natl Acad Sci U S A. 2007;104(34):13780-5.

152. Alam MT, Amos GCA, Murphy ARJ, Murch S, Wellington EMH, Arasaradnam RP. Microbial imbalance in inflammatory bowel disease patients at different taxonomic levels. Gut Pathog. 2020;12:1.

153. Manichanh C, Borruel N, Casellas F, Guarner F. The gut microbiota in IBD. Nat Rev Gastroenterol Hepatol. 2012;9(10):599-608.

154. Ambalam P, Raman M, Purama RK, Doble M. Probiotics, prebiotics and colorectal cancer prevention. Best Pract Res Clin Gastroenterol. 2016;30(1):119-31.

155. Rodriguez-Nogales A, Algieri F, Garrido-Mesa J, Vezza T, Utrilla MP, Chueca N, et al. Intestinal anti-inflammatory effect of the probiotic Saccharomyces boulardii in DSS-induced colitis in mice: Impact on microRNAs expression and gut microbiota composition. J Nutr Biochem. 2018;61:129-39.

156. Rodriguez-Nogales A, Algieri F, Garrido-Mesa J, Vezza T, Utrilla MP, Chueca N, et al. The Administration of Escherichia coli Nissle 1917 Ameliorates Development of DSS-Induced Colitis in Mice. Front Pharmacol. 2018;9:468.

157. Tarrah A, de Castilhos J, Rossi RC, Duarte VDS, Ziegler DR, Corich V, et al. In vitro Probiotic Potential and Anti-cancer Activity of Newly Isolated Folate-Producing Streptococcus thermophilus Strains. Front Microbiol. 2018;9:2214.

158. Van der Sluis M, De Koning BA, De Bruijn AC, Velcich A, Meijerink JP, Van Goudoever JB, et al. Muc2-deficient mice spontaneously develop colitis, indicating that MUC2 is critical for colonic protection. Gastroenterology. 2006;131(1):117-29.

159. Velcich A, Yang W, Heyer J, Fragale A, Nicholas C, Viani S, et al. Colorectal cancer in mice genetically deficient in the mucin Muc2. Science. 2002;295(5560):1726-9.

160. Uehara A, Fujimoto Y, Fukase K, Takada H. Various human epithelial cells express functional Toll-like receptors, NOD1 and NOD2 to produce anti-microbial peptides, but not proinflammatory cytokines. Mol Immunol. 2007;44(12):3100-11.

161. Wehkamp J, Harder J, Weichenthal M, Mueller O, Herrlinger KR, Fellermann K, et al. Inducible and constitutive beta-defensins are differentially expressed in Crohn's disease and ulcerative colitis. Inflamm Bowel Dis. 2003;9(4):215-23.

162. Hugot JP, Chamaillard M, Zouali H, Lesage S, Cezard JP, Belaiche J, et al. Association of NOD2 leucine-rich repeat variants with susceptibility to Crohn's disease. Nature. 2001;411(6837):599-603.

163. Ogura Y, Bonen DK, Inohara N, Nicolae DL, Chen FF, Ramos R, et al. A frameshift mutation in NOD2 associated with susceptibility to Crohn's disease. Nature. 2001;411(6837):603-6.

164. Economou M, Trikalinos TA, Loizou KT, Tsianos EV, Ioannidis JP. Differential effects of NOD2 variants on Crohn's disease risk and phenotype in diverse populations: a metaanalysis. Am J Gastroenterol. 2004;99(12):2393-404.

165. Na YR, Stakenborg M, Seok SH, Matteoli G. Macrophages in intestinal inflammation and resolution: a potential therapeutic target in IBD. Nat Rev Gastroenterol Hepatol. 2019;16(9):531-43.

166. Yona S, Kim KW, Wolf Y, Mildner A, Varol D, Breker M, et al. Fate mapping reveals origins and dynamics of monocytes and tissue macrophages under homeostasis. Immunity. 2013;38(1):79-91.

167. Cerovic V, Houston SA, Scott CL, Aumeunier A, Yrlid U, Mowat AM, et al. Intestinal CD103(-) dendritic cells migrate in lymph and prime effector T cells. Mucosal Immunol. 2013;6(1):104-13.

168. Bain CC, Scott CL, Uronen-Hansson H, Gudjonsson S, Jansson O, Grip O, et al. Resident and pro-inflammatory macrophages in the colon represent alternative context-dependent fates of the same Ly6Chi monocyte precursors. Mucosal Immunol. 2013;6(3):498-510.

169. McGarry MP, Stewart CC. Murine eosinophil granulocytes bind the murine macrophage-monocyte specific monoclonal antibody F4/80. J Leukoc Biol. 1991;50(5):471-8.

170. Schulz O, Jaensson E, Persson EK, Liu X, Worbs T, Agace WW, et al. Intestinal CD103+, but not CX3CR1+, antigen sampling cells migrate in lymph and serve classical dendritic cell functions. J Exp Med. 2009;206(13):3101-14.

171. Mowat AM. To respond or not to respond - a personal perspective of intestinal tolerance. Nat Rev Immunol. 2018;18(6):405-15.

172. Mikkelsen HB, Rumessen JJ. Characterization of macrophage-like cells in the external layers of human small and large intestine. Cell Tissue Res. 1992;270(2):273-9.

173. Smith PD, Smythies LE, Shen R, Greenwell-Wild T, Gliozzi M, Wahl SM. Intestinal macrophages and response to microbial encroachment. Mucosal Immunol. 2011;4(1):31-42.

174. Grainger JR, Wohlfert EA, Fuss IJ, Bouladoux N, Askenase MH, Legrand F, et al. Inflammatory monocytes regulate pathologic responses to commensals during acute gastrointestinal infection. Nat Med. 2013;19(6):713-21.

175. Bain CC, Bravo-Blas A, Scott CL, Perdiguero EG, Geissmann F, Henri S, et al. Constant replenishment from circulating monocytes maintains the macrophage pool in the intestine of adult mice. Nat Immunol. 2014;15(10):929-37.

176. Schlitzer A, McGovern N, Teo P, Zelante T, Atarashi K, Low D, et al. IRF4 transcription factor-dependent CD11b+ dendritic cells in human and mouse control mucosal IL-17 cytokine responses. Immunity. 2013;38(5):970-83.

177. Romagnani S. Lymphokine production by human T cells in disease states. Annu Rev Immunol. 1994;12:227-57.

178. Korn T, Bettelli E, Oukka M, Kuchroo VK. IL-17 and Th17 Cells. Annu Rev Immunol. 2009;27:485-517.

179. Geremia A, Biancheri P, Allan P, Corazza GR, Di Sabatino A. Innate and adaptive immunity in inflammatory bowel disease. Autoimmun Rev. 2014;13(1):3-10.

180. Monteleone G, Biancone L, Marasco R, Morrone G, Marasco O, Luzza F, et al. Interleukin 12 is expressed and actively released by Crohn's disease intestinal lamina propria mononuclear cells. Gastroenterology. 1997;112(4):1169-78.

181. Podolsky DK. Inflammatory bowel disease. N Engl J Med. 2002;347(6):417-29.

182. Biancheri P, Di Sabatino A, Corazza GR, MacDonald TT. Proteases and the gut barrier. Cell Tissue Res. 2013;351(2):269-80.

183. MacDonald TT, Biancheri P, Sarra M, Monteleone G. What's the next best cytokine target in IBD? Inflamm Bowel Dis. 2012;18(11):2180-9.

184. Di Sabatino A, Biancheri P, Rovedatti L, MacDonald TT, Corazza GR. New pathogenic paradigms in inflammatory bowel disease. Inflamm Bowel Dis. 2012;18(2):368-71.

185. Fuss IJ, Heller F, Boirivant M, Leon F, Yoshida M, Fichtner-Feigl S, et al. Nonclassical CD1d-restricted NK T cells that produce IL-13 characterize an atypical Th2 response in ulcerative colitis. J Clin Invest. 2004;113(10):1490-7.

186. Heller F, Florian P, Bojarski C, Richter J, Christ M, Hillenbrand B, et al. Interleukin-13 is the key effector Th2 cytokine in ulcerative colitis that affects epithelial tight junctions, apoptosis, and cell restitution. Gastroenterology. 2005;129(2):550-64.

187. Kadivar K, Ruchelli ED, Markowitz JE, Defelice ML, Strogatz ML, Kanzaria MM, et al. Intestinal interleukin-13 in pediatric inflammatory bowel disease patients. Inflamm Bowel Dis. 2004;10(5):593-8.

188. Vainer B, Nielsen OH, Hendel J, Horn T, Kirman I. Colonic expression and synthesis of interleukin 13 and interleukin 15 in inflammatory bowel disease. Cytokine. 2000;12(10):1531-6.

189. Heller F, Fuss IJ, Nieuwenhuis EE, Blumberg RS, Strober W. Oxazolone colitis, a Th2 colitis model resembling ulcerative colitis, is mediated by IL-13-producing NK-T cells. Immunity. 2002;17(5):629-38.

190. Ceponis PJ, Botelho F, Richards CD, McKay DM. Interleukins 4 and 13 increase intestinal epithelial permeability by a phosphatidylinositol 3-kinase pathway. Lack of evidence for STAT 6 involvement. J Biol Chem. 2000;275(37):29132-7.

191. Bernardo D, Vallejo-Diez S, Mann ER, Al-Hassi HO, Martinez-Abad B, Montalvillo E, et al. IL-6 promotes immune responses in human ulcerative colitis and induces a skin-homing phenotype in the dendritic cells and Tcells they stimulate. Eur J Immunol. 2012;42(5):1337-53.

192. Zhou L, Ivanov, II, Spolski R, Min R, Shenderov K, Egawa T, et al. IL-6 programs T(H)-17 cell differentiation by promoting sequential engagement of the IL-21 and IL-23 pathways. Nat Immunol. 2007;8(9):967-74.

193. Rovedatti L, Kudo T, Biancheri P, Sarra M, Knowles CH, Rampton DS, et al. Differential regulation of interleukin 17 and interferon gamma production in inflammatory bowel disease. Gut. 2009;58(12):1629-36.

194. Monteleone G, Monteleone I, Fina D, Vavassori P, Del Vecchio Blanco G, Caruso R, et al. Interleukin-21 enhances T-helper cell type I signaling and interferon-gamma production in Crohn's disease. Gastroenterology. 2005;128(3):687-94.

195. Sarra M, Monteleone I, Stolfi C, Fantini MC, Sileri P, Sica G, et al. Interferon-gamma-expressing cells are a major source of interleukin-21 in inflammatory bowel diseases. Inflamm Bowel Dis. 2010;16(8):1332-9.

196. O'Garra A, Vieira P. Regulatory T cells and mechanisms of immune system control. Nat Med. 2004;10(8):801-5.

197. Valencia X, Stephens G, Goldbach-Mansky R, Wilson M, Shevach EM, Lipsky PE. TNF downmodulates the function of human CD4+CD25hi T-regulatory cells. Blood. 2006;108(1):253-61.

198. Fantini MC, Rizzo A, Fina D, Caruso R, Sarra M, Stolfi C, et al. Smad7 controls resistance of colitogenic T cells to regulatory T cell-mediated suppression. Gastroenterology. 2009;136(4):1308-16, e1-3.

199. Kinchen J, Chen HH, Parikh K, Antanaviciute A, Jagielowicz M, Fawkner-Corbett D, et al. Structural Remodeling of the Human Colonic Mesenchyme in Inflammatory Bowel Disease. Cell. 2018;175(2):372-86 e17.

200. Smillie CS, Biton M, Ordovas-Montanes J, Sullivan KM, Burgin G, Graham DB, et al. Intra- and Inter-cellular Rewiring of the Human Colon during Ulcerative Colitis. Cell. 2019;178(3):714-30 e22.

201. Martin JC, Chang C, Boschetti G, Ungaro R, Giri M, Grout JA, et al. Single-Cell Analysis of Crohn's Disease Lesions Identifies a Pathogenic Cellular Module Associated with Resistance to Anti-TNF Therapy. Cell. 2019;178(6):1493-508 e20.

202. Huang B, Chen Z, Geng L, Wang J, Liang H, Cao Y, et al. Mucosal Profiling of Pediatric-Onset Colitis and IBD Reveals Common Pathogenics and Therapeutic Pathways. Cell. 2019;179(5):1160-76 e24.

203. Barnhoorn MC, Hakuno SK, Bruckner RS, Rogler G, Hawinkels L, Scharl M. Stromal Cells in the Pathogenesis of Inflammatory Bowel Disease. J Crohns Colitis. 2020;14(7):995-1009.

204. Gerling M, Buller NV, Kirn LM, Joost S, Frings O, Englert B, et al. Stromal Hedgehog signalling is downregulated in colon cancer and its restoration restrains tumour growth. Nat Commun. 2016;7:12321.

205. Roberts KJ, Kershner AM, Beachy PA. The Stromal Niche for Epithelial Stem Cells: A Template for Regeneration and a Brake on Malignancy. Cancer Cell. 2017;32(4):404-10.

206. Arnold M, Sierra MS, Laversanne M, Soerjomataram I, Jemal A, Bray F. Global patterns and trends in colorectal cancer incidence and mortality. Gut. 2017;66(4):683-91.

207. Welch HG, Robertson DJ. Colorectal Cancer on the Decline--Why Screening Can't Explain It All. N Engl J Med. 2016;374(17):1605-7.

208. Terzic J, Grivennikov S, Karin E, Karin M. Inflammation and colon cancer. Gastroenterology. 2010;138(6):2101-14 e5.

209. Balkwill F, Mantovani A. Inflammation and cancer: back to Virchow? Lancet. 2001;357(9255):539-45.

210. Morson BC. Cancer in ulcerative colitis. Gut. 1966;7(5):425-6.

211. Jones JH. Colonic cancer and Crohn's disease. Gut. 1969;10(8):651-4.

212. Eaden JA, Abrams KR, Mayberry JF. The risk of colorectal cancer in ulcerative colitis: a meta-analysis. Gut. 2001;48(4):526-35.

213. Canavan C, Abrams KR, Mayberry J. Meta-analysis: colorectal and small bowel cancer risk in patients with Crohn's disease. Aliment Pharmacol Ther. 2006;23(8):1097-104.

214. Jess T, Rungoe C, Peyrin-Biroulet L. Risk of colorectal cancer in patients with ulcerative colitis: a meta-analysis of population-based cohort studies. Clin Gastroenterol Hepatol. 2012;10(6):639-45.

215. Coussens LM, Werb Z. Inflammation and cancer. Nature. 2002;420(6917):860-7.

216. Choi CR, Al Bakir I, Ding NJ, Lee GH, Askari A, Warusavitarne J, et al. Cumulative burden of inflammation predicts colorectal neoplasia risk in ulcerative colitis: a large single-centre study. Gut. 2019;68(3):414-22.

217. O'Connor PM, Lapointe TK, Beck PL, Buret AG. Mechanisms by which inflammation may increase intestinal cancer risk in inflammatory bowel disease. Inflamm Bowel Dis. 2010;16(8):1411-20.

218. Kundu JK, Surh YJ. Inflammation: gearing the journey to cancer. Mutat Res. 2008;659(1-2):15-30.

219. Danese S, Mantovani A. Inflammatory bowel disease and intestinal cancer: a paradigm of the Yin-Yang interplay between inflammation and cancer. Oncogene. 2010;29(23):3313-23.

220. Grivennikov SI, Greten FR, Karin M. Immunity, inflammation, and cancer. Cell. 2010;140(6):883-99.

221. Kemper C, Atkinson JP. T-cell regulation: with complements from innate immunity. Nat Rev Immunol. 2007;7(1):9-18.

222. Nishina T, Deguchi Y, Ohshima D, Takeda W, Ohtsuka M, Shichino S, et al. Interleukin-11-expressing fibroblasts have a unique gene signature correlated with poor prognosis of colorectal cancer. Nat Commun. 2021;12(1):2281.

223. Karin M, Lin A. NF-kappaB at the crossroads of life and death. Nat Immunol. 2002;3(3):221-7.

224. Karin M, Greten FR. NF-kappaB: linking inflammation and immunity to cancer development and progression. Nat Rev Immunol. 2005;5(10):749-59.

225. Greten FR, Eckmann L, Greten TF, Park JM, Li ZW, Egan LJ, et al. IKKbeta links inflammation and tumorigenesis in a mouse model of colitis-associated cancer. Cell. 2004;118(3):285-96.

226. Shaked H, Hofseth LJ, Chumanevich A, Chumanevich AA, Wang J, Wang Y, et al. Chronic epithelial NF-kappaB activation accelerates APC loss and intestinal tumor initiation through iNOS up-regulation. Proc Natl Acad Sci U S A. 2012;109(35):14007-12.

227. Popivanova BK, Kitamura K, Wu Y, Kondo T, Kagaya T, Kaneko S, et al. Blocking TNF-alpha in mice reduces colorectal carcinogenesis associated with chronic colitis. J Clin Invest. 2008;118(2):560-70.

228. Onizawa M, Nagaishi T, Kanai T, Nagano K, Oshima S, Nemoto Y, et al. Signaling pathway via TNF-alpha/NF-kappaB in intestinal epithelial cells may be directly involved in colitis-associated carcinogenesis. Am J Physiol Gastrointest Liver Physiol. 2009;296(4):G850-9.

229. Su L, Nalle SC, Shen L, Turner ES, Singh G, Breskin LA, et al. TNFR2 activates MLCK-dependent tight junction dysregulation to cause apoptosis-mediated barrier loss and experimental colitis. Gastroenterology. 2013;145(2):407-15.

230. Waldner MJ, Neurath MF. Mechanisms of Immune Signaling in Colitis-Associated Cancer. Cell Mol Gastroenterol Hepatol. 2015;1(1):6-16.

231. Mitsuyama K, Sata M, Rose-John S. Interleukin-6 trans-signaling in inflammatory bowel disease. Cytokine Growth Factor Rev. 2006;17(6):451-61.

232. Blanchot-Jossic F, Jarry A, Masson D, Bach-Ngohou K, Paineau J, Denis MG, et al. Up-regulated expression of ADAM17 in human colon carcinoma: co-expression with EGFR in neoplastic and endothelial cells. J Pathol. 2005;207(2):156-63.

233. Becker C, Fantini MC, Schramm C, Lehr HA, Wirtz S, Nikolaev A, et al. TGF-beta suppresses tumor progression in colon cancer by inhibition of IL-6 trans-signaling. Immunity. 2004;21(4):491-501.

234. Matsumoto S, Hara T, Mitsuyama K, Yamamoto M, Tsuruta O, Sata M, et al. Essential roles of IL-6 trans-signaling in colonic epithelial cells, induced by the IL-6/soluble-IL-6 receptor derived from lamina propria macrophages, on the development of colitis-associated premalignant cancer in a murine model. J Immunol. 2010;184(3):1543-51.

235. Grivennikov S, Karin E, Terzic J, Mucida D, Yu GY, Vallabhapurapu S, et al. IL-6 and Stat3 are required for survival of intestinal epithelial cells and development of colitis-associated cancer. Cancer Cell. 2009;15(2):103-13.

236. Bollrath J, Phesse TJ, von Burstin VA, Putoczki T, Bennecke M, Bateman T, et al. gp130-mediated Stat3 activation in enterocytes regulates cell survival and cell-cycle progression during colitis-associated tumorigenesis. Cancer Cell. 2009;15(2):91-102.

237. Putoczki TL, Thiem S, Loving A, Busuttil RA, Wilson NJ, Ziegler PK, et al. Interleukin-11 is the dominant IL-6 family cytokine during gastrointestinal tumorigenesis and can be targeted therapeutically. Cancer Cell. 2013;24(2):257-71.

238. Clevers H. Wnt/beta-catenin signaling in development and disease. Cell. 2006;127(3):469-80.

239. Polakis P. The many ways of Wnt in cancer. Curr Opin Genet Dev. 2007;17(1):45-51.

240. MacDonald BT, Tamai K, He X. Wnt/beta-catenin signaling: components, mechanisms, and diseases. Dev Cell. 2009;17(1):9-26.

241. Parker TW, Neufeld KL. APC controls Wnt-induced beta-catenin destruction complex recruitment in human colonocytes. Sci Rep. 2020;10(1):2957.

242. Zhang L, Shay JW. Multiple Roles of APC and its Therapeutic Implications in Colorectal Cancer. J Natl Cancer Inst. 2017;109(8).

243. Robles AI, Traverso G, Zhang M, Roberts NJ, Khan MA, Joseph C, et al. Whole-Exome Sequencing Analyses of Inflammatory Bowel Disease-Associated Colorectal Cancers. Gastroenterology. 2016;150(4):931-43.

244. Jobin C, Morteau O, Han DS, Balfour Sartor R. Specific NF-kappaB blockade selectively inhibits tumour necrosis factor-alpha-induced COX-2 but not constitutive COX-1 gene expression in HT-29 cells. Immunology. 1998;95(4):537-43.

245. Eberhart CE, Coffey RJ, Radhika A, Giardiello FM, Ferrenbach S, DuBois RN. Up-regulation of cyclooxygenase 2 gene expression in human colorectal adenomas and adenocarcinomas. Gastroenterology. 1994;107(4):1183-8.

246. Chulada PC, Thompson MB, Mahler JF, Doyle CM, Gaul BW, Lee C, et al. Genetic disruption of Ptgs-1, as well as Ptgs-2, reduces intestinal tumorigenesis in Min mice. Cancer Res. 2000;60(17):4705-8.

247. Lal G, Ash C, Hay K, Redston M, Kwong E, Hancock B, et al. Suppression of intestinal polyps in Msh2-deficient and non-Msh2-deficient multiple intestinal neoplasia mice by a specific cyclooxygenase-2 inhibitor and by a dual cyclooxygenase-1/2 inhibitor. Cancer Res. 2001;61(16):6131-6.

248. Al-Salihi MA, Terrece Pearman A, Doan T, Reichert EC, Rosenberg DW, Prescott SM, et al. Transgenic expression of cyclooxygenase-2 in mouse intestine epithelium is insufficient to initiate tumorigenesis but promotes tumor progression. Cancer Lett. 2009;273(2):225-32.

249. Hamoya T, Fujii G, Miyamoto S, Takahashi M, Totsuka Y, Wakabayashi K, et al. Effects of NSAIDs on the risk factors of colorectal cancer: a mini review. Genes Environ. 2016;38:6.

250. Castellone MD, Teramoto H, Williams BO, Druey KM, Gutkind JS. Prostaglandin E2 promotes colon cancer cell growth through a Gs-axin-beta-catenin signaling axis. Science. 2005;310(5753):1504-10.

251. Shao J, Jung C, Liu C, Sheng H. Prostaglandin E2 Stimulates the beta-catenin/T cell factor-dependent transcription in colon cancer. J Biol Chem. 2005;280(28):26565-72.

252. Jones MK, Wang H, Peskar BM, Levin E, Itani RM, Sarfeh IJ, et al. Inhibition of angiogenesis by nonsteroidal anti-inflammatory drugs: insight into mechanisms and implications for cancer growth and ulcer healing. Nat Med. 1999;5(12):1418-23.

253. Khayrullina T, Yen JH, Jing H, Ganea D. In vitro differentiation of dendritic cells in the presence of prostaglandin E2 alters the IL-12/IL-23 balance and promotes differentiation of Th17 cells. J Immunol. 2008;181(1):721-35.

254. Ahern PP, Izcue A, Maloy KJ, Powrie F. The interleukin-23 axis in intestinal inflammation. Immunol Rev. 2008;226:147-59.

255. Langowski JL, Zhang X, Wu L, Mattson JD, Chen T, Smith K, et al. IL-23 promotes tumour incidence and growth. Nature. 2006;442(7101):461-5.

256. Grivennikov SI, Wang K, Mucida D, Stewart CA, Schnabl B, Jauch D, et al. Adenoma-linked barrier defects and microbial products drive IL-23/IL-17-mediated tumour growth. Nature. 2012;491(7423):254-8.

257. Gupta JW, Kubin M, Hartman L, Cassatella M, Trinchieri G. Induction of expression of genes encoding components of the respiratory burst oxidase during differentiation of human myeloid cell lines induced by tumor necrosis factor and gamma-interferon. Cancer Res. 1992;52(9):2530-7.

258. Qi H, Yang H, Xu G, Ren J, Hua W, Shi Y, et al. Therapeutic efficacy of IL-17A antibody injection in preventing the development of colitis associated carcinogenesis in mice. Immunobiology. 2015;220(1):54-9.

259. Hyun YS, Han DS, Lee AR, Eun CS, Youn J, Kim HY. Role of IL-17A in the development of colitis-associated cancer. Carcinogenesis. 2012;33(4):931-6.

260. Pickert G, Neufert C, Leppkes M, Zheng Y, Wittkopf N, Warntjen M, et al. STAT3 links IL-22 signaling in intestinal epithelial cells to mucosal wound healing. J Exp Med. 2009;206(7):1465-72.

261. Yu LZ, Wang HY, Yang SP, Yuan ZP, Xu FY, Sun C, et al. Expression of interleukin-22/STAT3 signaling pathway in ulcerative colitis and related carcinogenesis. World J Gastroenterol. 2013;19(17):2638-49.

262. Plava J, Cihova M, Burikova M, Matuskova M, Kucerova L, Miklikova S. Recent advances in understanding tumor stroma-mediated chemoresistance in breast cancer. Mol Cancer. 2019;18(1):67.

263. Guinney J, Dienstmann R, Wang X, de Reynies A, Schlicker A, Soneson C, et al. The consensus molecular subtypes of colorectal cancer. Nat Med. 2015;21(11):1350-6.

264. De Robertis M, Massi E, Poeta ML, Carotti S, Morini S, Cecchetelli L, et al. The AOM/DSS murine model for the study of colon carcinogenesis: From pathways to diagnosis and therapy studies. J Carcinog. 2011;10:9.

265. Tanaka T, Kohno H, Suzuki R, Yamada Y, Sugie S, Mori H. A novel inflammation-related mouse colon carcinogenesis model induced by azoxymethane and dextran sodium sulfate. Cancer Sci. 2003;94(11):965-73.

266. Takahashi M, Wakabayashi K. Gene mutations and altered gene expression in azoxymethane-induced colon carcinogenesis in rodents. Cancer Sci. 2004;95(6):475-80.

267. Neufert C, Heichler C, Brabletz T, Scheibe K, Boonsanay V, Greten FR, et al. Inducible mouse models of colon cancer for the analysis of sporadic and inflammation-driven tumor progression and lymph node metastasis. Nat Protoc. 2021;16(1):61-85.

268. Koliaraki V, Pasparakis M, Kollias G. IKKbeta in intestinal mesenchymal cells promotes initiation of colitis-associated cancer. J Exp Med. 2015;212(13):2235-51.

269. Henriques A, Koliaraki V, Kollias G. Mesenchymal MAPKAPK2/HSP27 drives intestinal carcinogenesis. Proc Natl Acad Sci U S A. 2018;115(24):E5546-E55.

270. Yuan Q, Gu J, Zhang J, Liu S, Wang Q, Tian T, et al. MyD88 in myofibroblasts enhances colitis-associated tumorigenesis via promoting macrophage M2 polarization. Cell Rep. 2021;34(5):108724.

271. Hamilton KE, Chatterji P, Lundsmith ET, Andres SF, Giroux V, Hicks PD, et al. Loss of Stromal IMP1 Promotes a Tumorigenic Microenvironment in the Colon. Mol Cancer Res. 2015;13(11):1478-86.

272. Li GC, Zhang HW, Zhao QC, Sun LI, Yang JJ, Hong L, et al. Mesenchymal stem cells promote tumor angiogenesis via the action of transforming growth factor beta1. Oncol Lett. 2016;11(2):1089-94.

273. Ljujic B, Milovanovic M, Volarevic V, Murray B, Bugarski D, Przyborski S, et al. Human mesenchymal stem cells creating an immunosuppressive environment and promote breast cancer in mice. Sci Rep. 2013;3:2298.

274. Li JH, Fan WS, Wang MM, Wang YH, Ren ZG. Effects of mesenchymal stem cells on solid tumor metastasis in experimental cancer models: a systematic review and meta-analysis. J Transl Med. 2018;16(1):113.

275. Christodoulou I, Goulielmaki M, Devetzi M, Panagiotidis M, Koliakos G, Zoumpourlis V. Mesenchymal stem cells in preclinical cancer cytotherapy: a systematic review. Stem Cell Res Ther. 2018;9(1):336.

276. Khakoo AY, Pati S, Anderson SA, Reid W, Elshal MF, Rovira, II, et al. Human mesenchymal stem cells exert potent antitumorigenic effects in a model of Kaposi's sarcoma. J Exp Med. 2006;203(5):1235-47.

277. Cousin B, Ravet E, Poglio S, De Toni F, Bertuzzi M, Lulka H, et al. Adult stromal cells derived from human adipose tissue provoke pancreatic cancer cell death both in vitro and in vivo. PLoS One. 2009;4(7):e6278.

278. Duijvestein M, Vos AC, Roelofs H, Wildenberg ME, Wendrich BB, Verspaget HW, et al. Autologous bone marrow-derived mesenchymal stromal cell treatment for refractory luminal Crohn's disease: results of a phase I study. Gut. 2010;59(12):1662-9.

279. Panes J, Garcia-Olmo D, Van Assche G, Colombel JF, Reinisch W, Baumgart DC, et al. Expanded allogeneic adipose-derived mesenchymal stem cells (Cx601) for complex perianal fistulas in Crohn's disease: a phase 3 randomised, double-blind controlled trial. Lancet. 2016;388(10051):1281-90.

280. Nasuno M, Arimura Y, Nagaishi K, Isshiki H, Onodera K, Nakagaki S, et al. Mesenchymal stem cells cancel azoxymethane-induced tumor initiation. Stem Cells. 2014;32(4):913-25.

281. Chen Z, He X, He X, Chen X, Lin X, Zou Y, et al. Bone marrow mesenchymal stem cells ameliorate colitis-associated tumorigenesis in mice. Biochem Biophys Res Commun. 2014;450(4):1402-8.

282. Tang RJ, Shen SN, Zhao XY, Nie YZ, Xu YJ, Ren J, et al. Mesenchymal stem cells-regulated Treg cells suppress colitis-associated colorectal cancer. Stem Cell Res Ther. 2015;6:71.

283. Zhang X, Wang S, Ding X, Guo J, Tian Z. Potential methods for improving the efficacy of mesenchymal stem cells in the treatment of inflammatory bowel diseases. Scand J Immunol. 2020;92(3):e12897.

284. Hu S, Yuan J, Xu J, Li X, Zhang G, Ma Q, et al. TNF-alpha and IFN-gamma synergistically inhibit the repairing ability of mesenchymal stem cells on mice colitis and colon cancer. Am J Transl Res. 2019;11(9):6207-20.

285. Beswick EJ, Johnson JR, Saada JI, Humen M, House J, Dann S, et al. TLR4 activation enhances the PD-L1-mediated tolerogenic capacity of colonic CD90+ stromal cells. J Immunol. 2014;193(5):2218-29.

286. Riehl TE, Alvarado D, Ee X, Zuckerman A, Foster L, Kapoor V, et al. Lactobacillus rhamnosus GG protects the intestinal epithelium from radiation injury through release of lipoteichoic acid, macrophage activation and the migration of mesenchymal stem cells. Gut. 2019;68(6):1003-13.

287. Zawahir S, Li G, Banerjee A, Shiu J, Blanchard TG, Okogbule-Wonodi AC. Inflammatory and Immune Activation in Intestinal Myofibroblasts Is Developmentally Regulated. J Interferon Cytokine Res. 2015;35(8):634-40.

288. Vicente-Suarez I, Larange A, Reardon C, Matho M, Feau S, Chodaczek G, et al. Unique lamina propria stromal cells imprint the functional phenotype of mucosal dendritic cells. Mucosal Immunol. 2015;8(1):141-51.

289. Inatomi O, Andoh A, Kitamura K, Yasui H, Zhang Z, Fujiyama Y. Butyrate blocks interferon-gamma-inducible protein-10 release in human intestinal subepithelial myofibroblasts. J Gastroenterol. 2005;40(5):483-9.

290. Willemsen LE, Koetsier MA, van Deventer SJ, van Tol EA. Short chain fatty acids stimulate epithelial mucin 2 expression through differential effects on prostaglandin E(1) and E(2) production by intestinal myofibroblasts. Gut. 2003;52(10):1442-7.

291. Gonzalez-Sarrias A, Larrosa M, Tomas-Barberan FA, Dolara P, Espin JC. NF-kappaB-dependent anti-inflammatory activity of urolithins, gut microbiota ellagic acid-derived metabolites, in human colonic fibroblasts. Br J Nutr. 2010;104(4):503-12.

292. Jacob N, Jacobs JP, Kumagai K, Ha CWY, Kanazawa Y, Lagishetty V, et al. Inflammation-independent TL1A-mediated intestinal fibrosis is dependent on the gut microbiome. Mucosal Immunol. 2018;11(5):1466-76.

293. Nagashima K, Sawa S, Nitta T, Tsutsumi M, Okamura T, Penninger JM, et al. Identification of subepithelial mesenchymal cells that induce IgA and diversify gut microbiota. Nat Immunol. 2017;18(6):675-82.

294. Krasnodembskaya A, Song Y, Fang X, Gupta N, Serikov V, Lee JW, et al. Antibacterial effect of human mesenchymal stem cells is mediated in part from secretion of the antimicrobial peptide LL-37. Stem Cells. 2010;28(12):2229-38.

295. Meisel R, Brockers S, Heseler K, Degistirici O, Bulle H, Woite C, et al. Human but not murine multipotent mesenchymal stromal cells exhibit broad-spectrum antimicrobial effector function mediated by indoleamine 2,3-dioxygenase. Leukemia. 2011;25(4):648-54.

296. Yang R, Liu Y, Kelk P, Qu C, Akiyama K, Chen C, et al. A subset of IL-17(+) mesenchymal stem cells possesses anti-Candida albicans effect. Cell Res. 2013;23(1):107-21.

297. Borges-Canha M, Portela-Cidade JP, Dinis-Ribeiro M, Leite-Moreira AF, Pimentel-Nunes P. Role of colonic microbiota in colorectal carcinogenesis: a systematic review. Rev Esp Enferm Dig. 2015;107(11):659-71.

298. Baxter NT, Zackular JP, Chen GY, Schloss PD. Structure of the gut microbiome following colonization with human feces determines colonic tumor burden. Microbiome. 2014;2:20.

299. Pochampally R. Colony forming unit assays for MSCs. Methods Mol Biol. 2008;449:83-91.

300. Garrido-Mesa J, Rodriguez-Nogales A, Algieri F, Vezza T, Hidalgo-Garcia L, Garrido-Barros M, et al. Immunomodulatory tetracyclines shape the intestinal inflammatory response inducing mucosal healing and resolution. Br J Pharmacol. 2018;175(23):4353-70.

301. Vezza T, Algieri F, Rodriguez-Nogales A, Garrido-Mesa J, Utrilla MP, Talhaoui N, et al. Immunomodulatory properties of Olea europaea leaf extract in intestinal inflammation. Mol Nutr Food Res. 2017;61(10).

302. Neufert C, Becker C, Neurath MF. An inducible mouse model of colon carcinogenesis for the analysis of sporadic and inflammation-driven tumor progression. Nat Protoc. 2007;2(8):1998-2004.

303. Wirtz S, Neufert C, Weigmann B, Neurath MF. Chemically induced mouse models of intestinal inflammation. Nat Protoc. 2007;2(3):541-6.

304. Becker C, Fantini MC, Neurath MF. High resolution colonoscopy in live mice. Nat Protoc. 2006;1(6):2900-4.

305. Camuesco D, Comalada M, Rodriguez-Cabezas ME, Nieto A, Lorente MD, Concha A, et al. The intestinal anti-inflammatory effect of quercitrin is associated with an inhibition in iNOS expression. Br J Pharmacol. 2004;143(7):908-18.

306. Rodriguez-Nogales A, Algieri F, Garrido-Mesa J, Vezza T, Utrilla MP, Chueca N, et al. Differential intestinal anti-inflammatory effects of Lactobacillus fermentum and Lactobacillus salivarius in DSS mouse colitis: impact on microRNAs expression and microbiota composition. Mol Nutr Food Res. 2017;61(11).

307. Magoc T, Salzberg SL. FLASH: fast length adjustment of short reads to improve genome assemblies. Bioinformatics. 2011;27(21):2957-63.

308. Bokulich NA, Subramanian S, Faith JJ, Gevers D, Gordon JI, Knight R, et al. Quality-filtering vastly improves diversity estimates from Illumina amplicon sequencing. Nat Methods. 2013;10(1):57-9.

309. Caporaso JG, Kuczynski J, Stombaugh J, Bittinger K, Bushman FD, Costello EK, et al. QIIME allows analysis of high-throughput community sequencing data. Nat Methods. 2010;7(5):335-6.

310. Edgar RC, Haas BJ, Clemente JC, Quince C, Knight R. UCHIME improves sensitivity and speed of chimera detection. Bioinformatics. 2011;27(16):2194-200.

311. Haas BJ, Gevers D, Earl AM, Feldgarden M, Ward DV, Giannoukos G, et al. Chimeric 16S rRNA sequence formation and detection in Sanger and 454-pyrosequenced PCR amplicons. Genome Res. 2011;21(3):494-504.

312. Edgar RC. UPARSE: highly accurate OTU sequences from microbial amplicon reads. Nat Methods. 2013;10(10):996-8.

313. Wang Q, Garrity GM, Tiedje JM, Cole JR. Naive Bayesian classifier for rapid assignment of rRNA sequences into the new bacterial taxonomy. Appl Environ Microbiol. 2007;73(16):5261-7.

314. Quast C, Pruesse E, Yilmaz P, Gerken J, Schweer T, Yarza P, et al. The SILVA ribosomal RNA gene database project: improved data processing and web-based tools. Nucleic Acids Res. 2013;41(Database issue):D590-6.

315. Thomson CA, Nibbs RJ, McCoy KD, Mowat AM. Immunological roles of intestinal mesenchymal cells. Immunology. 2020;160(4):313-24.

316. Wei W, Ao Q, Wang X, Cao Y, Liu Y, Zheng SG, et al. Mesenchymal Stem Cell-Derived Exosomes: A Promising Biological Tool in Nanomedicine. Front Pharmacol. 2020;11:590470.

317. Krampera M. Mesenchymal stromal cells: more than inhibitory cells. Leukemia. 2011;25(4):565-6.

318. Krampera M. Mesenchymal stromal cell 'licensing': a multistep process. Leukemia. 2011;25(9):1408-14.

319. Uccelli A, Moretta L, Pistoia V. Immunoregulatory function of mesenchymal stem cells. Eur J Immunol. 2006;36(10):2566-73.

320. Hidalgo-Garcia L, Galvez J, Rodriguez-Cabezas ME, Anderson PO. Can a Conversation Between Mesenchymal Stromal Cells and Macrophages Solve the Crisis in the Inflamed Intestine? Front Pharmacol. 2018;9:179.

321. Roulis M, Nikolaou C, Kotsaki E, Kaffe E, Karagianni N, Koliaraki V, et al. Intestinal myofibroblast-specific Tpl2-Cox-2-PGE2 pathway links innate sensing to epithelial homeostasis. Proc Natl Acad Sci U S A. 2014;111(43):E4658-67.

322. Davis MJ, Tsang TM, Qiu Y, Dayrit JK, Freij JB, Huffnagle GB, et al. Macrophage M1/M2 polarization dynamically adapts to changes in cytokine microenvironments in Cryptococcus neoformans infection. mBio. 2013;4(3):e00264-13.

323. He R, Han C, Li Y, Qian W, Hou X. Cancer-Preventive Role of Bone Marrow-Derived Mesenchymal Stem Cells on Colitis-Associated Colorectal Cancer: Roles of Gut Microbiota Involved. Front Cell Dev Biol. 2021;9:642948.

324. Zheng XB, He XW, Zhang LJ, Qin HB, Lin XT, Liu XH, et al. Bone marrow-derived CXCR4-overexpressing MSCs display increased homing to intestine and ameliorate colitis-associated tumorigenesis in mice. Gastroenterol Rep (Oxf). 2019;7(2):127-38.

325. Yin P, Gui L, Wang C, Yan J, Liu M, Ji L, et al. Targeted Delivery of CXCL9 and OX40L by Mesenchymal Stem Cells Elicits Potent Antitumor Immunity. Mol Ther. 2020;28(12):2553-63.

326. Jary M, Hasanova R, Vienot A, Asgarov K, Loyon R, Tirole C, et al. Molecular description of ANGPT2 associated colorectal carcinoma. Int J Cancer. 2020;147(7):2007-18.

327. Suzuki R, Miyamoto S, Yasui Y, Sugie S, Tanaka T. Global gene expression analysis of the mouse colonic mucosa treated with azoxymethane and dextran sodium sulfate. BMC Cancer. 2007;7:84.

328. Josse C, Bouznad N, Geurts P, Irrthum A, Huynh-Thu VA, Servais L, et al. Identification of a microRNA landscape targeting the PI3K/Akt signaling pathway in inflammation-induced colorectal carcinogenesis. Am J Physiol Gastrointest Liver Physiol. 2014;306(3):G229-43.

329. Sohn OS, Fiala ES, Requeijo SP, Weisburger JH, Gonzalez FJ. Differential effects of CYP2E1 status on the metabolic activation of the colon carcinogens azoxymethane and methylazoxymethanol. Cancer Res. 2001;61(23):8435-40.

330. Goretsky T, Bradford EM, Ye Q, Lamping OF, Vanagunas T, Moyer MP, et al. Beta-catenin cleavage enhances transcriptional activation. Sci Rep. 2018;8(1):671.

331. Joeris T, Muller-Luda K, Agace WW, Mowat AM. Diversity and functions of intestinal mononuclear phagocytes. Mucosal Immunol. 2017;10(4):845-64.

332. Alhmoud T, Gremida A, Colom Steele D, Fallahi I, Tuqan W, Nandy N, et al. Outcomes of inflammatory bowel disease in patients with eosinophil-predominant colonic inflammation. BMJ Open Gastroenterol. 2020;7(1):e000373.

333. Okba AM, Amin MM, Abdelmoaty AS, Ebada HE, Kamel AH, Allam AS, et al. Neutrophil/lymphocyte ratio and lymphocyte/monocyte ratio in ulcerative colitis as non-invasive biomarkers of disease activity and severity. Auto Immun Highlights. 2019;10(1):4.

334. Bischoff SC, Wedemeyer J, Herrmann A, Meier PN, Trautwein C, Cetin Y, et al. Quantitative assessment of intestinal eosinophils and mast cells in inflammatory bowel disease. Histopathology. 1996;28(1):1-13.

335. Shevyrev D, Tereshchenko V. Treg Heterogeneity, Function, and Homeostasis. Front Immunol. 2019;10:3100.

336. Yan JB, Luo MM, Chen ZY, He BH. The Function and Role of the Th17/Treg Cell Balance in Inflammatory Bowel Disease. J Immunol Res. 2020;2020:8813558.

337. Degirmenci B, Valenta T, Dimitrieva S, Hausmann G, Basler K. GLI1-expressing mesenchymal cells form the essential Wnt-secreting niche for colon stem cells. Nature. 2018;558(7710):449-53.

338. Xu L, Liu Y, Sun Y, Wang B, Xiong Y, Lin W, et al. Tissue source determines the differentiation potentials of mesenchymal stem cells: a comparative study of human mesenchymal stem cells from bone marrow and adipose tissue. Stem Cell Res Ther. 2017;8(1):275.

339. Powell DW, Mifflin RC, Valentich JD, Crowe SE, Saada JI, West AB. Myofibroblasts. II. Intestinal subepithelial myofibroblasts. Am J Physiol. 1999;277(2):C183-201.

340. Meisel R, Zibert A, Laryea M, Gobel U, Daubener W, Dilloo D. Human bone marrow stromal cells inhibit allogeneic T-cell responses by indoleamine 2,3-dioxygenase-mediated tryptophan degradation. Blood. 2004;103(12):4619-21.

341. Ciorba MA. Indoleamine 2,3 dioxygenase in intestinal disease. Curr Opin Gastroenterol. 2013;29(2):146-52.

342. Acovic A, Gazdic M, Jovicic N, Harrell CR, Fellabaum C, Arsenijevic N, et al. Role of indoleamine 2,3-dioxygenase in pathology of the gastrointestinal tract. Therap Adv Gastroenterol. 2018;11:1756284818815334.

343. Torres Crigna A, Uhlig S, Elvers-Hornung S, Kluter H, Bieback K. Human Adipose Tissue-Derived Stromal Cells Suppress Human, but Not Murine Lymphocyte Proliferation, via Indoleamine 2,3-Dioxygenase Activity. Cells. 2020;9(11).

344. Galipeau J, Krampera M, Barrett J, Dazzi F, Deans RJ, DeBruijn J, et al. International Society for Cellular Therapy perspective on immune functional assays for mesenchymal stromal cells as potency release criterion for advanced phase clinical trials. Cytotherapy. 2016;18(2):151-9.

345. Cui G, Li C, Xu G, Sun Z, Zhu L, Li Z, et al. Tumor-Associated Fibroblasts and Microvessels Contribute to the Expression of Immunosuppressive Factor Indoleamine 2, 3-Dioxygenase in Human Esophageal Cancers. Pathol Oncol Res. 2018;24(2):269-75.

346. West NR, Hegazy AN, Owens BMJ, Bullers SJ, Linggi B, Buonocore S, et al. Oncostatin M drives intestinal inflammation and predicts response to tumor necrosis factor-neutralizing therapy in patients with inflammatory bowel disease. Nat Med. 2017;23(5):579-89.

347. Caer C, Wick MJ. Human Intestinal Mononuclear Phagocytes in Health and Inflammatory Bowel Disease. Front Immunol. 2020;11:410.

348. Koelink PJ, Bloemendaal FM, Li B, Westera L, Vogels EWM, van Roest M, et al. Anti-TNF therapy in IBD exerts its therapeutic effect through macrophage IL-10 signalling. Gut. 2020;69(6):1053-63.

349. Nemeth K, Leelahavanichkul A, Yuen PS, Mayer B, Parmelee A, Doi K, et al. Bone marrow stromal cells attenuate sepsis via prostaglandin E(2)-dependent reprogramming of host macrophages to increase their interleukin-10 production. Nat Med. 2009;15(1):42-9.

350. Anderson P, Souza-Moreira L, Morell M, Caro M, O'Valle F, Gonzalez-Rey E, et al. Adipose-derived mesenchymal stromal cells induce immunomodulatory macrophages which protect from experimental colitis and sepsis. Gut. 2013;62(8):1131-41.

351. Chanput W, Mes JJ, Wichers HJ. THP-1 cell line: an in vitro cell model for immune modulation approach. Int Immunopharmacol. 2014;23(1):37-45.

352. Daigneault M, Preston JA, Marriott HM, Whyte MK, Dockrell DH. The identification of markers of macrophage differentiation in PMA-stimulated THP-1 cells and monocyte-derived macrophages. PLoS One. 2010;5(1):e8668.

353. Jiminez JA, Uwiera TC, Douglas Inglis G, Uwiera RR. Animal models to study acute and chronic intestinal inflammation in mammals. Gut Pathog. 2015;7:29.

354. Valatas V, Vakas M, Kolios G. The value of experimental models of colitis in predicting efficacy of biological therapies for inflammatory bowel diseases. Am J Physiol Gastrointest Liver Physiol. 2013;305(11):G763-85.

355. Mizoguchi E, Low D, Ezaki Y, Okada T. Recent updates on the basic mechanisms and pathogenesis of inflammatory bowel diseases in experimental animal models. Intest Res. 2020;18(2):151-67.

356. Lohan P, Treacy O, Morcos M, Donohoe E, O'Donoghue Y, Ryan AE, et al. Interspecies Incompatibilities Limit the Immunomodulatory Effect of Human Mesenchymal Stromal Cells in the Rat. Stem Cells. 2018;36(8):1210-5.

357. Ren G, Su J, Zhang L, Zhao X, Ling W, L'Huillie A, et al. Species variation in the mechanisms of mesenchymal stem cell-mediated immunosuppression. Stem Cells. 2009;27(8):1954-62.

358. Lee HK, Kim EY, Kim HS, Park EJ, Lee HJ, Lee TY, et al. Effect of Human Mesenchymal Stem Cells on Xenogeneic T and B Cells Isolated from Lupus-Prone MRL.Fas (lpr) Mice. Stem Cells Int. 2020;2020:5617192.

359. Kim JH, Lee YT, Hong JM, Hwang YI. Suppression of in vitro murine T cell proliferation by human adipose tissue-derived mesenchymal stem cells is dependent mainly on cyclooxygenase-2 expression. Anat Cell Biol. 2013;46(4):262-71.

360. Prockop DJ, Oh JY, Lee RH. Data against a Common Assumption: Xenogeneic Mouse Models Can Be Used to Assay Suppression of Immunity by Human MSCs. Mol Ther. 2017;25(8):1748-56.

361. Castelo-Branco MT, Soares ID, Lopes DV, Buongusto F, Martinusso CA, do Rosario A, Jr., et al. Intraperitoneal but not intravenous cryopreserved mesenchymal stromal cells home to the inflamed colon and ameliorate experimental colitis. PLoS One. 2012;7(3):e33360.

362. Wang M, Liang C, Hu H, Zhou L, Xu B, Wang X, et al. Intraperitoneal injection (IP), Intravenous injection (IV) or anal injection (AI)? Best way for mesenchymal stem cells transplantation for colitis. Sci Rep. 2016;6:30696.

363. Sala E, Genua M, Petti L, Anselmo A, Arena V, Cibella J, et al. Mesenchymal Stem Cells Reduce Colitis in Mice via Release of TSG6, Independently of Their Localization to the Intestine. Gastroenterology. 2015;149(1):163-76 e20.

364. Stzepourginski I, Nigro G, Jacob JM, Dulauroy S, Sansonetti PJ, Eberl G, et al. CD34+ mesenchymal cells are a major component of the intestinal stem cells niche at homeostasis and after injury. Proc Natl Acad Sci U S A. 2017;114(4):E506-E13.

365. Karpus ON, Westendorp BF, Vermeulen JLM, Meisner S, Koster J, Muncan V, et al. Colonic CD90+ Crypt Fibroblasts Secrete Semaphorins to Support Epithelial Growth. Cell Rep. 2019;26(13):3698-708 e5.

366. Goessling W, North TE, Loewer S, Lord AM, Lee S, Stoick-Cooper CL, et al. Genetic interaction of PGE2 and Wnt signaling regulates developmental specification of stem cells and regeneration. Cell. 2009;136(6):1136-47.

367. Soontararak S, Chow L, Johnson V, Coy J, Wheat W, Regan D, et al. Mesenchymal Stem Cells (MSC) Derived from Induced Pluripotent Stem Cells (iPSC) Equivalent to Adipose-Derived MSC in Promoting Intestinal Healing and Microbiome Normalization in Mouse Inflammatory Bowel Disease Model. Stem Cells Transl Med. 2018;7(6):456-67.

368. Seno H, Miyoshi H, Brown SL, Geske MJ, Colonna M, Stappenbeck TS. Efficient colonic mucosal wound repair requires Trem2 signaling. Proc Natl Acad Sci U S A. 2009;106(1):256-61.

369. Owen KA, Abshire MY, Tilghman RW, Casanova JE, Bouton AH. FAK regulates intestinal epithelial cell survival and proliferation during mucosal wound healing. PLoS One. 2011;6(8):e23123.

370. Dutra RC, Claudino RF, Bento AF, Marcon R, Schmidt EC, Bouzon ZL, et al. Preventive and therapeutic euphol treatment attenuates experimental colitis in mice. PLoS One. 2011;6(11):e27122.

371. Schmitt M, Schewe M, Sacchetti A, Feijtel D, van de Geer WS, Teeuwssen M, et al. Paneth Cells Respond to Inflammation and Contribute to Tissue Regeneration by Acquiring Stem-like Features through SCF/c-Kit Signaling. Cell Rep. 2018;24(9):2312-28 e7.

372. Plumas J, Chaperot L, Richard MJ, Molens JP, Bensa JC, Favrot MC. Mesenchymal stem cells induce apoptosis of activated T cells. Leukemia. 2005;19(9):1597-604.

373. Akiyama K, Chen C, Wang D, Xu X, Qu C, Yamaza T, et al. Mesenchymal-stem-cell-induced immunoregulation involves FAS-ligand-/FAS-mediated T cell apoptosis. Cell Stem Cell. 2012;10(5):544-55.

374. Goncalves Fda C, Schneider N, Pinto FO, Meyer FS, Visioli F, Pfaffenseller B, et al. Intravenous vs intraperitoneal mesenchymal stem cells administration: what is the best route for treating experimental colitis? World J Gastroenterol. 2014;20(48):18228-39.

375. Goncalves FDC, Luk F, Korevaar SS, Bouzid R, Paz AH, Lopez-Iglesias C, et al. Membrane particles generated from mesenchymal stromal cells modulate immune responses by selective targeting of pro-inflammatory monocytes. Sci Rep. 2017;7(1):12100.

376. Vega-Letter AM, Kurte M, Fernandez-O'Ryan C, Gauthier-Abeliuk M, Fuenzalida P, Moya-Uribe I, et al. Differential TLR activation of murine mesenchymal stem cells generates distinct immunomodulatory effects in EAE. Stem Cell Res Ther. 2016;7(1):150.

377. Watanabe T, Konishi T, Kishimoto J, Kotake K, Muto T, Sugihara K, et al. Ulcerative colitis-associated colorectal cancer shows a poorer survival than sporadic colorectal cancer: a nationwide Japanese study. Inflamm Bowel Dis. 2011;17(3):802-8.

378. Ou B, Zhao J, Guan S, Lu A. Survival of Colorectal Cancer in Patients With or Without Inflammatory Bowel Disease: A Meta-Analysis. Dig Dis Sci. 2016;61(3):881-9.

379. Alkhayyat M, Abureesh M, Gill A, Khoudari G, Abou Saleh M, Mansoor E, et al. Lower Rates of Colorectal Cancer in Patients With Inflammatory Bowel Disease Using Anti-TNF Therapy. Inflamm Bowel Dis. 2021;27(7):1052-60.

380. Gordillo J, Cabre E, Garcia-Planella E, Ricart E, Ber-Nieto Y, Marquez L, et al. Thiopurine Therapy Reduces the Incidence of Colorectal Neoplasia in Patients with Ulcerative Colitis. Data from the ENEIDA Registry. J Crohns Colitis. 2015;9(12):1063-70.

381. Cui G, Fan Q, Li Z, Goll R, Florholmen J. Evaluation of anti-TNF therapeutic response in patients with inflammatory bowel disease: Current and novel biomarkers. EBioMedicine. 2021;66:103329.

382. Scott FI, Mamtani R, Brensinger CM, Haynes K, Chiesa-Fuxench ZC, Zhang J, et al. Risk of Nonmelanoma Skin Cancer Associated With the Use of Immunosuppressant and Biologic Agents in Patients With a History of Autoimmune Disease and Nonmelanoma Skin Cancer. JAMA Dermatol. 2016;152(2):164-72.

383. Carvello M, Lightner A, Yamamoto T, Kotze PG, Spinelli A. Mesenchymal Stem Cells for Perianal Crohn's Disease. Cells. 2019;8(7).

384. Zhang Y, Pu W, Bousquenaud M, Cattin S, Zaric J, Sun LK, et al. Emodin Inhibits Inflammation, Carcinogenesis, and Cancer Progression in the AOM/DSS Model of Colitis-Associated Intestinal Tumorigenesis. Front Oncol. 2020;10:564674.

385. von Bahr L, Batsis I, Moll G, Hagg M, Szakos A, Sundberg B, et al. Analysis of tissues following mesenchymal stromal cell therapy in humans indicates limited long-term engraftment and no ectopic tissue formation. Stem Cells. 2012;30(7):1575-8.

386. Kawashima K, Onizawa M, Fujiwara T, Gunji N, Imamura H, Katakura K, et al. Evaluation of the relationship between the spleen volume and the disease activity in ulcerative colitis and Crohn disease. Medicine (Baltimore). 2022;101(1):e28515.

387. Wang K, Karin M. The IL-23 to IL-17 cascade inflammation-related cancers. Clin Exp Rheumatol. 2015;33(4 Suppl 92):S87-90.

388. Kobaek-Larsen M, Thorup I, Diederichsen A, Fenger C, Hoitinga MR. Review of colorectal cancer and its metastases in rodent models: comparative aspects with those in humans. Comp Med. 2000;50(1):16-26.

389. Becker C, Fantini MC, Wirtz S, Nikolaev A, Lehr HA, Galle PR, et al. IL-6 signaling promotes tumor growth in colorectal cancer. Cell Cycle. 2005;4(2):217-20.

390. Murch SH, Braegger CP, Walker-Smith JA, MacDonald TT. Location of tumour necrosis factor alpha by immunohistochemistry in chronic inflammatory bowel disease. Gut. 1993;34(12):1705-9.

391. Sheng H, Shao J, Washington MK, DuBois RN. Prostaglandin E2 increases growth and motility of colorectal carcinoma cells. J Biol Chem. 2001;276(21):18075-81.

392. Tessner TG, Muhale F, Riehl TE, Anant S, Stenson WF. Prostaglandin E2 reduces radiation-induced epithelial apoptosis through a mechanism involving AKT activation and bax translocation. J Clin Invest. 2004;114(11):1676-85.

393. Chun E, Lavoie S, Michaud M, Gallini CA, Kim J, Soucy G, et al. CCL2 Promotes Colorectal Carcinogenesis by Enhancing Polymorphonuclear Myeloid-Derived Suppressor Cell Population and Function. Cell Rep. 2015;12(2):244-57.

394. Bain CC, Schridde A. Origin, Differentiation, and Function of Intestinal Macrophages. Front Immunol. 2018;9:2733.

395. Popivanova BK, Kostadinova FI, Furuichi K, Shamekh MM, Kondo T, Wada T, et al. Blockade of a chemokine, CCL2, reduces chronic colitis-associated carcinogenesis in mice. Cancer Res. 2009;69(19):7884-92.

396. McClellan JL, Davis JM, Steiner JL, Enos RT, Jung SH, Carson JA, et al. Linking tumor-associated macrophages, inflammation, and intestinal tumorigenesis: role of MCP-1. Am J Physiol Gastrointest Liver Physiol. 2012;303(10):G1087-95.

397. Lei X, Lei Y, Li JK, Du WX, Li RG, Yang J, et al. Immune cells within the tumor microenvironment: Biological functions and roles in cancer immunotherapy. Cancer Lett. 2020;470:126-33.

398. Kay J, Thadhani E, Samson L, Engelward B. Inflammation-induced DNA damage, mutations and cancer. DNA Repair (Amst). 2019;83:102673.

399. Fedeles BI, Freudenthal BD, Yau E, Singh V, Chang SC, Li D, et al. Intrinsic mutagenic properties of 5-chlorocytosine: A mechanistic connection between chronic inflammation and cancer. Proc Natl Acad Sci U S A. 2015;112(33):E4571-80.

400. Takeda K, Nakayama M, Hayakawa Y, Kojima Y, Ikeda H, Imai N, et al. IFN-gamma is required for cytotoxic T cell-dependent cancer genome immunoediting. Nat Commun. 2017;8:14607.

401. Scott CL, Bain CC, Mowat AM. Isolation and Identification of Intestinal Myeloid Cells. Methods Mol Biol. 2017;1559:223-39.

402. Hedrick CC, Malanchi I. Neutrophils in cancer: heterogeneous and multifaceted. Nat Rev Immunol. 2021.

403. Shang K, Bai YP, Wang C, Wang Z, Gu HY, Du X, et al. Crucial involvement of tumor-associated neutrophils in the regulation of chronic colitis-associated carcinogenesis in mice. PLoS One. 2012;7(12):e51848.

404. He D, Li H, Yusuf N, Elmets CA, Li J, Mountz JD, et al. IL-17 promotes tumor development through the induction of tumor promoting microenvironments at tumor sites and myeloid-derived suppressor cells. J Immunol. 2010;184(5):2281-8.

405. Polosukhina D, Singh K, Asim M, Barry DP, Allaman MM, Hardbower DM, et al. CCL11 exacerbates colitis and inflammation-associated colon tumorigenesis. Oncogene. 2021;40(47):6540-6.

406. Ren G, Zhang L, Zhao X, Xu G, Zhang Y, Roberts AI, et al. Mesenchymal stem cell-mediated immunosuppression occurs via concerted action of chemokines and nitric oxide. Cell Stem Cell. 2008;2(2):141-50.

407. Hidalgo-Garcia L, Molina-Tijeras JA, Huertas-Pena F, Ruiz-Malagon AJ, Diez-Echave P, Vezza T, et al. Intestinal mesenchymal cells regulate immune responses and promote epithelial regeneration in vitro and in dextran sulfate sodium-induced experimental colitis in mice. Acta Physiol (Oxf). 2021;233(2):e13699.

408. Yan L, Zheng D, Xu RH. Critical Role of Tumor Necrosis Factor Signaling in Mesenchymal Stem Cell-Based Therapy for Autoimmune and Inflammatory Diseases. Front Immunol. 2018;9:1658.

409. Lim JY, Kim BS, Ryu DB, Kim TW, Park G, Min CK. The therapeutic efficacy of mesenchymal stromal cells on experimental colitis was improved by the IFN-gamma and poly(I:C) priming through promoting the expression of indoleamine 2,3-dioxygenase. Stem Cell Res Ther. 2021;12(1):37.

410. Chen K, Liu Q, Tsang LL, Ye Q, Chan HC, Sun Y, et al. Human MSCs promotes colorectal cancer epithelial-mesenchymal transition and progression via CCL5/beta-catenin/Slug pathway. Cell Death Dis. 2017;8(5):e2819.

411. Takeshita K, Motoike S, Kajiya M, Komatsu N, Takewaki M, Ouhara K, et al. Xenotransplantation of interferon-gamma-pretreated clumps of a human mesenchymal stem cell/extracellular matrix complex induces mouse calvarial bone regeneration. Stem Cell Res Ther. 2017;8(1):101.

412. Brandacher G, Perathoner A, Ladurner R, Schneeberger S, Obrist P, Winkler C, et al. Prognostic value of indoleamine 2,3-dioxygenase expression in colorectal cancer: effect on tumor-infiltrating T cells. Clin Cancer Res. 2006;12(4):1144-51.

413. Meireson A, Devos M, Brochez L. IDO Expression in Cancer: Different Compartment, Different Functionality? Front Immunol. 2020;11:531491.

414. Ni J, Wu GD, Albenberg L, Tomov VT. Gut microbiota and IBD: causation or correlation? Nat Rev Gastroenterol Hepatol. 2017;14(10):573-84.

415. Cheng Y, Ling Z, Li L. The Intestinal Microbiota and Colorectal Cancer. Front Immunol. 2020;11:615056.

416. Gong D, Gong X, Wang L, Yu X, Dong Q. Involvement of Reduced Microbial Diversity in Inflammatory Bowel Disease. Gastroenterol Res Pract. 2016;2016:6951091.

417. Chen W, Liu F, Ling Z, Tong X, Xiang C. Human intestinal lumen and mucosa-associated microbiota in patients with colorectal cancer. PLoS One. 2012;7(6):e39743.

418. Saffarian A, Mulet C, Regnault B, Amiot A, Tran-Van-Nhieu J, Ravel J, et al. Crypt- and Mucosa-Associated Core Microbiotas in Humans and Their Alteration in Colon Cancer Patients. mBio. 2019;10(4).

419. Vezza T, Algieri F, Garrido-Mesa J, Utrilla MP, Rodriguez-Cabezas ME, Banos A, et al. The Immunomodulatory Properties of Propyl-Propane Thiosulfonate Contribute to its Intestinal Anti-Inflammatory Effect in Experimental Colitis. Mol Nutr Food Res. 2019;63(5):e1800653.

420. Mori G, Rampelli S, Orena BS, Rengucci C, De Maio G, Barbieri G, et al. Shifts of Faecal Microbiota During Sporadic Colorectal Carcinogenesis. Sci Rep. 2018;8(1):10329.

421. Kasai C, Sugimoto K, Moritani I, Tanaka J, Oya Y, Inoue H, et al. Comparison of human gut microbiota in control subjects and patients with colorectal carcinoma in adenoma: Terminal restriction fragment length polymorphism and next-generation sequencing analyses. Oncol Rep. 2016;35(1):325-33.

422. Yang Y, Jobin C. Novel insights into microbiome in colitis and colorectal cancer. Curr Opin Gastroenterol. 2017;33(6):422-7.

423. Hall AB, Yassour M, Sauk J, Garner A, Jiang X, Arthur T, et al. A novel Ruminococcus gnavus clade enriched in inflammatory bowel disease patients. Genome Med. 2017;9(1):103.

424. Flemer B, Lynch DB, Brown JM, Jeffery IB, Ryan FJ, Claesson MJ, et al. Tumour-associated and non-tumour-associated microbiota in colorectal cancer. Gut. 2017;66(4):633-43.

425. Lee YK, Mehrabian P, Boyajian S, Wu WL, Selicha J, Vonderfecht S, et al. The Protective Role of Bacteroides fragilis in a Murine Model of Colitis-Associated Colorectal Cancer. mSphere. 2018;3(6).

426. Hajjar R, Richard CS, Santos MM. The role of butyrate in surgical and oncological outcomes in colorectal cancer. Am J Physiol Gastrointest Liver Physiol. 2021;320(4):G601-G8.

427. Zhang T, Li P, Wu X, Lu G, Marcella C, Ji X, et al. Alterations of Akkermansia muciniphila in the inflammatory bowel disease patients with washed microbiota transplantation. Appl Microbiol Biotechnol. 2020;104(23):10203-15.

428. Griffin LE, Djuric Z, Angiletta CJ, Mitchell CM, Baugh ME, Davy KP, et al. A Mediterranean diet does not alter plasma trimethylamine N-oxide concentrations in healthy adults at risk for colon cancer. Food Funct. 2019;10(4):2138-47.

429. Zhang T, Ji X, Lu G, Zhang F. The potential of Akkermansia muciniphila in inflammatory bowel disease. Appl Microbiol Biotechnol. 2021;105(14-15):5785-94.

430. Ciorba MA, Riehl TE, Rao MS, Moon C, Ee X, Nava GM, et al. Lactobacillus probiotic protects intestinal epithelium from radiation injury in a TLR-2/cyclo-oxygenase-2-dependent manner. Gut. 2012;61(6):829-38.

431. Ho YT, Shimbo T, Wijaya E, Kitayama T, Takaki S, Ikegami K, et al. Longitudinal Single-Cell Transcriptomics Reveals a Role for Serpina3n-Mediated Resolution of Inflammation in a Mouse Colitis Model. Cell Mol Gastroenterol Hepatol. 2021;12(2):547-66.

432. Signore M, Cerio AM, Boe A, Pagliuca A, Zaottini V, Schiavoni I, et al. Identity and ranking of colonic mesenchymal stromal cells. J Cell Physiol. 2012;227(9):3291-300.

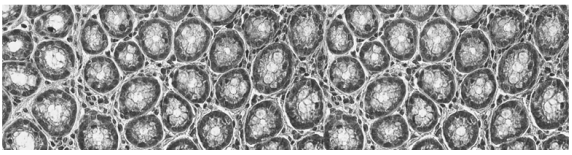

Abbreviations

ABRREVIATIONS

α-SMA	α smooth muscle actin
AOM	Azoxymethane
CAC	Colitis associated cancer
CD	Crohn's disease
CFSE	Carboxyfluorescein succinimidyl ester
CFU-F	Colony forming unit fibroblast
CM	Conditioned medium
COX-2	Cyclooxygenase-2
CRC	Colorectal cancer
DAI	Disease Activity Index
DCs	Dendritic cells
DMEM	Dulbecco's modified eagle's medium
DSS	Dextran Sodium Sulfate
DTT	Dithiothreitol
EDTA	Ethylenediaminetetraacetic acid
FACs	Fluorescence-activated cell sorting
FBS	Fetal bovine serum
FoxP3	Forkhead box P3
GAPDH	Glyceraldehyde 3-phosphate dehydrogenase
GSK3	Glycogen synthase kinase 3
GVHD	Graft versus host disease
HGF	Hepatocyte growth factor

HLA Human leukocyte antigen

H&E Hematoxylin and eosin

IBD Inflammatory Bowel Disease

ICAM-1 Intercellular adhesion molecule-1

IDO Indoleamine 2,3-dioxygenase

IFN Interferon

IL Interleukin

iMCs Intestinal mesenchymal cells

iMSCs Intestinal mesenchymal stromal cells

iNOS Inducible nitric oxide synthase

ISCT International Society for Cellular Therapy

LPS Lipopolisaccharide

MLNs Mesenteric Lymph Nodes

MMPs Matrix metalloproteinases

MSCs Mesenchymal Stromal Cells

NFAT Nuclear factor of activated T cells

NFkB Nuclear factor kappa B

NLR Nod-like receptors

NO Nitric oxide

PBMCs Peripheral Blood Mononuclear Cells

PD-L1 Programmed death-ligand 1

PFA Paraformaldehyde

PGE_2 Prostanglandin E2

PMA Phorbol 12-myristate 13-acetate

RNS Reactive nitrogen species

ROS Reactive oxygen species

SD Standard derivation

STAT Signal transducer and activator of transcription

TAMs Tumor associated macrophages

TGF Transcription growth factor

Th T helper

TLRs Toll-like receptors

Treg Regulatory T lymphocytes

TSG-6 Tumor Necrosis Factor α–Stimulated Gene 6

UC Ulcerative colitis

ZO-1 Zonula occludens-1

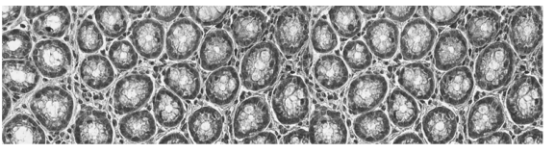

Annex

ANNEX

1.PUBLICATIONS

1. Can a Conversation Between Mesenchymal Stromal Cells and Macrophages Solve the Crisis in the Inflamed Intestine? **Hidalgo-Garcia L**, Gálvez J, Rodríguez-Cabezas ME, Anderson PO. Front Pharmacol. 2018 Mar 6;9:179. doi:10.3389/fphar.2018.00179. eCollection 2018.
2. Intestinal mesenchymal cells regulate immune responses and promote epithelial regeneration in vitro and in dextran sulfate sodium-induced experimental colitis in mice. **Hidalgo-Garcia L**, Molina-Tijeras JA, Huertas-Peña F, Ruiz-Malagón AJ, Diez-Echave P, Vezza T, Rodríguez-Sojo MJ, Morón R, Becerra-Massare P, Rodríguez-Nogales A, Gálvez J, Rodríguez-Cabezas ME, Anderson P. Acta Physiol (Oxf). 2021 Oct;233(2):e13699. doi:10.1111/apha.13699. Epub 2021 Jun 21.
3. Probiotic and Functional Properties of Limosilactobacillus reuteri INIA P572. Diez-Echave P, Martín-Cabrejas I, Garrido-Mesa J, Langa S, Vezza T, Landete JM, **Hidalgo-García L**, Algieri F, Mayer MJ, Narbad A, García-Lafuente A, Medina M, Rodríguez-Nogales A, Rodríguez-Cabezas ME, Gálvez J, Arqués JL. Nutrients. 2021 May 29;13(6):1860. doi:10.3390/nu13061860.
4. Silk fibroin nanoparticles enhance quercetin immunomodulatory properties in DSS-induced mouse colitis. Diez-Echave P, Ruiz-Malagón AJ, Molina-Tijeras JA, **Hidalgo-García L**, Vezza T, Cenis-Cifuentes L, Rodríguez-Sojo MJ, Cenis JL, Rodríguez-Cabezas ME, Rodríguez-Nogales A, Gálvez J, Lozano-Pérez AA. Int J Pharm. 2021 Sep 5;606:120935. doi:10.1016/j.ijpharm.2021.120935. Epub 2021 Jul 24.
5. Lactobacillus fermentum CECT5716 ameliorates high fat diet-induced obesity in mice through modulation of gut microbiota dysbiosis. Molina-Tijeras JA, Diez-Echave P, Vezza T, **Hidalgo-García L**, Ruiz-Malagón AJ, Rodríguez-Sojo MJ, Romero M, Robles-Vera I, García F, Plaza-Diaz J, Olivares M, Duarte J, Rodríguez-Cabezas ME, Rodríguez-Nogales A, Gálvez J. Pharmacol Res. 2021 May;167:105471. doi:10.1016/j.phrs.2021.105471. Epub 2021 Jan 30.
6. A recombinant glucocorticoid-induced leucine zipper protein ameliorates symptoms of dextran sulfate sodium-induced colitis by improving intestinal permeability. Gentili M, **Hidalgo-Garcia L**, Vezza T, Ricci E, Migliorati G, Rodríguez-Nogales A, Riccardi C, Galvez J, Ronchetti S. FASEB J. 2021 Nov;35(11):e21950. doi:10.1096/fj.202100778RRRR.
7. The Beneficial Effects of Red Sun-Dried Capsicum annuum L. Cv Senise Extract with Antioxidant Properties in Experimental Obesity are Associated with Modulation of the Intestinal Microbiota. Sinisgalli C, Vezza T, Diez-Echave P, Ostuni A, Faraone I, **Hidalgo-Garcia L**, Russo D, Armentano MF, Garrido-Mesa J, Rodríguez-Cabezas ME,

Rodríguez-Nogales A, Milella L, Galvez J. Mol Nutr Food Res. 2021 Feb;65(3):e2000812. doi:10.1002/mnfr.202000812. Epub 2020 Dec 28.

8. Allium-Derived Compound Propyl Propane Thiosulfonate (PTSO) Attenuates Metabolic Alterations in Mice Fed a High-Fat Diet through Its Anti-Inflammatory and Prebiotic Properties. Vezza T, Garrido-Mesa J, Diez-Echave P, **Hidalgo-García L**, Ruiz-Malagón AJ, García F, Sánchez M, Toral M, Romero M, Duarte J, Guillamón E, Baños Arjona A, Moron R, Galvez J, Rodríguez-Nogales A, Rodríguez-Cabezas ME. Nutrients. 2021 Jul 28;13(8):2595. doi: 10.3390/nu13082595.
9. The prebiotic properties of Hibiscus sabdariffa extract contribute to the beneficial effects in diet-induced obesity in mice. Diez-Echave P, Vezza T, Rodríguez-Nogales A, Ruiz-Malagón AJ, **Hidalgo-García L**, Garrido-Mesa J, Molina-Tijeras JA, Romero M, Robles-Vera I, Pimentel-Moral S, Borras-Linares I, Arráez-Román D, Segura-Carretero A, Micol V, García F, Duarte J, Rodríguez-Cabezas ME, Gálvez J. Food Res Int. 2020 Jan;127:108722. doi:10.1016/j.foodres.2019.108722. Epub 2019 Oct 8.
10. Anti-Inflammatory and Chemopreventive Effects of Bryophyllum pinnatum (Lamarck) Leaf Extract in Experimental Colitis Models in Rodents. Andrade AWL, Guerra GCB, de Souza Araújo DF, de Araújo Júnior RF, de Araújo AA, de Carvalho TG, Fernandes JM, Diez-Echave P, **Hidalgo-García L**, Rodríguez-Cabezas ME, Gálvez J, Zucolotto SM. Front Pharmacol. 2020 Jul 29;11:998. doi:10.3389/fphar.2020.00998. eCollection 2020.
11. The Beneficial Effects of Lippia Citriodora Extract on Diet-Induced Obesity in Mice Are Associated with Modulation in the Gut Microbiota Composition. Diez-Echave P, Vezza T, Rodríguez-Nogales A, **Hidalgo-Garcia L**, Garrido-Mesa J, Ruiz-Malagón A, Molina-Tijeras JA, Romero M, Robles-Vera I, Leyva-Jiménez FJ, Lozano-Sánchez J, Arráez-Román D, Segura-Carretero A, Micol V, García F, Morón R, Duarte J, Rodríguez-Cabezas ME, Gálvez J. Mol Nutr Food Res. 2020 Jul;64(13):e2000005. doi:10.1002/mnfr.202000005. Epub 2020 Jun 2.
12. Exopolysaccharide Producing Bifidobacterium animalis subsp. lactis Strains Modify the Intestinal Microbiota and the Plasmatic Cytokine Levels of BALB/c Mice According to the Type of Polymer Synthesized. Sabater C, Molinero-García N, Castro-Bravo N, Diez-Echave P, **Hidalgo-García L**, Delgado S, Sánchez B, Gálvez J, Margolles A, Ruas-Madiedo P. Front Microbiol. 2020 Nov 26;11:601233. doi:10.3389/fmicb.2020.601233. eCollection 2020.
13. Comparative Study of the Antioxidant and Anti-Inflammatory Effects of Leaf Extracts from Four Different Morus alba Genotypes in High Fat Diet-Induced Obesity in Mice. Leyva-Jiménez FJ, Ruiz-Malagón AJ, Molina-Tijeras JA, Diez-Echave P, Vezza T, **Hidalgo-García L**, Lozano-Sánchez J, Arráez-Román D, Cenis JL, Lozano-Pérez AA, Rodríguez-Nogales A, Segura-Carretero A, Gálvez J. Antioxidants (Basel). 2020 Aug 11;9(8):733. doi:10.3390/antiox9080733.

2. CONTRIBUTIONS TO CONGRESSES (ONLY THOSE RELATED TO THIS THESIS)

1. **Hidalgo-García L**, Ruiz-Malagón AJ, Huertas-Peña F, Mirón Pozo B, Molina-Tijeras JA, Rodríguez-Sojo MJ, Diez-Echave P, Vezza T, Morón R, Becerra-Massare P, Rodríguez-Nogales A, Gálvez J, Rodríguez-Cabezas ME, Anderson P. La modulación de la inflamación intestinal mediada por células mesenquimales estromales del intestino humano reduce el cáncer colorrectal asociado a colitis. II Congreso de Investigación del PTS Granada. Celebrado los días 9-11 de febrero de 2022 en Granada, España. Comunicación oral.
2. **Hidalgo-García L**; Molina-Tijeras JA; Huertas-Peña F; Ruiz-Malagón AJ; Díez-Echave P; Vezza T; Rodríguez-Sojo MJ; Morón R; Becerra-Massare P; Rodríguez Nogales A.; Gálvez J; Rodríguez Cabezas ME; Anderson P. Intestinal mesenchymal cells modulate gut microbiota composition in DSS-induced colitis in mice. XII Workshop Sociedad Española de Microbiota, Probióticos y Prebióticos (SEMiPyP 2021). Celebrado los días 15-18 de septiembre de 2021. Modalidad online. Comunicación oral.
3. **Hidalgo-García L**; Molina-Tijeras JA; Huertas-Peña F; Ruiz-Malagón AJ; Díez-Echave P; Vezza T; Rodríguez-Sojo MJ; Morón R; Becerra-Massare P; Rodríguez Nogales A.; Gálvez J; Rodríguez Cabezas ME; Anderson P. Intestinal mesenchymal cells regulate immune responses and promote epithelial regeneration in-vitro and in DSS-induced experimental colitis. LXXX Congreso de la Sociedad Española de Patología Digestiva. Celebrado los días 6-7 de mayo de 2021. Modalidad online. Comunicación oral.
4. **Hidalgo-García L**; Molina-Tijeras JA; Huertas-Peña F; Ruiz-Malagón AJ; Díez-Echave P; Vezza T; Rodríguez-Sojo MJ; Morón R; Becerra Massare; Rodríguez-Nogales A; Gálvez J; Rodríguez-Cabezas ME; Anderson P. Immunomodulatory properties of human intestinal mesenchymal cells on peripheral blood mononuclear cells, macrophages and epithelial cells. IV Congreso Nacional de Jóvenes Investigadores en Biomedicina. Celebrado los días 4-6 de noviembre de 2020. Modalidad online. Comunicación tipo póster.
5. **Hidalgo-García L**; Molina-Tijeras JA; Vezza T; Diez-Echave P; Ruiz-Malagón AJ; Rodríguez-Sojo MJ; Olivares M; Huertas F; Anderson P; Anderson P; Rodríguez-Cabezas ME. Analysis of mesenchymal stromal cells immunomodulation by different TLRs agonists and the probiotic Lactobacillus fermentum CECT5716. XI Reunión de Jóvenes Farmacólogos de Andalucía. Celebrada el día 31 de mayo de 2019 en Málaga, España. Comunicación oral.
6. **Hidalgo-García, L**.; Rodríguez-Cabezas, M.E.; Molina-Tijeras, J.A.; Vezza, T.; Diez-Echave, P.; Ruiz-Malagón, A.J.; Huertas, F.; Becerra-Massare, P.; Galvez, J.; Anderson, P. TNF-α and IFN-γ induce an antiinflammatory phenotype in intestinal mesenchymal stromal cells. Mesenchymal Cells in Inflammation, Immunity and Cancer EMBO

workshop. Celebrado los días 19-23 de mayo de 2019 en Atenas, Grecia. Comunicación tipo póster.

7. **Hidalgo-García, L**.; Rodriguez-Cabezas, M.E.; Molina-Tijeras, J.A.; Vezza, T.; Diez-Echave, P.; Ruiz-Malagón, A.J.; Huertas, F.; Becerra-Massare, P.; Galvez, J.; Anderson, P. TNF-a and IFN-y induce an anti-inflammatory phenotype in intestinal mesenchymal stromal cells. Falk symposium 212 2018. Celebrado los días 7-8 de septiembre de 2018 en Kyoto, Japón. Comunicación tipo póster.
8. **Hidalgo-García, L**; Anderson, P; de Araújo Farias, V; Rodríguez-Nogales, A; Algieri, F; Vezza, T; Garrido-Mesa, J; Utrilla, MP; Huertas, F; Diez-Echave, P; Becerra-Massare, P; Rodríguez-Cabezas, ME; Gálvez, J. Characterization of intestinal stromal stem cells for its future use in the treatment of inflammatory bowel disease. Falk symposium 209 2017. Celebrado los días 6-7 de octubre de 2017 en Berlín, Alemania. Comunicación tipo póster.

3. RESEARCH INTERNSHIPS

- Center: Biomedical Sciences Research Center Alexander Fleming, Vari, Greece. Institute or department: Immunology department. Supervisor: George Kollias. Duration: 31/05/2018 – 31/08/2018. 3 meses.
- Center: William Harvey Research Institute, London, United Kingdom. Institute or department: John Vane Science Centre. Supervisor: Dianne Cooper. Duration: 01/08/2019 – 30/09/2019. 3 meses.

4. TRAINING COURSES AND OTHER MERITS

- Capacitación para manipulación de material radiactivo no encapsulado de la IRA 1679 realizado en el Instituto de Biomedicina y parasitología “López-Neyra” (CSIC). Fecha de finalización 28/10/2016.
- Realización del curso “Introducción al diseño de nucleótidos para PCR” de 20 horas de duración organizado por la Universidad de Granada. Fecha de inicio-fin: 24/04/2018 - 26/04/2018.
- Introducción a la estadística en ciencias de la salud. Entidad de titulación: Universidad de Granada. Ciudad entidad titulación: Granada, Andalucía, España. Fecha de inicio-fin: 06/02/2018 - 08/02/2018.
- Curso de certificación de capacitación en protección y experimentación animal. Categorías A, B y C (FELASA). Fecha de titulación: 13/07/2018.
- Realización del curso “Bioinformática de muestras biológicas: bioestadística univariable y multivariable aplicada a resultados con muestras de secuenciación masiva (IV ed.) de 30 horas de duración organizado por el Centro Mediterráneo. Fecha de finalización: 17/07/2020.

- Realización del curso “Incorporación de datos ómicos a proyectos de investigación” de 20 horas de duración organizado por la Universidad de Granada. Fecha de finalización: 23/04/2021.
- Premio Arias Vallejo a la mejor comunicación en Gastroenterología Básica de los premios Fundación Española del Aparato Digestivo (FEAD) concedido por la Sociedad Española de Patología Digestiva. Título de la comunicación: Intestinal mesenchymal cells regulate immune responses and promote epithelial regeneration in-vitro and in DSS-induced experimental colitis. Autores: **Hidalgo-García L**; Molina-Tijeras JA; Huertas-Peña F; Ruiz-Malagón AJ; Díez-Echave P; Vezza T; Rodríguez-Sojo MJ; Morón R; Becerra-Massare P; Rodríguez Nogales A.; Gálvez J; Rodríguez Cabezas ME; Anderson P.
- Realización del “Curso Avanzado de Vesículas Extracelulares” de 40 horas de duración organizado por la Universidad Francisco de Vitoria. Fecha de finalización 09/06/2021.
- Realización del curso “Summer School 2021 módulo 4 – microbial genomics and metagenomics workshop” de 30 horas de duración organizado por Fundación FISABIO. Fecha de finalización 02/07/2021.
- Impartición de 180 horas de docencia repartidas entre los Grados en Farmacia, Medicina y Bioquímica durante los cursos académicos 2017-2018, 2018-2019 y 2019-2020.